

# The Role of the Wnt Receptor Frizzled-8 in Prostate Cancer Pathogenesis

-Doctoral Thesis-



Universidad  
del País Vasco

Euskal Herriko  
Unibertsitatea

Virginia Murillo Garzón

2018





# The Role of the Wnt Receptor Frizzled-8 in Prostate Cancer Pathogenesis

Virginia Murillo Garzón

Doctoral Thesis, 2018

Director: Dr. Robert Kypta

Doctorate Program: Molecular Biology and Biomedicine

Department: Biochemistry and Molecular Biology

University of the Basque Country (UPV)

This work has been performed at the Center for Cooperative Research in Biosciences (CIC bioGUNE) supported by the Basque Government PRE\_2015\_1\_0076.



**EUSKO JAURLARITZA**  
**GOBIERNO VASCO**

HEZKUNTZA, UNIBERTSITATE  
ETA IKERKETA SAILA  
DEPARTAMENTO DE EDUCACIÓN,  
UNIVERSIDADES E INVESTIGACIÓN



*“Vive como si fueras a morir mañana,  
aprende como si fueras a vivir para siempre”*

*Mahatma Gandhi*



## *Acknowledgements/ Agradecimientos*

First of all, I would to thank to my supervisor, Robert, who made this work possible and gave me the opportunity to learn every single day. Thanks for your help and support along these years. Your kind words, optimism and encouragement were very important for me.

Esta tesis no hubiera sido posible sin vosotras, ese gran equipo que forman las “Kypta’s girls”. Gracias Irantzu, por estar siempre ahí a lo largo de este camino, por tu ayuda en lo técnico, pero sobre todo por tener esa sonrisa cada día que lo hace todo más fácil. Gracias por tu capacidad para alentarnos y animarnos en cada momento. Mila esker. Gracias Esti, compañera de tesis de principio a fin, porque ir de la mano paso a paso ha creado un apoyo mutuo entre ambas. Gracias Inma, por lo que he podido aprender de tu experiencia, por tus consejos y tu guía, pero también por tu positividad para hacerme ver que todo es más fácil de lo que parece. Gracias Saray, por la alegría y energía que transmites, por estar siempre dispuesta a ayudar. Como no, gracias Nora que me ayudaste en los comienzos y lo sigues haciendo al final, incluso en la distancia. Gracias por tu maestría enseñando. Gracias también a Eder, por su disposición en cada momento. A todos los estudiantes que han pasado por el laboratorio, Michelle, Pierluigi, Carola e Igga que me han dado la oportunidad de enseñar pero que a la vez me han permitido aprender.

Por supuesto, agradecer también a “Vivanco’s lab”, con el que he podido compartir el día a día en el trabajo, pero también cada comida y muchos y grandes momentos fuera. En primer lugar, gracias María por todos tus consejos y comentarios constructivos a lo largo de esta tesis, que estoy segura han contribuido a mejorar mi trabajo. Gracias Miriam, por tu dedicación y capacidad para enseñar, pero también por tu forma de ser, alegre y protectora. Iskander, gracias por ser como eres, por tu ayuda en cada día del trabajo, pero, sobre todo, por cada uno de los momentos vividos fuera. Gracias Julia, por tu alegría y optimismo. Thank you So Young for your help with any issue, sharing your knowledge every time is possible. A Giacomo, por enseñarme cada uno de sus trucos y por todas las risas compartidas.

Esta tesis ha sido también posible gracias al gran ambiente de trabajo. Gracias a todos y cada uno de vosotros: Edurne´s, Anguita´s, Ashwin´s, Carracedo´s and Rosa´s labs. Gracias por vuestra ayuda siempre que ha sido posible.

Thanks to all the Finnish people, Matthias, Malin, Mervi, Jesse, Helena, Lea and Mikael, for the opportunity to complete my training and learn a new culture.

Gracias especialmente a Encarni, con quien compartí mis inicios en bioGUNE y de quien tuve la oportunidad de aprender tantas cosas. Gracias por tu apoyo y amistad durante todos estos años en los que me has permitido formar parte de tu cuadrilla o incluso de tu familia. Gracias por estar siempre ahí. Gracias también a Laura, por tu alegría, tu ilusión, tu optimismo y por tu apoyo en cada etapa de este camino. Y especialmente también a Cora, por tu voz que alegra el ambiente, por estar siempre pendiente de mí.

Gracias a tod@s, porque habéis pasado a formar parte de mi familia. Porque me habéis hecho sentir como en casa aun estando tan lejos de ella.

Una parte fundamental de esta tesis es debida a esa otra gran familia, mis amig@s, los que siempre estáis ahí. Gracias por vuestro interés tratando de entender mi trabajo, por vuestro apoyo durante este periodo en el que he estado un poco más lejos de vosotros, al menos físicamente. Por cada llamada, mensaje o abrazo que me hacen siempre tan feliz. Simplemente gracias.

Pero, sobre todo, esta tesis se ha materializado gracias a que he tenido la gran suerte de poder contar con vosotros. Gracias a mis padres, parte fundamental en mi vida, porque de vuestra mano he conocido la tenacidad, la honestidad, la humildad, la entereza, el respeto y el valor del trabajo. Vuestro ejemplo me ayuda día a día. Gracias a ti, hermanita, por estar siempre ahí, por valorarme tanto y hacerme sentir siempre grande en este mundo tan inmenso. Gracias al resto de los miembros de mi familia, a los que están y los que ya no están, a mis abuelos y a todos mis tíos y primos, porque sé que siempre puedo contar con vosotros.

Finalmente, gracias a ti, Loren, mi compañero, mi apoyo incondicional. Gracias por hacerme ver siempre el lado bueno de las cosas y hacerme disfrutar cada segundo. Gracias por acompañarme en el camino de la vida.







# INDEX

<b>ABBREVIATIONS</b> .....	<b>17</b>
<b>SUMMARY</b> .....	<b>21</b>
<b>RESUMEN</b> .....	<b>23</b>
<b>INTRODUCTION</b> .....	<b>25</b>
<b>1. The human prostate</b> .....	<b>27</b>
1.1 Structure and function of the human prostate gland .....	27
1.2 Prostate development .....	30
<b>2. Cancer</b> .....	<b>31</b>
2.1 Epithelial-mesenchymal transition (EMT) in cancer .....	32
<b>3. Prostate cancer</b> .....	<b>35</b>
3.1 Epidemiology and etiology .....	35
3.2 Histological variants of prostate cancer .....	36
3.3 Prostate cancer initiation and progression.....	38
3.4 Diagnosis .....	39
3.5 Classification and staging system .....	40
3.6 Treatment.....	42
<b>4. Androgen receptor signaling in prostate cancer</b> .....	<b>44</b>
<b>5. Wnt signaling: an overview</b> .....	<b>47</b>
5.1 Wnt proteins.....	47
5.2 Wnt biogenesis and secretion .....	49
5.3 Wnt signaling pathways.....	50
5.4 Wnt receptors.....	53
5.4.1 FZD receptors .....	53
5.4.1.1 FZD8 .....	57
5.4.2 LRP5/6 coreceptors .....	58
5.4.3 ROR1/2 coreceptors .....	59
5.4.4 Receptor tyrosine kinases (RYK, PTK7 and MuSK) and others.....	59
5.5 Regulation of Wnt signaling.....	60
<b>6. Wnt signaling in cancer</b> .....	<b>62</b>
6.1 Wnt alterations in prostate cancer .....	62
6.2 Targeting Wnt signaling.....	65
<b>7. Wnt signaling crosstalk with other pathways: TGF-<math>\beta</math> signaling</b> .....	<b>66</b>
7.1 TGF- $\beta$ signal transduction .....	67
7.2 TGF- $\beta$ receptors.....	68
7.3 Smad proteins.....	70
7.4 Dual role of TGF- $\beta$ .....	70
7.5 Wnt and TGF- $\beta$ signaling crosstalk .....	71
<b>8. Wnt-11 signaling</b> .....	<b>73</b>
8.1 Wnt-11 in development .....	73
8.2 Wnt-11 in cancer: implication in prostate cancer .....	74

---

<b>HYPOTHESIS AND AIMS</b> .....	<b>75</b>
<b>MATERIALS AND METHODS</b> .....	<b>79</b>
1. <b>Cell culture</b> .....	<b>81</b>
2. <b>Compounds</b> .....	<b>82</b>
3. <b>Plasmids and siRNAs</b> .....	<b>82</b>
4. <b>RNA analysis</b> .....	<b>84</b>
4.1 RNA extraction and cDNA synthesis .....	84
4.2 Primer design and setup .....	84
4.3 Quantitative Real-Time PCR .....	85
5. <b>Cell transfection and silencing</b> .....	<b>87</b>
6. <b>Generation of stable knockdown cells</b> .....	<b>88</b>
7. <b>Gene reporter assays</b> .....	<b>90</b>
8. <b>Cell migration and invasion assays</b> .....	<b>91</b>
9. <b>Protein analysis</b> .....	<b>92</b>
9.1 Protein extraction .....	92
9.2 Western blotting (WB) .....	92
9.3 Immunoprecipitation (IP) .....	94
10. <b>Immunofluorescence</b> .....	<b>94</b>
11. <b>Clinical samples</b> .....	<b>95</b>
12. <b>Immunohistochemistry</b> .....	<b>97</b>
13. <b>Miniaturized tridimensional (3D) assays</b> .....	<b>97</b>
13.1 Tridimensional (3D) culture and live-cell imaging .....	98
13.2 Tridimensional (3D) image acquisition, pre-processing and morphometric analyses .....	99
14. <b>Tumor growth assay on the chorioallantoic membrane (CAM)</b> .....	<b>100</b>
15. <b>Bioinformatics analysis</b> .....	<b>101</b>
16. <b>Statistical analysis</b> .....	<b>101</b>
<b>RESULTS</b> .....	<b>103</b>
<b>Chapter 1. Identification and characterization of Wnt-11 receptors in metastatic prostate cancer</b> .....	<b>105</b>
1.1 Screening of Wnt receptors with increased expression in prostate cancer cell lines .....	105
1.2 <i>In silico</i> screening of Wnt receptors with increased expression in prostate tumors .....	109
1.3 Identification of FZD receptors involved in Wnt-11 signaling.....	112
1.3.1 Colocalization of Wnt-11 with FZD family members .....	113
1.3.2 Evaluation of Wnt-11-FZD signaling.....	116
1.3.3 FZD8 as a major Wnt-11 receptor .....	118

<b>Chapter 2. Implication of FZD8 in prostate cancer pathogenesis .....</b>	<b>122</b>
2.1 Role of FZD8 in prostate tumorigenesis: <i>in vitro</i> analysis .....	122
2.1.1 Contribution of FZD8 to capacity for prostate cancer cell migration and invasion .....	122
2.1.1.1 Cell migration and invasion in conventional two-dimensional (2D) cell cultures .....	123
2.1.1.2 Cell invasion in organotypic tridimensional (3D) cultures .....	126
2.1.2 Role of FZD8 in the epithelial to mesenchymal transition (EMT) .....	131
2.1.2.1 EMT in standard 2D culture .....	131
2.1.2.2 Regulation of WNT11 by FZD8: potential positive-feedback loop ..	133
2.1.2.3 EMT in organotypic 3D cultures .....	134
2.2 Role of FZD8 in prostate pathogenesis: <i>in vivo</i> assays .....	135
2.2.1 <i>In vivo</i> chicken chorioallantoic membrane (CAM) model .....	135
2.2.2 <i>In vivo</i> mouse model .....	137
2.3 Role of FZD8 in prostate tumorigenesis: analysis of patient samples .....	138
2.3.1 Bioinformatics analysis of prostate cancer datasets .....	138
2.3.2 Analysis of FZD8 and Wnt-11 protein expression in prostate cancer patient TMAs .....	141
<b>Chapter 3. Elucidation of the mechanism underlying the effects of FZD8 in prostate cancer pathogenesis .....</b>	<b>145</b>
3.1 Involvement of FZD8 in TGF- $\beta$ signaling .....	145
3.1.1 Analysis of TGF- $\beta$ -dependent transcriptional activity .....	146
3.1.2 Evaluation of target gene expression and Smad phosphorylation ...	147
3.1.3 Analysis of TGF- $\beta$ -dependent cell invasion .....	148
3.1.4 Study of TGF- $\beta$ -dependent-EMT regulation.....	149
3.2 Mechanism of regulation of TGF- $\beta$ signaling by FZD8.....	152
3.2.1 Regulation at the intracellular level.....	152
3.2.2 Regulation at the cell membrane.....	154
3.2.2.1 FZD8 binds to TGF- $\beta$ receptors .....	154
3.2.2.2 Analysis of interacting domains .....	155
3.2.2.3 Effects of TGF- $\beta$ on the interaction .....	156
3.2.2.4 Implication of Wnt-11 in FZD8-TGF $\beta$ RI binding .....	157
<b>DISCUSSION .....</b>	<b>159</b>
<b>Chapter 1. Identification and characterization of Wnt-11 receptors in metastatic prostate cancer .....</b>	<b>162</b>
<b>Chapter 2. Implication of FZD8 in prostate cancer pathogenesis .....</b>	<b>166</b>
<b>Chapter 3. Elucidation of the mechanism underlying the effects of FZD8 in prostate cancer pathogenesis .....</b>	<b>171</b>
<b>CONCLUSIONS .....</b>	<b>175</b>
<b>BIBLIOGRAPHY .....</b>	<b>179</b>
<b>SCIENTIFIC CONTRIBUTIONS .....</b>	<b>199</b>
<b>RESUMEN: VERSIÓN EXTENDIDA.....</b>	<b>205</b>



## FIGURE INDEX

### INTRODUCTION

Figure 1. Human prostate anatomy.....	27
Figure 2. Histology and structure of the human prostate gland .....	29
Figure 3. Schematic representation of phases of prostate development .....	30
Figure 4. Hallmarks of cancer. ....	32
Figure 5. Classical model of reversible EMT-MET. ....	33
Figure 6. Plasticity through the transitional stages in EMT-MET.....	34
Figure 7. Prostate cancer epidemiology.....	36
Figure 8. Histology of prostate tissue. ....	38
Figure 9. Prostate cancer initiation and progression.....	39
Figure 10. Classification of prostate tumors based on stage system. ....	41
Figure 11. Gleason score representation. ....	42
Figure 12. Different treatment options during prostate cancer progression .....	43
Figure 13. Androgen receptor signaling. ....	45
Figure 14. Structure of Wnt proteins. ....	48
Figure 15. Wnt biogenesis and secretion .....	50
Figure 16. Wnt signaling pathways .....	52
Figure 17. Wnt receptors and coreceptors. ....	53
Figure 18. FZD receptors.....	55
Figure 19. Hypothetical model of Wnt signalosome assembly.....	56
Figure 20. FZD8 genetic alterations in prostate cancer datasets.....	58
Figure 21. Wnt signaling regulation.....	61
Figure 22. Wnt signaling regulation by RNF43/ZNRF3/RSPO.....	62
Figure 23. Drugs that target Wnt signaling. ....	66
Figure 24. Smad-dependent and Smad-independent pathways.....	68
Figure 25. Schematic illustration of the motifs of TGF- $\beta$ receptors. ....	69
Figure 26. Crosstalk between Wnt and TGF- $\beta$ signaling pathways. ....	72

### MATERIALS AND METHODS

Figure 27. Schematic process for the generation of stable knockdown cells.....	89
Figure 28. Schematic of lentivirus generation in HEK293T cell. ....	89
Figure 29. Basis of gene reporter assays.....	90
Figure 30. Schematic diagram for migration and invasion assays. ....	92
Figure 31. Schematic illustration of prostate cancer cells cultured in 3D and 2D.....	98
Figure 32. Schematic representation of the 3D culture technique. ....	99
Figure 33. Schematic representation of the CAM assay.....	101

### RESULTS

Figure 34. Expression levels of WNT11 and Wnt receptor genes in prostate cancer cell lines.....	107
Figure 35. Immunohistochemistry of Wnt receptors and coreceptors. ....	112
Figure 36. Wnt-11 and FZD receptor localization .....	114

Figure 36. Wnt-11 and FZD receptor localization (continuation).....	115
Figure 37. Wnt-11 activates the ATF2-dependent gene reporter.....	116
Figure 38. Involvement of FZD receptors in Wnt-11/ATF2 signaling in prostate cancer .....	117
Figure 39. Requirement for FZD8 in the response to Wnt-11 in prostate cancer cells. .....	119
Figure 40. FZD8 mediates Wnt-11 noncanonical signaling. ....	120
Figure 41. FZD8 binds Wnt-11 in vitro. ....	121
Figure 42. FZD8 is required for prostate cancer cell migration and invasion. ....	123
Figure 43. Effects of <i>FZD8</i> silencing on cell proliferation.....	124
Figure 44. Stable knockdown of <i>FZD8</i> reduces prostate cancer cell invasion .....	125
Figure 46. <i>FZD8</i> silencing reduces prostate cancer cell invasion in organotypic 3D cultures.....	127
Figure 47. Representative segmentation of live-cell confocal images by AMIDA.....	128
Figure 48. Quantification of phenotypic effects of <i>FZD8</i> silencing in organotypic 3D cultures. ....	129
Figure 49. Boxplots for the main parameters affected by <i>FZD8</i> silencing in organotypic 3D cultures. ....	130
Figure 50. FZD8 regulates the expression of EMT markers at the mRNA level.....	132
Figure 51. FZD8 regulates the expression of EMT markers at the protein level. ....	133
Figure 52. FZD8 regulates <i>WNT11</i> expression. ....	134
Figure 53. Immunostaining of <i>FZD8</i> silenced cells in organotypic 3D cultures. ....	135
Figure 54. FZD8 is required for tumor growth <i>in vivo</i> in the CAM.....	136
Figure 55. Immunohistochemistry of FZD8 and vimentin in the CAM. ....	137
Figure 56. Immunohistochemical staining of a lymph node metastasis from a PC-3 mouse xenograft. ....	138
Figure 57. <i>FZD8</i> is upregulated in patient prostate tumors.....	139
Figure 58. Correlation of <i>FZD8</i> and <i>WNT11</i> with prostate cancer relapse.....	140
Figure 59. <i>FZD8</i> and <i>WNT11</i> expression and disease free status. ....	141
Figure 60. FZD8 and Wnt-11 expression are increased in prostate cancer. ....	141
Figure 61. FZD8 and Wnt-11 are expressed in disseminated tumor cells.....	142
Figure 62. Both FZD8 and Wnt-11 expression are increased in tumor epithelia and reduced in prostate cancer stroma.....	143
Figure 63. Expression of the major components of the TGF- $\beta$ signaling pathway. ....	145
Figure 65. FZD8 is required for expression of TGF- $\beta$ target genes and TGF- $\beta$ -dependent Smad phosphorylation. ....	147
Figure 68. Effects of TGF- $\beta$ on EMT gene expression .....	150
Figure 69. FZD8 regulates TGF- $\beta$ -dependent expression of EMT-related genes. ....	151
Figure 70. ATF2 is required for TGF- $\beta$ -dependent gene reporter activity .....	152
Figure 71. ATF2 regulates TGF- $\beta$ -dependent expression of EMT-related genes. ....	153
Figure 72. ATF2 does not form a stable complex with Smad3. ....	153
Figure 73. FZD8 associates with TGF- $\beta$ receptors.....	154
Figure 74. FZD8 and TGF $\beta$ RI associate through their extracellular domains. ....	155
Figure 76. Implication of Wnt-11 in FZD8-TGF $\beta$ RI binding.....	157
Figure 77. Proposed model for FZD8 integration of Wnt-11 and TGF- $\beta$ signals. ....	158



## TABLE INDEX

### INTRODUCTION

Table 1. Key changes in Wnt signaling pathways components in prostate cancer. ....	64
--	----

### MATERIALS AND METHODS

Table 2. Characteristics of the prostate cancer cell lines.....	81
Table 3. List of plasmids used in this study. ....	82
Table 4. Table summarizing the siRNAs and dsRNA used in this study. ....	83
Table 5. Protocol for the retro-transcription procedure. ....	84
Table 6. List of primers used in this study. ....	87
Table 7. Protocol for cell transfection. ....	87
Table 8. Protocol for the preparation of acrylamide gels for WB.....	93
Table 9. List of antibodies used in WB assays. ....	93
Table 10. List of antibodies used for immunofluorescence experiments.....	95
Table 11. Clinical features of patients included in the analyzed TMA. ....	96
Table 12. Morphometric parameters used for the analysis of miniaturized 3D culture	100

### RESULTS

Table 13. Wnt receptor Ct values in prostate cancer cell lines used for normalization. .....	106
Table 14. Summary of Wnt receptor genes and <i>WNT11</i> expression in prostate cancer. .....	108
Table 15. Profiling of Wnt receptors genes in prostate tumors. ....	110
Table 16. <i>FZD4</i> , <i>FZD8</i> and <i>PTK7</i> expression in prostate cancer datasets. ....	111
Table 17. Quantification of Wnt-11 and FZD receptors colocalization. ....	113
Table 18. Correlation analysis of FZD8 and Wnt-11 protein expression in normal and cancer.....	142
Table 19. Correlation analysis of FZD8 and Wnt-11.....	143
Table 20. Statistical analysis of FZD8 and Wnt-11 expression in TMAs.....	144



## ABBREVIATIONS

<b>ADT:</b> Androgen deprivation therapy	<b>DBD:</b> DNA-binding domain
<b>ANOVA:</b> One-way analysis of variance	<b>DEP:</b> Disheveled, Egl-10 and Pleckstrin
<b>AP-1:</b> Activator protein-1	<b>DHEA:</b> Dehydroepiandrosterone
<b>APC:</b> Adenomatous polyposis coli	<b>DHEA-S:</b> Dehydroepiandrosterone sulphate
<b>APS:</b> Ammonium persulfate	<b>DHT:</b> Dihydrotestosterone
<b>AR:</b> Androgen receptor	<b>DIX:</b> Disheveled and Axin
<b>ARE:</b> Androgen response element	<b>DKK:</b> Dickkopf
<b>AR-Vs:</b> Variants of the AR	<b>DNA:</b> Deoxyribonucleic acid
<b>ATCC:</b> American Type Culture Collection	<b>DRE:</b> Digital rectal examination
<b>BCL9:</b> B-cell CLL/lymphoma 9	<b>dsiRNA:</b> Dicer-substrate small interfering RNA
<b>BCL9L:</b> B-cell CLL/lymphoma 9 like	<b>DVL:</b> Disheveled
<b>BM:</b> Basement membrane	<b>ECD:</b> Extracellular domain
<b>BMP:</b> Bone morphogenetic protein	<b>ECL:</b> Extracellular loop
<b>bp:</b> Base pair	<b>ECM:</b> Extracellular matrix
<b>BPH:</b> Benign prostatic hyperplasia	<b>EDD:</b> Embryo development day
<b>BSA:</b> Bovine serum albumin	<b>EGF:</b> Epidermal growth factor
<b>CAF:</b> Cancer associated fibroblast	<b>EMT:</b> Epithelial to mesenchymal transition
<b>CAM:</b> Chorioallantoic membrane	<b>ER:</b> Endoplasmic reticulum
<b>CaMKII:</b> Calmodulin-dependent kinase II	<b>ERG:</b> Erythroblast transformation-specific
<b>CBP:</b> CREB binding protein	<b>ETS:</b> E-twenty-six
<b>CK1:</b> Casein kinase 1	<b>ETV1:</b> ETS variant 1
<b>cm:</b> Centimeter	<b>Evi:</b> Evenness interrupted
<b>CRD:</b> Cysteine-rich-domain	<b>FBS:</b> Fetal bovine serum
<b>CREB:</b> cAMP response element binding protein	<b>FGF:</b> Fibroblast growth factor
<b>CRPC:</b> Castration resistant prostate cancer	<b>FKBP12:</b> FK506 binding protein-12
<b>CSS:</b> Charcoal stripped serum	<b>FSH:</b> Follicle-stimulating hormone
<b>CZ:</b> Central zone	<b>FZD:</b> Frizzled
<b>DAB:</b> 3,3'-diaminobenzidine	<b>GDF:</b> Growth and differentiation factor

<b>GPC:</b> Glypican	<b>min:</b> Minute
<b>GPCR:</b> G protein-coupled receptor	<b>MIS:</b> Mullerian inhibiting substance
<b>GSK3:</b> Glycogen synthase kinase-3	<b>mL:</b> Milliliter
<b>GTPase:</b> Guanosine triphosphate hydrolase	<b>mm:</b> Millimeter
<b>h:</b> Hour	<b>mM:</b> millimolar
<b>HBS:</b> HEPES buffered solution	<b>MMP:</b> Matrix metalloproteinase
<b>HGF:</b> Hepatocyte growth factor	<b>MMTV:</b> Mouse mammary tumor virus
<b>HGPIN:</b> High grade prostate intraepithelial neoplasia	<b>mRNA:</b> Messenger RNA
<b>HNSCC:</b> Head and neck squamous cell carcinoma	<b>MUSK:</b> Muscle skeletal receptor Tyr kinase
<b>HSP:</b> Heat shock protein	<b>MVB:</b> Multivesicular body
<b>ICD:</b> Intracellular domain	<b>NED:</b> Neuroendocrine-like differentiation
<b>ICL:</b> Intracellular loops	<b>NFAT:</b> Nuclear factor of activated T-cells
<b>IGF:</b> Insulin-like growth factor	<b>ng:</b> Nanogram
<b>IL:</b> Interleukin	<b>NLS:</b> Nuclear localization signal
<b>IP:</b> Immunoprecipitation	<b>nm:</b> Nanometer
<b>IUPHAR:</b> International Union of Basic and Clinical Pharmacology	<b>nM:</b> Nanomolar
<b>JNK:</b> Jun-N-terminal kinase	<b>NSE:</b> Neuron-specific enolase
<b>LAP:</b> Latent associated protein	<b>NTD:</b> N-terminal domain
<b>LATS:</b> Large Tumor Suppressor Kinase	<b>OST:</b> oligosaccharyl transferase complex
<b>LBD:</b> Ligand-binding domain	<b>PAM:</b> Palmitoleic acid motif
<b>LGR:</b> Leucine-rich repeat-containing G protein-coupled receptor	<b>PAP:</b> Prostatic acid phosphatase
<b>LH:</b> Luteinizing hormone	<b>PBS:</b> Phosphate buffered saline
<b>LHRH:</b> Luteinizing hormone-releasing hormone	<b>PCa:</b> Prostate cancer
<b>LRP:</b> Low-density lipoprotein receptor-related protein	<b>PCA3:</b> Prostate cancer gene 3
<b>LUT:</b> Lower urinary tract	<b>PCP:</b> Planar cell polarity
<b>MAPK:</b> Mitogen activated protein kinase	<b>PDZ:</b> Psd-95/Disc large/ZO-1 homologous
<b>MET:</b> Mesenchymal to epithelial transition	<b>PFA:</b> Para-formaldehyde
	<b>PI3K:</b> Phosphoinositide 3-kinase
	<b>PIN:</b> Prostate intraepithelial neoplasia
	<b>PKC:</b> Protein kinase C
	<b>PSA:</b> Prostate-specific antigen

<b>PSAP:</b> Prostate-specific acid phosphatase	<b>TGF-β:</b> Transforming growth factor beta
<b>PTK7:</b> Protein tyrosine kinase 7	<b>TGFβRI:</b> TGF-β receptor 1
<b>PZ:</b> Peripheral zone	<b>TGFβRII:</b> TGF-β receptor 2
<b>RIPA:</b> Radioimmunoprecipitation assay	<b>TGN:</b> Trans-Golgi network
<b>RNA:</b> Ribonucleic acid	<b>TMA:</b> Tissue microarray
<b>RNF43:</b> Ring Finger Protein 43	<b>TMD:</b> Trans-membrane domain
<b>ROCK:</b> Rho-associated kinase	<b>TME:</b> Tumor microenvironment
<b>ROR:</b> Receptor tyrosine kinase-like orphan receptor	<b>TMPRSS2:</b> Transmembrane protease serine 2
<b>RSPO:</b> R-spondin	<b>TNM:</b> Tumor-node-metastasis
<b>RT:</b> Room temperature	<b>TZ:</b> Transitional zone
<b>RTK:</b> Receptor tyrosine kinase	<b>UGE:</b> urogenital sinus epithelium
<b>RYK:</b> Receptor-like tyrosine kinase	<b>UGM:</b> Urogenital sinus mesenchyme
<b>SD:</b> Standard deviation	<b>UGS:</b> Urogenital sinus
<b>SDS:</b> Sodium dodecyl sulfate	<b>VANGL:</b> Vang-like protein
<b>sec:</b> Second	<b>VEGF:</b> Vascular endothelial growth factor
<b>sFRP:</b> Secreted Frizzled-Related Protein	<b>WB:</b> Western blotting
<b>siRNA:</b> Short interfering RNA	<b>Wg:</b> Wingless
<b>SMO:</b> Smoothened	<b>WHO:</b> World Health Organization
<b>SNP:</b> Single nucleotide polymorphism	<b>WIF:</b> Wnt inhibitory factor
<b>TAZ:</b> Transcriptional co-activator with PDZ-binding motif	<b>Wis:</b> Wntless
<b>TBS:</b> Tris buffered saline	<b>YAP:</b> Yes-associated protein
<b>TBST:</b> Tris buffered saline with Tween	<b>ZNRF3:</b> Zinc and Ring Finger 3
<b>TCF/LEF:</b> T-cell factor/lymphoid enhancer factor	<b>µg:</b> Microgram
<b>TEAD:</b> TEA domain family transcription factor	<b>µL:</b> Microliter
<b>TF:</b> Transcription factor	<b>µM:</b> Micromolar
	<b>2D:</b> Two-dimensional
	<b>3D:</b> Three-dimensional



## SUMMARY

Wnt-11 is a noncanonical Wnt ligand which is found upregulated in prostate cancer cell lines as well as in prostate tumors. It promotes cancer cell migration and invasion which suggest it has a role in prostate cancer progression and metastasis. Wnt ligands require binding to Frizzled (FZD) family of receptors in order to signal and therefore, this interaction provides an opportunity to inhibit Wnt signaling. However, the receptors that mediate Wnt-11 signaling in prostate cancer remain unknown. In this thesis, I provide evidence that FZD8 is a major Wnt-11 receptor in prostate cancer that integrates Wnt-11 and TGF- $\beta$  signals to promote cell invasion and epithelial to mesenchymal transition (EMT) and consequently, mediates prostate cancer progression. *FZD8* mRNA was upregulated in multiple prostate cancer datasets as well as in metastatic prostate cancer cell lines. Moreover, analysis of patient samples revealed increased levels of FZD8 in prostate cancer compared to benign tissues, correlating with increased expression of Wnt-11. In metastatic prostate cancer cells, FZD8 co-localized and co-immunoprecipitated with Wnt-11 and mediated Wnt-11 activation of ATF2 and AP-1 noncanonical signaling. Functionally, *FZD8* silencing reduced prostate cancer cell migration and invasion as well as three-dimensional (3D) organotypic cell invasion and expression of EMT-related genes. In addition, FZD8 was required for tumor growth in the chorioallantoic membrane (CAM) *in vivo* model. Finally, inhibition of TGF- $\beta$ /Smad-dependent signaling was observed when *FZD8* was silenced in prostate cancer cells and FZD8 was found to be required for TGF- $\beta$ -dependent cell invasion and expression of EMT genes. Surprisingly, FZD8 formed a TGF- $\beta$ -regulated complex with TGF- $\beta$  receptors that is mediated by the extracellular domains of both FZD8 and TGF $\beta$ RI. Together, these observations are consistent to a model in which FZD8 integrates Wnt and TGF- $\beta$  signaling pathways to promote cell migration, invasion and EMT, leading to prostate cancer metastasis. Consequently, FZD8 may constitute a useful therapeutic target in metastatic prostate cancer as its inhibition may block aberrant activation of both Wnt and TGF- $\beta$  signaling pathways.





## RESUMEN

Wnt-11 es un miembro no canónico de la familia de Wnt que se observa altamente expresado en líneas celulares de cáncer de próstata, así como en tumores de próstata. Wnt-11 promueve la migración y la invasión celular lo que sugiere que tiene un papel en la progresión y la metástasis del cáncer de próstata. Las proteínas Wnt necesitan unirse a la familia de receptores Frizzled (FZD) para activar la señalización de forma que esta interacción representa una oportunidad para inhibir la señalización de Wnt. Sin embargo, se desconocen los receptores que median la señalización de Wnt-11 en cáncer de próstata. En esta tesis, proporciono evidencia de que FZD8 es el principal receptor de Wnt-11 en cáncer de próstata y de que éste integra las señales de Wnt-11 y TGF- $\beta$  con el fin de promover la invasión celular y la transición epitelio-mesénquima (EMT) y así mediar la progresión del cáncer de próstata. La expresión de FZD8 a nivel de RNA mensajero se vio incrementada en múltiples bases de datos de cáncer de próstata, así como en líneas celulares de cáncer de próstata metastático. Asimismo, el análisis de muestras de pacientes mostró niveles aumentados de FZD8 en tejidos de próstata cancerosos comparados con tejido sanos de próstata, que también se relacionaron con niveles elevados de Wnt-11. En líneas celulares de cáncer de próstata metastático, FZD8 co-localizó y co-inmunoprecipitó con Wnt-11 además de mediar la activación que Wnt-11 produce en la señalización no-canónica de ATF2 y AP-1. Funcionalmente, el silenciamiento de *FZD8* redujo la migración y la invasión de las células cancerosas, así como la invasión en cultivo organotípico tridimensional (3D) y la expresión de genes implicados en EMT. Además, FZD8 resultó necesario para el crecimiento tumoral en el modelo *in vivo* de la membrana corioalantoidea (CAM). Finalmente, se observó una inhibición de la ruta de TGF- $\beta$ /Smad cuando *FZD8* se silenciaba en células de cáncer de próstata y FZD8 resultó ser necesario para la invasión celular dependiente de TGF- $\beta$  así como para la expresión de genes de EMT. Inesperadamente, FZD8 resultó formar un complejo regulado por TGF- $\beta$  con los receptores de TGF- $\beta$ , el cual está mediado por los dominios extracelulares de FZD8 y TGF $\beta$ RI. Todos estos resultados son consistentes con un modelo en el que FZD8 integra las rutas de señalización de Wnt y TGF- $\beta$  para promover la migración, invasión celular y el proceso de EMT, dando lugar a la metástasis del cáncer de próstata. Consecuentemente, FZD8 puede representar una óptima diana terapéutica en el cáncer de próstata metastático ya que su inhibición puede bloquear la activación aberrante de ambas rutas, Wnt y TGF- $\beta$ .

 **RESUMEN: VERSIÓN EXTENDIDA..... 205**





---

# INTRODUCTION

---



## 1. The human prostate

### 1.1 Structure and function of the human prostate gland

The human prostate is an exocrine gland with the size of a walnut and a weight about 10-20g that is part of the male reproductive system. The word “prostate” is taken from the Ancient Greek προστάτης, prostates, literally "one who stands before" which describes the position of the prostate gland being located below the bladder and the seminal vesicle and above the muscles of the pelvic floor. The rectum is behind the prostate which enables a clinician to feel the prostate in a rectal examination (Bhavsar & Verma 2014; PubMed Health 2016) (**Fig. 1**).

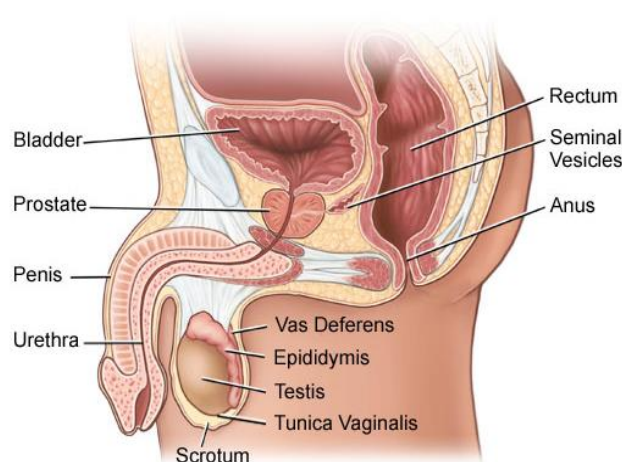


**Figure 1. Human prostate anatomy.** The illustration shows the location of the adult prostate and associated tissues within the male reproductive system. Taken from Stanford Children’s Health.

The main function of the prostate is the secretion of a slightly alkaline fluid, milky or white in appearance, which is mixed in the urethra together with sperm cells from the testicles, fluid from the seminal vesicle and the secretions released by the bulbourethral gland to constitute the male semen (Kumar & Majumder 1995; Bhavsar & Verma 2014). In humans, prostate secretions usually constitute approximately 30% of the semen volume and they are mainly composed of simple sugars with a protein content less than 1%, including proteolytic enzymes, prostatic acid phosphatase (PAP), beta-microseminoprotein, spermin, cholesterol and prostate-specific antigen (PSA) among others (Kumar & Majumder 1995). Zinc is also present in prostate secretions with a concentration 500–1,000 times the concentration in blood, working as an antibacterial agent (Kumar & Majumder 1995). The prostatic secretion is important for the proper functioning and motility of the sperm cells, and therefore also for fertility in men (PubMed Health 2016).

Apart from its secretory functions, the muscles of the prostate participate in the control of urine output from the bladder and ensure that the semen is forcefully pressed into the urethra and then expelled out during ejaculation (Kumar & Majumder 1995; Bhavsar & Verma 2014; PubMed Health 2016).

The microanatomy of the prostate reveals glandular and stromal components which are contained within a pseudocapsule (Bhavsar & Verma 2014). Histologically, the prostate comprises ducts and acini (**Fig. 2A**) containing secretory, basal and endocrine-paracrine cells (**Fig. 2B**). Secretory cells are the predominant cell type within the prostate gland which are mainly tall columnar cells, although there are areas of low cuboidal or squamous epithelium. At the molecular level, luminal cells are characterized by their expression of androgen receptor, as well as cytokeratins 8 and 18 and the cell surface marker CD57 (Abate-Shen & Shen 2000). These secretory cells, which also express prostatic specific antigen (PSA) and prostate-specific acid phosphatase (PSAP), are separated from the basal lamina and prostatic stroma by a layer of basal cells. These cells are generally flattened and they represent the stem cell population which gives rise to mature secretory cells (Kirby et al. 2004; American Urological Association 2017). Basal cells express cytokeratins 5 and 14 and CD44 as well as low levels of androgen receptor (although this is controversial), but do not produce prostatic secretory proteins (Abate-Shen & Shen 2000). In all zones of the prostate, the epithelium contains a small population of endocrine-paracrine cells which are androgen independent cells and contain neuron-specific enolase (NSE). However, their precise function remains unknown, although they are supposed to have a paracrine function supporting the growth of luminal cells and regulating the secretory process (Abate-Shen & Shen 2000; Kirby et al. 2004).

Structurally, although the prostate has an unlobulated appearance due to the presence of the pseudocapsule, this fibroelastic layer gives rise to septa which subdivide the prostate into different areas (Kumar & Majumder 1995). In 1912, Lowsley analyzed the anatomy of the fetal prostate and identified five lobes: the anterior, posterior, lateral (two), and medial, with the medial and the two lateral lobes the most prominent (Lowsley 1912; Kumar & Majumder 1995; Kirby et al. 2004). These terms, which were based on fetal studies and did not explain completely the morphology of the adult prostate, were traditionally used to describe prostate anatomy (Selman 2011). Nevertheless, later studies developed by McNeal using prostates obtained at autopsy divided the prostate gland into four different zones (McNeal 1981; Selman 2011; Reeves et al. 2016). A central zone (CZ), which surrounds the ejaculatory ducts and accounts approximately

for 2.5% of prostate cancers that tend to be more aggressive; a peripheral zone (PZ), surrounding the distal urethra, where 70-80% of prostate tumors originate; a transitional zone (TZ), which surrounds the proximal urethra, where the benign prostate hyperplasia (BPH) and 10-20% of cancers are initiated and a periurethral gland region. Apart from these glandular regions, the prostate also contains a fibromuscular zone which is also defined as a nonglandular region and accounts for one-third of the bulk of the prostate (Selman 2011; Reeves et al. 2016; Aaron et al. 2016) (**Fig. 2C**).

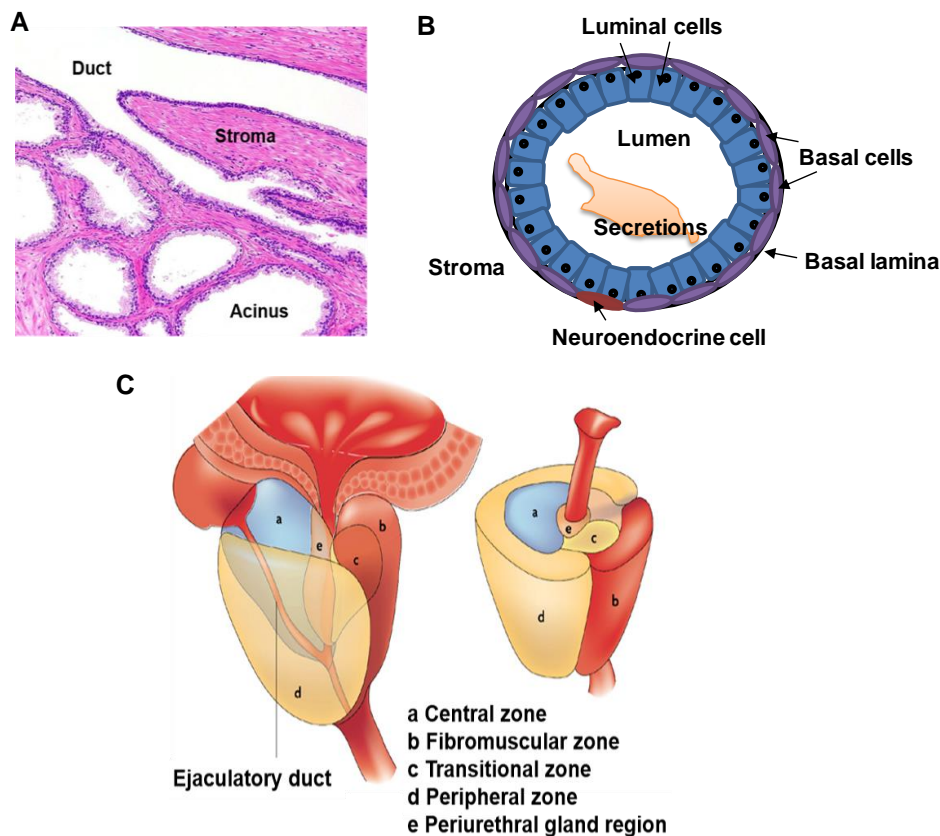


**Figure 2. Histology and structure of the human prostate gland.** (A) Microanatomy of prostate tissue by Hematoxylin & Eosin staining. Taken from American Urological Association. (B) Illustration showing the different cellular types in a histological section of a human prostate duct. Adapted from Abate-Shen & Shen 2000. (C) The prostatic zones described by McNeal (1983). Taken from Reeves et al. 2016.

The proper structure and function of the prostate is dependent on the presence of testicular hormones, mainly androgens (dihydrotestosterone (DHT) and testosterone) (Kumar & Majumder 1995; Aaron et al. 2016). In fact, different studies have shown that withdrawal of this hormonal support results in drastic metabolic changes including loss of secretory function and an accelerated rate of tissue involution in the prostate. Moreover, alterations at the subcellular levels in the nucleus, endoplasmic reticulum (ER), Golgi and ribosomes which result in decrease in deoxyribonucleic acid (DNA),



ribonucleic acid (RNA) and protein synthesis have also been described when removing androgens (Kumar & Majumder 1995).

## 1.2 Prostate development

In humans, development of the prostate is absolutely dependent on androgenic stimulation by the biologically active androgen, 5 $\alpha$ -DHT, which is produced by the local reduction of testosterone (produced in the testes) by the enzyme 5 $\alpha$ -reductase. However, other hormones such as estrogen also are involved in prostate development (Hayward & Cunha 2000; Aaron et al. 2016).

In humans, the cloaca functions as the combined excretory tract until 5 weeks post conception, which is then divided by the urorectal septum into urinary and digestive tract by 6 weeks. The ventral urinary compartment is called the urogenital sinus (UGS), which differentiates and becomes sexually dimorphic in response to androgens. Androgens begin to be excreted by Leydig cells in male gonads at around 8 weeks of gestation. By 10 weeks, the initial event in morphogenesis of the prostate is the outgrowth of solid epithelial buds from the urogenital sinus epithelium (UGE) into the surrounding urogenital sinus mesenchyme (UGM) (Meeks & Schaeffer 2011; Aaron et al. 2016). Androgens binds androgen receptor (AR) in the urogenital sinus mesenchyme (UGM) stimulating stromal cells to secrete other factors that then act on the epithelial cells and thereby, induce the epithelial budding, proliferation, and differentiation to form ductal structures. By 13 weeks, 70 primary ducts are present and have been differentiated into luminal and basal subtypes and exhibit secretory markers (Kirby et al. 2004; Aaron et al. 2016) (**Fig. 3**). Together with epithelial differentiation the UGM proliferates and differentiates into prostatic smooth muscle (which expresses AR) and interfascicular fibroblasts. Importantly, while androgens drive the development and growth of the prostate, they also play a key role in maintaining a growth quiescent adult organ (Aaron et al. 2016).

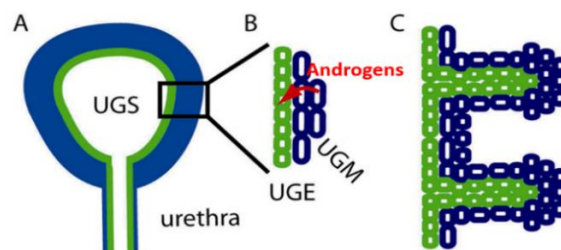


**Figure 3. Schematic representation of phases of prostate development.** A. The prostate develops from the urogenital sinus (UGS) which consists of both epithelium (green) and mesenchyme (blue). B. Androgens engage androgen receptor in the mesenchyme and induce epithelial budding. C. Epithelial buds elongate into solid cords of tissue that eventually canalize into ducts. Adapted from Meeks & Schaeffer 2011.



The human prostate is small in childhood, weighing around 2 g, but it undergoes a phase of exponential growth at puberty, increasing in size to about 20 g. This growth is due to the rise in serum testosterone to adult levels. Then, prostatic weight remains fairly constant until the end of the third decade of life when the mean prostatic weight begins to rise slowly. The human prostate is an extremely slow-growing organ, which is balanced by correspondingly low rates of apoptosis in the normal adult human prostate resulting in a growth-quiescent gland (Hayward & Cunha 2000).

## 2. Cancer

Cancer has been defined as the uncontrolled proliferation of cells that leads to the deregulation of cell homeostasis and the formation of an abnormal mass of cells named tumor. Although more than 100 distinct types of tumors can be found within specific organs, cancer is considered a complex disease involving lot of dynamic changes in the genome (Hanahan & Weinberg 2000). In this regard, oncogenes, tumor suppressors and genomic stability genes have been defined as crucial genes in the tumorigenesis process (Lee & Muller 2010).

During the last decades, strong efforts have been made to characterize common features in the cancer process. Hanahan and Weinberg defined six essential alterations in cell physiology that collectively dictate malignant growth. These alterations include: self-sufficiency in growth signals, insensitivity to growth-inhibitory (antigrowth) signals, evasion of programmed cell death (apoptosis), limitless replicative potential, sustained angiogenesis, and tissue invasion and metastasis (Hanahan & Weinberg 2000). Some years later, reprogramming of energy metabolism and evading immune destruction were also incorporated to the previously described panel of hallmarks, together with two enabling characteristic: genomic instability and mutation as well as tumor promoting inflammation (Hanahan & Weinberg 2011). Moreover, the tumor microenvironment constitutes another dimension of complexity which, together with these hallmarks, is crucial for cancer development and progression (Hanahan & Weinberg 2011; Wang et al. 2017) **(Fig. 4)**.

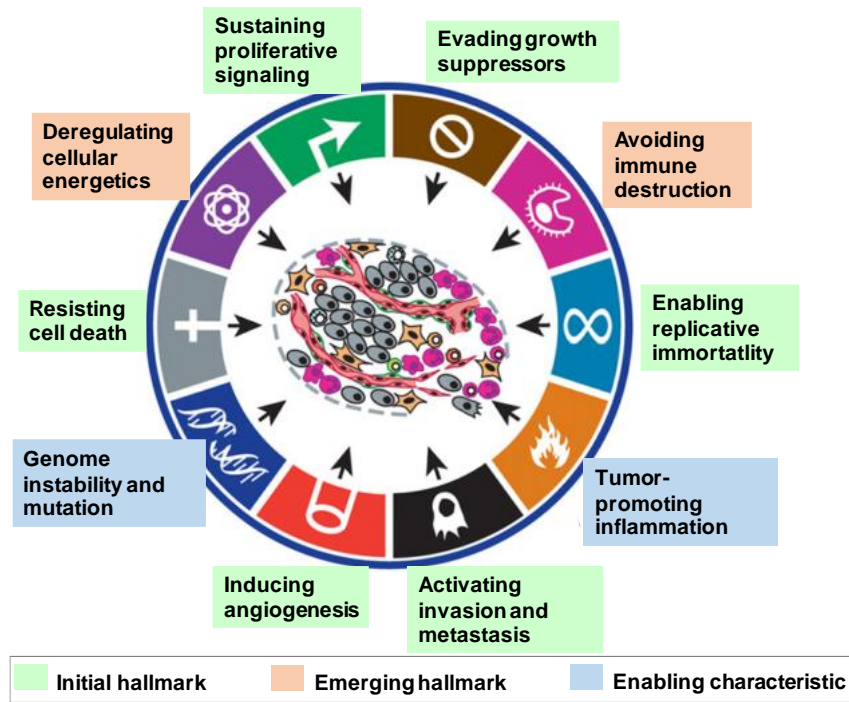


**Figure 4. Hallmarks of cancer.** Diagram showing the acquired capabilities necessary for tumor growth and progression. Green: six initial hallmarks described in 2000 by Hanahan and Weinberg; orange, the emerging hallmarks included in 2011 and blue, the derived enabling characteristic incorporated also in 2011. Adapted from Hanahan & Weinberg 2011.

## 2.1 Epithelial-mesenchymal transition (EMT) in cancer

Epithelial to mesenchymal transition (EMT) is classically defined as a reversible process in which epithelial cells acquire mesenchymal properties by altering their morphology, cellular architecture, adhesion, and migration capacity (Lee et al. 2006). The EMT process was firstly described in 1982 when it was observed that epithelial cells expressed characteristics of migrating mesenchymal cells when cultured in collagen (Greenburg & Hay 1982). Later on, EMT was shown to be involved in embryonic development, wound healing, fibrosis, but importantly, it has also been implicated in cancer progression and metastasis (Thiery 2002). In this regard, EMT has been shown to trigger the dissociation of carcinoma cells from primary carcinomas, which subsequently migrate and disseminate to distant sites. The reverse of the EMT process—mesenchymal-epithelial transition (MET)—is associated with a loss of this migratory capacity, with cells adopting an apico-basal polarization and expressing the junctional complexes that are hallmarks of epithelial tissues. Significantly, it is the MET that is then believed to trigger the cessation of migration, inducing the same cells to proliferate and seed the new tumor giving rise to a metastasis (Nieto et al. 2016; Jolly et al. 2017)

The EMT/MET molecular components have been classified into three groups: inducers, regulators and effectors (Banyard & Bielenberg 2015) (**Fig. 5**).

- a) Inducers: This group includes different growth factors and receptors which initiate the process such as epidermal growth factor (EGF), fibroblast growth factor (FGF), hepatocyte growth factor (HGF), vascular endothelial growth factor (VEGF), insulin-like growth factor (IGF), transforming growth factor beta (TGF- $\beta$ ), Wnt and Notch.
- b) Regulators: Transcription factors (TFs) called EMT-TFs (Nieto et al. 2016) such as Snail, Slug, Twist or Zeb1 and 2 are included in this group. Their expression profiles depend on cell and tissue type and on the degree of progression towards mesenchymal differentiation (Lamouille et al. 2014). In addition to EMT-TFs, multiple miRNAs are thought to regulate EMT, including miR-34 and miR-200 and epigenetic and post-translational regulators (Nieto et al. 2016).
- c) Effectors: The third category is formed by the EMT-associated proteins, which stimulate subsequent changes in cellular shape and invasive capacities. Cadherin switches, such as epithelial-cadherin (E-cadherin) to neural-cadherin (N-cadherin) are classic representative markers of the EMT process, but also other cell junction-related changes, including expression of catenins, claudins and desmocollins or cytoskeletal proteins, such as vimentin and keratins (Banyard & Bielenberg 2015).

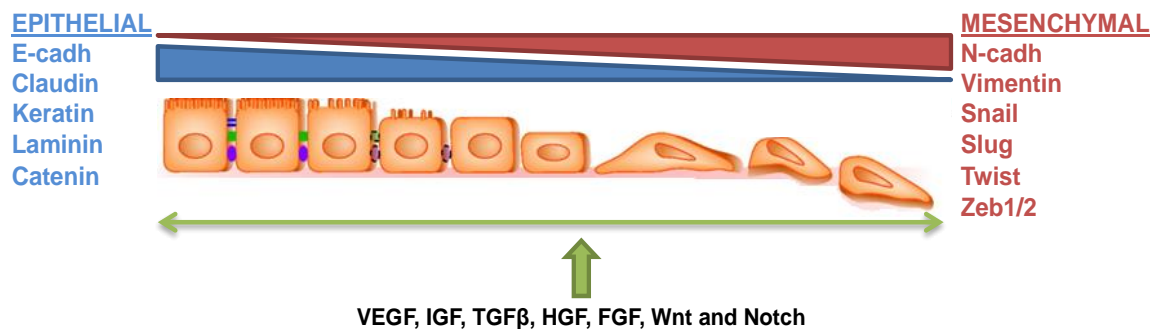


**Figure 5. Classical model of reversible EMT-MET.** Main inducers, regulators and effectors are shown.

Although traditionally EMT has been characterized as a transformation process between two alternative states, mesenchymal or epithelial, recent studies have made the concept evolve to a more dynamic and flexible process. In this regard, EMT is now considered a process characterized by the presence of plasticity and transitional states in which cells are no longer thought to oscillate between the full epithelial and full

mesenchymal states, but rather, they move through a spectrum of intermediary phases, being able to undergo a partial EMT (**Fig. 6**) (Nieto et al. 2016).

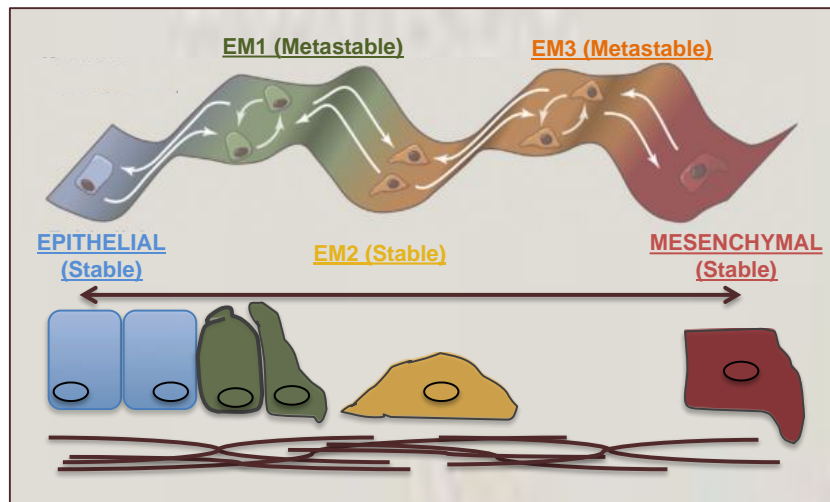


**Figure 6. Plasticity through the transitional stages in EMT-MET.** Intermediate EMT states have been defined having different stability. Adapted from Nieto et al. 2016.

Recent studies that categorized cells into E (epithelial), M (mesenchymal), and hybrid E/M, instead of just E and M, have proposed that tumor-initiating potential might be maximum when cells are in a hybrid E/M state (Jolly et al. 2017). However, considering the heterogeneity and unstable genetic background of tumor cells, it is common that cellular plasticity is often accompanied by a change in a varying cohort of EMT markers, which can differ among tumor cell types and EMT pathways (Banyard & Bielenberg 2015). Consequently, the presence of a partial or a full EMT may vary with the cancer type, making it necessary to investigate the contribution of these phenotypic transitions to invasion, dissemination and metastasis (Banyard & Bielenberg 2015; Jolly et al. 2017).

### 3. Prostate cancer


#### 3.1 Epidemiology and etiology

In 2017, prostate cancer (PCa) represents the most frequently diagnosed cancer in men and the third most common cause of cancer death in men in developed regions (**Fig. 7A**). An estimated 1.1 million men worldwide were diagnosed with prostate cancer in 2012 and 307,000 men were estimated to die in the same year (Siegel et al. 2017; Mottet et al. 2016).

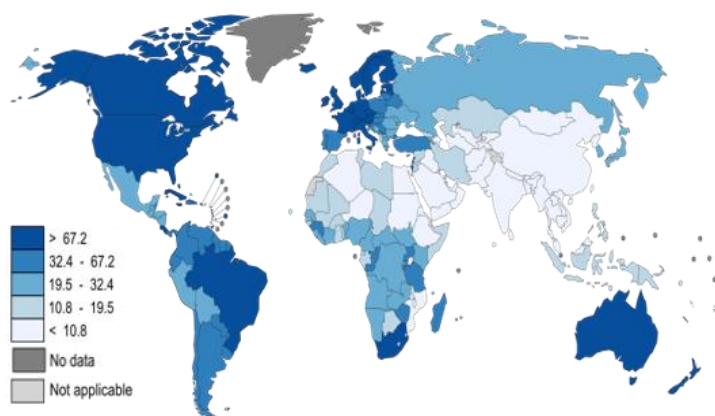
Prostate cancer is a disease of increasing significance worldwide with almost 70% of the cases appearing in more developed areas. Among these regions, incidence rates are higher in Australia/New Zealand and North America and in western and northern Europe. They are also relatively high in certain less developed regions such as the Caribbean, South Africa and South America, and remain low in Asian populations (Globocan 2012) (**Fig. 7B**). This wide variation in international PCa incidence rates is in part due to the substantial differences worldwide in the diagnosis of latent cancers through PSA testing of asymptomatic individuals, as well as during prostate surgery (Center et al. 2012).

Although incidence rates seem to be different worldwide, factors determining the risk of developing PCa remain unclear. Aside from age and ethnicity, the only established risk factor for prostate cancer is a family history of the disease being about twice the risk for first-degree relatives of men with prostate cancer than for men in the general population (Attard et al. 2016). Genetic factors are also considered important determinants of the variation in risk of PCa, since higher incidence in African Americans as well as a 50% higher risk in monozygotic twins than in dizygotic twins has been reported. In fact, several genetic studies have identified co-segregation of the *HOXB13* genetic region, 77 single nucleotide polymorphisms (SNPs) (including one in the vicinity of the oncogene *C-MYC*) as well as rare mutations in genes such as *BRCA2*, *BRCA1*, *MMR*, *NBS1* and *CHEK2* to be associated to prostate cancer risk (Attard et al. 2016) (**Fig. 7C**). Currently, exogenous factors such as diet or alcohol consumption have been studied as factors involved in the progression of the disease (Mottet et al. 2016).

A

Estimated New Cases			Males	Estimated Death		
Prostate	161,360	19%		Lung and bronchus	84,590	27%
Lung and bronchus	116,990	14%		Colon and rectum	27,150	9%
Colon and rectum	71,420	9%		Prostate	26,730	8%
Urinary bladder	60,490	7%		Pancreas	22,300	7%
Melanoma of the skin	52,170	6%		Liver and intrahepatic bile duct	19,610	6%
Kidney and renal pelvis	40,610	5%		Leukemia	14,300	4%
Non-Hodgkin lymphoma	40,080	5%		Esophagus	12,720	4%
Leukemia	36,290	4%		Urinary bladder	12,240	4%
Oral cavity and pharynx	35,720	4%		Non-Hodgkin lymphoma	11,450	4%
Liver and intrahepatic bile duct	29,200	3%		Brain and other nervous system	9,620	3%
All sites	836,150	100%	All sites	318,420	100%	

B



C

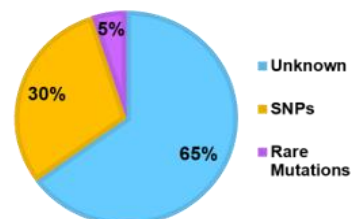


**Figure 7. Prostate cancer epidemiology.** (A) Estimated new cases and estimated dead in men per year in the United States in 2017. Adapted from Siegel, 2017. (B) Prostate cancer incidence worldwide. Taken from Globocan. (C) Susceptibility variants for excess familial risk of prostate cancer. Adapted from Attard, 2016.

### 3.2 Histological variants of prostate cancer

Prostate cancer displays significant phenotypic heterogeneity but it has been histologically divided into different types (Shen & Abate-Shen 2010; Humphrey et al. 2016) (**Fig. 8**):

a) Benign prostatic hyperplasia (BPH) is a non-cancerous type of growth of the prostate that consists of histopathological abnormalities of the prostatic epithelium primarily found in the transitional zone, which typically include expansion of the basal layer and stromal hyperproliferation (Abate-Shen & Shen 2000) (**Fig. 8**). In BPH, the prostate grows larger and squeezes the urethra, preventing the normal flow of urine and causing lower urinary tract symptoms (LUTs). BPH is a very common problem, being present in more than 50% of men aged over 60 years. For some men the symptoms may

be severe enough to need treatment or surgery (Humphrey et al. 2016; Thorpe & Neal 2003).

b) Prostate intraepithelial neoplasia (PIN) is considered the primary precursor of human prostate cancer. It is a specific type of lesion localized in the peripheral zone (Abate-Shen & Shen 2000), which generally is characterized by the appearance of luminal epithelial hyperplasia, reduction in basal cells, enlargement of nuclei and nucleoli, cytoplasmic hyperchromasia, and nuclear atypia (Shen & Abate-Shen 2010) **(Fig. 8)**. PIN can usually progress to high-grade PIN (HGPIN), a preneoplastic lesion which displays an important elevation of cellular proliferation markers and commonly progresses to prostate carcinoma (Abate-Shen & Shen 2000; Shen & Abate-Shen 2010).

c) Acinar adenocarcinoma represents 90% of prostate tumors **(Fig. 6)**. They originate in the secretory epithelial cells and typically are slow growing tumors. Different variants of acinar adenocarcinoma were defined in 2016 by the World Health Organization (WHO), including atrophic, pseudohyperplastic, microcystic, foamy gland, mucinous (colloid), signet ring-like cell, pleomorphic giant cell and sarcomatoid (Humphrey et al. 2016). This last type of cancer is comprised of a mixture of both epithelial and mesenchymal components. It is extremely rare and accounts for less than 0.1% of primary prostate cancer but generally occurs in younger men and is associated with poorer prognosis (Humphrey 2012; Humphrey et al. 2016).

d) Non-acinar prostate carcinoma accounts for 5-10% of prostate tumors and include different subtypes:

- Ductal adenocarcinoma: this is the most common histological variant of non-acinar prostatic carcinoma with an incidence of 3.2% of all prostatic carcinomas. It originates in the primary and secondary prostatic ducts and is considered to be more aggressive than acinar adenocarcinoma (Humphrey 2012; Humphrey et al. 2016).

- Transitional Cell carcinoma of the prostate is a carcinoma of urothelial origin that affects the urothelium normally lining the intraprostatic ducts (Angulo et al. 2010; Humphrey 2012; Humphrey et al. 2016).

- Squamous cell carcinoma: this type of prostate tumor has an incidence lower than 1% (Humphrey 2012). It is typically described as an aggressive cancer, with a median post-diagnosis survival of 14 months. Squamous cell carcinoma develops as a result of adverse stimuli affecting columnar cells, causing them to lose their ability to produce PSA and prostatic acid phosphatase (PAP) (Malik et al. 2011).

- Basal cell carcinoma usually arises in the transitional zone. Malignant tumors composed of basal cells have been designated as “adenoid cystic carcinoma” or



“adenoid basal cell tumor” when they share histologic features of salivary gland tumors, and more generically as “basaloid carcinoma” or “basal cell carcinoma” when they lack such similarity (Ali & Epstein 2007).

- Neuroendocrine tumors: this group includes adenocarcinoma with neuroendocrine differentiation, well-differentiated neuroendocrine tumors, large cell neuroendocrine carcinoma and small-cell neuroendocrine carcinoma, the last one being the most common neuroendocrine tumor in the prostate (Humphrey et al. 2016). They are extremely aggressive and often associated with disseminated disease being incidence estimates range from 0.3% to 1% of all prostatic carcinomas. They are significantly more common in men with castration resistant prostate cancer (CRPC) after androgen deprivation therapy (ADT) (Nadal et al. 2014). ERG (erythroblast transformation-specific) gene rearrangements are common in small-cell carcinoma of the prostate which can be helpful for diagnosis of this kind of prostate carcinomas (Humphrey 2012).

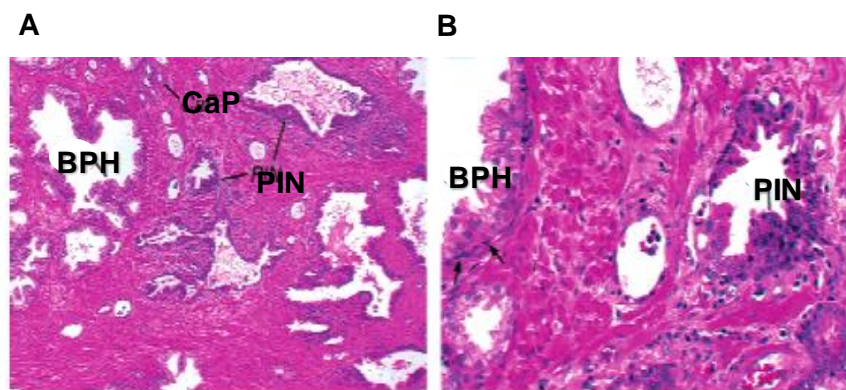


**Figure 8. Histology of prostate tissue. (A)** Section showing the heterogeneity of prostate tissue where BPH, PIN and PCa can be found. **(B)** Higher resolution section from A where BPH and PIN are shown. Arrows show basal cells present in BPH and absent in the region of PIN. Adapted from Abate-Shen & Shen 2000.

### 3.3 Prostate cancer initiation and progression

Prostate cancer initiates with prostatic intraepithelial neoplasia (PIN) that usually progress to high-grade PIN (HGPIN) and later to prostate carcinoma (Abate-Shen & Shen 2000; Shen & Abate-Shen 2010). Importantly, PIN lesions are distinguished from benign prostatic hyperplasia (BPH), which is not considered the precursor state for prostate cancer. After PIN, the progressive accumulation of further genetic alterations leads to more aggressive and malignant lesions, characterized by disruption of the basement membrane and invasion of the surrounding stroma, leading to an invasive carcinoma which can stay confined in the prostate or metastasize to different organs (Abate-Shen & Shen 2000; Shen & Abate-Shen 2010) **(Fig. 9)**.



At the molecular level, different parameters define prostate cancer initiation and progression, including characteristic patterns of chromosome abnormalities in prostate carcinoma that are indicative of stages of prostate cancer progression. Particularly, consistent allelic loss reflects the reduction or loss-of-function of putative tumor suppressor genes in prostate cancer, such as losses of heterozygosity at chromosomes 8p, 10q, 13q, and 17p, 6q, 7q, 16q, and 18q but also gains at chromosomes 8q and 7. Several reasonable candidate genes, including *Rb*, *P53*, *PTEN*, and *NKX3.1*, have been associated to these chromosome abnormalities during prostate cancer initiation and progression (Abate-Shen & Shen 2000) (**Fig. 9**).

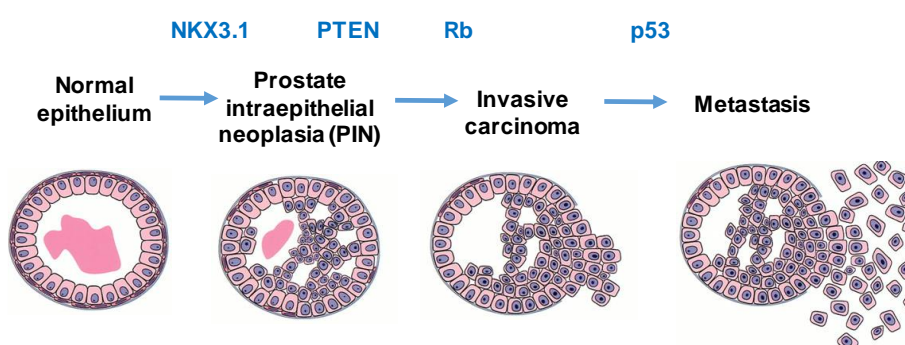


**Figure 9. Prostate cancer initiation and progression.** Different stages of prostate cancer are shown together with the most frequent molecular events associated with each stage. Adapted from Abate-Shen & Shen 2000.

### 3.4 Diagnosis

In the late 1960s and early 1970s, the absence of an efficient method to diagnose prostate cancer prompted many researchers to search for tumor-specific antigens that might be useful as biomarkers or targets for cancer therapy.

The discovery of prostate specific antigen (PSA), a kallikrein-related serine protease, was surrounded by high controversy, owing to its discovery in prostate tissue and semen by different scientists who gave it different names (Rao et al. 2008; Catalona 2014). Rubin Flocks in 1960 firstly identified “species-specific prostate antigens” and in 1966, Mitsuwo Hara reported a protein which he called “gamma-seminoprotein”. Tien Shun Li, Carl Beling and Richard Ablin were all involved in the discovery of PSA identifying different prostate antigens which later were shown to have similar sequences to PSA. In 1979, T. Ming Chu and his research group, most notably Ming C. Wang, purified and characterized PSA and suggested its potential clinical applications as a biomarker for prostate cancer (Rao et al. 2008; Catalona 2014). A later study analyzing 2200 serum samples from 699 patients, 378 of whom had prostate cancer, aimed to determine the

use of PSA as a tumor marker (Stamey et al. 1987). In fact, they showed that levels of PSA in the serum of patients correlated with the stage of prostate cancer as well as with the estimated volume of the tumor. Moreover, this study also showed that PSA reached undetectable levels in the serum after radical prostatectomy, which suggested PSA could be a useful marker to monitor the response of prostate cancer to radiation therapy and to detect residual or recurrent disease (Rao et al. 2008; Catalona 2014). Nowadays in many developed countries, men older than 50 years old are systematically examined through the analysis of PSA levels and digital rectal examination (DRE) (Mottet et al. 2016). There is no specific normal or abnormal level of PSA in the blood because PSA levels are not only affected by PCa but also by prostatitis and BPH. However, PSA levels above 4.0 ng/mL are considered as abnormal (NIH 2016; Mottet et al. 2016). In these cases, other tests, such as for Prostate Cancer gene 3 (PCA3), a prostate specific marker highly expressed by prostate cancer cells and detected in urine, are combined with PSA and DRE for prostate cancer diagnosis in order to avoid over-diagnosis and over-treatment in screening of PCa (Mottet et al. 2016).

After initial screening, when DRE and PSA levels are suspicious, the diagnosis is confirmed by histopathological examination of a biopsy and may be supplemented with bone scanning and computed tomography. The classification of the diagnosed tumor is established based on the tumor-node-metastasis (TNM) system and the Gleason criteria (Mottet et al. 2016) and specific treatments are applied based on this classification.

### 3.5 Classification and staging system

Strong efforts have been made to stratify prostate tumors into groups that could combine patients with similar clinical outcome. Two different criteria have been extensively used:

a) **Tumor stage:** this system uses the size and extension of the tumor (T), the number of nearby lymph nodes that the tumor has (N) as well as the presence of metastasis (M) (Schrlsder et al. 1992) to classify prostate tumors in different stages and sub-stages (**Fig. 10**).

	Stage	Substage	Definition	
T: Primary tumor	TX		Not possible to assess tumour	
	T0		Not evidence of tumour	
	T1	T1		
		T1a		Tumour finding in $\leq 5\%$ of tissue resected
		T1b		Tumour finding in $> 5\%$ of tissue resected
		T1c		Tumour identified by biopsy
	T2	T2		Tumour confined within the prostate
		T2a		Tumour involves one half or one lobe
		T2b		Tumour involves $>$ one half/one lobe but not two lobes
	T3	T2c		Tumour involves two lobes
T3			Tumour extends through the prostatic capsule	
T4	T3a		Invasion to the bladder neck	
	T3b		Invasion of seminal vesicle(s)	
	T4		Tumour invades sphincter, rectum, levator muscles or pelvic wall	
N: Regional lymph nodes	NX		Not possible to assess lymph node	
	N0		No lymph node metastasis	
	N1		Lymph node metastasis	
M: Distant metastasis	MX		Not possible to assess metastasis	
	M0		No metastasis	
	M1	M1		Metastasis
		M1a		Non-regional lymph nodes
		M1b		Bone
M1c		Other sites		

**Figure 10. Classification of prostate tumors based on stage system. TNM system.** Adapted from Mottet et al. 2016.

b) **Tumor grade:** this criterion classifies tumors attending to their prognosis, which is evaluated upon histological examination. Since most of the tumors typically have two histologic patterns, a score (Gleason score) (**Fig. 11**) was created in 1966 that added the two most common grade patterns in a tumor, with scores ranging from 2 to 10, the higher score having the greater risk (Gleason 1992; Harnden et al. 2007). In 2013, a study from Johns Hopkins Hospital and then validated in a multi-institutional study, includes five distinct Grade Groups based on the modified Gleason score groups. Grade Group 1 = Gleason score  $\leq 6$ , Grade Group 2 = Gleason score  $3 + 4 = 7$ , Grade Group 3 = Gleason score  $4 + 3 = 7$ , Grade Group 4 = Gleason score  $4 + 4 = 8$ , Grade Group 5 = Gleason scores 9 and 10. As this new grading system is simpler and more accurately reflects prostate cancer biology, it is recommended by the World Health Organization (WHO) to be used in conjunction with Gleason grading (Gordetsky & Epstein 2016).

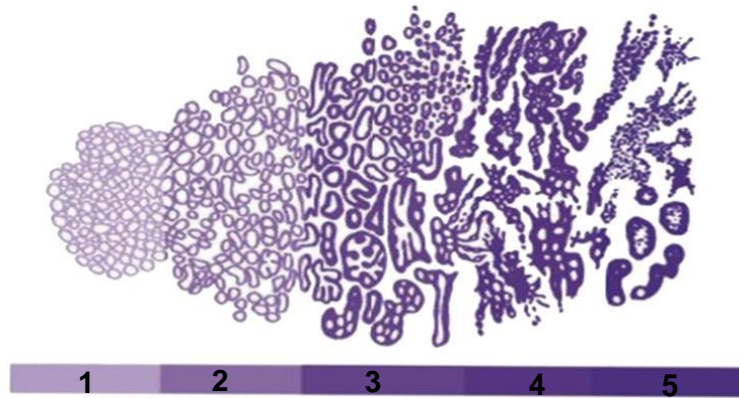


**Figure 11. Gleason score representation.** Gleason score criteria for different levels of tumor differentiation. Adapted from Harnden et al. 2007.

Currently, apart from tumor stage and grade, it is usual to classify PCa based on tumor risk which includes low-, intermediate-, and high-risk categories. These criteria were initially proposed by D'Amico and colleagues and are based on clinical stage, PSA and digital rectal examination results (Silberstein et al. 2013). According to this system, low-risk PCa has a Gleason score of 6 on prostate biopsy, clinical stage of T1a, T1c, or T2a and a PSA <10 ng/mL; intermediate risk prostate cancer has a Gleason of 7, a PSA of 10-20 ng/mL or a clinical stage of T2b or T2c and high-risk localized cancer has a Gleason score between 8 and 10, a PSA of >20 ng/mL or a clinical stage of T3a. Patients with T3b or T4 disease are classified as locally advanced (Silberstein et al. 2013).

### 3.6 Treatment

When a localized low risk tumor is diagnosed, watchful waiting and active surveillance are the standard of care due to the slow progression of the disease (Mottet et al. 2016) (**Fig. 12**). Upon examination of clinical progression, side-effects and potential benefit to survival, radical prostatectomy is the main treatment option (**Fig. 12**). It consists of removal of the entire prostate gland between the urethra and the bladder, and the resection of both seminal vesicles with sufficient surrounding tissue to obtain a negative margin. This procedure will try to preserve continence and whenever possible, potency. Moreover, radiotherapy is also often applied to localized prostate tumors that start progressing (Mottet et al. 2016).

Androgen deprivation therapy (ADT) is universally accepted as first-line treatment of symptomatic metastatic prostate cancer (**Fig. 12**). However, ADT is also used to treat localized prostate cancer, biochemical (PSA) recurrence after radical prostatectomy, locally advanced disease, lymph node metastases and asymptomatic metastatic disease

(Perlmutter & Lepor 2007). ADT can be achieved by different means, including surgical castration (which leads to a reduction in testosterone levels), chemical castration with luteinizing hormone-releasing hormone (LHRH) agonists (which results in the down-regulation of LHRH-receptors, suppressing luteinizing hormone (LH) and follicle-stimulating hormone (FSH) secretion and therefore testosterone production) and anti-androgens (which compete with androgens blocking androgen receptor in prostate cancer cells) (Perlmutter & Lepor 2007). Recent studies have shown that combination of ADT plus docetaxel or abiraterone in newly diagnosed metastatic non-castrate prostate cancer offers a survival benefit as compared with ADT alone (Morris et al. 2018).

However, after ADT, the development of castration resistant prostate cancer (CRPC) is very frequent and is considered as progression of the disease, despite medical or surgical castration, either clinical (development of metastatic disease, progression of pre-existing disease) or biochemical (three consecutive rises in PSA levels above nadir) in the presence of castrate levels of circulating testosterone (Chandrasekar et al. 2015). In these cases, chemotherapy (docetaxel and/or prednisone) and radiotherapy has been the first-line therapy. However, newer agents including antiandrogens (abiraterone acetate, enzalutamide and apalutamide), novel chemotherapy (taxane-based), immunotherapy (sipuleucel-T) and bone metastasis therapy (radium-223 dichloride) are also applied (Nevodomskeya et al. 2018; Wang et al. 2018) (**Fig. 12**). However, these novel therapies have shown limited benefits and more trials are needed to demonstrate efficacy (Nevodomskeya et al. 2018). Therefore, further research on the mechanisms driving resistance in prostate cancer will encourage the identification of new targets to treat the disease.

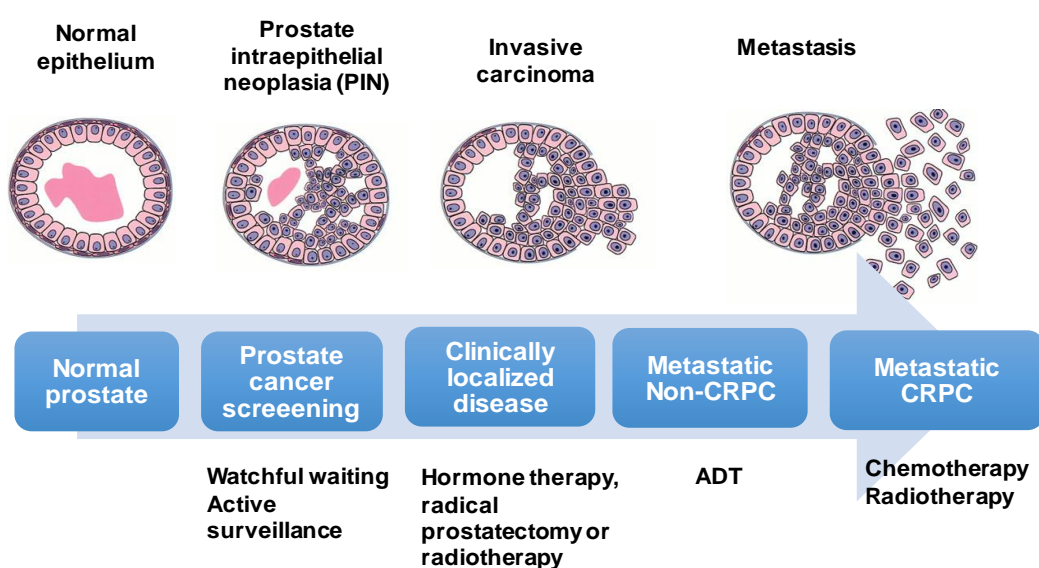


**Figure 12. Different treatment options during prostate cancer progression.** Adapted from Shen & Abate-Shen 2010.

#### 4. Androgen receptor signaling in prostate cancer

Androgens and androgen receptor (AR) play a pivotal role in the development and normal growth of the prostate gland but this pathway is also crucial in prostate carcinogenesis and progression to androgen-independent disease (Peter E Lonergan 2011).

The *AR* gene is a transcription factor located on chromosome X that encodes a 110-kDa protein consisting of 919 amino acids structurally divided into an N-terminal domain (NTD), DNA-binding domain (DBD) and a ligand-binding domain (LBD), all of which are essential for receptor function. Both testosterone and DHT binding to the LBD domain can activate AR under physiological conditions, with DHT having a significantly greater affinity for AR (Peter E Lonergan 2011). In the absence of ligands, AR remains in the cytoplasm tethered by heat shock proteins (HSPs). When testosterone or DHT are present, they induce conformational changes in AR that mediates dimerization of the receptor and its translocation to the nucleus, where it binds through the DBD domain to androgen response elements (AREs) on the promoters of target genes, such as PSA and transmembrane protease serine 2 (*TMPRSS2*), recruiting various coregulatory proteins to facilitate transcription and leading to responses such as growth and survival (Feldman & Feldman 2001; Peter E Lonergan 2011; Tan et al. 2015) (**Fig. 13**).

Androgens and the AR control the constant growth of prostate cancer cells by stimulating cell proliferation and inhibiting apoptosis (Feldman & Feldman 2001; Tan et al. 2015). The initiation of prostate cancer can in many cases be attributed to the activation of distinct growth-promoting pathways, such as the androgen-dependent upregulation of members of the E-twenty-six (*ETS*) family of transcription factors by gene fusions between the AR-regulated *TMPRSS2* gene promoter and the coding region of the *ETS* family member erythroblast transformation-specific (*ERG*) and *ETS* variant 1 (*ETV1*), which have been estimated to occur in ~50% of prostate tumors. These fusions confer androgen responsiveness to *ETS* transcription factors, leading to cell-cycle progression (Tan et al. 2015).

Androgens are not the only steroid hormones involved in prostate tumorigenesis. Estrogens can directly and indirectly affect the development and homeostasis of the prostate gland and also play a pivotal role in prostate tumor initiation and progression (Bonkhoff & Berges 2009). Moreover, other signals are involved in prostate cancer initiation and progression, including those involving phosphoinositide 3-kinase (PI3K), RAS/RAF and Wnt signaling (Tan et al. 2015).



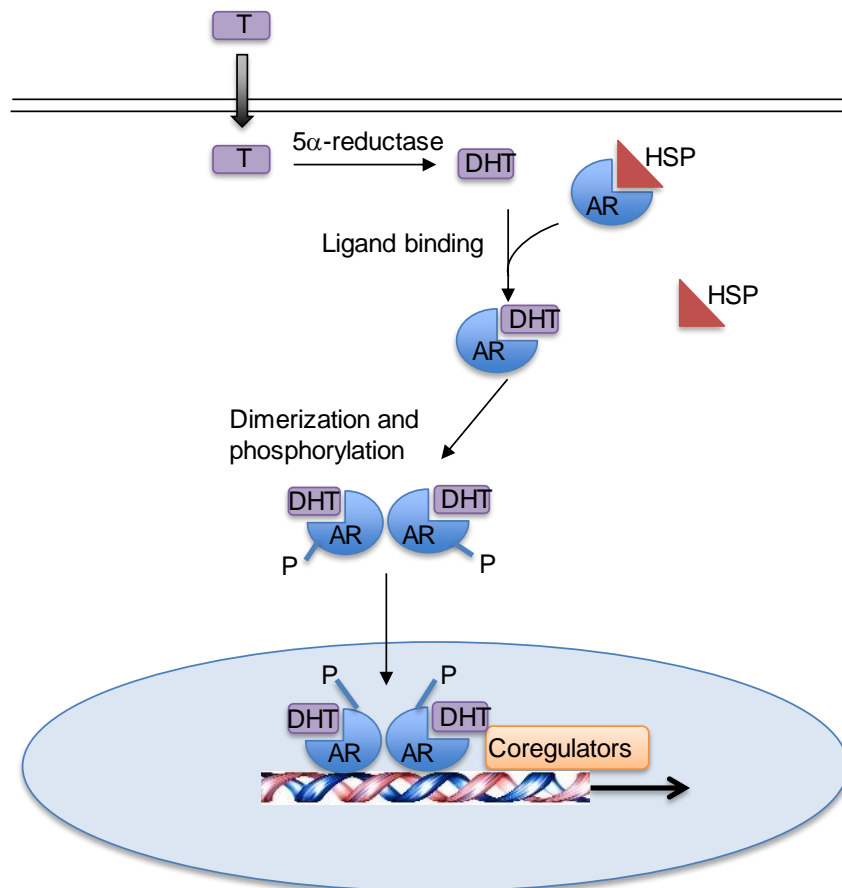


**Figure 13. Androgen receptor signaling.** Upon binding to dihydrotestosterone, androgen receptor translocates to the nucleus, binds to its target genes and regulates their expression. Adapted from Feldman & Feldman, 2001.

Since 1941, when Huggins and Hodges demonstrated the androgen dependency of PCa growth and progression, androgens and AR have been shown as the crucial players in both localized and advanced disease, as well as the major targets for therapeutic treatment of prostate cancer (Karen E. Livermore et al. 2016). Depriving tumors of androgens such as DHT and testosterone or blocking their actions has represented the main therapeutic option for the disease (Tan et al. 2015). Despite ADT, tumors progress to CRPC being then characterized by the reactivation of the AR signaling axis, which can take place through different mechanisms (Feldman & Feldman 2001; Chandrasekar et al. 2015; Watson et al. 2015):

a) Ligand dependent mechanisms:

- AR amplification and mutations: low levels of androgens persist despite androgen blockade with ADT. Amplification of the AR has been identified in a significant portion of CRPC cell lines, which may enable CRPC to be hypersensitive to low androgen levels and promote progression of the disease (hypersensitivity pathway). Also, different mutations in the AR gene have been identified to increase AR activity in the presence of

low levels of androgens and other androgen-like molecules (promiscuous pathway).

- Co-activators and co-repressors: The AR normally recruits a series of co-regulator complexes, which can function to either enhance (co-activators) or repress (co-repressors) transcriptional activity, thereby modulating AR signaling. Several studies have found upregulation of some of these coactivators in CRPC including FKBP51, SRC and p300/CBP. On the other hand, co-repressors were found downregulated.

b) Ligand independent mechanisms:

- Aberrant activation (post-translational modification)/outlaw pathway: multiple growth factors, cytokines and kinases increase AR signaling, thereby promoting progression to castration resistance in a ligand-independent manner. PI3K, Src, NFkB and IGF are among these pathways.

- Altered steroidogenesis: alternative androgen production of adrenal origin can lead to the production of dehydroepiandrosterone (DHEA) and its sulfated form (DHEA-S), which are not affected by ADT and can be converted to the highly active DHT in the “5 $\alpha$ -dione” pathway, promoting prostate cancer progression.

- AR variants: recent studies have identified the presence of splice variants of AR (AR-Vs) that are constitutively active, typically due to the loss of the C-terminal LBD. The predominant variants are ARV1, ARV7 and ARV 567 with ARV7 being the most studied.

Since, unfortunately, most patients progress to CRPC, new drugs that have been approved in the last few years only extend the life of patients for months rather than years and resistance to these treatments is still common. Therefore, the identification of alternative targets not relying on AR signaling could lead to significant improvements in the treatment of prostate cancer.



## 5. Wnt signaling: an overview

### 5.1 Wnt proteins

Wnt proteins are a family of secreted lipoglycoproteins that play fundamental roles in different processes including neural patterning and organogenesis, cell proliferation, cell fate determination, cell polarity and migration, stem cell self-renewal and survival (Logan & Nusse 2004; Willert & Nusse 2012; Klaus & Birchmeier 2008; Clevers 2006; MacDonald et al. 2009). According to these fundamental roles, perturbation of the levels of Wnt ligands or altered activities of the proteins involved in Wnt signal transduction can result in defects in embryonic development, as well as in diseases such as cancer (Anastas & Moon 2013).

The first Wnt gene, mouse *Wnt-1*, was discovered in 1982 (Nusse & Varmus 1982). Experiments conducted in mouse identified an insertion site of viral integration of mouse mammary tumor virus (MMTV) within the promoter of a gene called *Int-1* (for 'integration'), which resulted in increased expression of full-length Int-1 protein leading to mammary tumorigenesis (Nusse & Varmus 1982). Sequence analysis showed 5 years later that *Int-1* was orthologous to the *Drosophila* segment polarity gene *Wingless (Wg)* (Rijsewijk et al. 1987) and the terms were combined to produce the name 'Wnt' for the mammalian *Int-1* gene and its paralogs (Nusse & Varmus 1992).

Later studies led to the isolation of more than 100 Wnt sequences in different species, all of which are highly evolutionarily conserved in metazoans (Komiya & Habas 2008). In mammals, 19 members of the Wnt family of proteins are present: Wnt-1, Wnt-2, Wnt-2b/13, Wnt-3, Wnt-3a, Wnt-4, Wnt-5a, Wnt-5b, Wnt-6, Wnt-7a, Wnt-7b, Wnt-8a, Wnt-8b, Wnt-9a, Wnt-9b, Wnt-10a, Wnt-10b, Wnt-11 and Wnt-16 (MacDonald et al. 2009; Nusse 2018).

Wnt proteins are cysteine-rich proteins of about 350-400 amino acids that harbor an N-terminal region containing a palmitoleic acid group (PAM) crucial for their secretion, several highly charged amino-acid residues, many potential glycosylation sites and a characteristic distribution of 23-25 cysteine residues which suggest the formation of multiple intramolecular disulfide bonds (MacDonald et al. 2009; Mikels & Nusse 2006) **(Fig. 14A and B)**.

The tridimensional structure of *X.laevis* Wnt-8 in complex with the cysteine-rich domain (CRD) of mouse FZD8 was solved in 2012 (Janda et al. 2012) and showed that XWnt-8 has a distinctive donut shape which seems to resemble a hand that extends thumb (N-terminal) and index (C-terminal) fingers from a central "palm" domain **(Fig.**

**14C).** XWnt-8 comprises an N-terminal  $\alpha$ -helical domain (NTD) from residues ~32 to 250 that contains the lipid-modified thumb, and a C-terminal cysteine-rich domain (CTD) from residues 261 to 338 (**Fig. 14B**). The XWnt-8 NTD is composed of a seven- $\alpha$ -helical bundle palm, containing two large interhelical loop insertions that are stabilized by four disulfide bonds. The principal feature of the CTD is a long  $\beta$ -strand hairpin that is also stabilized by an extensive network of disulfide bonds. Two asparagines (Asn104, and Asn263) are glycosylation sites on XWnt-8 (Janda et al. 2012) (**Fig. 14B**).

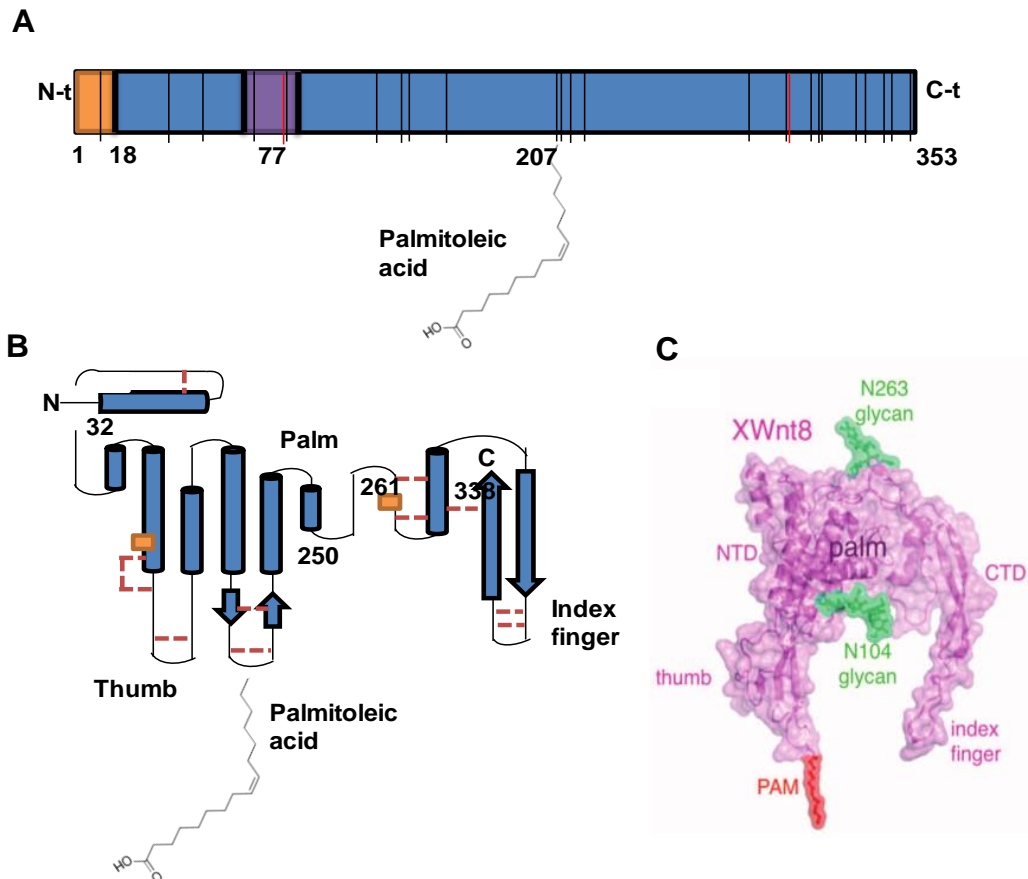


**Figure 14. Structure of Wnt proteins. (A)** Schematic representation of mouse Wnt-3a. Black lines indicates cysteine and red lines potential glycosylation sites. Yellow region shows the N-terminal signal sequence and purple region shows the porcupine binding area. Adapted from Coudreuse & Korswagen 2007. **(B)** Secondary-structure diagram of the XWnt-8 fold. Disulfide bonds are shown by red lines and glycosylation sites are shown with yellow boxes. Adapted from Janda et al. 2012. **(C)** Tridimensional structure of XWnt-8. The palmitoleic acid (PAM) group is shown in red. Palm, thumb and index fingers are shown. Taken from Janda et al. 2012.

## 5.2 Wnt biogenesis and secretion

Wnt proteins are heavily modified through glycosylation (Smolich et al. 1992) and palmitoylation (Willert et al. 2003) prior to transport and secretion, which take place in the endoplasmic reticulum (ER) and are both required for proper intracellular processing and signaling activity (Willert & Nusse 2012). These modifications make Wnts more hydrophobic than they should be according to their sequence and explain the low solubility of active Wnt molecules (Logan & Nusse 2004; Willert & Nusse 2012; Takada et al. 2017). In the case of glycosylation, the oligosaccharyl transferase complex (OST) attaches N-linked oligosaccharide chains to the appropriate residues that can differ in the numbers of attachments among different Wnts (Coudreuse & Korswagen 2007; Willert & Nusse 2012) (**Fig. 15**). For palmitoylation, the acyltransferase Porcupine, a multipass transmembrane ER protein that is conserved across multiple species (Mikels & Nusse 2006), transfers acyl groups, such as a palmitoyl group, to substrates in cysteine and serine/threonine residues (**Fig. 15**). Willert et al reported a palmitic acid linked to a conserved cysteine residue (Cys77) and later on, Takada et al reported a palmitoleic acid motif (PAM) linked via an oxyester to a conserved serine residue (Ser209) (Willert & Nusse 2012). However, the crystal structure of *Xenopus* Wnt-8 in complex with mouse FZD8-CRD published in 2012 (Janda et al. 2012) indicates that only the conserved serine residue is lipidated, whereas the conserved cysteine is occupied in a disulfide linkage, arguing that Wnt proteins are modified by a single lipid moiety (Janda et al. 2012). Although glycosylation and palmitoylation occurs in all Wnt proteins, other post-transductional modifications may occur in specific Wnts (Willert & Nusse 2012).

After modification of Wnts in the ER, different proteins are involved in their release from producing cells to the extracellular space including the multipass transmembrane protein Wntless (Wls)/Evenness interrupted (Evi)/Mom-3. This protein is located in the Golgi as well as in vesicles and in the plasma membrane and it associates and accompanies modified Wnts to the cell surface (Mikels & Nusse 2006; Willert & Nusse 2012). But also other proteins such as TMEM9/p24 act as Wnt cargo proteins, promoting Wnts exit from the ER (Willert & Nusse 2012). After Wnt release, Wls needs to be retrieved back to the trans-Golgi network (TGN) to maintain Wnt secretion and this process is mediated through the retromer complex (Yang et al. 2008) (**Fig. 15**). Following release of Wnts, different studies have shown that they can be tethered to the plasma membrane via their lipid moieties but also be found in a biologically active form in the conditioned media. Alternatively, Wnt proteins may become incorporated into lipoprotein complexes (Willert & Nusse 2012).

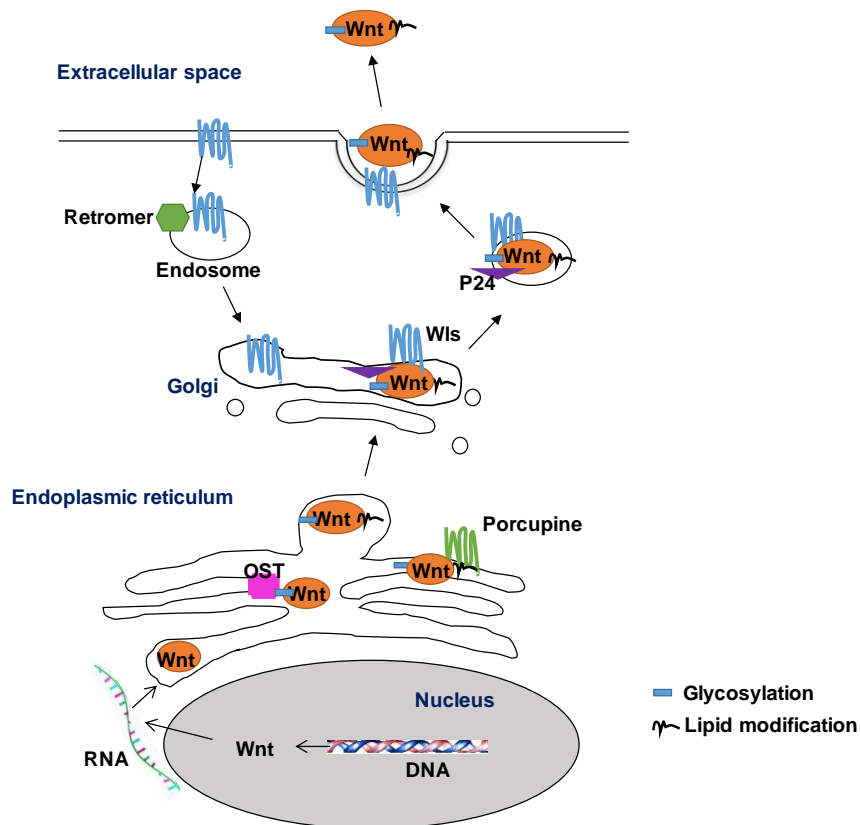


**Figure 15. Wnt biogenesis and secretion.** Wnt proteins are palmitoylated in the ER by porcupine and secreted through the Golgi by Wls. After Wnt release, the retromer complex mediates Wls return to the trans-Golgi network (TGN). Adapted from Willert & Nusse, 2012.

### 5.3 Wnt signaling pathways

Traditionally, Wnt signals have been classified into canonical or  $\beta$ -catenin dependent and noncanonical or  $\beta$ -catenin independent pathways. However, novel branches have been recently characterized that increase the complexity of Wnt signaling (**Fig. 16**).

A hallmark of canonical Wnt signaling is the stabilization and nuclear translocation of  $\beta$ -catenin, which in the absence of Wnt ligands is recruited and degraded by the destruction complex, whose components include Axin, glycogen synthase kinase-3 (GSK-3), casein kinase 1 (CK1) and adenomatous polyposis coli (APC) (Komiya & Habas 2008). Wnt binding to frizzled (FZD) receptor and low density lipoprotein (LRP5/6) coreceptors leads to the phosphorylation of the latter by CK1 and GSK-3, which promotes the assembly of an intracellular signalosome driven by Disheveled (DVL) and Axin co-polymerization at the plasma membrane. Recent evidence suggests that FZD and LRP5/6 participate in the assembly of this signalosome by forming regulatory scaffolds which stabilize DVL and Axin adapters, thereby disrupting the destruction complex (DeBruine et al. 2017). This leads to the stabilization of  $\beta$ -catenin, which accumulates in the cytoplasm and enters the nucleus, binding to T-cell factor

(TCF)/lymphoid enhancer factor (LEF) family transcription factors and co-activators, such as cAMP response element binding protein (CREB) binding-protein (CBP)/p300, B-cell CLL/lymphoma 9 (BCL9) and B Cell CLL/Lymphoma 9 Like (BCL9L) thereby regulating the expression of Wnt target genes (Komiya & Habas 2008).

Noncanonical Wnt signals are less well characterized being traditionally sub-divided into Planar Cell Polarity (PCP) and Wnt/Ca<sup>2+</sup> pathways (Komiya & Habas 2008). However, additional  $\beta$ -catenin/TCF-independent signals have been described (van Amerongen 2012; Park et al. 2015). Noncanonical Wnt signals are activated upon Wnt binding to FZD receptors and tyrosine kinase-like co-receptors, leading to the recruitment and activation of DVL. The PCP pathway has two parallel branches involving small guanosine triphosphate hydrolase (GTPases): Rho, which activates Rho-associated kinase (ROCK) and Rac, which is linked to Jun-N-terminal kinase (JNK) and signaling by activator protein-1 (AP-1) family transcription factors. Cytoskeletal and transcriptional changes associated with these small GTPases regulate cell adhesion and migration (Komiya & Habas 2008; van Amerongen 2012; M. T. Veeman et al. 2003; Eferl & Wagner 2003). Activation of the Wnt/Ca<sup>2+</sup> pathway stimulates Ca<sup>2+</sup> release from the endoplasmic reticulum, promoting activation of G-proteins, protein kinase C (PKC) and Ca<sup>2+</sup>/calmodulin-dependent kinase II (CaMKII). These events can also lead to the activation of transcription factors, such as nuclear factor of activated T-cells (NFAT), which promotes cell growth, survival, invasion and angiogenesis (van Amerongen 2012; M. T. Veeman et al. 2003; Kohn AD 2005; Mancini & Toker 2009).

More recently, novel links have been identified between Wnt and Hippo signaling, which regulates organ size, tissue homeostasis and patterning. Hippo signals are transduced by YAP (Yes-associated protein), TAZ (transcriptional co-activator with Psd-95/Disc large/ZO-1 homologous (PDZ) -binding motif) and TEADs (TEA domain family transcription factors) (Zanconato et al. 2016). YAP/TAZ antagonize canonical Wnt signaling by binding to components of the destruction complex, such as Axin (Azzolin et al. 2014), and regulating nuclear translocation of  $\beta$ -catenin. In addition, a noncanonical Wnt-YAP/TAZ signaling axis has also been described, where Wnt binding to FZD and to receptor tyrosine kinase-like orphan receptor (ROR) activates G $\alpha$ 12/13, Rho and LATS1/2 (Large Tumor Suppressor Kinase) to induce YAP/TAZ and TEAD-mediated transcription (Park et al. 2015).

A novel branch of Wnt signaling, Wnt-STOP (Acebron et al. 2014), has been described, whose signal is initiated by Wnt binding to LRP6 and whose effects are transcription-independent, involving Cyclin Y, rather than  $\beta$ -catenin (Acebron et al. 2014).

Wnt-STOP signals promote protein stabilization at mitosis and cell growth, which suggest it could play an important role in cancer (Acebron & Niehrs 2016).

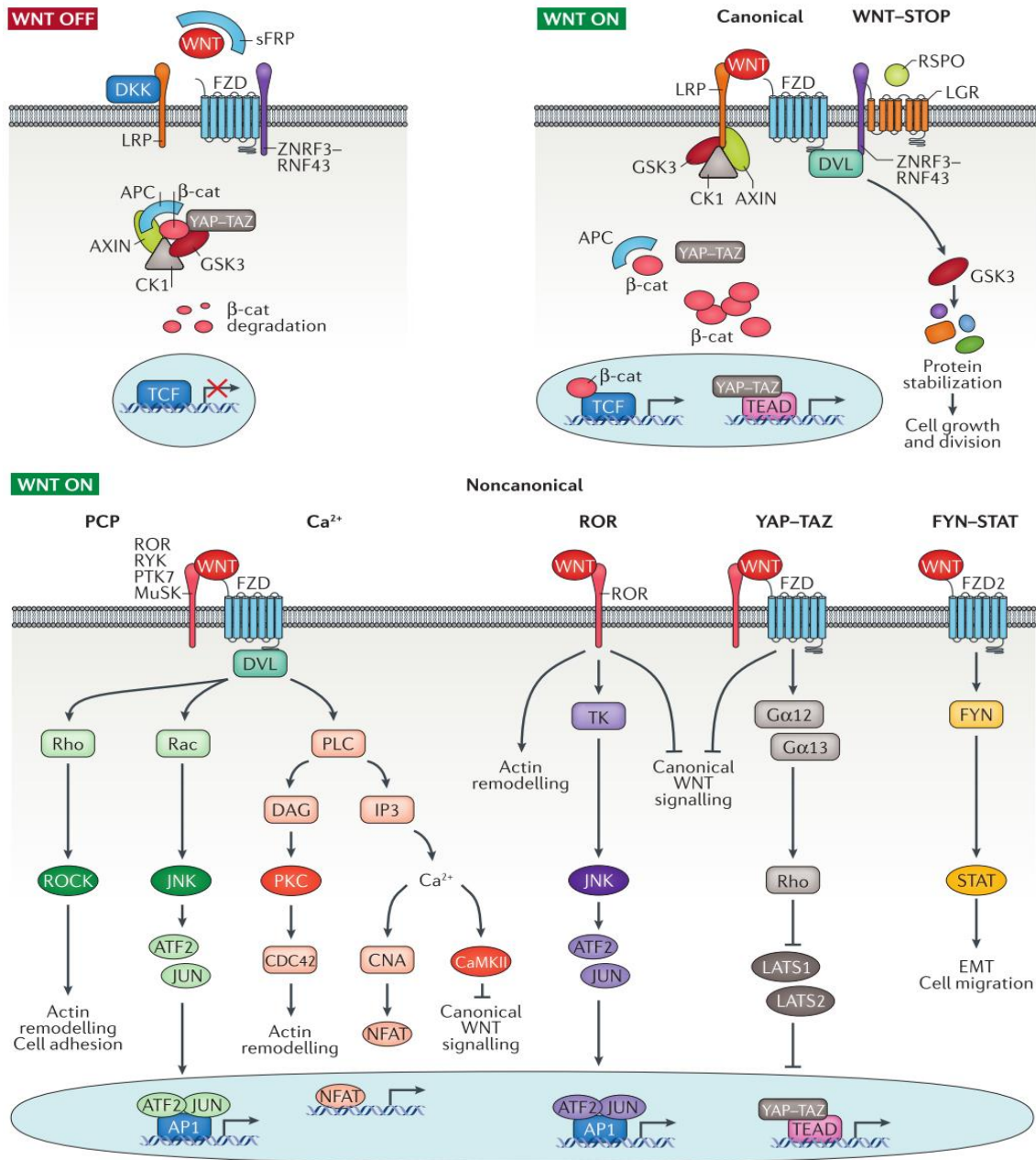


**Figure 16. Wnt signaling pathways.** In the absence of Wnt ligands (WNT OFF), β-catenin is degraded by the destruction complex (APC, Axin, GSK-3, CK1 and YAP/TAZ) and Wnt target genes are repressed. Binding of Wnt ligands to FZD and either LRP5/6 or ROR1/2-RYK-PTK7-MuSK (WNT ON) activates canonical and noncanonical signaling, respectively. Canonical signals disrupt the destruction complex, stabilizing β-catenin, which enters the nucleus and binds TCF/LEF transcription factors to activate gene expression. The WNT-STOP pathway is a transcription-independent pathway involving LRP coreceptors and cyclin Y. Noncanonical signals activate small GTPases and various kinases, mobilize Ca<sup>2+</sup> and activate AP-1 family and NFAT transcription factors. New noncanonical signals involve activation of YAP/TAZ and tyrosine-protein kinase Fyn (FYN)/ signal transducer and activator of transcription (STAT) signaling. Taken from Murillo-Garzón & Kypta 2017.

## 5.4 Wnt receptors

After processing and secretion, Wnt proteins can enhance different signals by binding and activating different receptors at the cell membrane, including members of the Frizzled (FZD), low-density lipoprotein receptor-related protein (LRP) 4 to LRP6, receptor tyrosine kinase-like orphan receptor (ROR), protein tyrosine kinase 7 (PTK7), receptor tyrosine kinase (RYK), muscle skeletal receptor tyrosine kinase (MUSK) and proteoglycan families (glypican 4-6, GPC4-6) (Niehrs 2012) (**Fig. 17**)

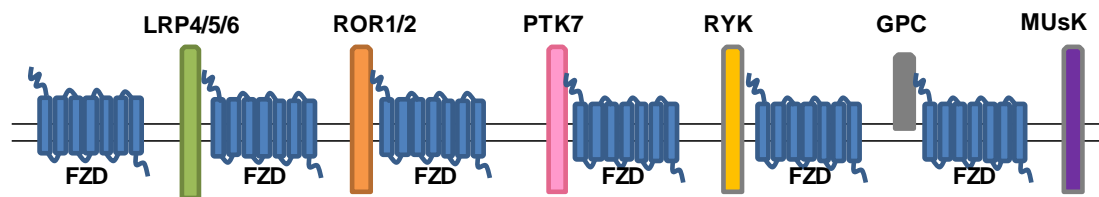


**Figure 17. Wnt receptors and coreceptors.** Variety of Wnt receptors and coreceptors. Adapted from Niehrs, 2012.

### 5.4.1 FZD receptors

The seven-pass transmembrane family of Frizzled (FZD) receptors were firstly discovered in *Drosophila* (Vinson & Adler 1987; Vinson et al. 1989) being later characterized their homologues in mammals (Bhanot et al. 1996). According to the International Union of Basic and Clinical Pharmacology (IUPHAR) classification, Frizzled receptors have been defined as a separate family, the Class Frizzled receptors, although some studies have shown similarity between them and G-protein-coupled receptors (GPCR) (Schulte & Bryja 2007; Schulte 2010). Mammalian Frizzled receptors contains 10 members, FZD1-10, as well as the Hedgehog pathway protein Smoothened (SMO). Phylogenetic analysis of FZD proteins identifies different clusters based on their identity, which can vary from 20 to 40% being even higher between different clusters. Five main clusters group FZD proteins as follows: FZD1/2/7 (75% identity), FZD3/6 (50%), FZD5/8 (70%) and FZD4/9/10 (65%) (**Fig. 18A**) (Schulte & Bryja 2007; MacDonald, B.T & He 2012; Schenkelaars et al. 2015). Several *FZD* genes appear to lack introns including *FZD1*, *FZD2*, and *FZD7* to *FZD10*, but others such as *FZD5* contain one intron, although the entire open reading frame is encoded by a single exon (Huang & Klein 2004).

FZD receptors range in length from about 500 to 700 amino acids (Huang & Klein 2004). The N-terminal region is extracellular and contains a cysteine rich domain (CRD) that is connected to the transmembrane domain (TMD) through a variable 70-120 amino acid linker region (MacDonald, B.T & He 2012; Niehrs 2012) (**Fig. 18B**). The seven



transmembrane region contains three intracellular loops (ICL) and three extracellular loops (ECL) ending with a C terminal domain of variable length. Although the CRD within all members is remarkably conserved, each cluster shares a hallmark characteristic: FZD5 and FZD8 receptors have exceptionally long CRD-to-TMD linkers; FZD3 and FZD6 receptors have long cytoplasmic tails with many regulatory elements; FZD4, FZD9 and FZD10 have very short C-terminal tails and the shortest CRD-to-TMD linkers; and FZD1, FZD2 and FZD7 seem to possess a CRD most different in sequence and structure from other FZD receptors (DeBruine et al. 2017). Apart from cysteines in the CRD, FZD receptors contain conserved cysteines in the ECL 1 and 2, which could engage in stabilizing disulfide bonds (Schulte 2010; MacDonald, B.T & He 2012) (**Fig. 18B**). The intracellular loops of FZD receptors contain essential sites for post-translational modifications such as phosphorylation, ubiquitination and proteolysis, which are known to regulate their function (Schulte 2010; Niehrs 2012). The C-terminal domain of FZD proteins contains the conserved KTxxxW domain which is essential for FZD signaling through its interaction with the Disheveled (DVL) PDZ domain. However, other residues in intracellular loops 1 and 3 are also required for DVL interaction and FZD signaling (Schulte & Bryja 2007; Schulte 2010; MacDonald, B.T & He 2012) (**Fig. 18B**).

The FZD CRD is a highly conserved domain in FZD that mediates high affinity interactions with Wnt proteins (Niehrs 2012). The resolution of the structure of *Xenopus* Wnt-8 in complex with the CRD of mouse FZD8 (Janda et al. 2012) led to important new insights into Wnt biochemistry. In the complex structure, XWnt-8 appears to grasp the FZD8-CRD at two opposing sites in FZD-CRD: “site 1” and “site 2” respectively, which resembles a hand that extends thumb (N-terminal) and index (C-terminal) fingers from a central “palm” domain. The N-terminal domain of Wnt-8 is dominated by the palmitoleic lipid projecting into a groove in the FZD8-CRD. This interaction is mediated by amino acid residues that are conserved among Wnt and FZD family members, which may explain the promiscuous interactions among many Wnt and FZD proteins. Wnt-FZD CRD interactions in the C-terminal domain of Wnt-8 are mediated between amino acid residues that are highly conserved in all Wnts and a small depression in the FZD8-CRD structure that harbors some residues that are not conserved among other FZD CRDs. Therefore, it is possible that the specificity in Wnt–FZD binding arises from the interaction of the Wnt index finger with this surface domain in FZD (Janda et al. 2012) (**Fig. 18C**).

The crystal structure also provides knowledge about Wnt formation of ternary complexes with coreceptors necessary for both canonical and noncanonical signaling (Janda et al. 2012) (**Fig. 18C**). Through conservation analysis of 20 Wnt sequences, four



main regions of conserved residues were identified in XWnt-8, including the thumb and index finger, the core of the N-terminal domain helical bundle and a large continuous patch composed of 10 residues. The location of this patch at the opposite end of XWnt-8 from the FZD CRD domain and its solvent exposure suggest a potential binding site for interaction with Wnt coreceptors such as LRP5/6, ROR1/2, PTK7 and RYK (Niehrs 2012; Janda et al. 2012).

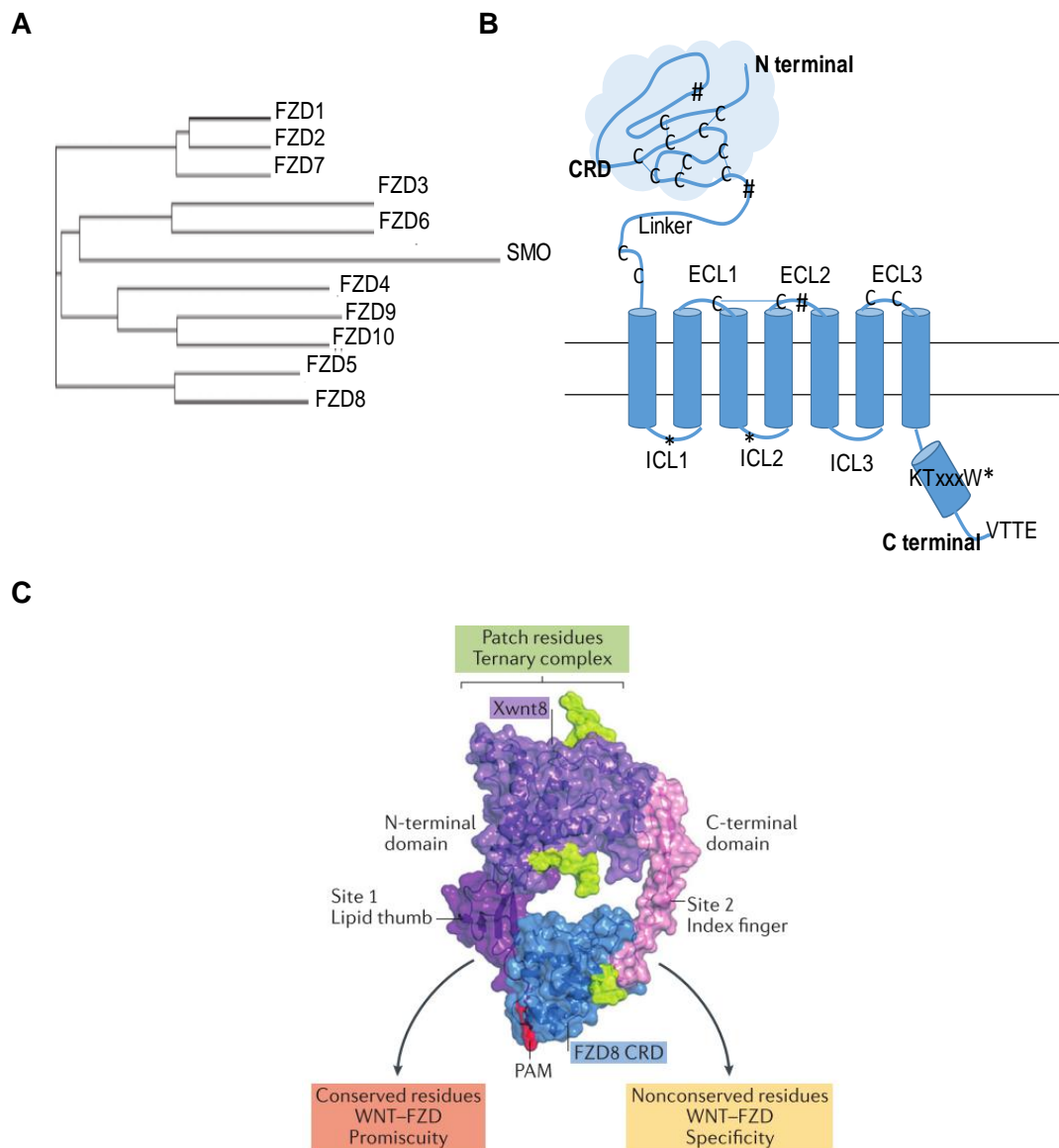


**Figure 18. FZD receptors.** (A) Phylogenetic tree of the family of FZD receptors. Adapted from Schulte, 2007. (B) Structure of FZD receptors showing the CRD domain with cysteines (C) forming 5 disulphide bonds. ECL and ICL: extracellular and intracellular loops \* represents potential phosphorylation sites and # potential glycosylation sites. The transmembrane domain and the C-terminal domain with the conserved KTxxxW\* sequence and the less conserved VTTE sequences are also shown. Adapted from Schulte, 2007 and MacDonald, 2012. (C) Crystal structure of XWnt-8 in complex with FZD8 CRD. Sites of interaction between Wnt and FZD are shown as well as the patch residues involved in the formation of ternary complexes. Taken from Murillo-Garzón & Kypta 2017.

During the last year, two independent structural studies of FZD CRDs revealed novel insight into Wnt-FZD interactions (Nile et al. 2017; Debruine et al. 2017). The structures of FZD7 and FZD5 CRD (Nile et al. 2017) and the FZD4-CRD (Debruine et al. 2017) suggest that the Wnt acyl group is required for FZD CRD dimerization, supporting a 1:2 stoichiometry model for Wnt-FZD complexes (Nile et al. 2017; Debruine et al. 2017). Moreover, palmitoylated Wnt-5a and Wnt-8a were found to stabilize the FZD4 CRD-CRD interaction, suggesting that FZD receptors form signalosomes upon Wnt binding and that the Wnt palmitoyl group is crucial for this interaction (Debruine et al. 2017). However, although hypothetical models have been created, further studies will be required to determine how these interactions orchestrate Wnt signalosome assembly (**Fig. 19**).

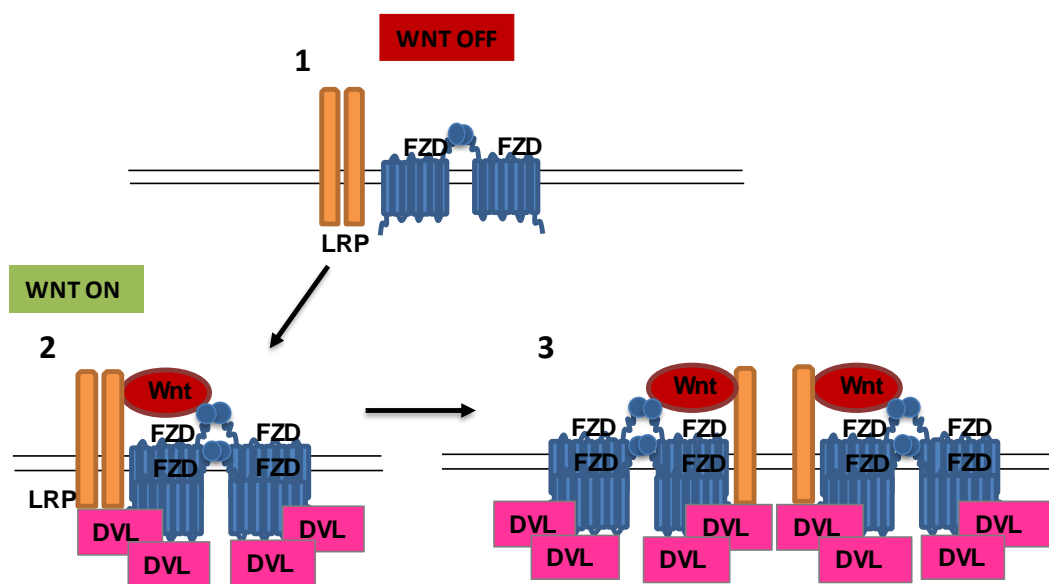


**Figure 19. Hypothetical model of Wnt signalosome assembly.** (1) LRP5/6 and FZD receptors exist as inactive dimers; (2) Wnt stabilizes LRP5/6 and FZD receptors and allows DVL dimerization; (3) Multiple Wnts may drive assembly of large receptor signalosomes. Adapted from DeBruine et al, 2017.

The two most prominent intracellular binding partners for FZD receptors are the scaffold protein DVL and GPCRs (Dijksterhuis et al. 2014). In humans, there are three variants of DVL (DVL1, DVL2 and DVL3) all of which contain three functional domains: the N-terminal domain, which contains the DIX (Disheveled and Axin) polymerization domain; the C-terminal region, where the DEP (Disheveled, Egl-10 and Pleckstrin) domain is located and which is functionally involved in the regulation of small GTPases and in addition, a central PDZ (Psd-95/Disc large/ZO-1 homologous) binding domain, which enables interactions with other proteins. DVL-FZD interaction is mainly based on three mechanisms involving the KTxxxW–DVL interaction, the DEP domain interaction with a bipartite motif in the ICL3 of FZD and DEP-domain-mediated electrostatic

interactions with the negatively charged head groups of membrane lipids. In this regard, DVL plays not only an important role in the  $\beta$ -catenin-dependent but also in the independent signaling pathways (Dijksterhuis et al. 2014).

Although FZD receptors share features with GPCRs (seven transmembrane segments, an extracellular N-terminal domain, and a cytoplasmic C-terminal tail), they lack hallmarks of prototypical GPCRs and they are classified as nonconventional GPCRs. However, other studies have shown that FZDs can directly interact with GPCRs and signal through them to activate Wnt/Ca<sup>2+</sup> and Wnt/cAMP signaling (Nichols et al. 2013; Dijksterhuis et al. 2014).

Apart from being Wnt receptors, FZD proteins have been described to bind to Clostridium difficile toxin B (TcdB) through the CRD of FZD which therefore, can result on competition with Wnt for binding to FZDs, blocking Wnt signaling (Tao et al. 2016; Chen et al. 2018).

#### 5.4.1.1 FZD8

FZD8 is one of the best characterized FZD family members since the structure of mouse FZD8 CRD was solved in complex with *Xenopus* Wnt-8. FZD8 is located on chromosome 10 and encodes for a protein of 694 amino acids with a molecular mass of 69 kDa (Saitoh et al. 2001). As shown before, the homology between FZD receptors is extremely high with FZD5 the closest family member (**Fig. 18**) (Schulte & Bryja 2007; MacDonald, B.T & He 2012). FZD8 is expressed in fetal kidney and brain as well as in adult kidney, heart, pancreas and skeletal muscle (Saitoh et al. 2001). Like other FZD receptors, FZD8 is regulated through ubiquitination by Zinc and Ring Finger 3 (ZNRF3) which leads to its degradation by the proteasome. Moreover, it is glycosylated at Asparagines 49, 152 and 475. Independent studies have shown the involvement of FZD8 in the canonical pathway (Wang et al. 2012; Albers et al. 2013; Yin et al. 2013; Bravo et al. 2013; Q. Jiang et al. 2015; Fu et al. 2016; Yang et al. 2017; Li et al. 2017; Kramer et al. 2017). However, FZD8 has also been implicated in noncanonical signaling (Gregory et al. 2010; Kumawat et al. 2013; Wang et al. 2015; A. I. R. Spanjer et al. 2016; Murillo-Garzón et al. 2018), which again highlights the promiscuity of FZD receptors to activate different pathways in different contexts.

Most of the alterations described for FZD8 have been related to different cancer types, such as renal cell carcinoma (Janssens et al. 2004; Yang et al. 2017), acute lymphoblastic leukemia (Khan et al. 2007; Gregory et al. 2010) and lung cancer (Wang et al. 2012; Bravo et al. 2013), where it was found upregulated. It has also been

implicated in triple negative breast cancer, where it mediates drug resistance (Yin et al. 2013), in head and neck squamous carcinoma, where FZD8 was found to be a target for elimination of cancer stem cells (Sun et al. 2014), and in colon cancer progression, where it mediates Wnt-2 signaling (Kramer et al. 2017). Particularly in prostate cancer, FZD8 has been found upregulated in prostate tumors (Pascal et al. 2009; Li et al. 2017) but genetic alterations of FZD8 are not very frequent (**Fig. 20**).

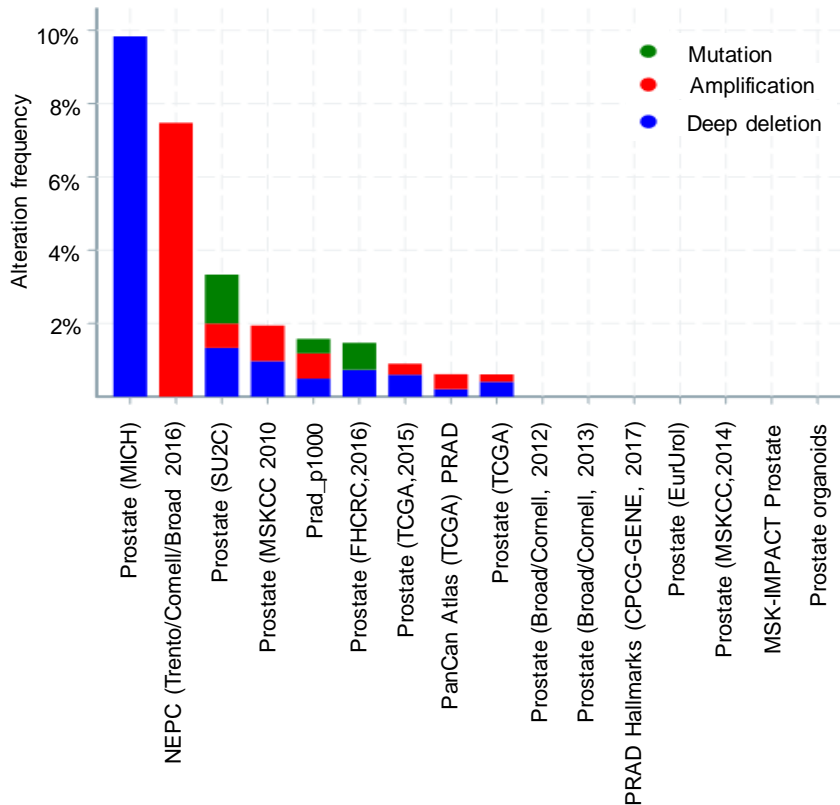


**Figure 20. FZD8 genetic alterations in prostate cancer datasets.** Taken from cBioPortal.org.

Last but not least, FZD8 alterations have also been linked to other diseases, such as rheumatoid arthritis (Miao et al. 2015), asthma pathogenesis (Kumawat et al. 2013; A. I. R. Spanjer et al. 2016), chronic bronchitis (Anita I.R. Spanjer et al. 2016), high glucose stress (Pang et al. 2016), corneal defects (Benson et al. 2017) and psoriasis (Shen et al. 2017). Moreover, a human-accelerated regulatory enhancer (HARE5) of FZD8 has been implicated in brain development and size (Boyd et al. 2015).

#### 5.4.2 LRP5/6 coreceptors

LRP5 and LRP6 are members of the low-density lipoprotein receptor family, which act as coreceptors in Wnt-  $\beta$ -catenin dependent signaling. Both have more than 1600 amino acids, sharing around 70% sequence identity (MacDonald, B.T & He 2012). Their single

pass transmembrane structure contains an extracellular domain (ECD) that mediates the interaction with Wnt and FZD, leading to ternary complexes, and an intracellular domain (ICD) that contains five Pro-Pro-Pro-Ser/Thr-Pro (PPPSP) repeats whose phosphorylation by GSK3 and CK1 is required for  $\beta$ -catenin-dependent signaling (Niehrs 2012). Once LRP6 is fully phosphorylated at PPPSPXS sites, it binds Axin and GSK3, leading to recruitment of the  $\beta$ -catenin destruction complex and inhibition of GSK3 through its sequestration in multivesicular bodies (MVBs). These events protect  $\beta$ -catenin from phosphorylation, escaping ubiquitination and proteasomal degradation and promoting its accumulation in the cytoplasm and nucleus (Niehrs 2012). The role of LRP5/6 coreceptors promoting canonical Wnt signaling can be regulated by the secreted protein SOST or sclerostin, which binds LRP5/6 coreceptors and consequently, disrupts the formation of the Wnt-FZD-LRP complex and inhibit canonical Wnt signaling (Semënov et al. 2005).

#### **5.4.3 ROR1/2 coreceptors**

The receptor tyrosine kinase-like orphan receptors (RORs) are transmembrane proteins included within the receptor tyrosine kinase (RTK) family. Both ROR1 and ROR2 have about 940 amino acids and share about 58% identity (Masiakowski & Carroll 1992). They contain an extracellular domain consisting of an immunoglobulin-like motif, a cysteine-rich frizzled domain, which harbors high homology to the FZD CRD and mediates ligand binding and a Kringle domain involved in protein-protein and protein-ligand interactions. The intracellular region includes a tyrosine kinase domain whose functionality has been extensively debated, and a proline-rich domain flanked by two serine-threonine-rich regions (Green & Nusse 2014; Borcharding et al. 2014). They were named orphan receptors because their ligands had not been discovered. However, different studies have shown that they can associate with different Wnt ligands, such as Wnt-5a, transducing mostly PCP signaling (Niehrs 2012; van Amerongen 2012; Rebagay et al. 2012; Green & Nusse 2014; Borcharding et al. 2014).

#### **5.4.4 Receptor tyrosine kinases (RYK, PTK7 and MuSK) and others**

RYK (receptor-like tyrosine kinase) is a single pass transmembrane receptor that binds Wnt ligands. It contains an extracellular domain resembling the Wnt inhibitory factor (WIF) protein, which has been proposed to interact directly with the lipid modification on the Wnt protein (Green & Nusse 2014). The cytoplasmic portion of RYK has a tyrosine kinase motif that is not considered to be active (Green & Nusse 2014). Hence, RYK may act as a coreceptor rather than as a primary signal transducing

receptor and has been implicated in  $\beta$ -catenin-dependent, PCP and WNT–Ca<sup>2+</sup> signaling (van Amerongen 2012; Niehrs 2012; Green & Nusse 2014).

Protein Tyrosine Kinase 7 (PTK7) is a single pass transmembrane receptor with seven extracellular immunoglobulin-like domains, a transmembrane region, a juxtamembrane region and a catalytically inactive cytoplasmic tyrosine kinase domain (Niehrs 2012; Peradziryi et al. 2012). PTK7 is mainly involved in the PCP pathway (Peradziryi et al. 2012; Hayes et al. 2013; Martinez et al. 2015) but some reports also showed its involvement in  $\beta$ -catenin dependent signaling in *X.laevis* (Puppo et al. 2011). Therefore, it may activate both canonical and noncanonical pathways (Niehrs 2012).

Muscle Specific Kinase (MuSK) is a type I, single-pass transmembrane glycoprotein that acts as Wnt receptor specifically in muscle and that has been linked to PCP signaling (Niehrs 2012). Its extracellular region contains three immunoglobulin-like domains (Ig1-3) and a cysteine-rich domain (CRD) that is similar to the FZD CRD. A single transmembrane helix connects the extracellular domain to the cytoplasmic region, which contains the tyrosine kinase domain that can be auto-phosphorylated on three tyrosine residues (Gnanasambandan 2013).

Even though they are less well characterized, other proteins have also been reported as Wnt receptors or coreceptors, including VANG like proteins 1 and 2 (VANGL1/2), which are mainly involved in the PCP pathway (Hatakeyama et al. 2014) and proteoglycans such as glypican-4 (GPC4), which regulates the signaling at the level of the interaction between the ligand and receptor (Capurro et al. 2014). Some other receptors including CD146, have also been reported to bind Wnt ligands, such as Wnt-5a, to activate JNK and regulate cell migration (Ye et al. 2013).

## 5.5 Regulation of Wnt signaling

Regulation of Wnt signaling is very complex and is mediated through different effectors that can function as agonists or antagonists (**Fig. 21**). Antagonists can be classified depending on their mechanism of action. Some of them are secreted regulators that bind Wnt proteins, for example sFRPs (secreted Frizzled-Related Proteins), WIF-1 (Wnt inhibitory factor 1) and Cerberus (Kawano & Kypta 2003; Malinauskas & Jones 2014; Cruciat & Niehrs 2013). Other antagonists such as Dickkopf (DKK) proteins (Kawano & Kypta 2003; Malinauskas & Jones 2014; Cruciat & Niehrs 2013) and SOST (Semenov et al. 2005) associate with Wnt co-receptors LRP5/6, or Shisa (Cruciat & Niehrs 2013) which binds to FZD receptors in the ER, preventing its translocation to the membrane (Yamamoto et al. 2005). Among Wnt agonists, Norrin directly activates Wnt

signaling by binding to FZD4 (Cruciat & Niehrs 2013). Adding further complexity, sFRPs can also bind to FZD receptors and activate or inhibit Wnt signaling in different contexts (Kawano & Kypta 2003; Bovolenta et al. 2008).

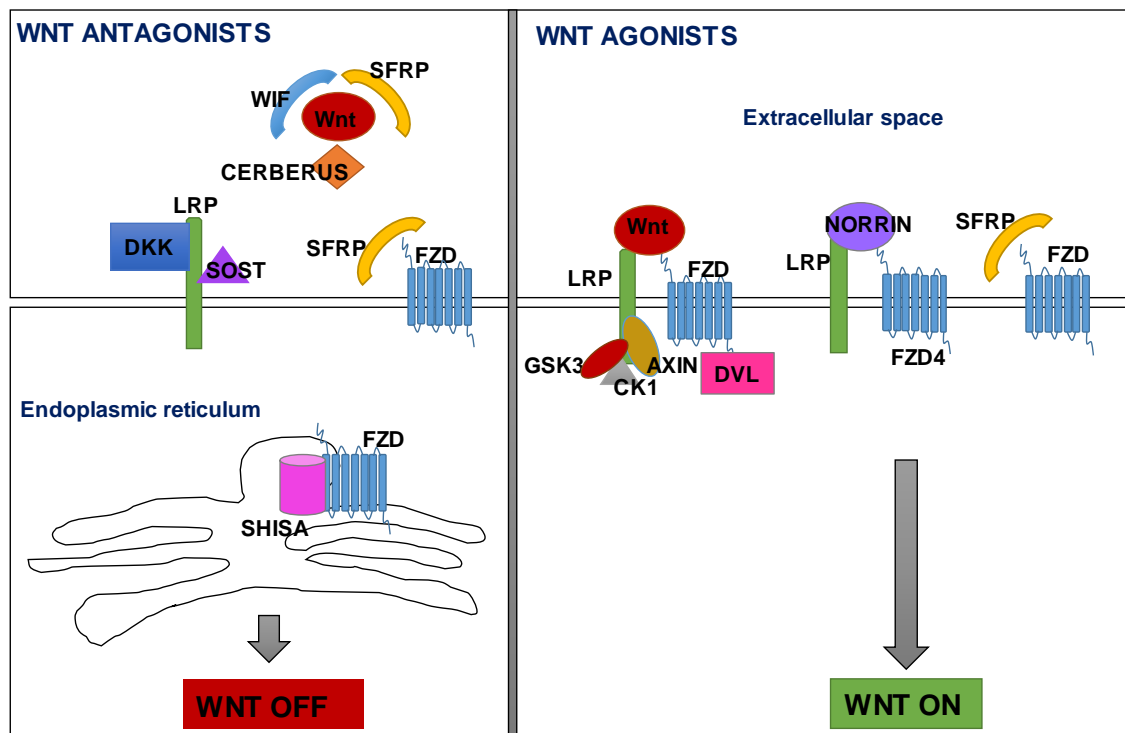


**Figure 21. Wnt signaling regulation.** Schematic overview of the different antagonist and agonist of the Wnt signaling.

Recent studies have revealed additional mechanisms of regulation of Wnt signaling at the membrane (Cruciat & Niehrs 2013; Malinauskas & Jones 2014; Hao et al. 2016). The transmembrane E3 ubiquitin ligases ZNRF3 (Zinc and Ring Finger 3) and RNF43 (Ring Finger Protein 43) inhibit Wnt signaling by targeting FZD receptors for ubiquitination and degradation. ZNRF3 and RNF43, in turn, are regulated by R-Spondins (RSPO1-4), secreted proteins that enhance Wnt signaling by simultaneously binding ZNRF3/RNF43 and leucine-rich repeat-containing G protein-coupled receptors (LGR4-6) to promote ubiquitination and membrane clearance of ZNRF3/RNF43, thus facilitating FZD receptor stabilization (Hao et al. 2012; Hao et al. 2016) (**Fig. 22**).

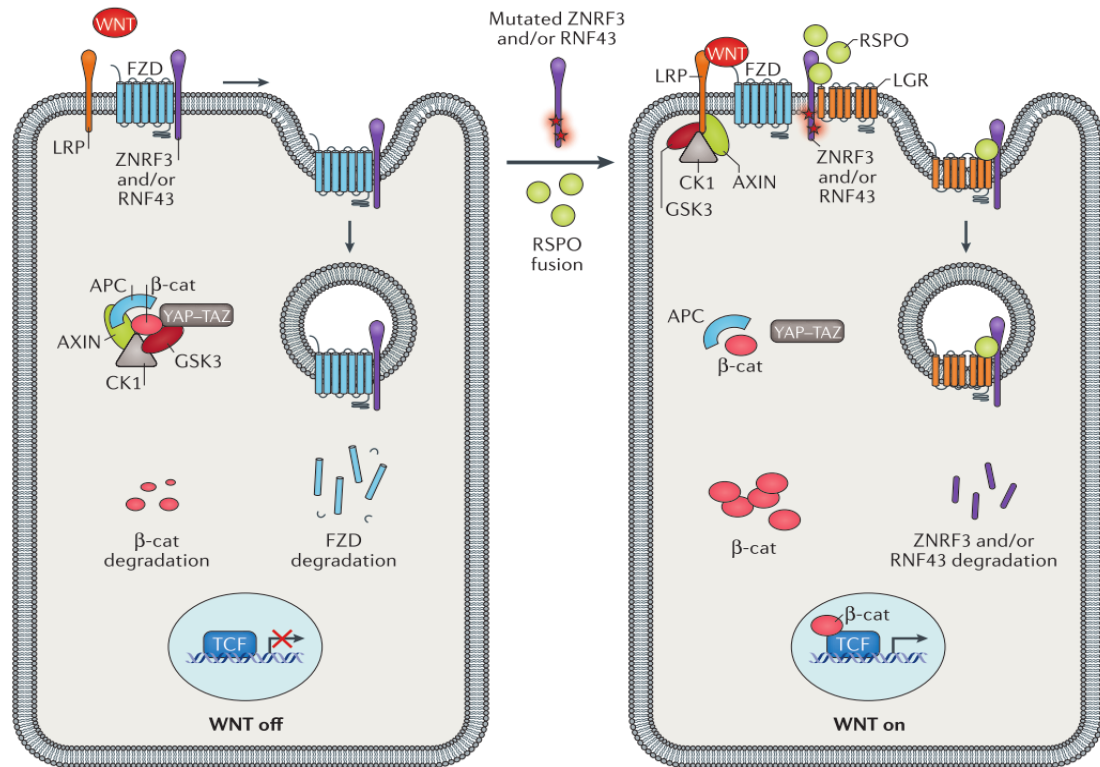


**Figure 22. Wnt signaling regulation by RNF43/ZNRF3/RSPO.** RNF43 and ZNRF3 ubiquitin ligases inhibit Wnt signaling by ubiquitinating FZD receptors, promoting their degradation. R-Spondin (RSPO) binds RNF43/ZNRF3 and LGR5, resulting in membrane clearance of RNF43 and ZNRF3 and increased FZD stability. Mutations in *RNF43* and *ZNRF3* or overexpression of RSPO as a result of a RSPO gene fusion activate Wnt signaling. Taken from Murillo-Garzón & Kypta, 2017.

## 6. Wnt signaling in cancer

A role for Wnts in cancer was first described three decades ago in mouse models of mammary cancer and in human and mouse colon cancer (Nusse & Varmus 1982; Korinek et al. 1997; Morin et al. 1997). Since then, alterations in Wnt signaling have been described in different types of cancer, including colon, breast, lung and prostate (Polakis 2000; Clevers 2006; Polakis 2012; Anastas & Moon 2013) among others. Different roles have been defined for Wnt signaling in a cancer-stage-specific and a cancer-type-specific manner. In this regard, Wnt signaling is able to either promote or inhibit tumor initiation, growth and metastases and is also involved in drug resistance (Anastas & Moon 2013).

### 6.1 Wnt alterations in prostate cancer

Activating mutations in the gene encoding  $\beta$ -catenin (*CTNNB1*) and inactivating mutations in the genes that encode proteins in the destruction complex (*APC* and *AXIN1*) increase Wnt– $\beta$ -catenin signaling in many types of cancer, particularly colorectal cancer,



but are infrequent in prostate cancer (Murillo-Garzón & Kypta 2017). Nevertheless, recent studies analyzing 150 CRPC tumors revealed genomic alterations affecting *APC* and *CTNNB1* in 18% of samples (Robinson et al. 2015). Moreover, high expression of  $\beta$ -catenin and  $\beta$ -catenin partners such as AR have been found to be associated with high Gleason grade, disease progression and PSA levels (Murillo-Garzón & Kypta 2017) **(Table 1)**.

The low frequency of Wnt signaling pathway gene mutations in the majority of prostate tumors has encouraged the study of upstream components of the pathway. In this respect, alterations in Wnt ligands such as Wnt-5a, Wnt-7b or Wnt-11 and Wnt regulators including sFRP and DKK have been reported (Murillo-Garzón & Kypta 2017). Particularly, mutations in the ubiquitin ligases *RNF43* and *ZNRF3* and gene fusions that increase expression of *RSPO2* were detected at an overall frequency of 6% in a panel of 150 metastatic CRPC tumors (Robinson et al. 2015), suggesting novel therapeutic options might be a possibility for some patients with prostate cancer **(Table 1)**.

Perturbations in the levels of Wnt receptors have also been described in prostate cancer. *FZD2* was found as a Wnt-5a receptor involved in the activation of PKC and JNK (Yamamoto et al. 2010). Moreover, *FZD2* was required for prostate cancer cell invasion and expression of metalloproteinase-1 (MMP-1), thereby promoting aggressiveness of prostate cancer (Yamamoto et al. 2010). Increased expression of *FZD2* as a Wnt-5a receptor has also been reported in prostate tumors and their expression is associated with EMT and higher Gleason score (Sandsmark et al. 2017). The oncogene *ERG*, expressed in prostate tumors with *TMPRSS2-ERG* rearrangements, has been found to increase the expression of several FZD receptors, including *FZD3*, *FZD5* and *FZD7* (Brase et al. 2011) and *FZD8* (Brase et al. 2011; Chakravarthi et al. 2018), and also *FZD4*, which has a role in EMT (Gupta et al. 2010). Independent studies reported increased expression of *FZD8* (Pascal et al. 2009) and its closest relative protein, *FZD5*, in advanced prostate cancer (Thiele et al. 2011). Among the coreceptors, ROR1 protein was shown to be expressed at high levels in 19 of 21 prostate tumors (S. Zhang et al. 2012) **(Table 1)**.

<b>WNT pathway component</b>	<b>Alteration</b>	<b>Disease stage</b>	<b>Effect on WNT signaling, on prostate cancer cells and on patients if known</b>
<b>β-catenin (CTNNB1)</b>	Activating mutations	CRPC	Disease progression (mice)
<b>APC</b>	Inactivating mutations SNPs	CRPC Advanced prostate cancer	Disease progression (mice) Decreased PSA-free survival
<b>Ligands</b>			
<b>WNT5A</b>	Upregulation	CTCs from CRPC and ADT patients with tumors and metastases Localized cancer	Noncanonical; increased CRPC growth, bone metastasis; metastasis and recurrence Increased survival, improved outcome
<b>WNT7B</b>	Upregulation	Tumor CTCs from patients receiving ADT	Noncanonical; induces osteoblastic response in bone
<b>WNT11</b>	Upregulation	ADT, metastases	Noncanonical; promotes invasion and neuroendocrine-like differentiation
<b>WNT16B</b>	Upregulation	Tumor stroma	Canonical; therapy resistance
<b>Receptors</b>			
<b>FZD2</b>	Upregulation	CRPC	Recurrence
<b>FZD4</b>	Upregulation	ERG positive tumors	Canonical and noncanonical: EMT
<b>FZD5</b>	Upregulation	Tumors	Noncanonical
<b>FZD8</b>	Upregulation	Tumors	Canonical and noncanonical
<b>ROR1</b>	Upregulation	Tumors	Not canonical; not known
<b>Regulators</b>			
<b>SFRP1</b>	Downregulation	Tumors	Reduced survival
<b>SFRP2</b>	Upregulation	Tumor stroma	Potentialiation of WNT-16B; therapy resistance
<b>DKK1</b>	Upregulation	Serum, tumors	Increased tumor growth, bone metastases and osteolytic lesions in mice; poor prognosis in patients
<b>DKK3</b>	Downregulation	Tumors	Inhibits tumor growth and metastasis
<b>ZNRF3/RNF43</b>	Inactivating mutations	CRPC	Potentialiation of WNT signals
<b>RSPO2</b>	Upregulation (gene fusion)	CRPC	Potentialiation of WNT signals

**Table 1. Key changes in Wnt signaling pathways components in prostate cancer.** Adapted from Murillo-Garzón & Kypta 2017.

## 6.2 Targeting Wnt signaling

Specific Wnt pathway inhibitors has been developed that can be classified into functional groups (Murillo-Garzón & Kypta 2017) (**Fig. 23**):

- a) Inhibition of Wnt secretion: this strategy has relied on targeting porcupine which is responsible for Wnt palmitoylation. Drugs in this group include IWPs (Chen et al. 2009), Wnt-C59 (Proffitt et al. 2013), LGK974 (Liu et al. 2013), and ETC-159 (Madan et al. 2016).
- b) Regulation of Wnt antagonists or agonists: in this approach are included for example the use of recombinant SFRP1 protein (Ghoshal et al. 2015), as well as an adenoviral vector expressing DKK3 (Veeck & Dahl 2012) and RSPO blocking antibodies such as OMP-131R10 (Storm et al. 2015).
- c) Preventing DVL activation: since DVL is crucial for signal transduction different inhibitors have been developed, for example 3289-8625 (Grandy et al. 2009).
- d) Stabilizing the destruction complex: this strategy is based on tankyrase inhibitors that target Axin for proteasomal degradation. This group include inhibitors such as IWR (Haikarainen et al. 2014), XAV-939 or NVP-TNKS656 (Shultz et al. 2013)
- e) Targeting nuclear  $\beta$ -catenin partners: drugs such as iCRTs (Gonsalves et al. 2011), which prevent  $\beta$ -catenin/TCF interaction or ICG-001 (Emami et al. 2004) or PRI-724 (El-Khoueiry et al. 2013), both preventing  $\beta$ -catenin interaction with CBP coactivator, might provide new therapies.
- f) Blocking Wnt-receptor interactions: approaches focused on specific Wnts, FZD receptors or other signaling components at the cell membrane might, in principle, be more selective than manipulating the pathway at the level of its cytosolic or nuclear components and hence, better positioned to lead to clinically viable strategies. These inhibitors include drugs such as Wnt-5a antibodies (Hanaki et al. 2012) or a peptide targeting Wnt-5a (Foxy5) (Säfholm et al. 2006; Säfholm et al. 2008); OMP-54F28 (Le et al. 2015), a decoy Wnt receptor which competes with the native FZD8 for its ligand; OMP-18R5 (Gurney et al. 2012), which target FZD1,2,5,7 and 8; OTSA10 (Fukukawa et al. 2008), targeting FZD10 or UC-961 (Kolb et al. 2016), which targets ROR1.

Several drugs that target Wnt signaling are currently in clinical trials, but very few of them are being tested for the treatment of prostate cancer. However, the increased frequency of *APC* mutations, identification of novel mutations in CRPC, and the growing

evidence that noncanonical Wnt signals are active in prostate cancer, are anticipated to stimulate further interest in this area of drug development (Murillo-Garzón & Kypta 2017).

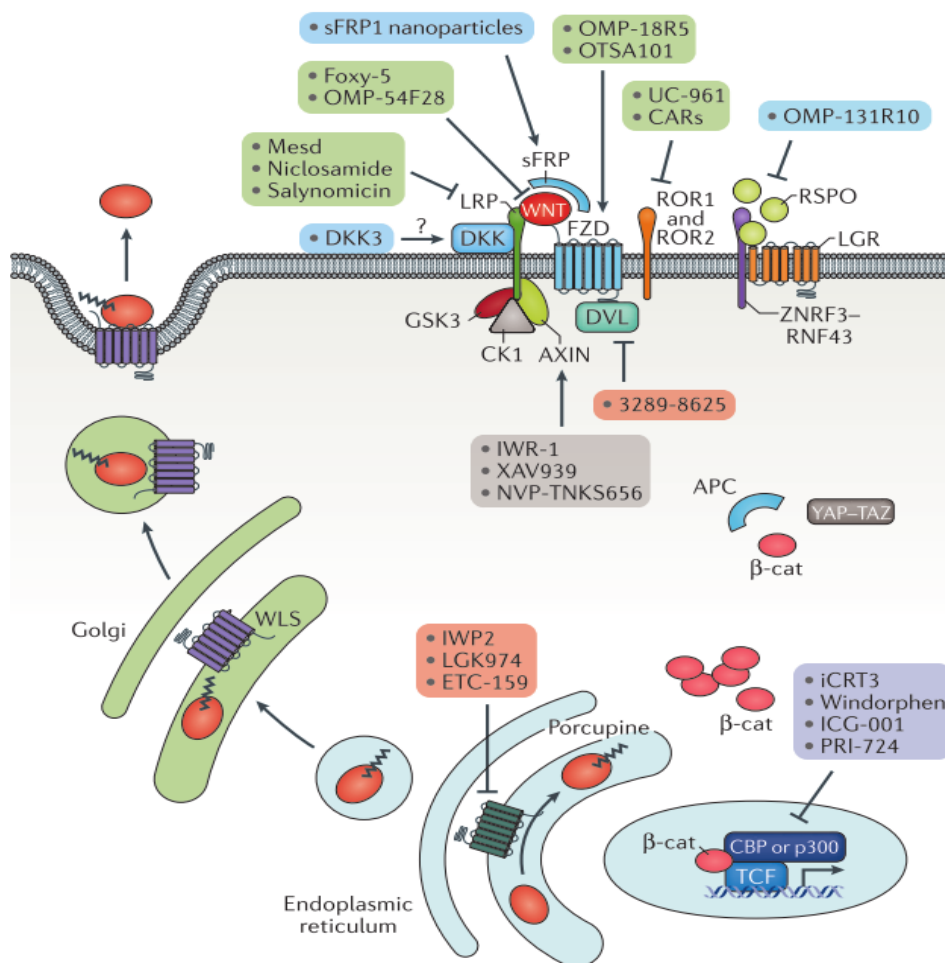


**Figure 23. Drugs that target Wnt signaling.** Many drugs have been developed that act on different targets at different levels in the Wnt signaling pathway. The therapeutics are inhibitors of Wnt secretion (red), regulators of Wnt antagonist and antagonist function (blue), drugs that target Wnt receptor interactions (green), drugs that prevent disheveled (DVL) activation (pink), drugs that stabilize the destruction complex (grey), and drugs that target β-catenin (β-cat) partners in the nucleus (purple). Taken from Murillo-Garzón & Kypta, 2017.

## 7. Wnt signaling crosstalk with other pathways: TGF-β signaling

The Transforming Growth Factor beta (TGF-β) family of cytokines, characterized by six conserved cysteine residues, contains two subfamilies, the TGF-β/Activin/Nodal subfamily and the BMP (bone morphogenetic protein)/GDF (Growth and Differentiation Factor)/MIS (Mullerian Inhibiting Substance) subfamily (Shi & Massagué 2003). Most members of this family exist in different forms, with the TGF-β cytokine consisting of three isoforms: TGF-β1, TGF-β2, and TGF-β3.

TGF- $\beta$  ligands are synthesized within the cell as 75-kDa homodimers that are then cleaved in the Golgi to produce mature 25-kDa TGF- $\beta$  homodimers. TGF- $\beta$  homodimers bind latency-associated proteins (LAPs) through a disulphide bond, generating a large latent complex in the ER. These complexes are secreted to the extracellular matrix to interact with fibronectin fibrils and heparan sulfate proteoglycans at the cell membrane and are stored in fibrillin-rich microfibrils in the extracellular matrix (Cao & Kyprianou 2015). Latent TGF- $\beta$  is activated and released from the latent complex by proteases, reactive oxygen species, integrins and thrombospondin 1 to form active signaling molecules (Padua & Massagué 2009; Cao & Kyprianou 2015).

TGF- $\beta$  uses a simple mechanism to signal from the cell membrane to the nucleus that involves binding to specific kinase receptors at the surface of target cells and the activation of Smad family transcription factors. However, non-Smad pathways have also been described (Shi & Massagué 2003; Kubiczkova et al. 2012)

### 7.1 TGF- $\beta$ signal transduction

For initiation of TGF- $\beta$  signaling, active TGF- $\beta$  homodimers bind to two pairs of type I and type II serine/threonine kinases receptors forming a heterotetrameric receptor complex. The constitutively active type II receptor comes in close contact with the type I receptors whose interaction can be negatively regulated by the pseudo-receptor BAMBI by intercalating in the receptor complex (Massagué et al. 2005). TGF $\beta$ RII binding to TGF $\beta$ RI causes the phosphorylation of a 30-amino-acid regulatory segment called the GS region, located immediately upstream of the kinase domain. Phosphorylation of the type I receptor disrupts the interaction between the kinase domain and a TGF- $\beta$  signaling inhibitor, FKBP12 (FK506 binding protein-12). With the release of FKBP12 from the active site, the Smad transcription factors are then able to form a heteromeric complex with the receptors and be phosphorylated by them at their C-terminal domains (Massagué 2000; Padua & Massagué 2009). Smad phosphorylation by receptors causes their activation and translocation to the nucleus, where they assemble complexes with other nuclear cofactors to directly control target gene expression (Massagué 2000; Shi & Massagué 2003) (**Fig. 24**). Members of many other DNA-binding protein families participate as Smad cofactors, including FOX, HOX, RUNX, E2F, AP-1, CREB/ATF, Zinc-finger and other families and these interaction facilitates target gene specificity (Kubiczkova et al. 2012).

However, the diversity of TGF- $\beta$  signaling in cells is determined not only by various ligands, receptors, Smad mediators and Smad-interacting partners, but also by the ability

of TGF- $\beta$  to activate other signaling pathways. These Smad-independent pathways include various branches of mitogen-activated protein kinase (MAPK) pathways, Rho-like GTPase signaling pathways, and PI3K/AKT pathways (Zhang 2009; Kubiczkova et al. 2012) (**Fig. 24**).

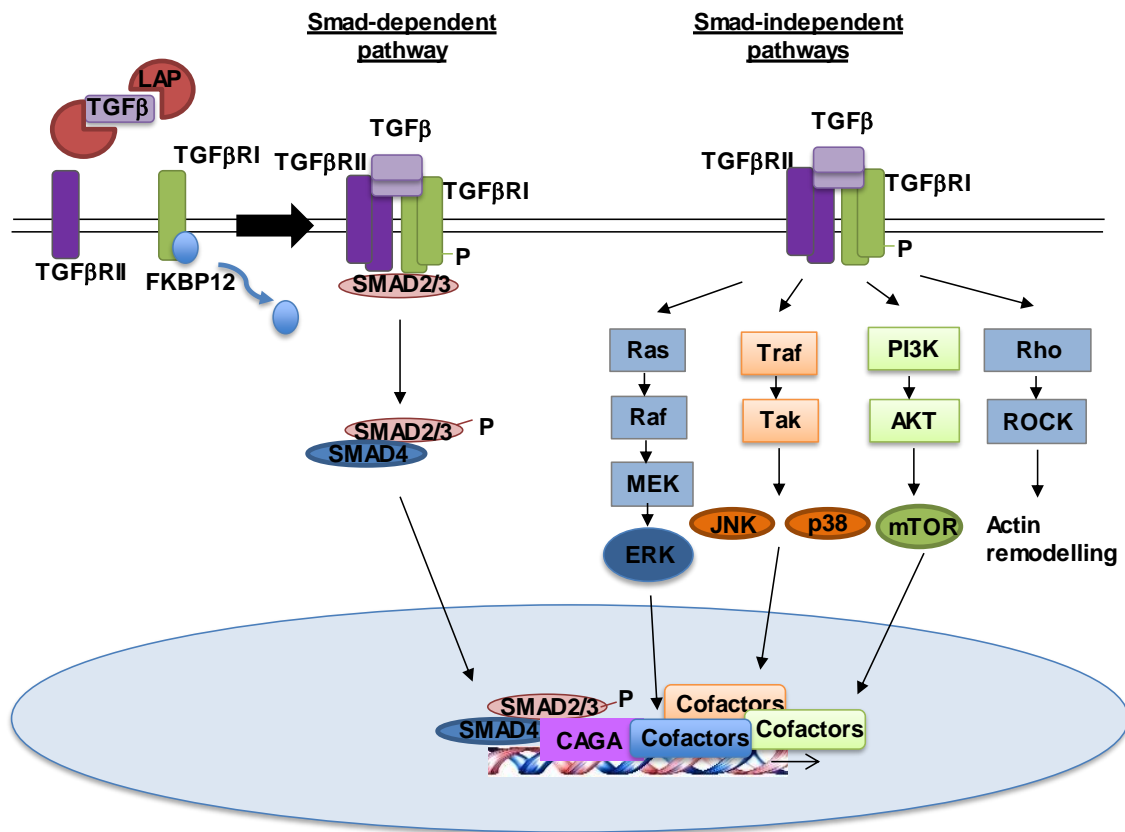


**Figure 24. Smad-dependent and Smad-independent pathways.** In the inactive state, TGF- $\beta$  remains latent bound to latency associated proteins (LAPs) and FKBP21 blocks the phosphorylation site of TGF- $\beta$ RI. When TGF- $\beta$  is active, a heteromeric complex is formed with TGF- $\beta$ RII and I and the latter is phosphorylated by TGF- $\beta$ RII. This phosphorylation allows Smad phosphorylation and its translocation to the nucleus where it binds to other cofactors to regulate gene expression. The TGF- $\beta$  complex can also activate non-Smad pathways involving ERK/JNK/PI3K or Rho GTPases. Adapted from Padua & Masagué, 2009 and Zhang, 2009.

## 7.2 TGF- $\beta$ receptors

This family of receptors have structural characteristics similar to both serine/threonine and tyrosine kinases although they are more often referred to as serine/threonine kinase receptors (Heldin & Moustakas 2016). The human genome encodes seven type I receptors (ALKs 1-7) and five type II receptors (ActR-IIa, ActR-IIB, BMPRII, AMHRII, and TGF- $\beta$ RII) that function as receptor complexes for various members of the TGF- $\beta$  family. The type II receptors range from 85 to 110 kDa, while the type I receptors are smaller ranging from 65 to 70 kDa (Kubiczkova et al. 2012). The TGF- $\beta$ 1 ligand, which is the

most abundant isoform, preferentially signals through the TGF $\beta$ RII receptor and the ALK5 type I receptor, TGF $\beta$ RI. In addition to these two classes of receptors, type III receptors such as betaglycan, help TGF- $\beta$  ligands bind more efficiently to their receptors (Padua & Massagué 2009). The structural motifs of the receptors include small cysteine-rich extracellular domains, a transmembrane domain and a kinase domain that harbors a very short C-terminal tail (Heldin & Moustakas 2016). The type I, but not type II, receptors contain a characteristic SGSGSG sequence, termed the GS domain, immediately N-terminal to the kinase domain (Shi & Massagué 2003) (**Fig. 25**).

The activities of both TGF $\beta$ RI and TGF $\beta$ RII are regulated by several phosphorylation events. After ligand-induced assembly of the heterotetrameric TGF- $\beta$  receptor complex, the constitutively active TGF $\beta$ RII phosphorylates TGF $\beta$ RI in the GS domain, located just upstream of the kinase domain. Moreover, TGF $\beta$ RI can be phosphorylated at Ser165 in the juxtamembrane domain and auto-phosphorylated on serine/threonine residues, as well as on tyrosine residues. The kinase activity of TGF $\beta$ RII is regulated positively by auto-phosphorylation at Ser213 and Ser409, and negatively by auto-phosphorylation at Ser416. In addition, TGF $\beta$ RII can be auto-phosphorylated on tyrosine residues, including Tyr259, Tyr336, Tyr424 and Tyr470, which may also contribute to the regulation of the kinase activity of TGF $\beta$ RII, and by Src at Tyr284 and Tyr470 (Heldin & Moustakas 2016). But apart from phosphorylation, TGF- $\beta$  receptor activity and stability are also regulated by ubiquitination, neddylation and sumoylation (Heldin & Moustakas 2016). Not only that, localization of TGF- $\beta$  receptors has been shown to be regulated by endocytosis and microRNAs have been shown to negatively regulate the expression level of TGF- $\beta$  receptors (Heldin & Moustakas 2016).

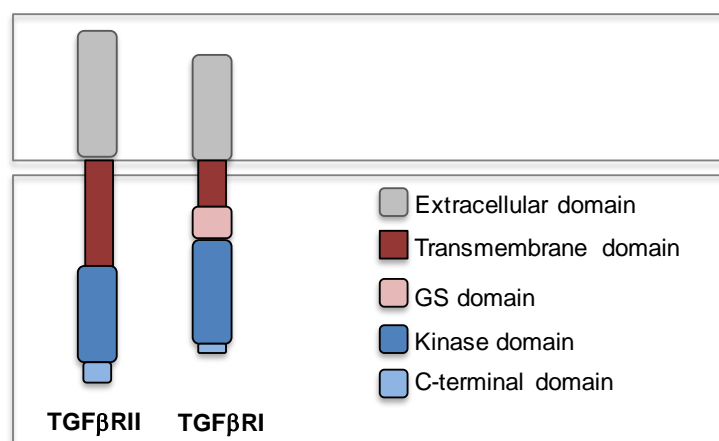


**Figure 25. Schematic illustration of the motifs of TGF- $\beta$  receptors.** Adapted from Heldin & Moustakas, 2016.

### 7.3 Smad proteins

Smad proteins are key elements in the transduction of TGF- $\beta$  signaling. In humans, the Smad family includes eight members, but only five of them (Smad1, Smad2, Smad3, Smad5, and Smad8) act as substrates for TGF- $\beta$  family receptors, being commonly named as receptor-regulated Smads, or RSmads. Smad1, 5, and 8 serve principally as substrates for the BMP and anti-Mullerian hormone receptors, and Smad2 and 3 for the TGF- $\beta$ , activin, and Nodal receptors. Apart from RSmads, Smad4, serves as a common partner for all RSmads, and Smad6 and Smad7 are inhibitory Smads (Massagué et al. 2005).

Smad proteins are ~500 amino acids in length consisting of two globular domains coupled by a linker region. The N-terminal domain, or “Mad-homology 1” (MH1) domain, is highly conserved in all RSmads and Smad4 but not in Smad6 and 7. The linker region is quite divergent between the various subgroups, whereas the C-terminal or MH2 domain is conserved in all Smad proteins. The MH1 domain is a DNA-binding module stabilized by a tightly bound zinc atom. The MH2 domain is one of the most versatile protein-interacting modules in signal transduction. RSmads have a conserved C-terminal motif, Ser–X–Ser, that is phosphorylated by the activated receptor (Massagué et al. 2005).

Smad proteins undergo a constant process of nucleo-cytoplasmic shuttling where the nuclear translocation is mediated through Smad interaction with nucleoporins. Smad nuclear accumulation results from receptor-mediated phosphorylation events that decrease the affinity of RSmads for cytoplasmic anchors and increase their affinity for nuclear factors. Subsequent de-phosphorylation of RSmads causes their return to the cytoplasm for another round of receptor-mediated phosphorylation and nuclear translocation (Massagué et al. 2005).

### 7.4 Dual role of TGF- $\beta$

All members of the TGF- $\beta$  family play important roles during development, as well as in normal physiological and disease processes, by regulating an extensive range of cellular processes, including cell growth, differentiation, migration, apoptosis, and extracellular matrix production

In cancer, a dual role of TGF- $\beta$  has been described, in which it is able to act either as a proto-oncogene or as a tumor suppressor, depending on cell context and tumor stage (Kubiczkova et al. 2012). TGF- $\beta$  is a potent anti-tumor agent because it strongly inhibits



the growth of epithelial cells. However, in a different cellular context, TGF- $\beta$  can also promote tumor progression because it is able to induce changes in transcriptional activities that re-program epithelial cells into mesenchymal cells, thereby facilitating tumor metastasis and invasion (Zhang 2009).

In the case of prostate cancer, TGF- $\beta$  plays a positive role as a tumor suppressor in normal prostate epithelial cells and premalignant lesions (high-grade intraepithelial neoplasia). However, elevation of TGF- $\beta$  expression will quickly drive tumor progression, invasion and metastasis; thus the characterization of the temporal events responsible for the transition from growth suppressor to growth promoter are key to use TGF- $\beta$  as a therapeutic target in prostate cancer (Jones et al. 2009).

### 7.5 Wnt and TGF- $\beta$ signaling crosstalk

Aberrations in Wnt signaling pathways usually drive tumorigenesis in cooperation with other signaling pathways, oncogenes and tumor suppressors. Some of these pathways include PI3K/AKT, Ras, mTOR, Notch, Hedgehog as well as EGF, FGF, VEGF or TGF- $\beta$  (Thompson et al. 2011). Among them, crosstalk between Wnt and TGF- $\beta$  signaling has been extensively studied during the last years (Guo & Wang 2009; Attisano & Wrana 2013).

There is a remarkable synchronization between Wnt and TGF- $\beta$  signaling pathways during an animal development, in which the levels of both ligands reciprocally regulated each other. Nevertheless, this synchronization takes place not only during development but also in tumor progression (Guo & Wang 2009). The best-characterized scenario of this crosstalk is the nucleus, where Smad proteins have been found to associate with  $\beta$ -catenin/Tcf/LEF complexes to regulate the expression of shared target genes (Guo & Wang 2009). However, Smads not only interact with  $\beta$ -catenin/Tcf/LEF complexes but have also been found to associate with AP-1 family transcription factors, which mediate  $\beta$ -catenin-independent Wnt signals (Padua & Massagué 2009) (**Fig. 26**)

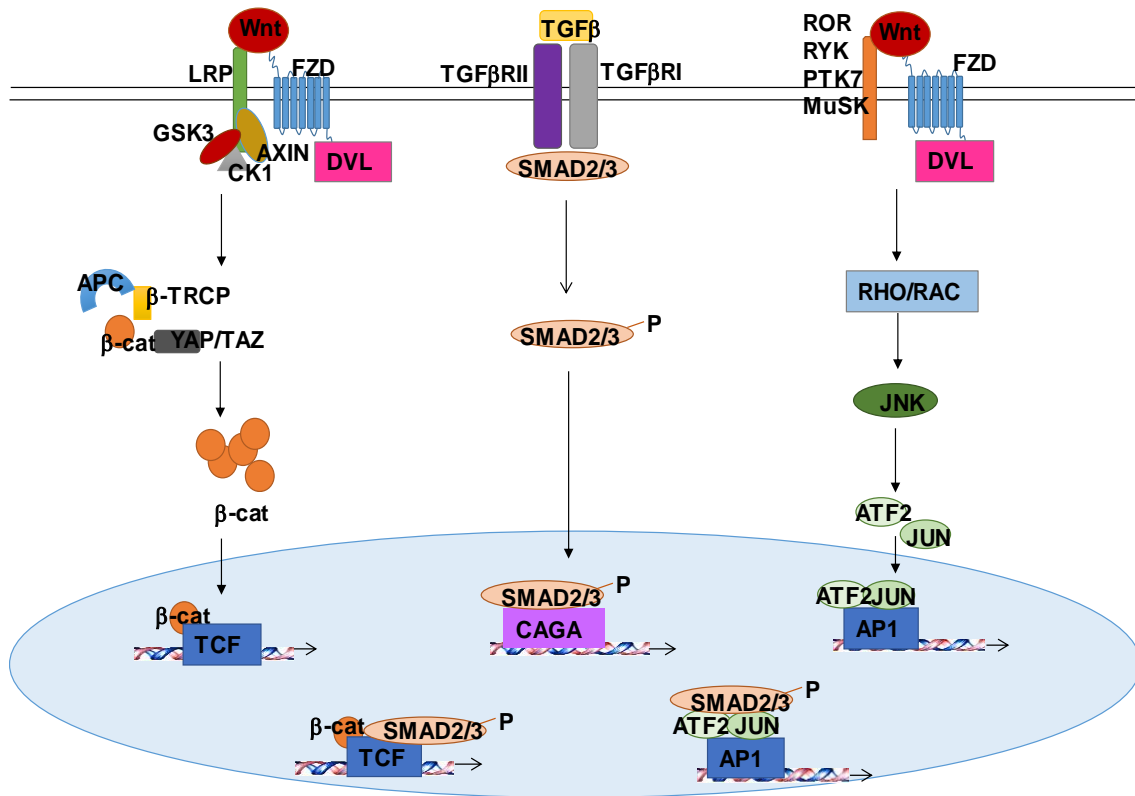


**Figure 26. Crosstalk between Wnt and TGF- $\beta$  signaling pathways.** TGF- $\beta$  communicates with Wnt signaling at several levels. Physical interactions between pathway components can occur leading to changes in target gene expression.

In prostate cancer, different studies have shown the contribution of both pathways to the progression of the disease. A paracrine TGF- $\beta$ /Wnt-3a signaling was observed to promote prostate cancer progression since it was observed that in mouse models, secretion of stromal Wnt-3a activates canonical Wnt signaling in the epithelium, facilitating progression of PIN lesions to adenocarcinoma and resistance to androgen deprivation (X. Li et al. 2008). Moreover, studies from Brase et al in 2011 showed an upregulation of target genes from Wnt and TGF- $\beta$  pathways in *TMPRSS-ERG* fusion positive tumors, which are present in approximately 50% of prostate cancer patients (Brase et al. 2011). Furthermore, some years ago Wnt signaling was found to promote progression to prostate adenocarcinoma leading to increased reactive stroma and TGF- $\beta$  signaling in mouse models of prostate cancer (Carstens et al. 2014). All these studies support the potential of combined strategies that target both TGF- $\beta$  and Wnt signaling pathways in order to improve prostate cancer treatment.

## 8. Wnt-11 signaling

Among the large family of Wnt ligands, Wnt-11 is traditionally defined as a noncanonical Wnt (Uysal-Onganer & Kypta 2012). Although its downstream effectors have not been fully characterized, Wnt-11 can activate PKC and JNK (Flaherty et al. 2008) and CREB family members (Zhou et al. 2007) and inhibit  $\beta$ -catenin dependent signaling (Railo et al. 2008; Maye et al. 2004).

### 8.1 Wnt-11 in development

Wnt-11 is best known for its role during embryonic development (Lako et al. 1998; Majumdar et al. 2003). In fact, Wnt-11 was shown to promote convergent extension movements during zebrafish gastrulation (Heisenberg et al. 2000) as well as to increase cell contact persistence to coordinate cell movements during gastrulation through accumulation of FZD7 on adjacent sites of cell contacts (Witzel et al. 2006). The involvement of Wnt-11 in convergence and extension movements has been reported to implicate its binding to ROR2 (Bai et al. 2014).

Wnt-11 was also involved in axis formation in *Xenopus* embryos (Tao et al. 2005). As previously described in zebrafish, later studies in *Xenopus* also showed that Wnt-11 induces accumulation of FZD7 at apical adherens junctions, together with polarized accumulation of Disheveled (Yamanaka & Nishida 2007). Furthermore, RYK was found to cooperate with FZD7 to mediate Wnt11-stimulated endocytosis of Disheveled and activation of the noncanonical Wnt pathway to regulate convergent extension movements (Kim et al. 2008).

In mouse kidney development, *Wnt11* mutation results in ureteric branching morphogenesis defects and consequent kidney hypoplasia in newborn mice. In this study, Wnt-11 cooperates in a positive autoregulatory feedback loop with Ret/Gdnf, a mesenchymally produced ligand that is crucial for normal ureteric branching, (Majumdar et al. 2003). Moreover, FZD4 and FZD8 act as Wnt-11 receptors during this process (Ye et al. 2011).

The role of Wnt-11 in cardiomyocyte differentiation has also extensively described (Pandur et al. 2002; Flaherty et al. 2008; He et al. 2011; Abdul-Ghani et al. 2011), where the effects of Wnt-11 involve activation of noncanonical pathway in all cases.

## 8.2 Wnt-11 in cancer: implication in prostate cancer

Apart from its role in development, Wnt-11 has also been linked to different types of cancer such as colon (Dwyer et al. 2010; Ouko et al. 2004; Nishioka et al. 2013), lung (Bartis et al. 2013) and prostate (Zhu et al. 2004; Dwyer et al. 2010; Uysal-Onganer et al. 2010), where it promotes cancer cell migration, adhesion and survival, all hallmarks of advanced disease. However, some controversy exists since a tumor suppressor role for Wnt-11 has been described in hepatocellular carcinoma, where it reduces cell migration by activating Rho and inhibiting Rac (Toyama et al. 2010), and in ovarian cancer where Wnt-11 overexpression reduces cell migration and invasion as well as tumor growth and metastasis *in vivo* (Azimian-Zavareh et al. 2018).

Particularly, in prostate cancer, *WNT11* messenger RNA (mRNA) levels are elevated in a subset of high-grade prostatic tumors, in CRPC xenografts and in tumor metastases (Zhu et al. 2004; Uysal-Onganer et al. 2010). Inhibition of AR signaling increases expression of *WNT11*, and Wnt-11, in turn, inhibits AR-dependent transcriptional activity and AR-dependent proliferation (Zhu et al. 2004) and promotes prostate tumor cell survival, migration and invasion and neuroendocrine-like differentiation (NED) (Uysal-Onganer et al. 2010). Moreover, Wnt-11 has been reported to be a direct target of ERG transcription factor (Mochmann et al. 2011; Sreenath et al. 2011; Wu et al. 2013). *WNT11* expression was also found elevated in tumors from patients receiving ADT, which supports its involvement in prostate cancer progression (Volante et al. 2016).

Different FZD family receptors can interact with Wnt-11, including FZD7 in *Xenopus* (Djiane et al. 2000; Penzo-Mendéz et al. 2003; Yamanaka & Nishida 2007), FZD5 (Cavodeassi et al. 2005) and FZD7 (Witzel et al. 2006) in zebrafish, FZD4 in differentiating cardiomyocytes (Abdul-Ghani et al. 2011; Ye et al. 2011) and FZD4 and FZD8 in the developing kidney (Ye et al. 2011). Given the known complexity of Wnt signaling, it is likely that the Wnt-11-receptor signaling will be determined not only by the specific member(s) of the FZD family involved, but also by cell context and the pool of other receptors expressed (Grumolato et al. 2010; Niehrs 2012).

Even though some Wnt receptors have been implicated in prostate cancer progression (see 6.1 Wnt alterations in prostate cancer), the specific receptors that transduce Wnt-11 signals in prostate cancer still remain unknown and their identification may provide novel therapeutic targets for this disease.



---

# **HYPOTHESIS AND AIMS**

---



Previous results from Dr.Kypta's group demonstrated that Wnt-11 was elevated in a subset of high-grade prostatic tumors, in CRPC xenografts and in tumor metastases (Zhu et al. 2004; Uysal-Onganer et al. 2010). Moreover, Wnt-11 was found to promote prostate cancer cell migration and invasion (Uysal-Onganer et al. 2010), both hallmarks of advance disease. Independent studies also reported that *WNT11* was highly expressed in tumors from patients receiving ADT which supports its involvement in prostate cancer progression (Volante et al. 2016).

Since Wnt-11 receptors in prostate cancer are not known, we hypothesize that identifying and characterizing the receptors that mediate Wnt-11 migration and invasion in prostate cancer cells could represent potential therapeutic target to treat this disease.

Based on this knowledge, the main aims of the project are to identify Wnt-11 receptors in metastatic prostate cancer and characterize their requirement for the pathway and their functional effects on prostate cancer progression.

The specific aims of the project are:

- a) To identify highly expressed Wnt receptors in metastatic prostate cancer through screening analysis in a panel of prostate cancer cell lines as well as through *in silico* profiling in prostate tumors.
- b) To characterize the Wnt-11/receptor signaling pathway through evaluation of canonical/noncanonical reporters, study of target genes as well as the analysis of Wnt-11/receptor interaction and localization.
- c) To evaluate the functional effects of Wnt-11 receptors driving prostate cancer cell invasion and metastasis through *in vitro* and *in vivo* models.
- d) To characterize the molecular mechanism underlying Wnt-11/receptor signaling in prostate cancer cells.
- e) To analyze the potential relevance of Wnt-11 receptors as biomarkers for prostate cancer progression as well as their potential use as therapeutic targets.







---

**MATERIALS AND  
METHODS**

---



## 1. Cell culture

The prostate cancer cell lines LNCaP, PC-3 and VCaP were from the American Type Culture Collection (ATCC) as were human embryonic kidney HEK293T cells. PC-3M cells were provided by Scott Fraser and Mustafa Djamgoz (Imperial College London), LNCaP and C4-2B cells were from Charlotte Bevan (Imperial College London) and DU145 cells were from John Masters (University College London) and Magali Williamson (Kings College London). Cell lines were authenticated by DNA profiling (Eurofins Genomics, Germany) and cells were routinely tested for mycoplasma. Low passage cell stocks were cultured for up to six months after thawing. LNCaP, C4-2B, PC3, PC-3M and DU145 cells were cultured at 37°C, 5% CO<sub>2</sub> in RPMI-1640 with GlutaMAX™ (Invitrogen) supplemented with 10% fetal bovine serum (FBS; First Link, UK) and antibiotics (100 units/mL penicillin, 100 µg/mL streptomycin, Invitrogen, UK). For some experiments LNCaP cells were cultured in medium containing 5% charcoal-stripped serum (CSS, First Link, UK) for 3 or 6 days. VCaP cells were cultured in DMEM/Ham's F12, 10% FBS, antibiotics, 0.5% sodium pyruvate and 1.5 mM glutamine. HEK293T cells were cultured in DMEM, 10% FBS and antibiotics. For transfections, cells were cultured in OptiMEM (Gibco). The main features of the used prostate cancer cell lines are summarized in **Table 2**.

Cell line	First isolation	Hormone status	AR	PSA	Other markers
<b>LNCaP</b>	Lymph node metastatic prostate adenocarcinoma (1980)	Androgen dependent	Positive	Positive	p53 wild type/PTEN negative
<b>LNCaP C4-2B</b>	Subline of LNCaP mouse xenografts (1994)	Androgen independent	Positive	Positive	Low levels of p53 /PTEN negative
<b>VCaP</b>	Vertebral metastatic lesion (2001)	Androgen dependent	Positive	Positive	p53 mutation/ PTEN positive/TMPRSS2-ERG gene rearrangement
<b>PC-3</b>	Vertebral metastatic prostate tumor (1979)	Androgen independent	Negative	Negative	p53 deletion/PTEN negative
<b>PC-3M</b>	Subline of PC-3 mouse xenografts	Androgen independent	Negative	Negative	p53 deletion/PTEN negative
<b>DU145</b>	Brain metastatic prostate tumor (1975)	Androgen independent	Negative	Negative	p53 mutation P53/PTEN positive

**Table 2. Characteristics of the prostate cancer cell lines.**

## 2. Compounds

TGF- $\beta$ 1 (R&D Systems) was added in gene reporter assays at a concentration of 0.1 or 1 ng/mL 4 h after transfection of reporter and incubated for 24 h. For q-RT-PCR analysis, cells were treated with 1 ng/mL TGF- $\beta$  for 24 h. For evaluation of TGF- $\beta$ -induced Smad phosphorylation, 1 ng/mL TGF- $\beta$  was added to cells 48 h after silencing for 30 min. Inhibitor 1 (3235-0367) and 2 (2124-0331) from the ChemDiv library (Lee et al. 2015) were used in migration experiments at 10  $\mu$ M for 24 h. For miniaturized tridimensional (3D) cultures and the chicken chorioallantoic membrane (CAM) assays, phenol red free matrigel (BD Biosciences, Vantaa, Finland) was used at a concentration of 8 ng/mL.

## 3. Plasmids and siRNAs

Different plasmids were used in this work which are described in **Table 3**.

Plasmid	Source	Reference
pcDNA Wnt-11		(Uysal-Onganer et al. 2010)
PA-Wnt11	Junichi Takagi	(Mihara et al. 2016)
pRL-Tk	Promega	
Super8XTOP/FOPFlash	Randall Moon (Addgene Plasmid #12456)	(M. Veeman et al. 2003)
AP-1-luc		(Vivanco et al. 1995)
CAGA12-luc		(Dennler et al. 1998)
ATF2-luc	Christof Niehrs	(van der Sanden et al. 2004)
pRK5 mFzd1-10-1D4	Chris Garcia and Jeremy Nathans (Addgene #42263-42272).	(Yu H, Ye X, Guo N 2012)
CMV500	Charles Vinson (Addgene #33348)	(Rishi et al. 2004)
CMV500 $\Delta$ -ATF2	Charles Vinson (Addgene #33362)	(Rishi et al. 2004)
3TP-lux	Joan Massagué and Jeff Wrana (Addgene #11767)	(Wrana et al. 1992)
HA-FZD8	Jeffrey Rubin	
pRK5 TGF $\beta$ RI-Flag	Rik Derynck (Addgene #14831)	(Feng & Derynck 1996)
pCMV5B TGF $\beta$ RII wild-type (N-term HA)	Jeff Wrana (Addgene #24801)	
pRK5 mFz8CRD IgG	Xi He (Addgene #16689)	(Semenov et al. 2001)
pCS2 LRP6N-IgG	Xi He (Addgene #27279)	(Tamai et al. 2000)
pRK5-Flag-ALK5-HA (ecto)	Rik Derynck (Addgene #31720)	
Flag-SMAD3	Wei Cui	
HA-ATF2	Pedro Lazo	

**Table 3. List of plasmids used in this study.**

SMARTpool siRNAs were purchased from Dharmacon, ThermoFisher and dsRNA from Integrative DNA Technologies (IDT, Leuven Belgium). The siRNAs and dsRNA used are listed in **Table 4**.

Distributor	siRNA /dsiRNA	Sequence 5'3'	siRNA /dsiRNA Concentration (nM)
SMARTpool (Dharmacon, Thermo Fisher)	FZD2	CCACGUACUUGGUAGACAU	25-50
		GAACUGCGCUUCUCCUGU	
		GGAGGAAGUUCUACACUCG	
		GCUACAAGUUUCUGGGCGA	
SMARTpool (Dharmacon, Thermo Fisher)	FZD3	CCAAAUACUCCUAUCAUAA	25-50
		ACAGAUCACUCCAGGCAUA	
		GUUCGAAGCUCAUGGAGAU	
		UGAUUGAUGUCACAAGAUU	
SMARTpool (Dharmacon, Thermo Fisher)	FZD4	GAUCGAUUCUUCUAGGUUU	25-50
		UCACACCGCUCAUCCAGUA	
		GGACAAAGACAGACAAGUU	
		CCAAGGAGUUCACUGAUAU	
SMARTpool (Dharmacon, Thermo Fisher)	FZD5	GCAUUGUGGUGGCCUGCUA	25-50
		GCACAUGCCCAACCAGUUC	
		AAAUCACGGUGCCCAUGUG	
		GAUCCGCAUCGGCAUCUUC	
SMARTpool (Dharmacon, Thermo Fisher)	FZD8	AGACAGGCCAGAUUCGUAA	25-50
		ACACCUACAUGCCCAAUCA	
		UCACCGUGCCGCUGUGUAA	
		CGGCGAGCUCCGUGUCUUA	
Integrated DNA Technologies (IDT)	dsiFZD8	rArGrCrUrCrCrGrUrGrUrCrUr UrArUrCrCrArArGrCrAGA	25-50
		rUrCrUrGrCrUrUrUrGrGrArUr ArArGrArCrArCrGrGrArGrCrU CG	

**Table 4.** Table summarizing the siRNAs and dsRNA used in this study.

## 4. RNA analysis

### 4.1 RNA extraction and cDNA synthesis

Total cellular RNA from prostate cancer cells was extracted using TRIzol (Invitrogen Life Technologies, Burlington, ON) according to the manufacturer's protocol. For the silencing experiments, RNA was extracted using illustra™ RNAspin Mini Isolation Kit (GE Healthcare). DNase treatment was performed on columns, as instructed by manufacturer. In both cases, the concentration and purity of RNA samples was determined by the spectrophotometric measurement of the absorbance at 260nm and 280nm using ND-1000 spectrophotometer (NanoDrop Technologies). In general, 2 µg of total RNA was used for cDNA synthesis using M-MLV Reverse Transcriptase and RNase OUT Ribonuclease Inhibitor (Invitrogen), according to manufacturer's instructions. Amounts of reagents for cDNA synthesis of one sample are described in **Table 5** and they were scaled up as necessary.

Reagent	Stock concentration	Final concentration	Volume (ul)
Ramdon primers (Life technologies)	100ng/µL	5 ng/µL	2
dNTP mix (Bioline)	10mM (2,5mM each)	1 mM (250 uM/each)	4
5X First Strand Buffer (Invitrogen)	5X	1X	8
DTT (Invitrogen)	0,1M	5mM	2
M-MLV-Reverse transcriptase (Life Technologies)	200U/µL	5,U/µL	1
RNase OUT (Life Technologies)	40UµL	1U/µL	1
RNA+ H2O (Sigma)	Variable	Variable	22

**Table 5. Protocol for the retro-transcription procedure.** Original and final concentrations are described.

### 4.2 Primer design and setup

Primers were designed using the Primer-BLAST tool (<https://www.ncbi.nlm.nih.gov/tools/primer-blast/>) aiming to detect as many genetic isoforms as possible targeting a unique sequence for each gene of 80-150bp. When possible, primers were separated by an intron to avoid genomic DNA amplification. Melting temperature about 61-63°C, minimum self-complementarity, GC content between 30-55% and minimum differences between forward and reverse melting temperature were established as optimal parameters in order to obtain high efficient primers.

The USC Genome Browser (<https://genome.ucsc.edu/>) was used to double-check that the designed primers were amplifying the target genes. After that, primer amplification efficiency was tested by serial dilution of cDNA (1X, 0.5X, 0.2X, 0.1X, 0.05X) and standard Curve analysis using the  $\Delta\Delta\text{CT}$  method. Amplicons were run on agarose gels to confirm their correct size.

### 4.3 Quantitative Real-Time PCR

Quantitative-PCR was performed using PerfeCTa SYBR® Green Supermix, Low Rox (Quanta, Barcelona, Spain) in a Viia7 Real-Time PCR System (Applied Biosystems, Madrid, Spain) with the following conditions: Taq polymerase activation 95°C 3 min, denaturation 95°C 15 sec, annealing/extension 62°C 1 min, melting curve 95°C 15 sec, 60°C 1 min, 95°C 15 sec, 40 cycles. All reactions were done in a final volume of 6 $\mu\text{L}$  (5 $\mu\text{L}$  of mix and 1 $\mu\text{L}$  cDNA). Relative levels of mRNA were determined according to the  $\Delta\Delta\text{CT}$  quantification method, relative to the housekeeping gene 36B4. The primers used are listed in **Table 6**.

Primer	Sequence 5-->3'	Primer concentration (nM)
FZD1 F	CATTCTCTAGTGTCTAAAACCT	300
FZD1 R	TAACATTTTATAACCCATATCTTC	300
FZD2 F	ATTCGCTGCACCAAGTGCTTC	300
FZD2 R	CGAATGCTTCCCCTAGACATGA	300
FZD3 F	TGATGGCTCTCATAGTTGGCA	300
FZD3 R	ACCTGTGGCTCTCATTACAC	300
FZD4 F	GACAACCTTTCACACCGCTCA	900
FZD4 R	TCTTCTCTGTGCACATTGGC	900
FZD5 F	GTACCCAGCCTGTGCTAAA	300
FZD5 R	CCGAGAAGAGCAGACAGTCC	300
FZD6 F	TCCCAGATGTATGAAAATGGC	900
FZD6 R	CCAGATTTGCGAGAGGAAGA	900
FZD7 F	GCCTCTGTTGCTACCTC	300
FZD7 R	GTCGTGTTTCATGATGGTGC	300
FZD8 F	GCTCTACAACCGCGTCAAGA	900
FZD8 R	GCTGAAAAAGGGGTTGTGGC	900
FZD9 F	TGGCGGTCTTCATGCTCAA	300
FZD9 R	TATCTTGCGGTAGCACAGGC	300
FZD10 F	CCGCCTCACACCCAGTGGAT	300
FZD10 R	TTCTGTCTTGACAGAGACTATT	300
VANGL1 F	GCTTCTACAGCCTGGGACAC	300
VANGL1 R	GCTCGGAATTTGGAGGCTGT	300
VANGL2 F	AAGTCGGGCCACTCCCGCAG	300
VANGL2 R	CCCATCTCGACTCTTAGAGC	300

<b>ROR1 F</b>	AAAGAGCTACCTCTTTCTGCTGTACG	300
<b>ROR1 R</b>	CTTCTTGTTGAAATCCCGTCCATTG	900
<b>ROR2 F</b>	GGCAGAACCCATCCTCGTG	300
<b>ROR2 R</b>	CRACTGCGAATCCAGGACC	300
<b>RYK F</b>	TCTCTACCTGAGCGAGGACG	300
<b>RYK R</b>	CCAGGTGAAAGTGCAGGAAAT	300
<b>PTK7 F</b>	GTTGCCTCTGCTCAGCGT	300
<b>PTK7 R</b>	CCCTGCAGTGCATCCTG	300
<b>LGR4 F</b>	GGCCTTGCTGGGTTGAAAG	300
<b>LGR4 R</b>	CAAAGCACTCAGCCCTCGAA	300
<b>LGR5 F</b>	GGGAGCATTCACTGGCCTTTA	300
<b>LGR5 R</b>	TCCAGACGCAGGGATTGAAG	300
<b>LRP4 F</b>	GGTCTTGGTCAGCCATGTGT	300
<b>LRP4 R</b>	ACACGCTGGATTGACTTGGT	300
<b>LRP5 F</b>	AAGAGGAAGGAGATCCTGAGTG	300
<b>LRP5 R</b>	ATTGTCCTCCTCACAGCGAGT	300
<b>LRP6 F</b>	TGAGGGTCTGCGTGAAATCC	300
<b>LRP6 R</b>	TGGGAACAACCCCATTTGTC	300
<b>GPC4 F</b>	TCGTGACTGTGAAGCCATGT	300
<b>GPC4 R</b>	TCTAGCCTCTCTGCCACCAT	300
<b>MuSK F</b>	CCCACCATCACCTGGATTGAA	300
<b>MuSK R</b>	TGTGTAGAGTCCTGGCTTGG	300
<b>WNT11 F</b>	AGACCGGCGTGTGCTATG	900
<b>WNT11 R</b>	CACCTGTGCAGACACCAGAC	900
<b>ATF2 F</b>	AGTCCTTTACCTCACCCAGAGT	300
<b>ATF2 R</b>	GATGTGGGCTGTGCAGTTTG	300
<b>JUN F</b>	TGAGTGACCGCGACTTTTCA	300
<b>JUN R</b>	TTAAGATGCCTCCCGCACTC	300
<b>CREB F</b>	AGCCCAGCCACAGATTGCCAC	300
<b>CREB R</b>	GTTACGGTGGGAGCAGATGAT	300
<b>AXIN2 F</b>	AAGTGCAAACCTTTGCGCAAC	300
<b>AXIN2 R</b>	ACAGGATCGCTCCTCTTGAA	300
<b>CDH1 F</b>	AGCAGAACTAACACACGGGG	600
<b>CDH1 R</b>	ACCCACCTCTAAGGCCATCT	600
<b>CLDN1 F</b>	CTGTCATTGGGGGTGCGATA	600
<b>CLDN1 R</b>	CTGGCATTGACTGGGGTCAT	600
<b>CDH2 F</b>	CATGAAGGACAGCCTCTTCTCAA	300
<b>CDH2 R</b>	GCTTCTCACGGCATAACCCAT	300
<b>VIM F</b>	GCTTCAGAGAGAGGAAGCCG	600
<b>VIM R</b>	AAGGTCAAGACGTGCCAGAG	600
<b>SNAI F</b>	CCCTGGCTGCTACAAGGC	600
<b>SNAI R</b>	TGAGTGGGTCTGGAGGTGG	600
<b>SNAI2 F</b>	GCCAAACTACAGCGAACTGG	300
<b>SNAI2 R</b>	AGTGATGGGGCTGTATGCTC	300
<b>TWIST1 F</b>	GCCACTGAAAGGAAAGGCATC	600
<b>TWIST1 R</b>	TGGTTTTGCAGGCCAGTTTG	600



<b>ZEB1 F</b>	AAGAATTCACAGTGGAGAGAAGCCA	300
<b>ZEB1 R</b>	CGTTTCTTGCAGTTTGGGCATT	300
<b>MMP9 F</b>	TTGGTCCACCTGGTTCAACT	300
<b>MMP9 R</b>	TCAACTTGGTCCACCTGGTT	300
<b>PAI1 F</b>	CAATCGCAAGGCACCTCTGA	600
<b>PAI1 R</b>	TTCACCAAAGACAAGGGCCA	600
<b>TGF<math>\beta</math>1 F</b>	TGTCACCGGAGTTGTGCGGC	300
<b>TGF<math>\beta</math>1 R</b>	GCAGTGGGCGCTAAGGCGAA	300
<b>TGF<math>\beta</math>RI F</b>	GAAAGTGGCGGGGAGAAGAA	600
<b>TGF<math>\beta</math>RI R</b>	AATCTCTGCCTCACGGAACC	600
<b>TGF<math>\beta</math>RII F</b>	TCCTGAAGACGGCTCCCTAA	600
<b>TGF<math>\beta</math>RII R</b>	GTTCTTTGGTGAGAGGGGCA	600
<b>SMAD2 F</b>	AACCGAAATGCCACGGTAGA	600
<b>SMAD2 R</b>	GCACTCAGCAAAAATTCCCC	600
<b>SMAD3 F</b>	GAAACTCAAGAAGACGGGGCAG	900
<b>SMAD3 R</b>	CGATGGGACACCTGCAACC	900
<b>36B4 F</b>	GTGTTTCGACAATGGCAGCAT	300
<b>36B4 R</b>	AGACACTGGCAACATTGCGGA	300

**Table 6. List of primers used in this study.** Sequences and concentrations are described.

## 5. Cell transfection and silencing

Cells were plated 24 h before transfection to be 70-80% confluent at the moment of transfection. Lipofectamine LTX with PLUS reagents (LifeTechnologies), were used for cell transfection as instructed by the manufacturer. Briefly, OptiMEM was added to the cells after a previous OptiMEM wash to remove antibiotics. After that, the required plasmids and Plus reagent were incubated in OptiMEM for 15 min and Lipofectamine LTX was also individually incubated in OptiMEM for 5 min. Mixing of both DNA/lipid mixes was done in 1:1 ratio and further incubated together for 15 min. DNA-lipid mix was then added to the cells and transfection analyzed after 24 h. DNA/LTX/Plus amounts are summarized in **Table 7**.

Plate	Experiment	DNA/well (ng)	LTX/well ( $\mu$ L)	Plus/well ( $\mu$ L)
<b>24 well</b>	Immunofluorescence	250	0,75	0,25
<b>12 well</b>	Gene Reporter	500	1,5	0,5
<b>6 cm</b>	Immunoprecipitation	2500	4,5	1,5

**Table 7. Protocol for cell transfection.** The reagent amounts used in cell transfections in different types of experiments are indicated.

For silencing experiments, 24 h before transfection, cells were plated to be 60% confluent at transfection. RNAimax (Invitrogen) was used for cell silencing as instructed by the manufacturer. Briefly, OptiMEM was added to the cells after a previous OptiMEM

wash to remove antibiotics. After that, siRNA or dsRNAs (**Table 3**) were incubated in OptiMEM to be at a final concentration in the well of 25 or 50 nM, depending of the gene. RNAimax was mixed with OptiMEM and then the RNA/lipid was mixed in a 1:1 ratio and incubated for 5 min. DNA-lipid complexes were then added to the cells and silencing was evaluated after 48 h.

In both cases, cell transfection and silencing, fresh media were added to the cells 4h after transfection.

## 6. Generation of stable knockdown cells

For stable knockdown of *FZD8*, lentiviral pLKO and shFZD8 constructs (TRC Lentiviral Human shRNA, RHS4533, Dharmacon) were used. For generation of lentiviruses, two cell cell lines were used: a packaging cell line (HEK293T) and the target cell line in which the transgene wants to be knocked down (PC-3M).

The general protocol for lentivirus infection is performed in different steps (**Fig. 27**):

- **Day 1:**
  - Morning: Packaging cells were seeded at high density ( $2 \times 10^6$  cells/100mm plate)
  - Afternoon: Packaging cells were transfected.
- **Day 2:** Packaging cells media was changed to fresh culture media and the target cell line was seeded.
- **Day 3:** Target cells were first infected with virus containing supernatant from packaging cells. For this, 7 mL of supernatant from packaging cells was filtered with 0.45  $\mu$ m filters and 3 mL of fresh media were added to a total of 10 mL. Protamine sulfate was added to the mixture (1:1000 dilution) to increase infection efficiency. After infection, fresh media was added to packaging cells for further virus production.
- **Day 4:** A second infection of target cells was performed with virus containing supernatant and the packaging cells were discarded.
- **Day 5:** Target cells were subjected to selection with puromycin at 2  $\mu$ g/mL and the efficiency of *FZD8* knockdown was evaluated by q-RT-PCR.

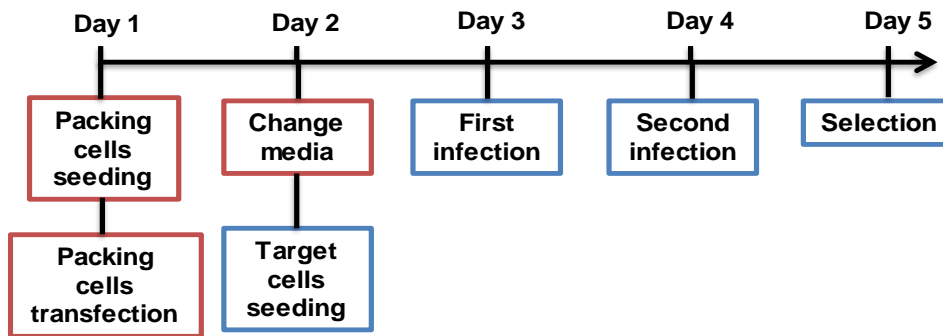


**Figure 27. Schematic process for the generation of stable knockdown cells.**

HEK293T cell transfections were performed using 5  $\mu\text{g}$  of pLKO and shFZD8 constructs together with 2.5  $\mu\text{g}$  of psPAX2 (provides integrase, reverse transcriptase and structural proteins) and 2.5  $\mu\text{g}$  of VSV-G (provides the envelope proteins) (**Fig. 28**). 50  $\mu\text{L}$  of calcium chloride ( $\text{CaCl}_2$ ) per condition were added in a final volume of 500  $\mu\text{L}$ . The DNA solution was mixed with 500  $\mu\text{L}$  of HEPES-buffered solution (HBS) (50 mM HEPES, 280 mM NaCl, 10 mM KCl, 1.5 mM  $\text{Na}_2\text{HPO}_4 \cdot 2\text{H}_2\text{O}$ , 12 mM dextrose, pH=7.05) in the presence of oxygen by making bubbles to favor the formation of calcium phosphate crystals.

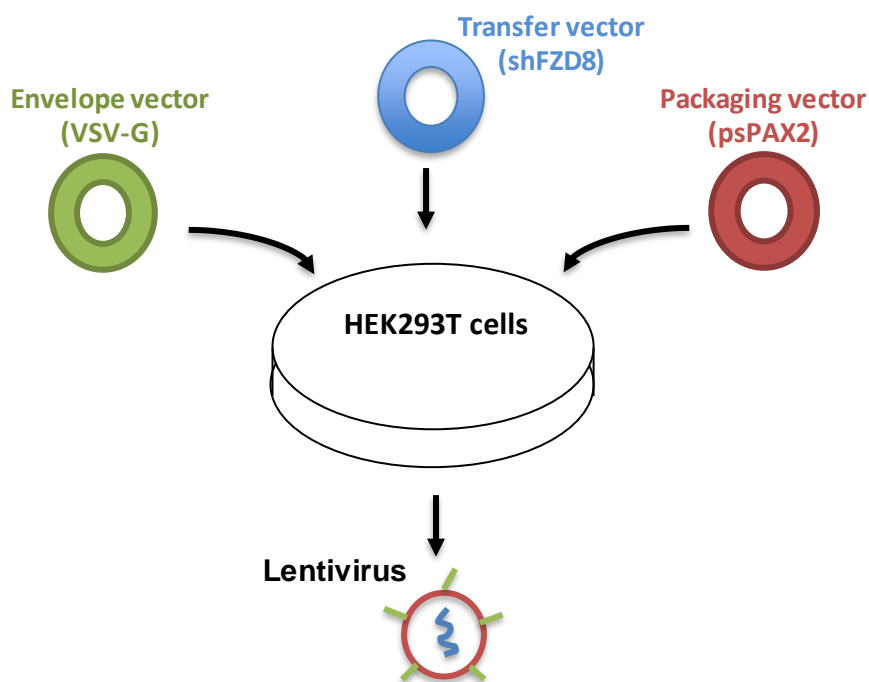


**Figure 28. Schematic of lentivirus generation in HEK293T cell.**

## 7. Gene reporter assays

Gene reporter assays have been widely used in order to measure the expression of genes of interest at the transcriptional level. They are based on the direct fusion between the promoter of the gene of interest with specific firefly reporters. Luciferase reporter (firefly) from *Photinus pyralis* is one of the most widely used reporters due to the rapid production of light when combined with the substrate luciferin, which can be measured through luminescence (Yun & DasGupta 2015). This assay is complemented with the use of the renilla reporter from *Renilla reniformis*, which is expressed under the control of a constitutive promoter working as an internal control for normalization of transfected cell number (Yun & DasGupta 2015) (**Fig. 29**).

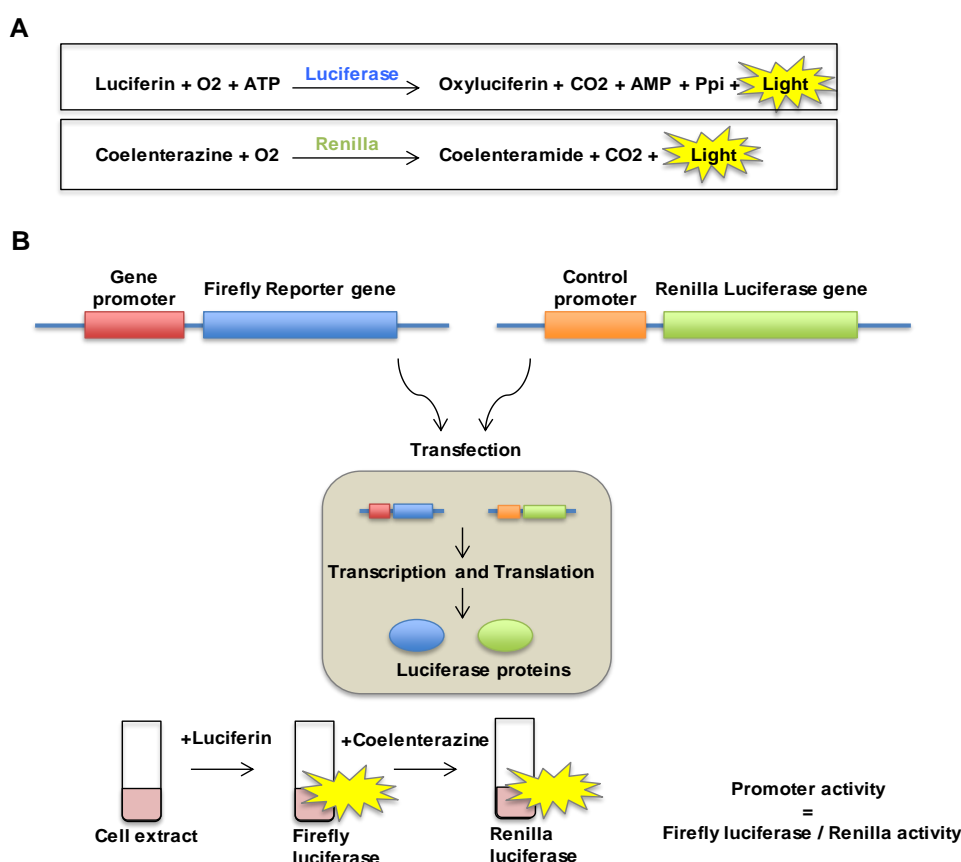


**Figure 29. Basis of gene reporter assays. (A)** Chemical reactions of Luciferase and Renilla. **(B)** Schematic illustration of gene reporter assays.

In our gene reporter assays, 100,000 (C4-2B) or 80,000 (PC-3M and DU145) cells per well were plated in 12-well plates. Transfections were normally carried in triplicate wells 24 h after plating. Cells were transfected with 250 ng of ATF2/AP-1/TOP/FOP luciferase reporters, 50 ng of Renilla (pRL-tk) and 200 ng empty vector or Wnt-11 plasmid. For CAGA luciferase analysis, cells were transfected with 450 ng of CAGA reporter and 50 ng pRL-tk. When FZD plasmids were co-transfected, 150 ng of ATF2

luciferase reporter was used together with 50/100 ng of FZD plasmid. In experiments involving gene silencing, reporters and other plasmids were transfected 24 h after siRNAs.

24 h after transfection of reporters, cells were washed twice with PBS (Phosphate buffered saline) and lysed in 150  $\mu$ L per well of Passive Lysis Buffer (Promega). Lysates were shaken at room temperature (RT) for 10 min and then frozen at  $-80^{\circ}\text{C}$  for 20 min to facilitate lysis. After that, lysates were collected and centrifuged at 15,000 g for 5 min. Two different Luciferase Assay System were used. When the Dual Glo Luciferase Assay Systems (Promega) was used, 50  $\mu$ L of lysate was added to white luminometer plates (PerkinElmer) and 50  $\mu$ L of luciferase reagent was added on top. After 10 min of incubation, luciferase activity was measured using a Veritas microplate luminometer (Turner biosystems). After this measurement, 50  $\mu$ L of renilla reagent (substrate: buffer; 1:100) was added on top. After 10 min incubation, Renilla activity was measured. When the Luciferase Assay Kit (PJK, Germany) was used, 30  $\mu$ L of lysate was added to white luminometer plates and 80  $\mu$ L of luciferase PJK was added on top. In different wells, 25  $\mu$ L of lysate was also plated and 25  $\mu$ L of Renilla (substrate: buffer; 1:50) was added. After 5 min of incubation at RT, luciferase activity was measured. In both cases, gene reporter activities were calculated as luciferase/renilla and TOP/FOP ratios when required.

## 8. Cell migration and invasion assays

For migration and invasion assays, 250,000 PC-3M or DU145 cells per well were plated in 6-well plates and transfected with control and FZD8 siRNA for 48 h. Afterwards, cells were trypsinized and resuspended in RPMI with 1% FBS and 50,000 cells/well were added to duplicate uncoated or Matrigel-coated 8  $\mu$ m pore transwell filters with a polycarbonate membrane (BD Biosciences) for migration and invasion assays, respectively (**Fig. 30**). When the effects of inhibitors 1 and 2 (I1, I2) were tested, DMSO or inhibitors were added at 10  $\mu$ M to 50,000 cells/well on uncoated 8  $\mu$ m pore transwell filters for migration assays. For TGF- $\beta$ -dependent invasion assays, siRNA-transfected cells were cultured overnight in media with 0.2% FBS and then treated with 5 ng/mL TGF- $\beta$ 1 for 24 h. Cells were then trypsinized and resuspended in media containing 0.2% FBS and 5 ng/mL TGF- $\beta$ 1. 50,000 cells/well were added to Matrigel-coated 8  $\mu$ m pore transwell filters. In all cases, inserts were set in 24-well plates with media containing 20% FBS in the lower chamber. As a control for cell viability, cells were plated in parallel at the same density in 24-well plates.

Migration and invasion were evaluated after 24 and 48 h, respectively. Non-migrating/invasive cells were removed using a cotton swab and migrating/invasive cells retained in the polycarbonate membrane of the insert were stained using 0.1% crystal violet, 20% methanol, 0.36% para-formaldehyde (PFA) in PBS (**Fig. 30**). After that, pictures were taken of 5 different fields of the insert and the average numbers of migrating/invasive cells per insert was determined by counting stained cells. The control plate was also stained using crystal violet and absorbance measured at 595 nm after solubilizing in methanol. These data were then used to normalize the numbers of migrating/invasive cells to the numbers of viable cells. Results were shown as relative cell migration/invasion.

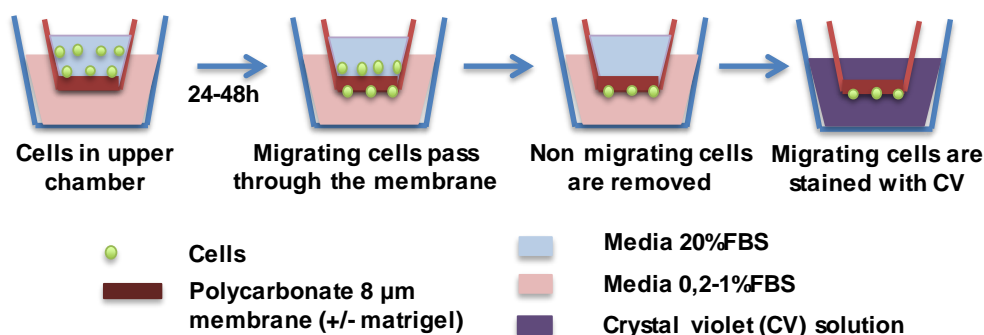


**Figure 30.** Schematic diagram for migration and invasion assays.

## 9. Protein analysis

### 9.1 Protein extraction

For total cell extracts, cells were lysed for 10 min in radioimmunoprecipitation assay (RIPA) lysis buffer (50 mM Tris-HCl, pH 7.4, 150 mM NaCl, 0.25% deoxycholic acid, 1% NP-40, 1 mM EDTA (Millipore)) with cOmplete™ Mini EDTA-free Protease Inhibitor Cocktail (Roche), PhosSTOP Phosphatase Inhibitor Cocktail Tablets (Roche) and 0.1% sodium dodecyl sulfate (SDS) (LifeTechnologies) and then centrifuged for 12 min at 15,000 g. Supernatants were combined with 2X Laemmli buffer (Sigma) and heated at 37°C or 95°C for 10 or 5 min, respectively, depending on the assay. Remaining extracts were store at -80°C.

### 9.2 Western blotting (WB)

After protein sample preparation, extracts were separated on SDS polyacrylamide gels using a Mini Protean System (BioRad). Gels were prepared as shown in **Table 8**, adjusting for gel percentage according to target protein size.

Reagent	Volume (ml) 8% resolving gel	Volume (ml) stacking gel
H <sub>2</sub> O	2.3	0.68
30% Acrylamide (Sigma)	1.3	0.17
1.5M Tris (pH 8,8)	1.3	
1.5M Tris (pH 6,8)		0.13
10% Sodium dodecyl sulphate (SDS) (Gibco)	0.05	0.01
10% Ammonium persulfate (APS) (Sigma)	0.05	0.01
TEMED (Sigma)	0.003	0.002

**Table 8. Protocol for the preparation of acrylamide gels for WB.**

Gels were run at 15 mA/gel for 1,5-2h and transferred to nitrocellulose 0.2 µm pore size (Millipore) at 10-12V for 30-40 min using a semi-dry transfer cell (BioRad). PageRuler™ Plus Prestained Protein Ladder (Thermo Scientific) was used as protein size marker with a range of 250-10 kDa. Membranes were washed with TBST (Tris-buffered saline 0.05% Tween (Sigma)) and incubated in blocking buffer containing 3% BSA (Bovine serum albumin, Sigma) in TBST for 1h.

Primary antibodies (**Table 9**) were incubated with blots at 4° C overnight. After 3-4 TBST washes, blots were incubated for 1h at RT in blocking buffer with HRP-conjugated secondary antibodies (1: 20,000, Jackson ImmunoResearch). Membranes were washed again 3-4 times with TBST and then developed using chemiluminescence (Amersham ECL western blotting detection reagents, GE Healthcare).

Antigen	Company	Catalog number	Species	Concentration
pSMAD2	Cell Signaling	138D4	Rabbit	1:1000
pSMAD3	Abcam	ab52903	Rabbit	1:2000
SMAD2/3	Santa Cruz	sc-133098	Rabbit	1:1000
PA tag	Novus Biological	NBP-03952	Rat	1:1000
1D4 tag	Santa Cruz	sc-57432	Mouse	1:2000
HA tag	Santa Cruz	sc-805	Rabbit	1:1000
Flag tag	Sigma-Aldrich	F1804	Mouse	1:1000
FZD8	LS Bio	LS-C120599	Rabbit	1:2000
IgG	GenScript	A00166	Human	1:5000
Wnt-11	RyD	AF2647	Goat	1:2000
N-cadherin	Santa Cruz	sc-393933	Mouse	1:500
Vimentin	Santa Cruz	sc-373717	Mouse	1:500
Claudin-1	Santa Cruz	sc-166338	Mouse	1:500
β-Tubulin	Sigma-Aldrich	T5293	Mouse	1:5000
GAPDH	SIGMA	G8795	Mouse	1:2000

**Table 9. List of antibodies used in WB assays.**

### 9.3 Immunoprecipitation (IP)

For immunoprecipitation (IP) assays, 500,000 PC-3M cells were plated in 6 cm plates and transfected with 2.5  $\mu$ g of total DNA (1:2 ratio for FZD8-1D4: Wnt-11-PA, FZD8-1D4: TGF $\beta$ RI-Flag/HA-TGF $\beta$ RII, FZD8-CRD-IgG: TGF $\beta$ RI-Flag/HA-TGF $\beta$ RII and FZD8-CRD-IgG: Flag-ALK5-HA(ecto)). After 24 h, cells were washed twice with PBS and lysed in 1 mL of IP lysis buffer (50 mM Tris-HCl, pH 8, 150 mM NaCl, 1% Triton X-100, 1 mM EDTA with cOmplete™ EDTA-free Protease Inhibitor Cocktail and PhosSTOP Phosphatase Inhibitor Cocktail Tablets) for 5 min on ice. Samples were then centrifuged at 4°C for 12 min at 15,000 g. For inputs, 50  $\mu$ L of supernatant was combined with 2x Laemmli Buffer and heated for 10 min at 37 °C (this temperature was used to reduce FZD aggregation) or stored at -80 °C. For IPs, supernatants were incubated for 90 min on ice with 1  $\mu$ g of antibody (anti-PA or anti-1D4). Protein A/G PLUS-Agarose (Santa Cruz) was added to each sample and incubated for 1 h on a rotating wheel at 4 °C. For fusion proteins, immunoprecipitation was performed without antibody incubation. IPs were then collected by centrifugation at 500 g for 30 sec. Pellets were washed three times with IP buffer and once with ice-cold TBS. After washes, samples were resuspended in 15  $\mu$ L of 2X Laemmli Buffer and heated for 10 min at 37 °C. Western blotting was performed as described above. Primary antibodies used for blotting are listed in **Table 9**.

### 10. Immunofluorescence

For immunofluorescence assays, PC-3M cells were plated on coverslips at 40,000 cells per well in a 24-well plate. 24 h after plating, cells were transfected with 170 ng Wnt-11 and 80/40 ng FZDs plasmids depending on the FZD construct. The following day, cells were fixed in 4% PFA in PBS (Santa Cruz) for 20 min at RT and permeabilized using 0.1% Triton X-100 in PBS for 10 min at RT. Blocking was performed using 2% BSA, 50 mM glycine, 0.01% NaN<sub>3</sub> in PBS for 40 min to 1 h. Primary antibodies (**Table 10**) were added overnight at 4°C. Coverslips were washed three times with PBS and secondary antibodies were prepared in blocking buffer at 1:500 (AlexaFluor488, AlexaFluor594, AlexaFluor647, Life Technologies) and incubated for 1h at RT. After three washes with PBS, coverslips were mounted using Vectashield mounting medium with DAPI (Vector Labs). Stained cells were visualized using a confocal microscope (Leica TCS SP2) with a 63x oil immersion objective. For analysis of colocalization, 10 cells from two independent experiments were quantified using Image J and the Coloc 2 plug-in and Pearson's correlation coefficient determined.



When immunofluorescence was performed on miniaturized 3D cultures the corresponding wells from the 96 well Angiogenesis  $\mu$ -slides plate (Ibidi GmbH, Martinsried, Germany) were fixed in 4% PFA in PBS for 30 min and washed three times with cold PBS. Permeabilization was performed with 1% Triton X-100 (Sigma-Aldrich) and blocking in 20% horse serum for 45 min at RT. Primary antibodies (**Table 10**) were also added overnight at 4°C. Vimentin staining was used to visualize invasive and mesenchymal structures and anti-laminin- $\alpha$ 1 was used to stain the basal membrane of non-differentiated structures. Secondary antibodies (AlexaFluor® 488 and 568 (Life Technologies)) were added at 1:500 for 1h at RT. Nuclei were stained with Draq5 (Thermo Fisher Scientific). Images were taken with a Zeiss LSM780 laser scanning confocal microscope, using a 20x objective.

Antigen	Company	Catalog number	Species	Application	Concentration
1D4 tag	Santa Cruz	sc-57432	Mouse	IF	1:200
HA tag	Santa Cruz	sc-805	Rabbit	IF	1:200
Flag tag	Sigma-Aldrich	F1804	Mouse	IF	1:200
Wnt-11	RyD	AF2647	Goat	IF	1:50
FZD8	LS Bio	LS-C120599	Rabbit	IF	1:50
Vimentin	Abcam	Ab16700	Rabbit	IF	1:100
Laminin- $\alpha$ 1	Santa Cruz	Sc-59849	Mouse	IF	1:100

**Table 10.** List of antibodies used for immunofluorescence experiments.

## 11. Clinical samples

Tissue arrays (TMAs) were generated at the Imperial College Experimental Cancer Medicine Centre (ECMC) using tissue from surgical resections from 99 prostate cancer patients provided by the Imperial College Healthcare NHS Trust Tissue Bank (ICHTB; project R15043), which is supported by the National Institute for Health Research (NIHR) Biomedical Research Centre, based at Imperial College Healthcare NHS Trust and Imperial College London. The clinical characteristics of the patients are summarized in **Table 11**. Other investigators may have received samples from these same tissues. TMAs contained two cores from regions containing cancer and two cores from regions without cancer from each patient. A histopathologist (James Carton) examined representative haematoxylin and eosin-stained sections to evaluate their pathology. Nine cores did not contain cancer and three showed low quality staining or loss of sample and were not analyzed further. The staining intensities of FZD8 and Wnt-11 were scored independently by two people (Virginia Murillo and Robert Kypta) and divergences in

scores were re-evaluated until consent was found. Each core was scored based on the staining intensity as 0 (no staining), 1 (weak staining), 2 (moderate staining) or 3 (strong staining).

<b>Characteristic</b>	<b>Number of patients</b>
<b>Gleason (patients)</b>	
3 + 3	6
3 + 4	59
4 + 3	27
4 + 4	0
4 + 5	7
<b>Stage</b>	
pT2a	1
pT2b	1
pT2c	48
pT3a	29
pT3b	11
<b>Lymph node metastasis</b>	
Yes	1
No	89
<b>Perineural invasion</b>	
Yes	37
No	53
<b>Lymphovascular invasion</b>	
Yes	7
No	83
<b>Inflammation</b>	
Yes	27
No	72
<b>Gleason (sections analyzed)</b>	
3 + 3	47
3 + 4	21
4 + 3	14
4 + 4	7
4 + 5	1
No cancer	9

**Table 11. Clinical features of patients included in the TMA.**

## 12. Immunohistochemistry

Paraffin blocks containing lymph node metastases surgically removed from mice 31 days after orthotopic implantation of  $2 \times 10^6$  PC-3M-luc cells were provided by Genscript (Piscataway, NJ, USA). Sections from these blocks, from TMAs and from CAM sections were de-paraffinized with Histo-Clear II (National Diagnosis, USA) and then transferred through four changes of 100%, 96%, 70% ethanol and water. Antigen retrieval was performed in a pressure cooker filled with sodium citrate buffer at pH 6.0. Endogenous peroxidase activity was quenched for 10 min with 3% hydrogen peroxide. Blocking was performed for 15 min with Avidin followed by 15 min with Biotin (Avidin/Biotin blocking kit (Vector Labs)). Samples were washed with PBS and blocked with 5% horse serum for 30 min at RT to reduce nonspecific staining. After washing, primary antibodies to FZD8 (LS Bio, Rabbit, 1:100) and Wnt-11 (R&D, Goat, 1:100) were applied overnight at 4°C. Sections were incubated with biotinylated secondary antibody (Vector Labs) for 30 min followed by Vectastain® Elite ABC reagent (Vector Labs) for 30 min. Liquid 3,3'-diaminobenzidine (DAB) (DAKO) was used as a chromogenic agent for 1-2 min and sections were counterstained with Mayer's haematoxylin. Images were taken on an AxioImager D1 light microscope.

## 13. Miniaturized tridimensional (3D) assays

Tridimensional cell cultures have emerged as a technique that allows the researcher to work with a cellular model that mimics the functions of living tissues (Pampaloni et al. 2007). In this model, organotypic acinar structures named organoids are formed that display physiologically relevant cell-cell and cell-matrix interactions, epithelial polarization and differentiation, recapitulating human cancer histology *in vivo* (Pampaloni et al. 2007; Härma et al. 2010). Specifically, prostate cancer cells such as PC-3 or PC-3M initially differentiate into hollow organoids (days 4-5) and later spontaneously de-differentiate into invasive stellate structures (days 8-12) (Härma et al. 2010) (**Fig. 31**). In this regard, 3D cultures represent a very useful model to study cell invasion in more physiological conditions.

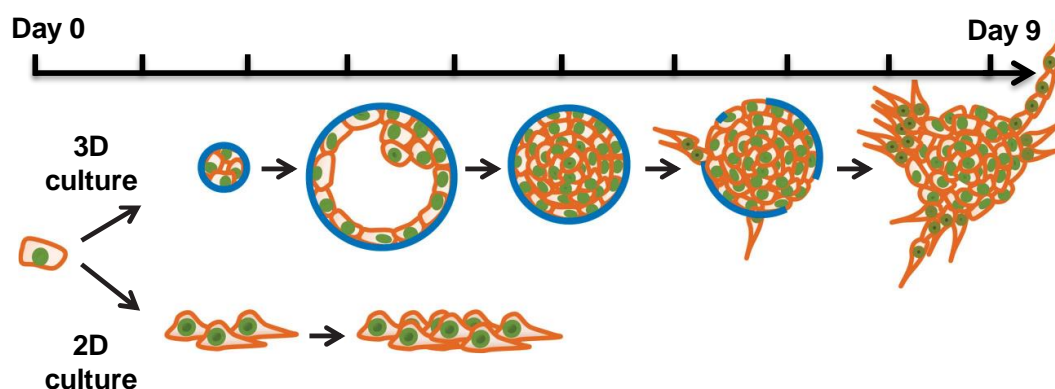


**Figure 31. Schematic illustration of prostate cancer cells cultured in 3D and 2D.** The former allows organotypic organoid formation, acinar differentiation and invasion. The basement membrane is depicted in blue. (Adapted from Björk et al., 2016).

### 13.1 Tridimensional (3D) culture and live-cell imaging

For miniaturized 3D cultures, PC-3 and PC-3M cells were plated on 6 well plates at a cell density of 150,000 cells/well and the following day they were silenced with Ctrl and FZD8 siRNAs. 48 h after silencing, 3D cultures were set up by embedding silenced cells between two layers of Matrigel and culturing them for 8-9 days on uncoated 96 well Angiogenesis  $\mu$ -slides (Ibidi GmbH, Martinsried, Germany). Wells were filled with 10  $\mu$ L of Matrigel/culture medium (1:1) and kept at 37°C for 1 h until polymerization. Cells were then trypsinized and counted and 20  $\mu$ L of a second layer of Matrigel (1:4) containing 650 PC-3 and PC-3M cells per well were added on top of the well and kept at 37°C for 4 h until polymerization. Wells were then filled up with 60  $\mu$ L of medium and humidity was maintained by adding sterile PBS between the wells. Media were changed every second day.

Live cell imaging was performed using Incucyte (Essen BioScience, Hertfordshire, UK), which is a flexible platform that allows real time monitoring of cell cultures through automatic acquisition and analysis of images around the clock. In our case, images were captured every two hours for 8-9 days (**Fig. 32**).

For monitoring silencing efficiency during the 3D culture, silenced cells were replated onto 12-well plates and RNA was extracted at day 4 and day 8. Gene expression was analyzed by q-RT-PCR.

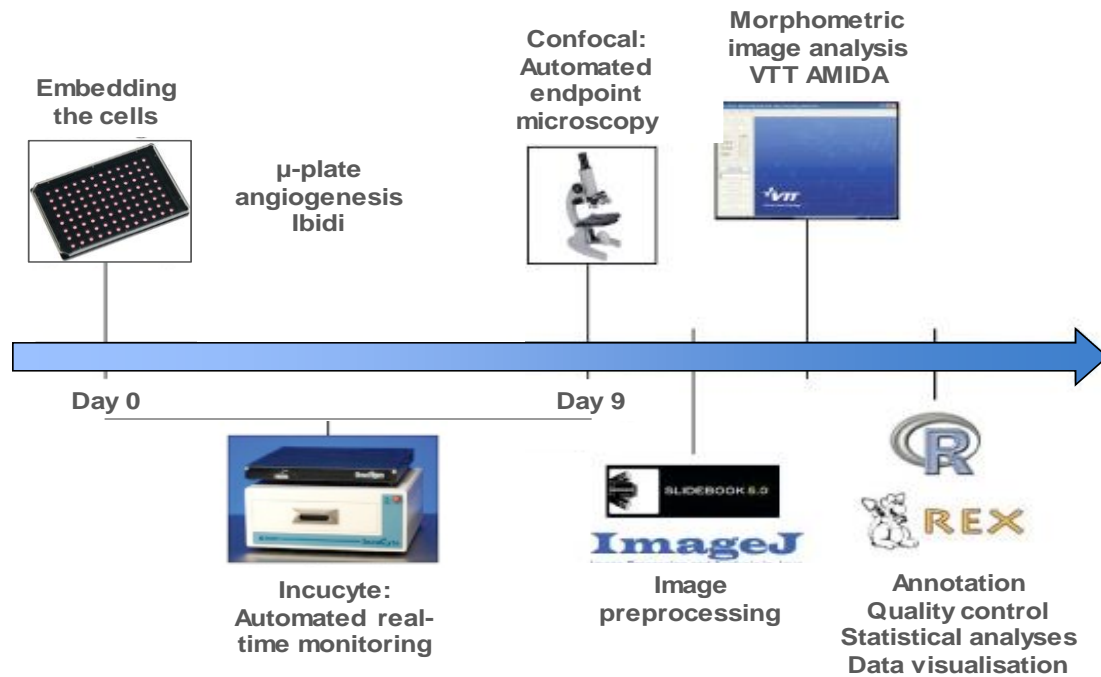


**Figure 32. Schematic representation of the 3D culture technique.** The different tools needed for the imaging and analysis are shown. Adapted from Härma et al. 2014.

### 13.2 Tridimensional (3D) image acquisition, pre-processing and morphometric analyses

At the experimental endpoints multicellular structures were double stained with 1  $\mu\text{M}$  of calcein 488 and ethidium homodimer 647 in media at 37°C for 30 min. Calcein allows to stain for live cells through the conversion of nonfluorescent calcein to fluorescent calcein. This reaction is mediated by the removal of the acetomethoxy group by esterases, which are only present in live but not in dead cells. On the contrary, ethidium homodimer allows the detection of apoptotic cells due to its ability to bind DNA of dead cells passing through their broken membrane.

Confocal images were taken of 4 different fields per well with a Zeiss spinning disk confocal unit using a 5x objective. Intensity projections were created with SlideBook (Intelligent Imaging Innovations Inc, Denver, CO, USA) and background noise was removed by normalization, also using SlideBook. Finally, confocal images were analyzed with VTT's AMIDA software (Härma et al. 2014) and raw numerical data were statistically processed and visualized with R/Bioconductor (**Fig. 32**). Morphometric parameters used in the analysis can be found in **Table 12**.

Parameter	Explanation	Unit
<b>Area</b>	Area of the segmented structure	pixels
<b>AreaR</b>	Area of apoptotic cells	pixels
<b>Roundness</b>	Roundness of the segmented structure	%
<b>Roughness</b>	Roughness of the surface of the segmented structure	%
<b>AppIndex</b>	Indexes the severity of the invasiveness by utilizing Roundness and Roughness parameters	ratio
<b>MaxApp</b>	Estimate for the maximum length of appendages of the segmented structure	pixels

**Table 12. Morphometric parameters used for the analysis of miniaturized 3D culture.** For an extended explanation of the parameters see Härma et al. 2014.

#### 14. Tumor growth assay on the chorioallantoic membrane (CAM)

Fertilized white Leghorn chicken eggs were cleaned with water and 70% ethanol to remove bacteria. Afterwards, eggs were placed into the eggs incubator with the pointed end in the bottom (embryo development day 0, EDD0). Incubation is performed at 37 °C under constant humidity (60%) and rotation of 100 degrees every 20 min. No method of randomization was used. Separation of the developing CAM was induced on EDD4 by drilling a hole of approximately 2 mm of diameter in the pointed end of the eggs. After covering holes with tape, eggs were placed again in the incubator. On EDD7, egg holes were enlarged to a final size of approximately 1 cm of diameter and a plastic ring was set above blood vessels of the CAM membrane. After that, 500,000 PC3 cells/egg silenced for 48 h for Ctrl and FZD8 siRNAs were suspended in PBS and Matrigel (1:1) and 20 µL/egg of the mix were implanted in the middle of the ring on the CAM. On EDD10, eggs were placed on ice for 1 h to anesthetized embryos. Holes were enlarged and tumors were photographed *in ovo* and excised. Tumor area was measured blind using photographs from three independent experiments, each with 15 eggs per condition, using ImageJ (NIH, Bethesda, MD, USA). Tumor specimens were excised from the CAM and placed in 4% PFA, paraffin embedded and cut in 5 µm sections for immunohistochemical analysis (**Fig. 33**).

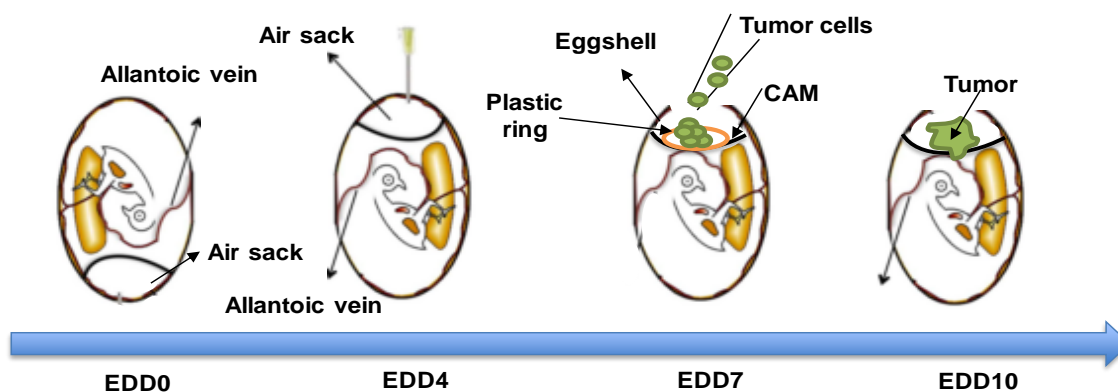


Figure 33. Schematic representation of the CAM assay. Adapted from Crespo & Casar, 2016.

## 15. Bioinformatics analysis

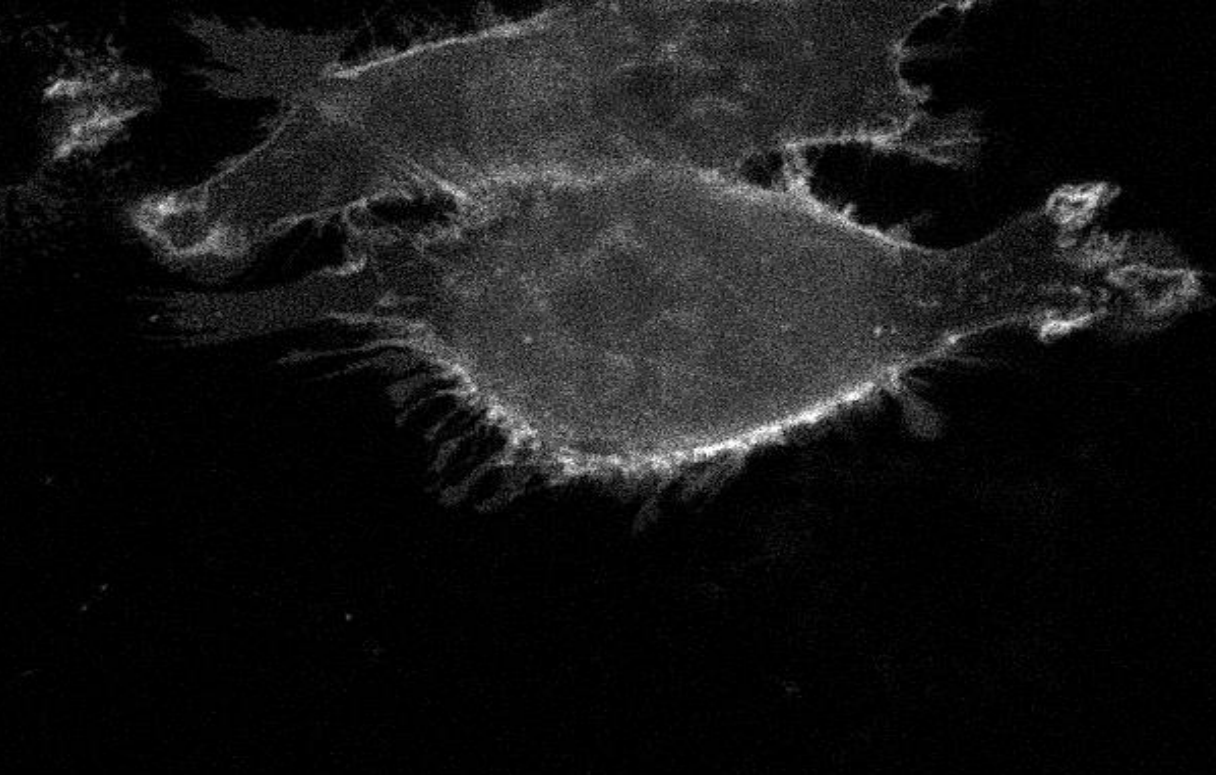
The Oncomine database ([www.oncomine.org](http://www.oncomine.org)) was used to examine the expression of Wnt receptors in prostate cancer datasets. Cancer *versus* Normal comparison with  $p$ -value  $< 0.05$  and fold change  $> 1.5$  were considered significant. The cBioPortal database ([www.cbioportal.org](http://www.cbioportal.org)) was used to obtain correlation levels between *FZD8* and *ERG* as well as *FZD8* and *WNT11* and EMT markers. This database was also used to analyze the correlation between *FZD8* and *WNT11* expression levels with freedom from biochemical recurrence. Analysis of the MSKCC dataset was performed through R/bioconductor in order to stratify samples into normal, cancer and metastasis as well as to differentiate Gleason score, stage and lymph node invasion status. The CamcAPP database (<http://bioinformatics.cruk.cam.ac.uk/apps/camcAPP/>) was used to determine the disease free status based on *FZD8* and *WNT11* expression levels.

## 16. Statistical analysis

Results are presented as the mean  $\pm$  standard deviation (SD). All experiments were repeated at least three times. Statistical evaluations were performed with GraphPad Prism 5.0 (GraphPad, La Jolla, CA, USA) using Student's  $t$  test for single comparisons or one-way analysis of variance (ANOVA) with post-hoc Tukey for multiple group comparisons. A two-tailed  $p$  value  $\leq 0.05$  was considered to indicate statistical significance. For TMA analysis, patients were divided into low (0, 1) and high (2, 3) *FZD8* and *Wnt-11* expression and Gleason scores  $\geq 4+3$  and  $\leq 3+4$  and analyzed by one-way  $\chi^2$  test, Chi-squared test with Yates correction or Fisher's exact test, two-sided. Correlation analysis was calculated using Phi-correlations to test association between expression of *FZD8* and *Wnt-11*. All TMA analyses were performed using SPSS v16 (IBM Corp., Somers, NY, USA).



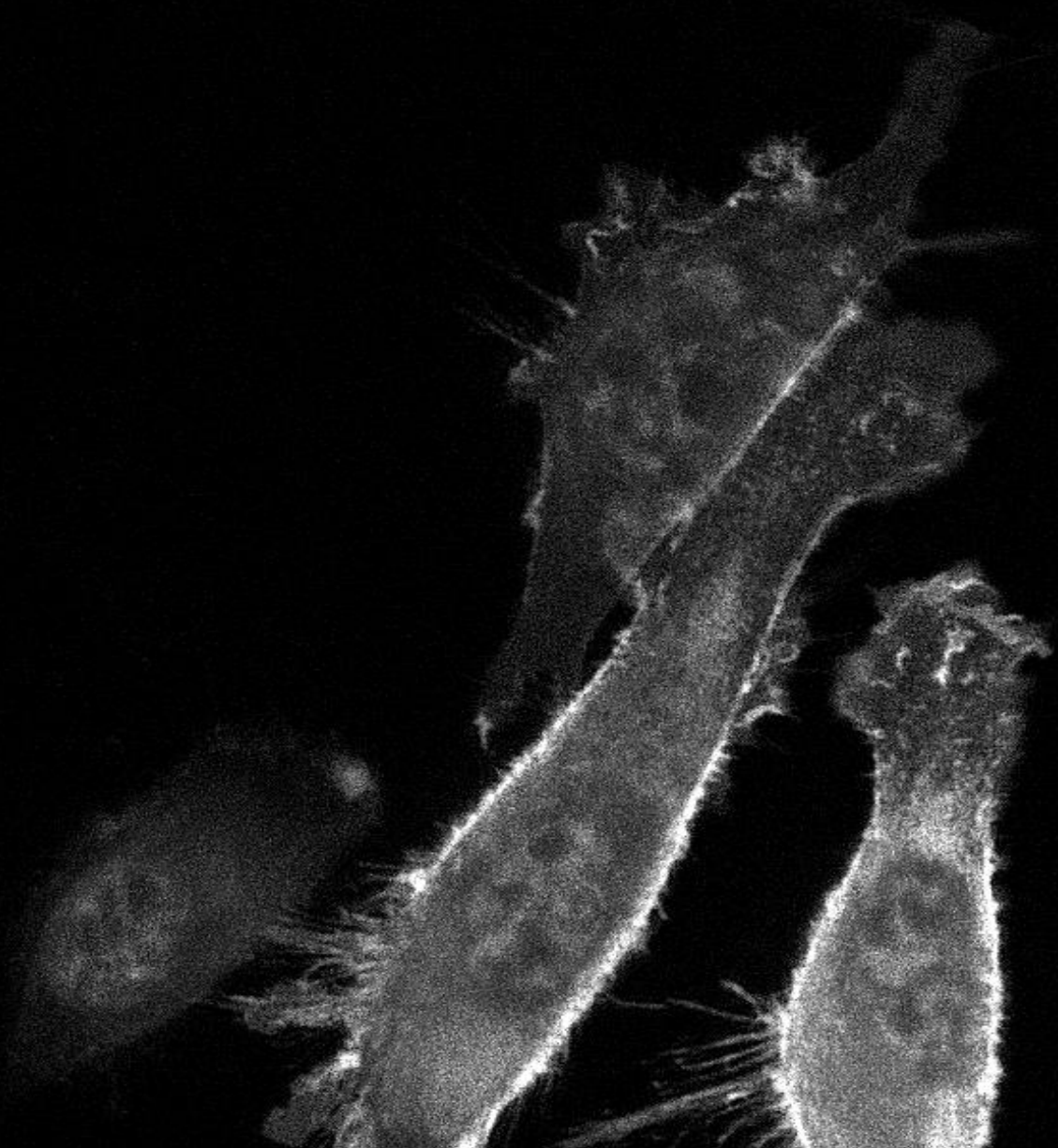




---

# RESULTS

---





## Chapter 1. Identification and characterization of Wnt-11 receptors in metastatic prostate cancer

The involvement of Wnt-11 in prostate cancer was previously reported by our group showing that Wnt-11 expression is elevated in prostate tumors and particularly in patient metastases (Uysal-Onganer et al. 2010). *WNT11* expression was also found upregulated in hormone-depleted LNCaP cells as well as in castration-resistant LNCaP cell tumor xenografts (Zhu et al. 2004).

All members of the Wnt family of proteins mediate their signaling through binding and activation of different receptors and coreceptors at the cell membrane, which then promotes the consequent activation of the intracellular canonical or noncanonical signaling cascades, and the regulation of target genes expression (M. T. Veeman et al. 2003; Komiya & Habas 2008; Niehrs 2012; Zhan et al. 2017)

Based on previous studies showing the involvement of Wnt-11 in prostate cancer metastasis and on the well-known requirement of Wnt receptors for activation of all branches of Wnt pathways, we first aimed to identify which of the Wnt receptors show an increased expression in prostate cancer and therefore could play a role in prostate cancer progression and metastasis. A variety of receptors and co-receptors are able to bind Wnt ligands in different types of cancer, including the frizzled family members (FZD1-10), VANGL1 and 2, tyrosine kinase-like receptors (ROR1, ROR2, RYK, PTK7 and MuSK), LRP4-6, LGR4 and 5 and GPC4 (Niehrs 2012). The strategy to elucidate the implication of Wnt receptors in prostate cancer was divided into two screening approaches, based on *in vitro* experiments using different prostate cancer cell lines and on *in silico* analysis of prostate tumor databases.

### 1.1 Screening of Wnt receptors with increased expression in prostate cancer cell lines

In order to identify candidate receptors involved in prostate cancer progression we characterized the expression pattern of a panel of 23 Wnt receptors by q-RT-PCR in different prostate cancer cell lines representing a range of prostate tumor types. These cell lines included LNCaP cells and a castrate-resistant derivative, C4-2B, both of which express high levels of AR and low levels of WNT11; VCaP cells, which harbor a TMPRSS2-ERG gene fusion and express high levels of AR and WNT11, and PC-3M, a metastatic AR-negative cell line that expresses moderate levels of WNT11. We also examined Wnt receptor gene expression in LNCaP cells cultured in hormone-depleted

medium, which is known to reduce proliferation and induce neuroendocrine-like differentiation, concomitant with an increase in *WNT11* expression.

As a way to mimic prostate cancer progression, the different prostate cancer cell lines used in the q-RT-PCR analysis were arranged from lower to higher malignant potential; expression in C4-2B cells was used for normalization in all experiments. When receptors were undetectable (UND) in C4-2B cells, values from PC-3M or VCaP cells were used instead (**Table 13**).

	Ct C4-2B	Ct PC-3M	Ct VCaP
<b>FZD1</b>	UND	UND	UND
<b>FZD2</b>	26		
<b>FZD3</b>	23		
<b>FZD4</b>	21		
<b>FZD5</b>	21		
<b>FZD6</b>	22		
<b>FZD7</b>	25		
<b>FZD8</b>	26		
<b>FZD9</b>	26		
<b>FZD10</b>	UND	UND	27
<b>VANGL1</b>	21		
<b>VANGL2</b>	28		
<b>ROR1</b>	24		
<b>ROR2</b>	30		
<b>RYK</b>	20		
<b>PTK7</b>	25		
<b>LGR4</b>	21		
<b>LGR5</b>	UND	27	
<b>LRP4</b>	31		
<b>LRP5</b>	20		
<b>LRP6</b>	21		
<b>GPC4</b>	23		
<b>MuSK</b>	UND	28	
<b>WNT11</b>	30		

**Table 13. Wnt receptor Ct values in prostate cancer cell lines used for normalization.** Q-RT-PCR Ct values for listed genes in C4-2B cells used for normalization in Figure 15; PC-3M or VCaP were used for normalization in cases where a gene was undetectable (UND) in C4-2B cells, except for FZD1, which was not expressed in any prostate cancer cell line.

At first glance, examination of expression patterns in the different prostate cancer cell lines revealed that genes encoding several Wnt receptors (*FZD2-5*, *FZD8*, *VANGL1*, *ROR1*, *RYK*, *LGR4*, *LRP5* and *LRP6* and *GPC4*) were highly expressed in at least three prostate cancer cell lines, suggesting a role for them in prostate cancer (**Fig. 34**). Of note, *FZD1* expression was undetectable in any of the prostate cancer cell lines, suggesting this receptor is unlikely to be involved in prostate cancer.

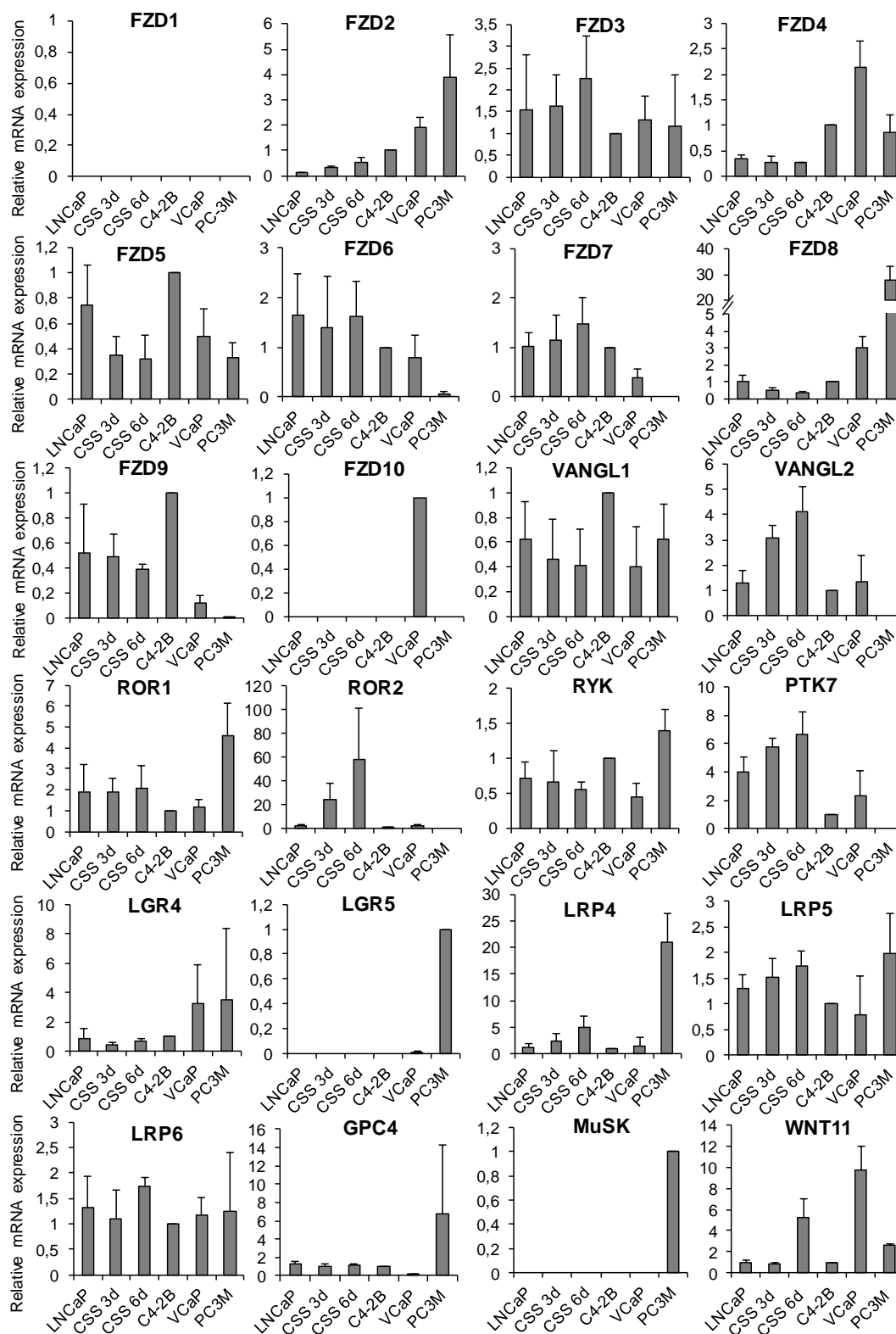


**Figure 34. Expression levels of WNT11 and Wnt receptor genes in prostate cancer cell lines.** Q-RT-PCR analysis showing expression levels of the indicated genes, normalized to 36B4, in LNCaP cells, CSS (LNCaP cells that were hormone-depleted by culture in medium containing 5% charcoal-stripped serum for 3 or 6 days), C4-2B, PC-3M and VCaP cells. PC-3M or VCaP were used for normalization in cases where a gene was undetectable (UND) in C4-2B cells (see Table 13); error bars show SD for three independent experiments.

Trying to simplify the large amount of data obtained after this q-RT-PCR analysis (**Fig. 34**), the different prostate cancer cell lines were classified according to the features of prostate cancer that they represent and grouped the expression of the different Wnt receptors into these categories (**Table 14**). These groups included: neuroendocrine-like differentiation (NED), when receptor expression was increased upon CSS treatment; androgen independence (AI), when receptor expression was increased in C4-2B cells, compared to parental LNCaP cells; metastatic prostate cancer (mPCa), when there was an increased expression in the prostate cancer cell lines derived from patient metastasis (VCaP and PC-3M); and restricted expression, when the receptor expression was limited to a single cell line.

Receptor	UP in NED	UP in AI PCa	UP in mPCa	Restricted expression
<b>FZD2</b>	X	X	X	
FZD3				
<b>FZD4</b>		X	X	
FZD5		X		
FZD6				
FZD7	X			
<b>FZD8</b>			X	
FZD9		X		
FZD10				X
VANGL1		X		
VANGL2	X			
ROR1			X	
ROR2	X			
RYK		X	X	
PTK7	X			
LGR4			X	
LGR5				X
LRP4	X		X	
LRP5	X			
LRP6				
GPC4			X	
MuSK				X
WNT11	X	X	X	

**Table 14. Summary of Wnt receptor genes and *WNT11* expression in prostate cancer.** Wnt receptor and *WNT11* mRNA expression in prostate cancer cell lines with neuroendocrine-like differentiation (NED), androgen-independence (AI PCa), capacity for metastasis (mPCa) and restricted expression to one cell line (for details see Figure 34); *FZD2*, *FZD4* and *FZD8* (grey highlight) were highly expressed in cells with the most aggressive features.

The reorganization and categorization of the q-RT-PCR data allowed us to further analyze which of these Wnt receptors might mediate Wnt-11 signaling in prostate cancer through a deeper comparison of Wnt receptors and *WNT11* expression profiles. Interestingly, although many other *FZD* receptors were highly expressed in the more aggressive prostate cancer cell lines, only some of them showed a pattern of expression similar to that of *WNT11*. Among them, *FZD2* correlated best with *WNT11*, as it was more highly expressed in PC-3M and VCaP cells than in LNCaP and C4-2B cells and it was also upregulated in hormone-depleted LNCaP cells, where *WNT11* expression was increased (**Fig. 34, Table 14**). *FZD4* and *FZD8* expression also showed a partial correlation with that of *WNT11*. In fact, *FZD4* and *FZD8* expression were higher in the more aggressive prostate cancer cells, VCaP and PC-3M, as was *WNT11* expression, suggesting a possible role for these receptors in prostate cancer progression and metastasis. However, *FZD4* also showed increased expression in the androgen-independent C4-2B cell line, in contrast to *WNT11*, and *FZD8* showed lower mRNA levels in hormone-depleted LNCaP cells, where *WNT11* is upregulated (**Fig. 34, Table 14**).

In conclusion, the results from these initial screens highlight the upregulation of several Wnt receptors in prostate cancer cell lines as well as the similar expression patterns of some of them with *WNT11*, suggesting that these candidates may be implicated in prostate cancer progression through mediation of Wnt-11 signaling.

## 1.2 *In silico* screening of Wnt receptors with increased expression in prostate tumors

It is complicated to determine which of the previously identified candidate Wnt receptors is crucial for prostate cancer progression and could function as a Wnt-11 receptor. To complete the initial profiling in prostate cancer cell lines, we used a second approach based on *in silico* analysis of prostate cancer databases, in order to evaluate the expression of Wnt receptors in prostate tumors.

Thus, we examined the expression levels of the 23 Wnt receptors in the Oncomine™ database. Oncomine is a cancer microarray database and web-based data-mining platform which facilitates discovery from genome-wide expression analyses. Oncomine contains more than 65 gene expression datasets comprising nearly 48 million gene expression measurements from over 4700 microarray experiments and allows the analysis of gene expression in most of the major types of cancer in comparison with the

respective normal tissues, as well as a variety of cancer subtypes and clinical-based and pathology-based analyses (Rhodes et al. 2004).

In this screen, we focused on datasets with p-values smaller than 0.05 ( $p < 0.05$ ) and fold changes higher than 1.5 ( $FC > 1.5$ ). At a first glance, when analyzing the data, we could observe that, consistent with our previous results in prostate cancer cell lines, among all the Wnt receptors examined only *FZD4*, *FZD8* and the coreceptor, *PTK7* were clearly upregulated in prostate cancer compared to normal tissue (**Table 15**). However, in contrast to what observed in our screen using prostate cancer cell lines, *FZD2* expression was only found upregulated in a single dataset being also downregulated in one dataset (**Table 15**), which reduces its potential as receptor involved in prostate cancer progression and as a mediator of Wnt-11 signaling.

Receptor	UP in PCa	DOWN in PCa
FZD1	1	6
FZD2	1	1
FZD3	1	1
<b>FZD4</b>	4	
FZD5		1
FZD6		
FZD7	1	6
<b>FZD8</b>	6	
FZD9		
FZD10		2
VANGL1		
VANGL2		1
ROR1		1
ROR2		6
RYK		1
<b>PTK7</b>	2	
LGR4		1
LGR5		2
LRP4		2
LRP5		
LRP6	1	1
GPC4		1
MUSK		1

**Table 15. Profiling of Wnt receptors genes in prostate tumors.** Analysis of Wnt receptor expression profiles using datasets from OncoPrint™; *FZD4*, *FZD8* and *PTK7* (grey highlight) were found to be most frequently upregulated; only datasets with  $p < 0.05$  and fold-change  $> 1.5$  were considered.



A deeper analysis of the Oncomine datasets revealed that *FZD4*, *FZD8* and *PTK7* were not only upregulated in prostate cancer compared to benign prostate tissue in multiple datasets but also in PIN lesions compared to benign prostate, which are thought to be the precursor of prostate cancer (**Table 16**). Therefore, these results implicate these receptors in disease progression. It is important to take into account that not all the analyzed datasets have a large enough sample size for considering the observed differences as biologically significant, but the consistency of the results in all of them support the involvement of *FZD4*, *FZD8* and *PTK7* in prostate cancer.

	Dataset	Comparison	Sample number	P-value	Fold change
<b>FZD4</b>	Lapointe	Carcinoma vs Normal	112	1.61E-11	1,724
	Varambally	Carcinoma vs Normal	13	1.03E-04	1,761
	Tomlins	PIN vs Normal	36	1.63E-04	3,917
	Luo	Carcinoma vs Normal	30	0.023	1,523
<b>FZD8</b>	Tomlins	Carcinoma vs Normal	52	3.67E-06	5,057
		PIN vs Normal	35	2.26E-04	2,462
	Varambally	Carcinoma vs Normal	13	0.002	2,803
	Arredouani	Carcinoma vs Normal	21	0.001	1,811
	Grasso	Carcinoma vs Normal	85	1.47E-05	1,717
<b>PTK7</b>	Tomlins	Carcinoma vs Normal	47	0.001	2,208
		PIN vs Normal	29	4.02E-04	3,466

**Table 16. *FZD4*, *FZD8* and *PTK7* expression in prostate cancer datasets.** Only datasets with  $p < 0.05$  and fold-change  $> 1.5$  were considered.

Since analysis of Oncomine datasets is only based on gene expression, we also used the Protein Atlas database ([www.proteinatlas.org](http://www.proteinatlas.org)) to examine the expression of Wnt receptors at the protein level. The Human Protein Atlas is a Swedish-based program initiated in 2003 with the aim of mapping all the human proteins in cells, tissues and organs using integration of various omics technologies, including antibody-based imaging, mass spectrometry-based proteomics, transcriptomics and systems biology. All the data in the knowledge resource is open access to allow to free exploration of human proteome data. Consistent with the analysis from the Oncomine database, *FZD8* protein expression levels were low in normal prostate and moderately high in prostate cancer, suggesting a possible role for *FZD8* in prostate cancer. In contrast, *FZD4* and *PTK7* protein levels were similar (low and high, respectively) in normal prostate and prostate cancer tissues (**Fig. 35**), which did not support their possible involvement of these receptors in prostate cancer.

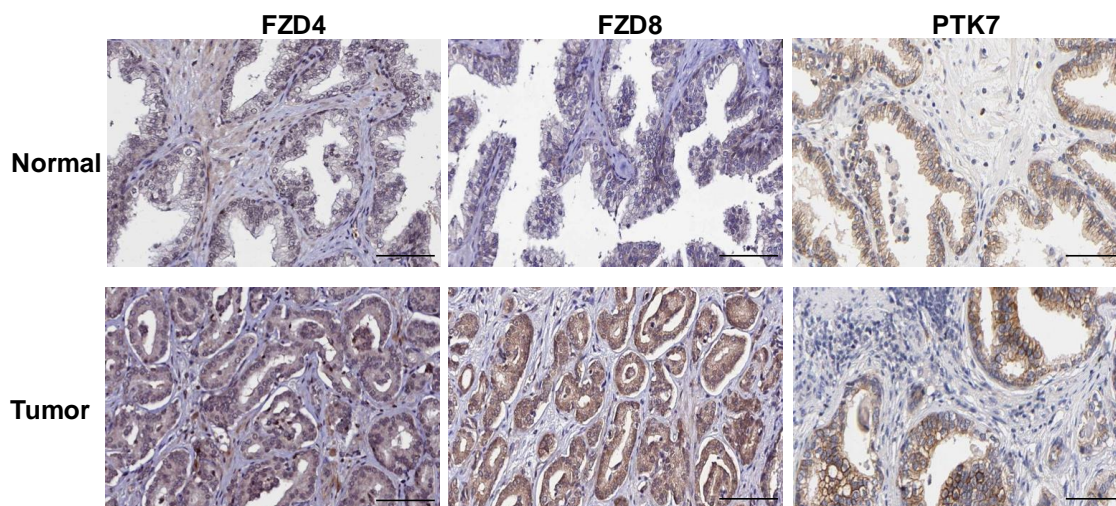


**Figure 35. Immunohistochemistry of Wnt receptors and coreceptors.** Detection of FZD4, FZD8 and PTK7 in sections of normal prostate and prostate cancer; images were collected from [www.ProteinAtlas.org](http://www.ProteinAtlas.org). Scale bar 100  $\mu$ m.

In summary, the analysis of Wnt receptor expression in prostate tumors allowed us to identify potential candidates that are upregulated in prostate cancer and therefore may play a role in the pathogenesis of prostate cancer. Although PTK7 was also found upregulated in prostate cancer and coreceptors are important for Wnt signaling, we will focus our efforts on FZD receptors, since they are essential in all branches of Wnt signaling.

### 1.3 Identification of FZD receptors involved in Wnt-11 signaling

The analysis from both screening approaches in prostate cancer cell lines and in prostate tumors led us to conclude that FZD2, FZD4 and FZD8 may be involved in prostate cancer pathogenesis. However, clarifying their roles as potential Wnt-11 receptors in metastatic prostate cancer required further investigation. Although some FZD receptors have been reported to bind Wnt-11 in different models, such as FZD7 in *Xenopus* (Djiane et al. 2000; Penzo-Mendèz et al. 2003; Yamanaka & Nishida 2007), FZD5 (Cavodeassi et al. 2005) and FZD7 (Witzel et al. 2006) in zebrafish, FZD4 in differentiating cardiomyocytes (Abdul-Ghani et al. 2011; Ye et al. 2011) and FZD4 and FZD8 in the developing kidney (Ye et al. 2011), to date there was no evidence for which FZDs transduce Wnt-11 signals in prostate cancer.

### 1.3.1 Colocalization of Wnt-11 with FZD family members

The analysis of the cell line data led us to hypothesize that FZD2, FZD4 and FZD8 may be involved in prostate cancer pathogenesis, and as they show similar expression patterns to that of Wnt-11, they may also mediate Wnt-11 signaling in prostate cancer cells. However, the high expression of some other FZD family members in PCa cells meant that we could not rule them out.

To further explore this possibility, immunofluorescence was used to examine which of the FZD family members is capable of co-localizing with Wnt-11 in prostate cancer cells. PC-3M prostate cancer cells were co-transfected with Wnt-11 and epitope-tagged forms of each of the members of the FZD family (FZD1-10). Subsequent staining for FZD-tag and Wnt-11 revealed very different patterns of expression and Wnt-11 colocalization among the FZD members. A deeper analysis of the staining showed a strong colocalization between Wnt-11 and FZD8, as shown by a Pearson coefficient of correlation of 0.686 (**Table 17 and Fig. 36**). Of note, moderate colocalization was also found between Wnt-11 and FZD6 (Pearson of 0.459) and Wnt-11 and FZD10 (Pearson of 0.529) (**Table 17 and Fig. 36**). However, no or weak colocalization was observed for the other FZD family members (**Table 17 and Fig. 36**).

	<b>Pearson (-1 &lt; x &lt; 1)</b>
FZD1	-0.016 ± 0.009
FZD2	0.062 ± 0.025
FZD3	0.181 ± 0.063
FZD4	0.125 ± 0.082
FZD5	0.224 ± 0.102
<b>FZD6</b>	0.459 ± 0.068
FZD7	-0.002 ± 0.014
<b>FZD8</b>	0.686 ± 0.030
FZD9	-0.037 ± 0.026
<b>FZD10</b>	0.529 ± 0.050

**Table 17. Quantification of Wnt-11 and FZD receptor colocalization.** ImageJ analysis of colocalization for 10 cells per experiment (see Methods). FZD6, FZD8 or FZD10 (grey highlight) showed strong colocalization.

Since our q-RT-PCR analysis showed that FZD6 was not highly expressed in metastatic prostate cancer cell lines and that FZD10 expression was restricted to a single cell line, this colocalization analysis supports a role of FZD8 as the FZD receptor that mediates Wnt-11 signaling in metastatic prostate cancer.

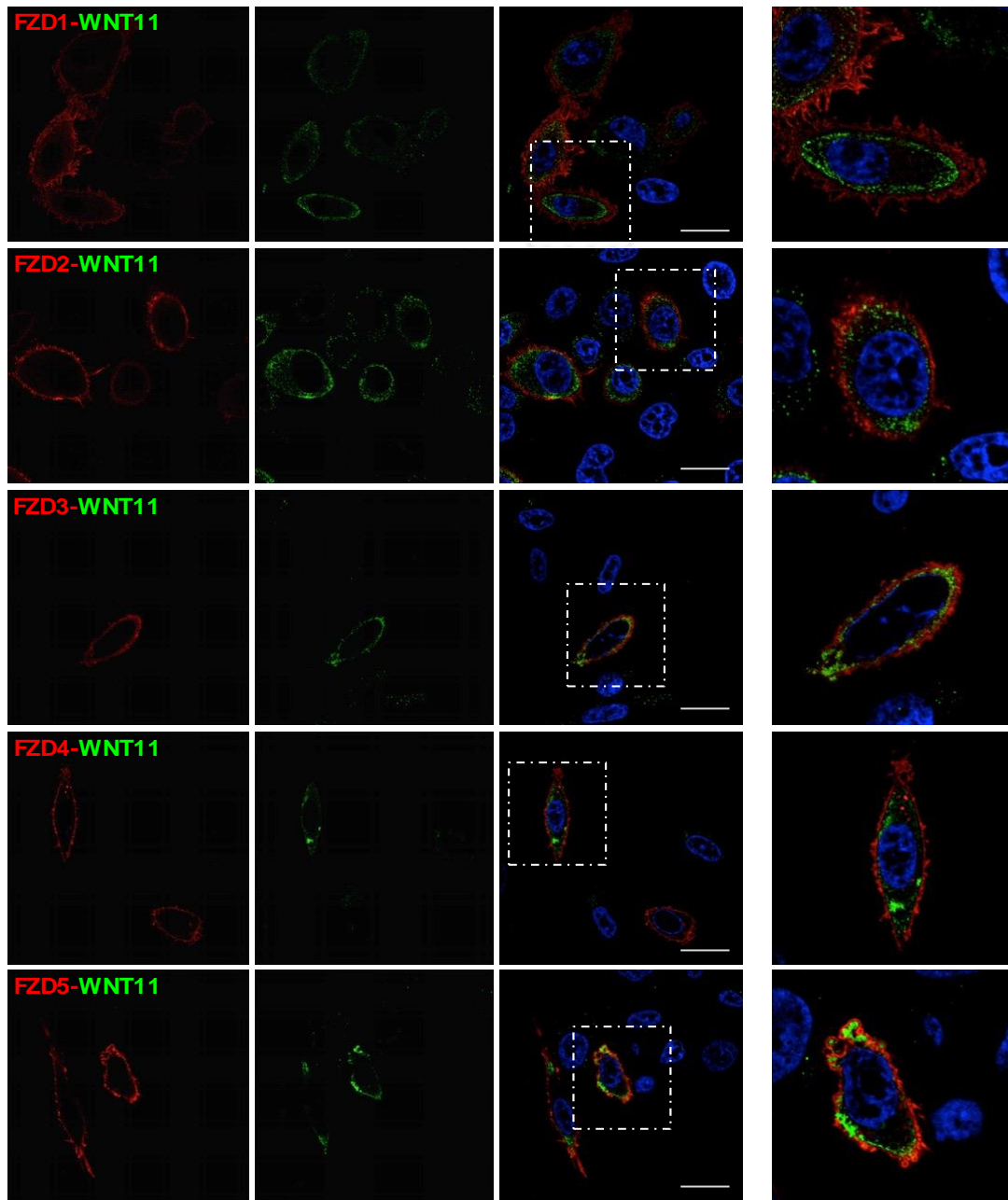


**Figure 36. Wnt-11 and FZD receptor localization.** Immunofluorescence analysis of PC-3M cells transfected with 1D4-tagged FZD1-10 (red) and Wnt-11 (green) for 24 h; images are representative of three independent experiments, blue staining shows cell nuclei (DAPI), scale bar 20  $\mu$ m.

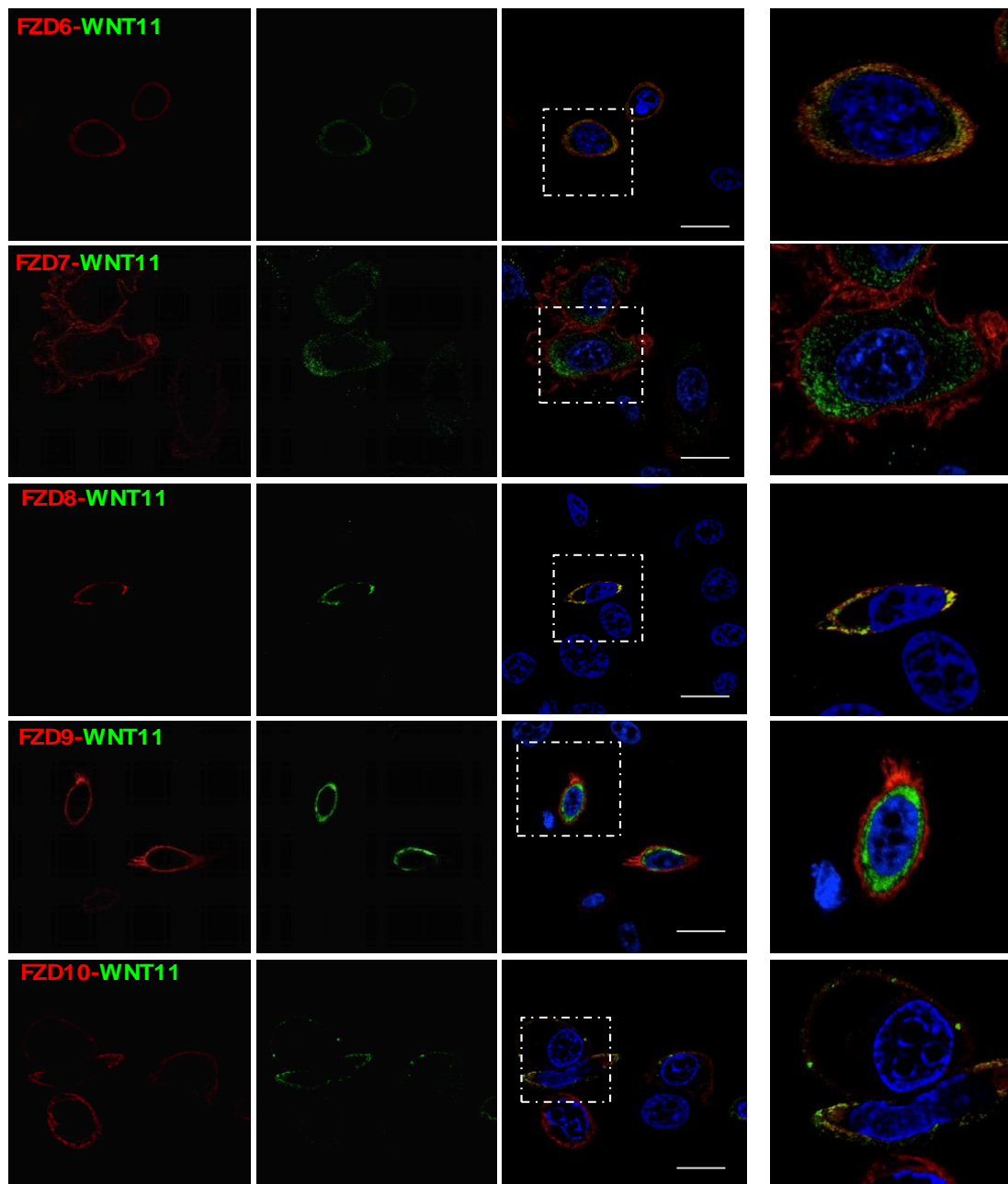


**Figure 36. Wnt-11 and FZD receptor localization (continuation).** Immunofluorescence analysis of PC-3M cells transfected with 1D4-tagged FZD1-10 (red) and Wnt-11 (green) for 24 h; images are representative of three independent experiments, blue staining shows cell nuclei (DAPI), scale bar 20  $\mu$ m.

### 1.3.2 Evaluation of Wnt-11-FZD signaling

The results from our initial screen and the colocalization assays indicate that FZD8 satisfies several criteria to be a Wnt-11 receptor in metastatic prostate cancer. However, since other FZD family members were also highlighted in our studies, we decided to explore the potential role of all of them as Wnt-11 receptors through further analysis. Since Wnt proteins mediate signaling by activating different transcription factors, gene reporter assays are widely used tool to monitor the activation of this pathway.

In a variety of cell contexts, including cardiac tissue morphogenesis (Zhou et al. 2007), *Xenopus* embryo development (Ohkawara & Niehrs 2011) and avian facial morphogenesis (Geetha-Loganathan et al. 2014), Wnt-11 has been found to activate ATF2 dependent gene reporter activity, which is considered a reporter of the noncanonical pathway. In this regard, our first goal was to determine whether Wnt-11 was also able to activate an ATF2-dependent luciferase reporter (Ohkawara & Niehrs 2011) in prostate cancer cells. With this purpose, we used two different prostate cancer cell lines, C4-2B and PC-3M, which harbor low and relatively high levels of endogenous Wnt-11, respectively and performed gene reporter assays. Consistent with observations in other models, transfection of Wnt-11 in both prostate cancer cell lines showed a significant activation of the reporter (**Fig. 37**) supporting the activation of this noncanonical signal by Wnt-11 in prostate cancer cells.

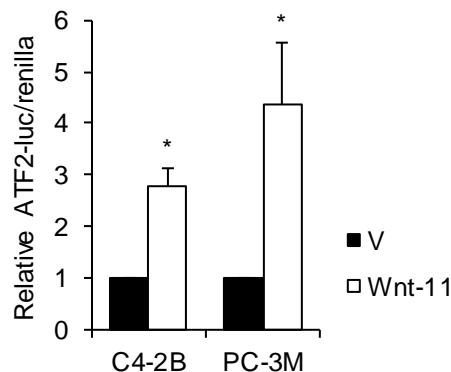


**Figure 37. Wnt-11 activates the ATF2-dependent gene reporter.** Relative ATF2 luciferase/renilla activity in C4-2B and PC-3M cells transfected with empty vector (V) or Wnt-11.

Aiming to determine which FZD family members might be capable of transducing Wnt-11 signals in prostate cancer, we co-transfect Wnt-11 together with the ten members of the FZD family. The gene reporter assay revealed that ATF2-dependent transcriptional activity in PC-3M cells was significantly enhanced upon transfection of seven members of the FZD family (**Fig. 38A**). Among them, FZD8 and FZD10 showed the strongest

increases and their effects were further boosted by Wnt-11 (**Fig. 38A**), suggesting that these receptors can mediate Wnt-11 signaling in prostate cancer. Importantly, the amount of each receptor plasmid used (**Fig. 38A**) was adjusted based on the level of protein expression when cotransfected with Wnt-11 (**Fig. 38B**) in order to reduce the possibility of effects on ATF2 reporter activity resulting from different protein expression levels. Of note, expression of FZD3 and FZD10 was substantially lower than other FZD family members even though higher amounts of plasmid were transfected, which suggests that FZD3 and FZD10 are less stable. Despite its low expression, FZD10 was able to activate ATF2 luciferase, suggesting the lack of effect of FZD3 is not related to its lower expression.

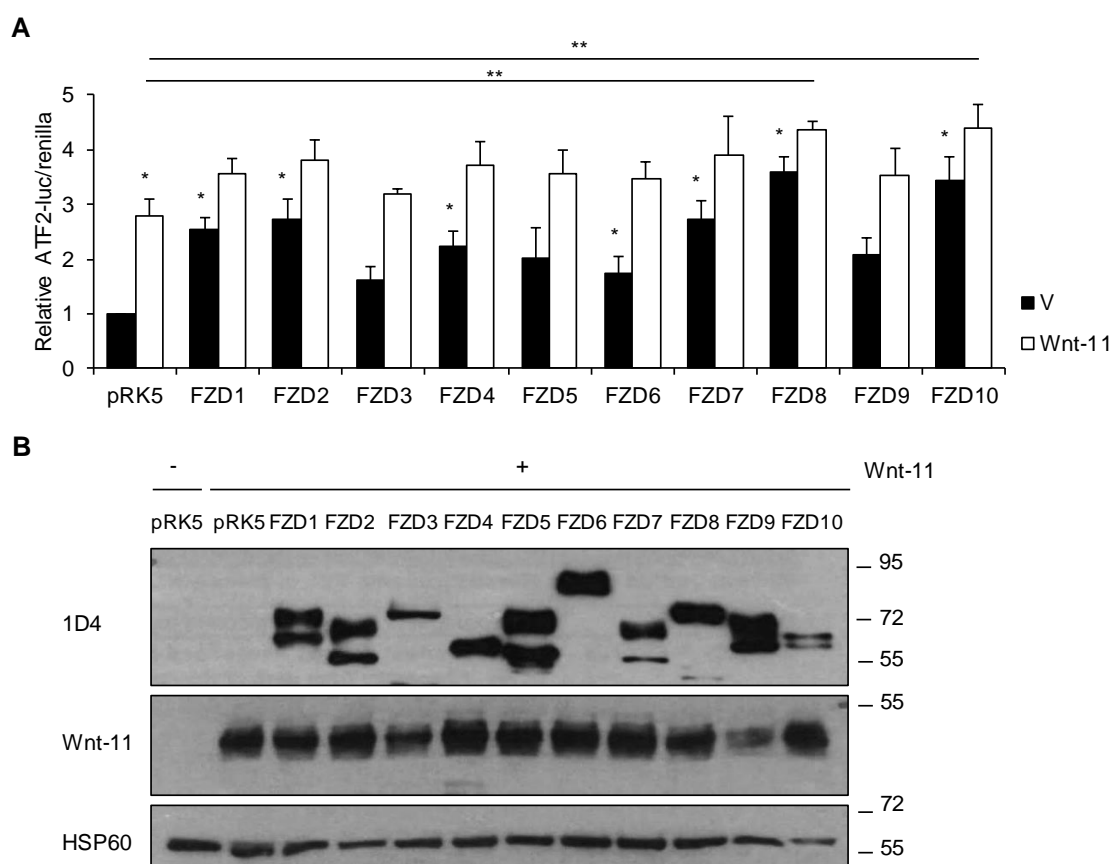


**Figure 38. Involvement of FZD receptors in Wnt-11/ATF2 signaling in prostate cancer. (A)** Relative ATF2 luciferase/renilla activity in C4-2B cells transfected with empty vector (pcDNA) or Wnt-11 and FZD1-10; results are normalized to pRK5. **(B)** Western blot of C4-2B cells transfected with and without Wnt-11 and the same amounts of FZD1-10 as in **(A)**.

### 1.3.3 FZD8 as a major Wnt-11 receptor

All the previous results are consistent with FZD8 mediating the Wnt-11 response. However, it was still unclear if endogenous FZD8 transduces Wnt-11 signals in prostate cancer, as several other FZD family members are also highly expressed.

To address this issue, gene reporter assays were carried out in PC-3M cells silenced with siRNAs targeting the highly expressed FZD family members. According to our data from the initial profiling in prostate cancer cell lines, *FZD2-5* and *FZD8* were highly expressed in the more metastatic cell lines, showing Ct values between 20 to 22 by q-RT-PCR (**Table 13,14 and Fig. 34**). Gene reporter assays after silencing of these receptors and transfection of Wnt-11 revealed that, *FZD8* silencing reduced Wnt-11 activation of ATF2-dependent transcription by approximately 40% (**Fig. 39A**). This analysis also showed that *FZD2* silencing reduced it by 20%, while silencing of *FZD3*, *FZD4* and *FZD5* had no effect (**Fig. 39A**). Of note, *FZD8* silencing also mildly reduced *FZD5* expression (**Fig. 39B**), which is related in sequence to *FZD8*. However, *FZD5* was not highly expressed in the more aggressive prostate cancer cell lines (**Table 14 and Fig. 34**) and *FZD5* silencing did not affect Wnt-11 activation of ATF2-dependent transcription (**Fig. 39A**), consistent with endogenous FZD8, rather than FZD5, mediating the Wnt-11 response.

To confirm this results, an unrelated Dicer-substrate siRNA (dsiRNA) was used to silence *FZD8*. In fact, this dsiRNA also inhibited Wnt-11 activation of ATF2-dependent transcription (**Fig. 39C**), supporting the role of FZD8 in transducing the Wnt-11 signal. Importantly, the effect of *FZD8* siRNA on ATF2 transcriptional activity could be rescued by transfection of mouse FZD8, which is not recognized by the *FZD8* siRNA (**Fig. 39D**). Together, these findings indicate that endogenous FZD8 is a major mediator of Wnt-11 signaling in prostate cancer.



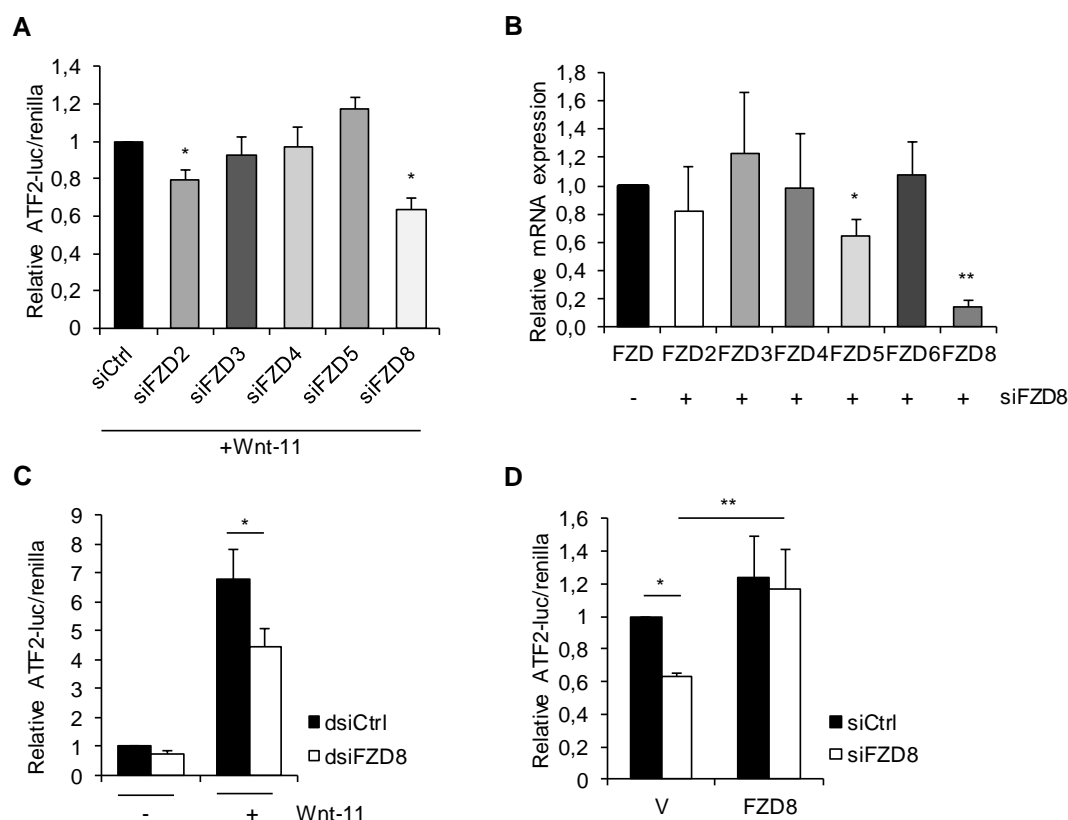


**Figure 39. Requirement for FZD8 in the response to Wnt-11 in prostate cancer cells. (A)** Relative ATF2 luciferase/renilla activity in PC-3M cells silenced for the indicated FZDs and then transfected with Wnt-11; results are normalized to siCtrl. **(B)** Relative expression levels of the indicated genes, normalized to 36B4, in PC-3M cells silenced for *FZD8*. **(C)** Relative ATF2 luciferase/renilla activity in PC-3M cells silenced for *FZD8* with dsiRNAs and then transfected with Wnt-11. **(D)** Relative ATF2 luciferase/renilla activity in PC-3M cells silenced for *FZD8* siRNAs and transfected with empty vector pRK5 (V) or *FZD8* plasmid. Error bars in **(A)** to **(D)** show SD for three independent experiments; \*  $p < 0.05$ , \*\*  $p < 0.001$  by Student's *t* test or ANOVA with Tukey post-hoc test where appropriate

ATF2 is a component of the AP-1 complex, in which it forms homo- or hetero-dimers with JUN, FOS and MAF (musculoaponeurotic fibrosarcoma) transcription factors (Eferl & Wagner 2003; Lopez-bergami 2011). Since Wnt-11 is also known to regulate AP-1 signaling (Y. Li et al. 2008) and we have previously shown that FZD8 is involved in ATF2 signaling, we decided to corroborate the implication of FZD8 in transducing Wnt-11/AP-1 noncanonical signaling using an AP-1-dependent gene reporter (Vivanco et al. 1995). Analysis of these data showed that *FZD8* silencing also reduced Wnt-11 activation of AP-1-dependent transcription (**Fig. 40A**), which supports our previous results involving FZD8 in noncanonical Wnt signaling.

Although Wnt-11 usually inhibits Wnt/ $\beta$ -catenin signaling due to its activation of noncanonical pathways (Uysal-Onganer & Kypta 2012), FZD8 has been reported to be involved in Wnt/ $\beta$ -catenin signaling in some cell types (Miao et al. 2015; Sun et al. 2014;

Yin et al. 2013; Albers et al. 2013). However, *FZD8* silencing in PC-3M prostate cancer cells did not inhibit  $\beta$ -catenin/Tcf-dependent transcriptional activity, as measured using the Super8xTOPFlash reporter and its nonresponsive control Super8xFOPFlash (**Fig. 40B**). In agreement with these results, *FZD8* silencing reduced expression of *ATF2* mRNA but not expression of the  $\beta$ -catenin/Tcf target gene *AXIN2*, which actually increased (**Fig. 40C**). Together, these data corroborate the role of FZD8 in  $\beta$ -catenin-independent Wnt signaling in prostate cancer.

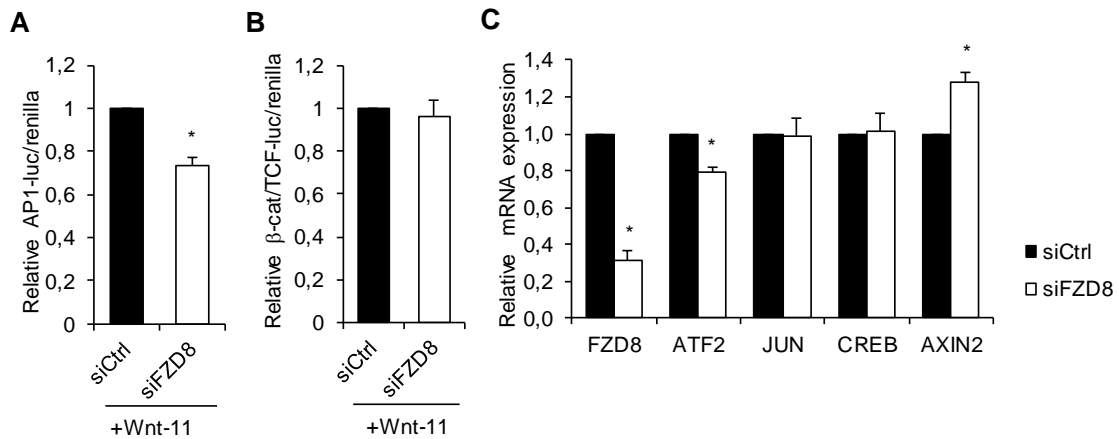


**Figure 40. FZD8 mediates Wnt-11 noncanonical signaling. (A)** Relative AP-1 luciferase/renilla activity in PC-3M cells transfected with siCtrl or siFZD8 and then with Wnt-11. **(B)** Relative  $\beta$ -catenin/TCF activity (TOPFlash/FOPFlash) in PC-3M cells transfected with siCtrl or siFZD8 and then with Wnt-11. **(C)** Q-RT-PCR analysis showing mRNA expression of the indicated genes, relative to 36B4, in PC-3M cells transfected with control (Ctrl) and FZD8 siRNAs. Error bars in (A) – (C) show SD from at least three independent experiments; \* p < 0.05, \*\* p < 0.001 by Student's t test or ANOVA with Tukey post-hoc test.

Interaction of Wnt proteins with FZD receptors is an essential step in activation of both canonical and noncanonical Wnt signals (Mikels & Nusse 2006). Since our results support the role of FZD8 as major Wnt-11 receptor in metastatic prostate cancer and we also found that Wnt-11 and FZD8 strongly colocalize in prostate cancer cells, we hypothesized that Wnt-11 and FZD8 should be able to form a stable complex, which mediates activation of signaling. In order to corroborate our hypothesis, immunoprecipitation analyses were carried out using PC-3M cells transfected with tagged forms of Wnt-11 and FZD8. As expected, the results indicated that Wnt-11 and FZD8 can form a stable complex (**Fig. 41**) in prostate cancer cells, further supporting a role for Wnt-11- FZD8 signaling in prostate cancer.

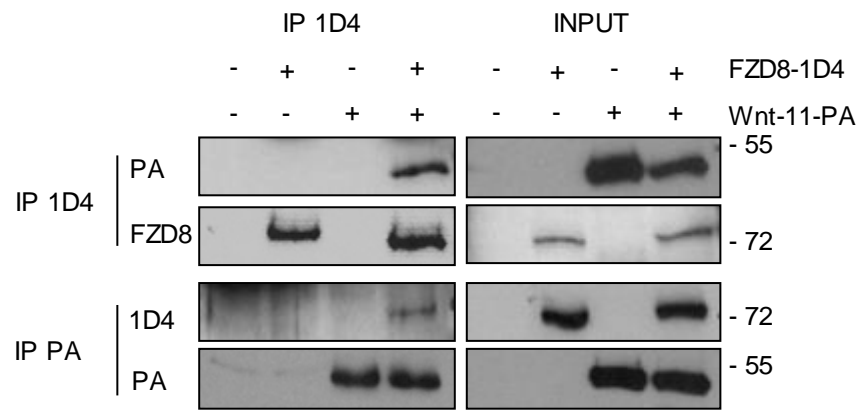


**Figure 41. FZD8 binds Wnt-11 in vitro.** Western blots of anti-1D4 and anti-PA immunoprecipitates (IP) and extracts (Input) from PC-3M cells transfected with plasmids encoding 1D4-tagged FZD8 and PA-tagged Wnt-11 were probed for Wnt-11 (PA) or FZD8 (1D4); blots are representative of three independent experiments and the positions of molecular mass markers are indicated.

## Chapter 2. Implication of FZD8 in prostate cancer pathogenesis

Prostate cancer, as any other type of cancer, is a complex disease involving a lot of dynamic changes in the genome which together lead to cancer development and progression. Different alterations such as self-sufficiency in growth signals, insensitivity to growth-inhibitory signals, evasion of apoptosis, limitless replicative potential, sustained angiogenesis, genomic instability and mutation, tumor promoting inflammation and tissue invasion and metastasis have been identified as drivers of tumorigenesis (Hanahan & Weinberg 2000; Hanahan & Weinberg 2011).

Due to our previous results showing the increased expression of FZD8 as well as its role as a Wnt-11 receptor in metastatic prostate cancer cell lines, we hypothesized that FZD8 could have a role in prostate cancer progression driving the metastatic process. We therefore decided to explore our hypothesis using three different strategies combining *in vitro* and *in vivo* assays, as well as samples from prostate cancer patients.

### 2.1 Role of FZD8 in prostate tumorigenesis: *in vitro* analysis

In order to study the implication of FZD8 in tumor progression and metastasis, we firstly aimed to evaluate different features of tumor cells that have been described as essential during the metastatic process, such as the acquisition of cell motility and the regulation of the epithelial to mesenchymal transition (EMT).

#### 2.1.1 Contribution of FZD8 to capacity for prostate cancer cell migration and invasion

The loss of cell-cell adhesion capacity allows malignant tumor cells to dissociate from the primary tumor mass and the changes in cell-matrix interaction enable the cells to invade the surrounding stroma. This process involves the secretion of substances to degrade the basement membrane and extracellular matrix and also the expression/suppression of proteins involved in the control of motility and migration. After acquiring these properties, the motile cells then journey through the circulatory system invading the vascular basement membrane and the extracellular matrix in the process of extravasation. Later, these cells will attach at a new location and proliferate to produce the secondary tumor (Martin et al. 2000). Since migration and invasion are among the key events leading the course of tumor progression and metastasis and it was previously reported that Wnt-11 is required for prostate cancer cell migration and invasion (Uysal-Onganer et al. 2010), we hypothesized that FZD8 could be required for these functions in prostate cancer cells.

### 2.1.1.1 Cell migration and invasion in conventional two-dimensional (2D) cell cultures

As a first approach, we performed migration and invasion assays using conventional 2D cell culture. In order to do that, two independent metastatic prostate cancer cell lines: PC-3M (which metastasizes to the bone) and DU145 (which is derived from a metastasis in the brain) were transiently silenced for *FZD8* for 48 h and then subjected to migration and invasion assays. Analysis of both assays revealed that *FZD8* silencing significantly reduced cell migration (**Fig. 42A and B**) and invasion through Matrigel (**Fig. 42C and D**) in both cell lines. Of note, *FZD8* silencing also had a small effect on cell number, reducing it by up to 20% (**Fig. 43A and B**). However, this effect was already accounted for when measuring the effects of *FZD8* silencing on cell migration and invasion. Taken together, these results indicate that *FZD8* contributes to the migratory and invasive capacities of metastatic prostate cancer cells.

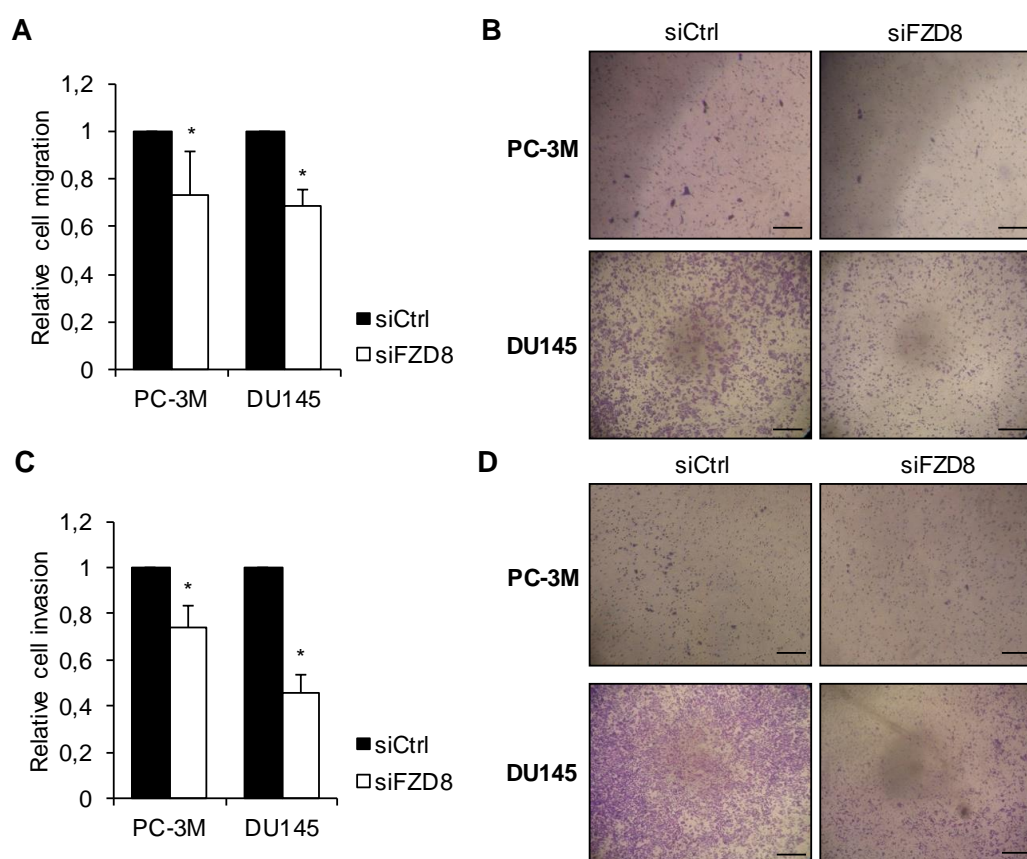


**Figure 42. FZD8 is required for prostate cancer cell migration and invasion.** (A) Migration assays for PC-3M and DU145 cells silenced with control (siCtrl) and FZD8 siRNAs, values are relative to siCtrl and normalized to viable cell number of silenced cells plated in parallel; error bars show SD for at least four independent experiments. (B) Representative images of migrated cells, scale bar 100  $\mu$ m. (C) Invasion assays for PC-3M and DU145 cells silenced with control (siCtrl) and FZD8 siRNAs, values are relative to siCtrl and normalized to viable cell number; error bars show SD for at least three independent experiments. (D) Representative images of invaded cells, scale bar 100  $\mu$ m. \*  $p < 0.05$  by Student's t test.

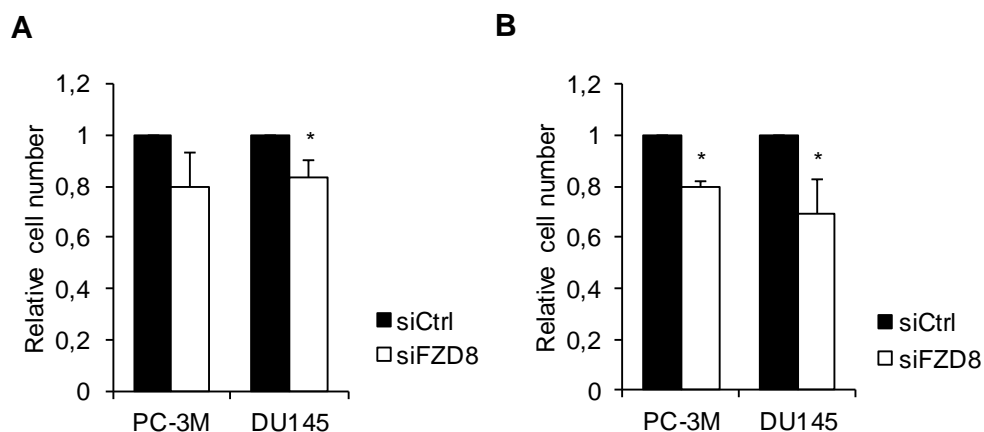


**Figure 43. Effects of *FZD8* silencing on cell proliferation. (A) and (B)** Cell number analysis of PC-3M and DU145 cells transfected with control of *FZD8* siRNAs used to normalize numbers of migrating (**Fig. 42A**) and invading (**Fig. 42C**) cells; error bars show SD of at least three independent experiments. \*  $p < 0.05$  by Student's t test.

To corroborate the requirement for *FZD8* in cell invasion, PC-3M cell lines in which *FZD8* was stably silenced were generated using two independent lentiviral sh*FZD8* constructs. The analysis of invasion assays showed that, in agreement with the results obtained by transient silencing, stable *FZD8* knockdown significantly reduced prostate cancer cell invasion (**Fig. 44A and B**). The extent of *FZD8* silencing was confirmed by q-RT-PCR (**Fig. 44C**) and its effect on cell number (**Fig. 44D**) was taken into account when analyzing the effect on cell invasion. Taken together, these results indicate that, as for Wnt-11, *FZD8* contributes to the migratory and invasive activities of metastatic prostate cancer cells.

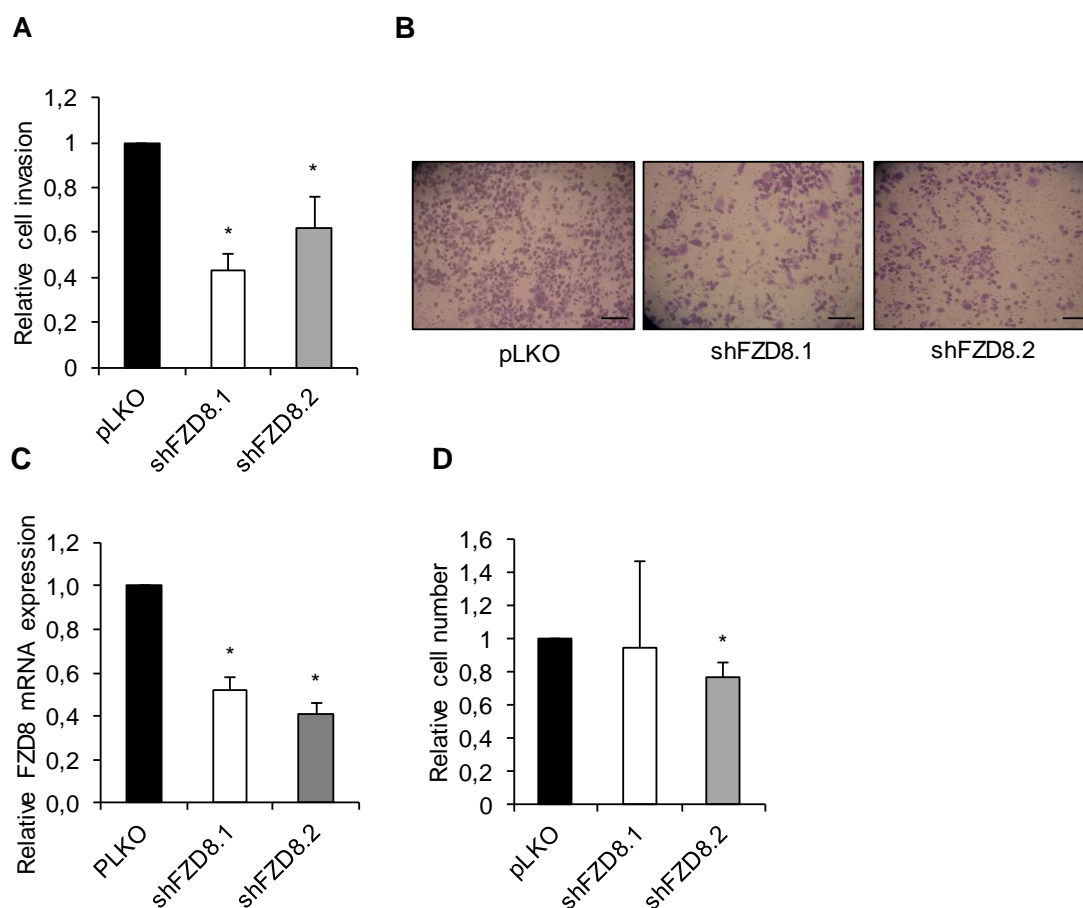


**Figure 44. Stable knockdown of *FZD8* reduces prostate cancer cell invasion.** (A) Invasion assays using PC-3M cells stably silenced for FZD8 using lentiviruses expressing two different FZD8 shRNAs (shFZD8.1 and shFZD8.2), values are relative to pLKO and normalized to numbers of viable cells plated in parallel (Figure 44D); error bars show SD for three independent experiments. (B) Representative images of invaded cells, scale bar 100  $\mu$ m. (C) Relative mRNA expression levels of FZD8 measured by q-RT-PCR in shFZD8 PC-3M cells; error bars represent SD of three independent experiments. (D) Cell number of stable PC-3M cells expressing the indicated shRNAs; error bars show SD of three independent experiments. This data was used to normalize numbers of invading cells. \*  $p < 0.05$  by ANOVA with Tukey post-hoc test

A recent study reported small molecule inhibitors of Wnt signaling that target the Wnt binding site on FZD8 (Lee et al. 2015). Structure-based virtual screening and cell-based assays were used to identify five small molecules that have low IC<sub>50</sub> values in the micromolar range. Their binding to the FZD8 CRD was confirmed by NMR experiments and their ability to inhibit canonical Wnt signaling was shown with TOP/FOP reporter assays and analysis of LRP6 phosphorylation (Lee et al. 2015). Based on these studies, we selected two of these compounds: inhibitor 1 (3235-0367) and 2 (2124-0331) and tested their effects on prostate cancer cell migration. Consistent with our *FZD8* silencing studies, both compounds significantly reduced PC-3M cell migration (Fig. 45A and B) without affecting cell number (Fig. 45C), providing further support for FZD8 as a therapeutic target in metastatic prostate cancer.

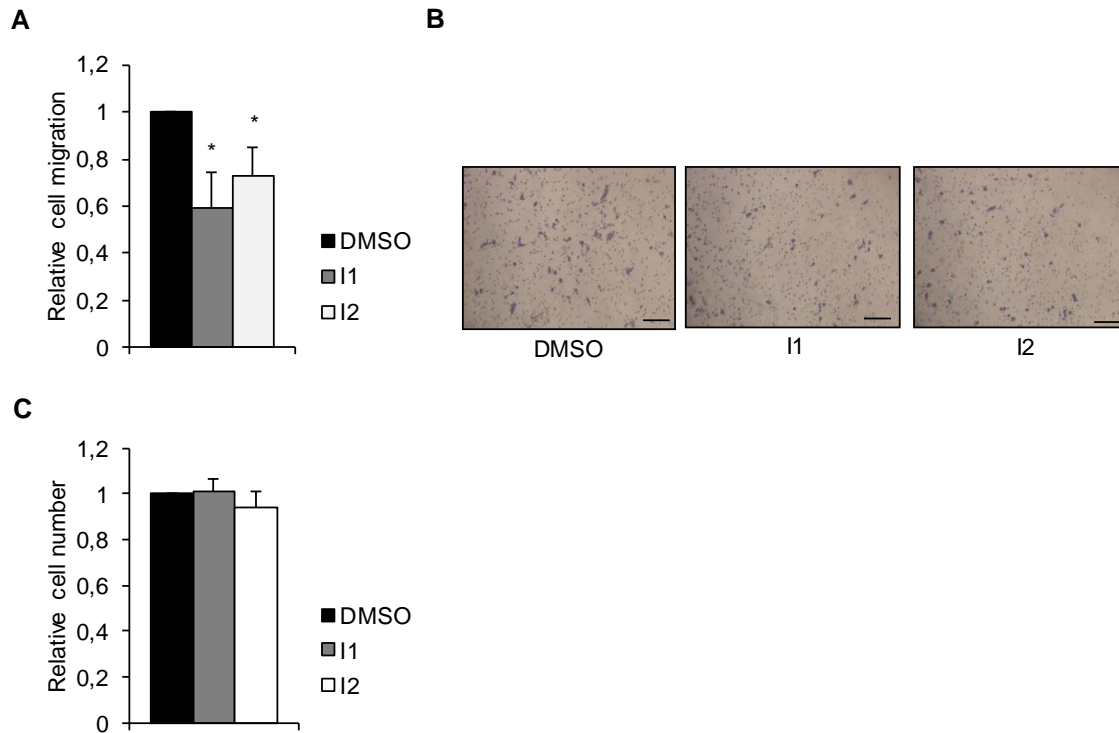


**Figure 45. Wnt/FZD inhibitors reduce prostate cancer cell migration. (A)** Migration assays for PC-3M cells treated with DMSO or inhibitors 1 (I1) and 2 (I2) at 10  $\mu$ M for 24 h; values are relative to DMSO and normalized to viable cell number; error bars show SD for four independent experiments. **(B)** Representative images of migrated cells, scale bar 100  $\mu$ m. **(C)** Cell proliferation analysis of PC-3M cells treated with DMSO, inhibitor 1 (I1) and inhibitor 2 (I2); error bars show SD for four independent experiments. These data were used for normalization the migration experiments in **(A)**. \*  $p < 0.05$  by ANOVA with Tukey post-hoc test

### 2.1.1.2 Cell invasion in organotypic tridimensional (3D) cultures

Our results highlight a role for FZD8 in prostate cancer cell motility through regulation of migration and invasion of prostate cancer cells. In order to perform a better examination of the role of FZD8 in this context, we took advantage of a three-dimensional (3D) organotypic cell culture model that includes Matrigel to mimic the tissue extracellular matrix (ECM). Previous studies have shown that in this assay, PC-3 and PC-3M metastatic prostate cancer cells initially differentiate into hollow organoids (days 4-5) and later spontaneously de-differentiate into invasive stellate structures (days 8-12) (Härma et al. 2010).

To determine the effects of FZD8 silencing using this assay, *FZD8* was silenced in both PC-3 and PC-3M cells and they were cultured as organoids, monitoring morphology, polarization and growth for up to 9 days using the IncuCyte™ system. Evaluation of the 3D assay revealed that cells transfected with control siRNA initially matured into well-differentiated organoids and then formed invasive and multicellular structures at days 8-



9 (**Fig. 46A and B**). In contrast, as anticipated based on the results from the 2D experiments, *FZD8*-silenced cells matured into well-differentiated organoids but did not form invasive structures by the end of the assay (**Fig. 46A and B**). Of note, these effects were completely evident at the endpoint of the assay, despite recovery of basal *FZD8* mRNA expression levels by day 8, which suggests that phenotypical changes occur early in the process (**Fig. 46C and D**).

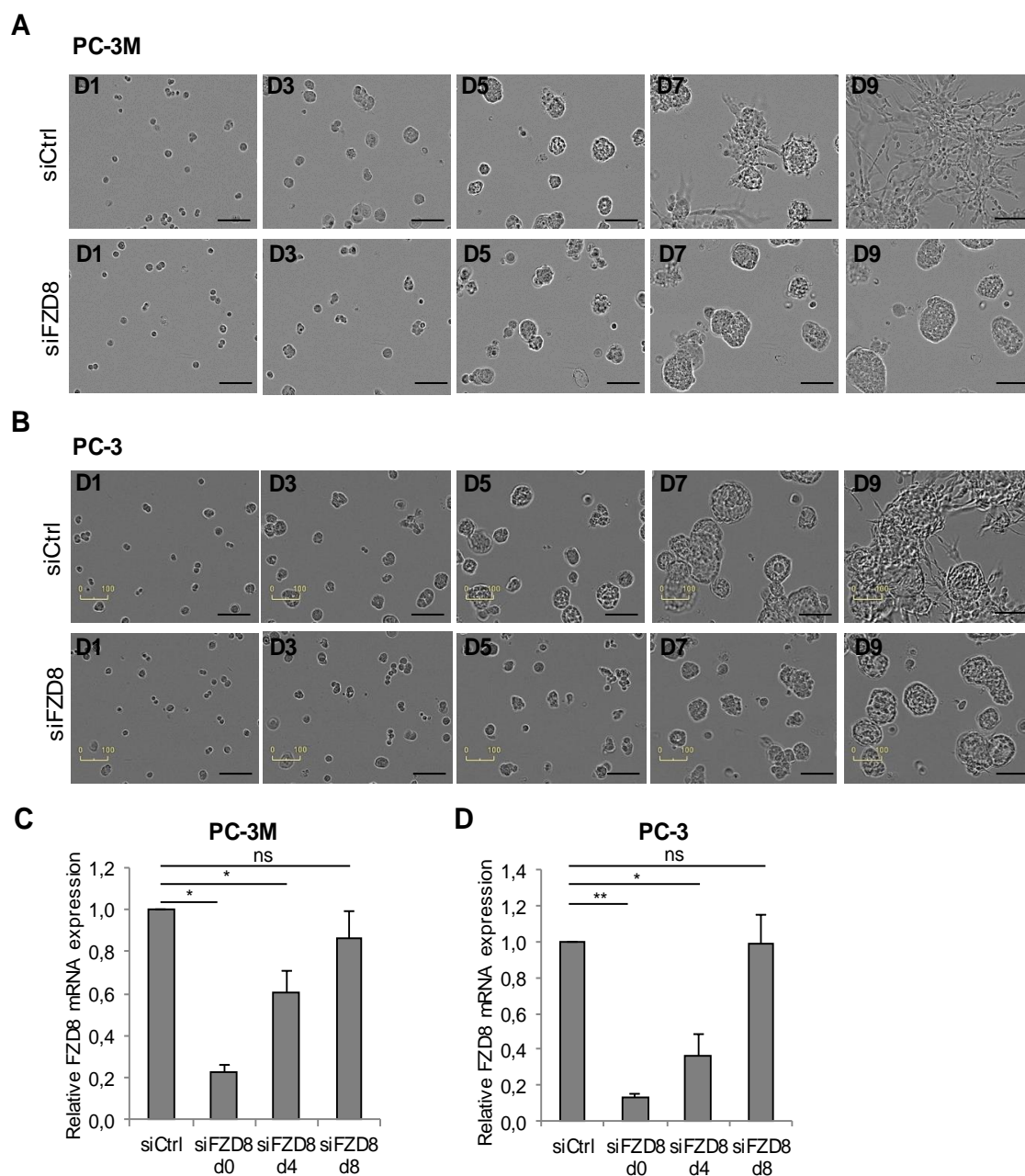


**Figure 46. *FZD8* silencing reduces prostate cancer cell invasion in organotypic 3D cultures.** (A) Representative images from Incucyte live-cell imaging of 3D cultures of control and *FZD8*-silenced in PC-3M (upper panel) and PC-3 (lower panel) cells at days 1 to 9; scale bar 100  $\mu$ m. (C) and (D) *FZD8* expression levels in *FZD8*-silenced cells at days 0, 4 and 8 of 3D culture in PC-3M (C) and PC-3 (D); error bars show SD for three independent experiments. \*  $p < 0.05$  \*\*  $p < 0.001$  by ANOVA with Tukey post-hoc test.

In order to quantify the phenotypic changes observed during the 3D culture, at least 1,000 organoids were examined using high-content, automated morphometric image data analysis (AMIDA) software, which allows the segmentation and quantitative measurement of large numbers of images with different shapes, sizes and textures (Härma et al. 2014). For this purpose, organoids were live-stained with calcein and ethidium homodimer at the endpoint of the 3D culture and visualized by confocal microscopy. After imaging, all the pictures were segmented (**Fig. 47**) and analyzed using AMIDA. This analysis revealed that *FZD8* silencing significantly reduced the severity (AppIndex) and length (MaxApp) of invasive multicellular structures, accompanied by reductions in the numbers of small filopodia-like cellular extensions (Roughness) and organoid size (Area), as well as by a rounder shape (Roundness) (**Fig. 48 and 49**). Of note, *FZD8* silencing in PC-3M cells significantly reduced the frequency of cell death (AreaRatioR), which in theory could promote the subsequent formation of invasive structures. However, this is not the case for *FZD8* silencing, which significantly reduced parameters involved in cell invasion (**Fig. 48A**).

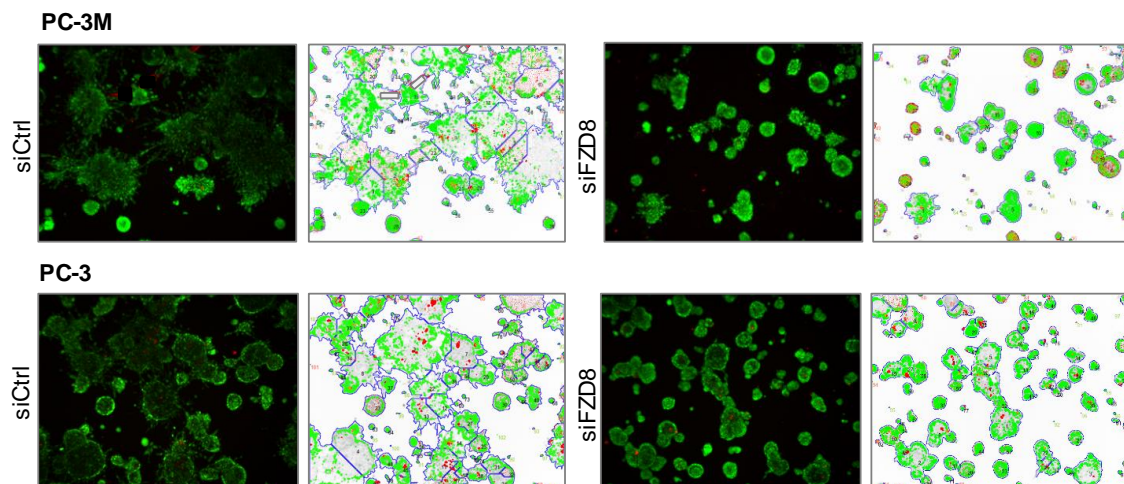


**Figure 47. Representative segmentation of live-cell confocal images by AMIDA.** *FZD8*-silenced PC-3M (upper panel) and PC-3 (lower panel) cell organoids cultured in 3D for 9 days were stained with ethidium homodimer-1 (red) to detect apoptotic cells and with calcein (green) to detect live cells. Confocal images were segmented with AMIDA for posterior quantification of effects.

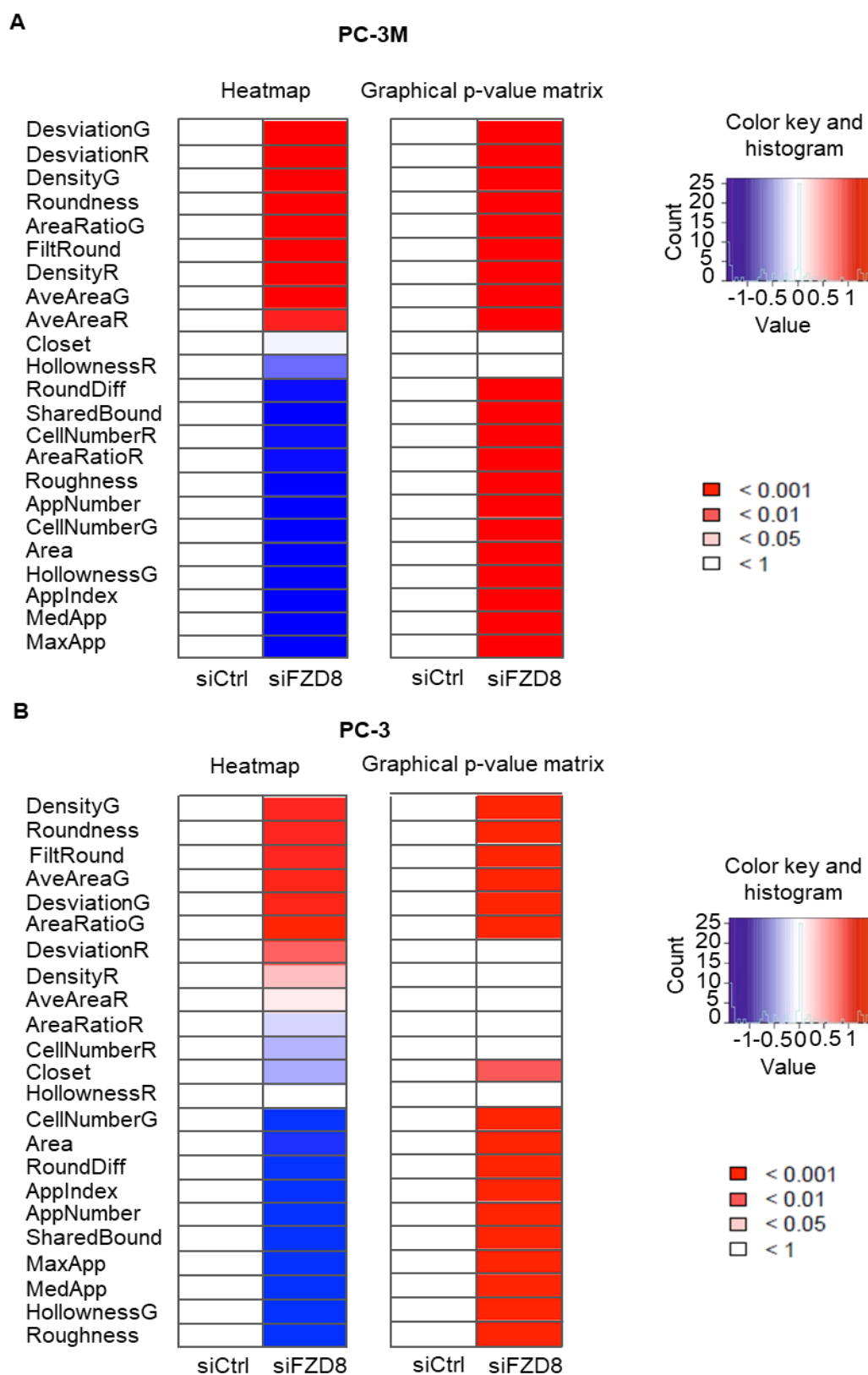


**Figure 48. Quantification of phenotypic effects of *FZD8* silencing in organotypic 3D cultures.** Heatmaps and graphical p-value matrix of morphometric parameters measured by AMIDA and altered by *FZD8* silencing in PC-3M (**A**) and PC-3 (**B**) cell organoids (red, increased and blue decreased). P values are Bonferroni-corrected from t-tests, comparing siFZD8 and siCtrl.

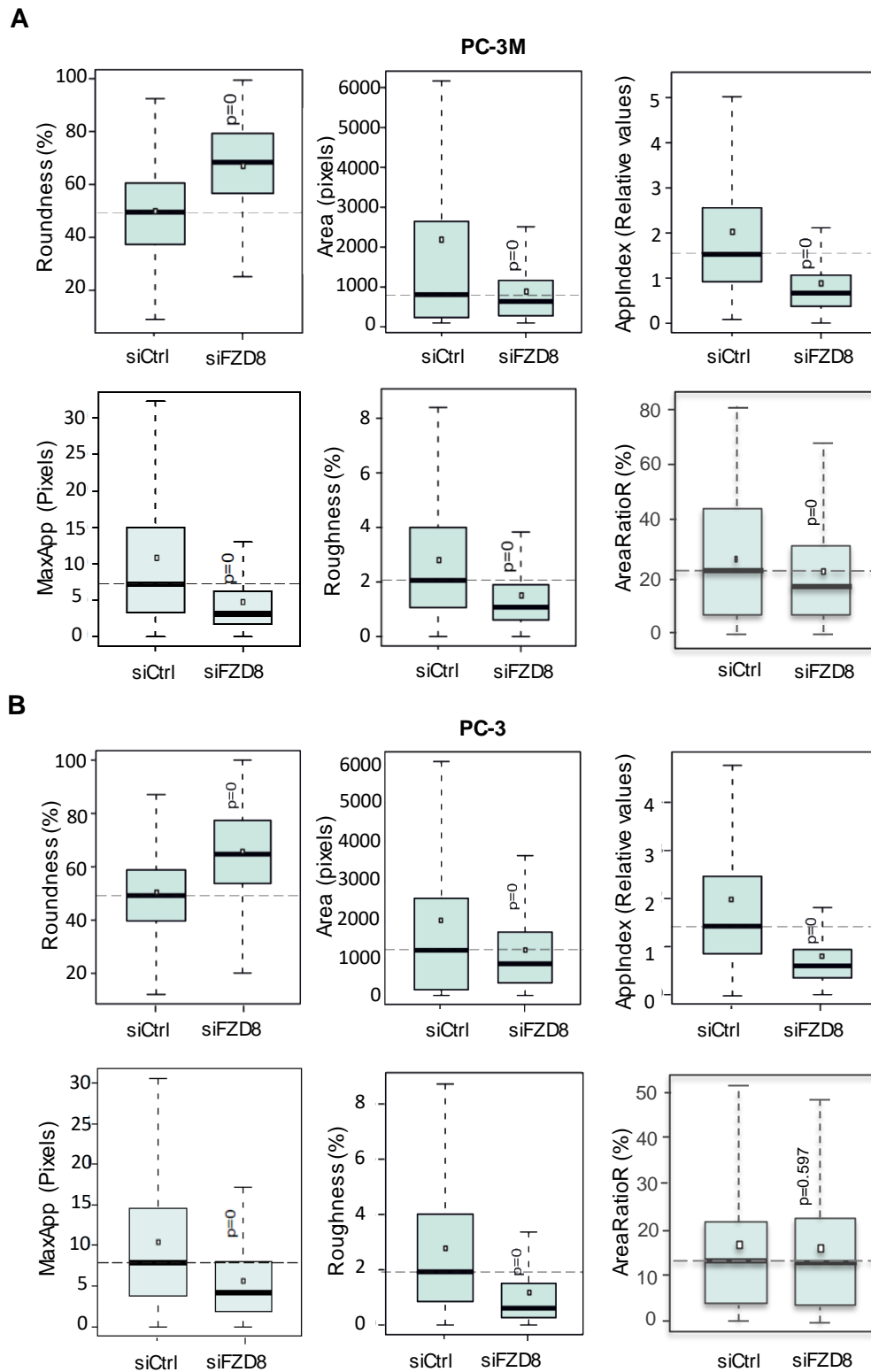


**Figure 49. Boxplots for the main parameters affected by *FZD8* silencing in organotypic 3D cultures.** Box and whisker plots of selected parameters from heatmaps in Fig. 48 in PC-3M (**A**) and PC-3 (**B**) cells; p=0 indicates p-value <0.001.

## 2.1.2 Role of FZD8 in the epithelial to mesenchymal transition (EMT)

The epithelial-mesenchymal transition (EMT) is a reversible and flexible process in which epithelial cells acquire mesenchymal properties moving through a spectrum of intermediate phases in which they alter their morphology, cellular architecture, adhesion and migratory capacities (Lee et al. 2006; Nieto et al. 2016). EMT has been reported to drive the dissociation of carcinoma cells from primary carcinomas, which as a result, migrate and disseminate to distant sites. Later, the reverse of EMT (MET) is proposed to cause cessation of migration, inducing the same cells to proliferate and giving rise to a new tumor mass (Nieto et al. 2016).

Given that Wnt signaling is one of the pleiotropic factors that induce the EMT program (Banyard & Bielenberg 2015) and our previous results support the role of FZD8 in prostate cancer progression through regulation of cell migration and invasion, we hypothesized that FZD8 could be also involved in the regulation of EMT.

### 2.1.2.1 EMT in standard 2D culture

In order to corroborate the idea of FZD8 involvement in EMT in prostate cancer, we first used conventional 2D culture techniques. To do this, the levels of EMT-associated genes were analyzed by q-RT-PCR in PC-3M and DU145 cells, in which *FZD8* was transiently silenced for 48 h. *FZD8* silencing in PC-3M cells (**Fig. 50A**) significantly reduced the expression of the mesenchymal genes encoding N-cadherin (*CDH2*) and Vimentin (*VIM*), as well as the mesenchymal transcription factors Snail (*SNA1*), *TWIST1* and *ZEB1*, but not the expression of Slug (*SNAI2*). In addition, *FZD8* silencing increased expression of the epithelial cell marker Claudin 1 (*CLDN1*). The effects of *FZD8* silencing in DU145 cells were, on the whole, similar (**Fig. 50B**), reducing the expression of Vimentin (*VIM*), Snail (*SNAI1*), Slug (*SNAI2*) and *ZEB1*. However, *FZD8* silencing did not affect *TWIST1* nor *CLDN1* in DU145 cells. Although there are some differences in the subset of EMT genes regulated by FZD8 in both cell lines, these results suggest that FZD8 is required for the expression of EMT genes in metastatic prostate cancer cells.

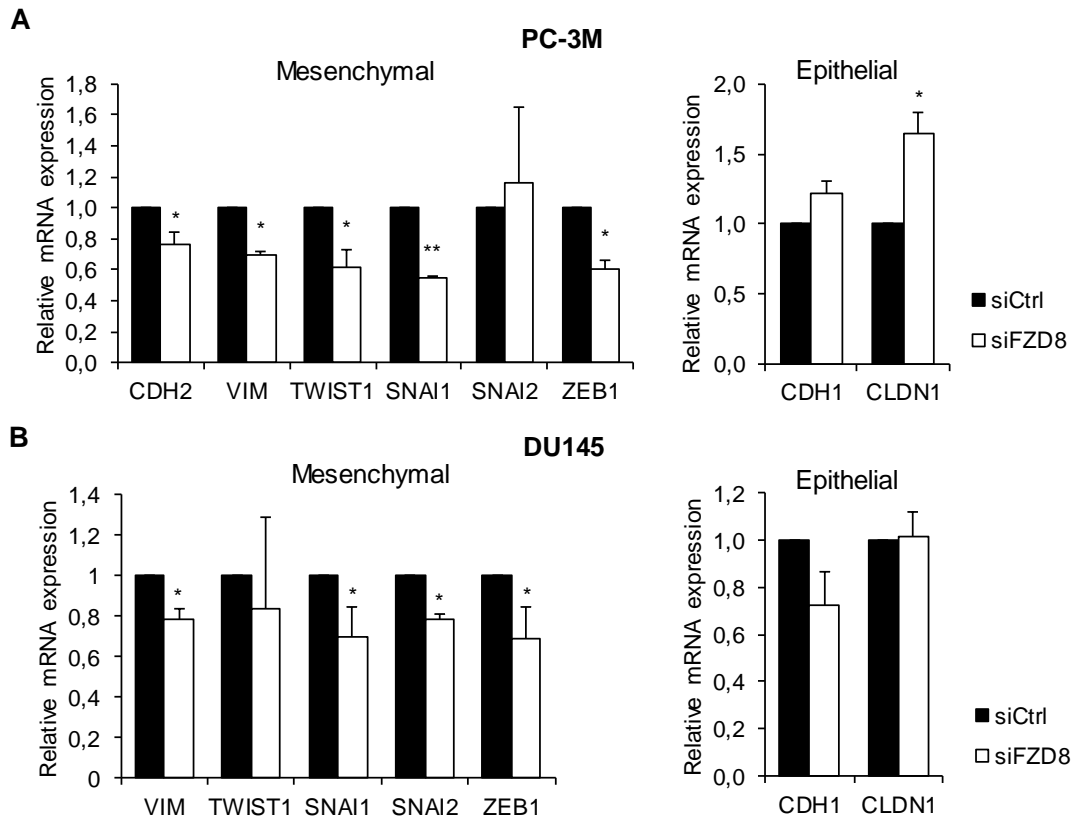


**Figure 50. FZD8 regulates the expression of EMT markers at the mRNA level.** Q-RT-PCR analysis showing expression levels of the indicated genes, normalized to 36B4, in PC-3M (**A**) and DU145 (**B**) cells, respectively silenced with control (siCtrl) or FZD8 siRNAs; error bars show SD for four independent experiments \*  $p < 0.05$  \*\*  $p < 0.001$  by Student's t test.

Since the analysis by q-RT-PCR showed that FZD8 could be mediating the EMT process in metastatic prostate cancer cells, we decided to further analyze FZD8 effects on the expression of EMT markers at the protein level. With that purpose, western blot assays were carried out in PC-3M cells silenced for *FZD8*. Consistent with the mRNA data, there was a significant reduction in the protein levels of N-cadherin and Vimentin (mesenchymal markers) together with an increase in the epithelial marker Claudin 1 (**Fig. 51A**). In order to investigate further the correlation between FZD8 and Wnt-11 with EMT marker expression, we carried out bioinformatics analysis using the MSKCC dataset from cBioPortal. As anticipated based on our results, both *FZD8* and *WNT11* expression correlated with expression of the mesenchymal genes *SNAI1*, *SNAI3*, *TWIST1* and *TWIST2*, and negatively correlated with the expression of the epithelial markers *CDH1* and *CTNNB1*, further supporting the link between Wnt-11-FZD8 signaling and EMT (**Fig. 51B**).

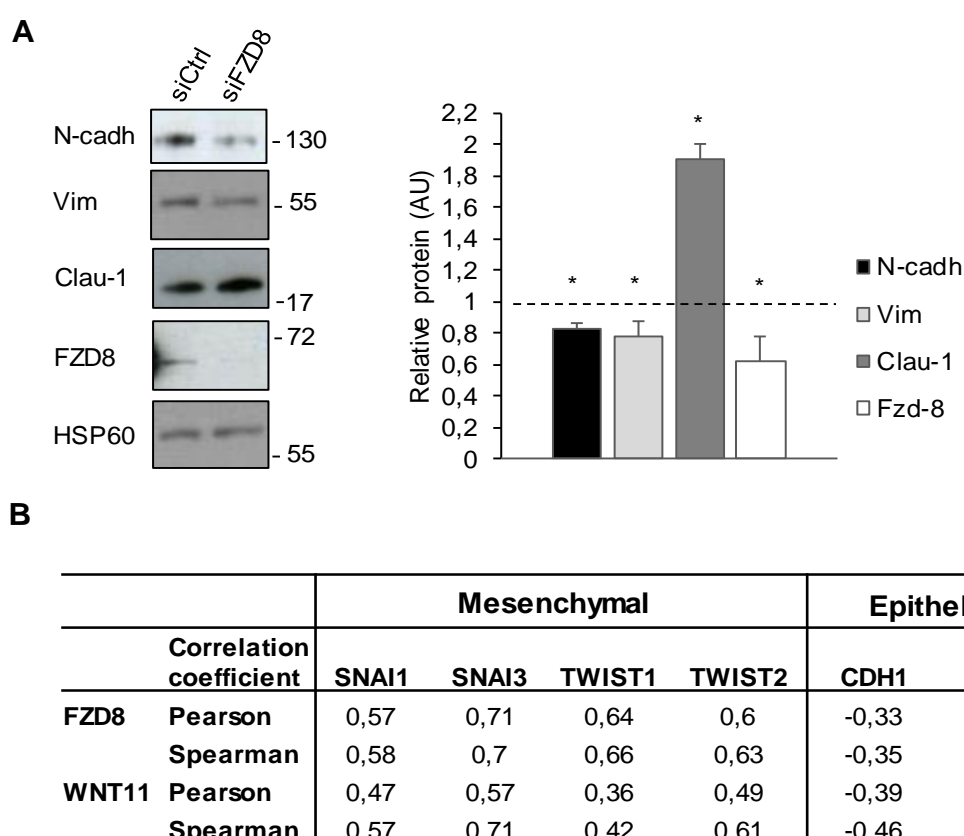


**Figure 51. FZD8 regulates the expression of EMT markers at the protein level. (A)** Extracts from PC-3M silenced cells blotted for the indicated proteins; graph shows average relative protein levels, determined by densitometry analysis of blots from three independent experiments, normalized to HSP60 and relative to control siRNA. **(B)** Correlation analysis of *FZD8* and *WNT11* mRNA expression with the indicated EMT genes in the MSKCC dataset calculated using cBioPortal; Pearson and Spearman coefficients were used to measure correlation. \*  $p < 0.05$  by Student's t test.

### 2.1.2.2 Regulation of WNT11 by FZD8: potential positive-feedback loop

The fact that FZD8 is required for the EMT process in prostate cancer, together with reports describing *WNT11* as an EMT gene in kidney epithelial cells (P. Zhang et al. 2012; He et al. 2011) led us to analyze *WNT11* expression in *FZD8* silenced cells. *FZD8* silencing significantly reduced *WNT11* expression both in PC-3M and DU145 cells (**Fig. 52A**). Moreover, there was a positive correlation between *FZD8* and *WNT11* expression in the MSKCC dataset (**Fig. 52B**). These observations together suggest that there may be a positive-feedback loop in the pathway, in which FZD8 signaling increases expression of its ligand. However, further studies will be required to explore the mechanism of this regulation.

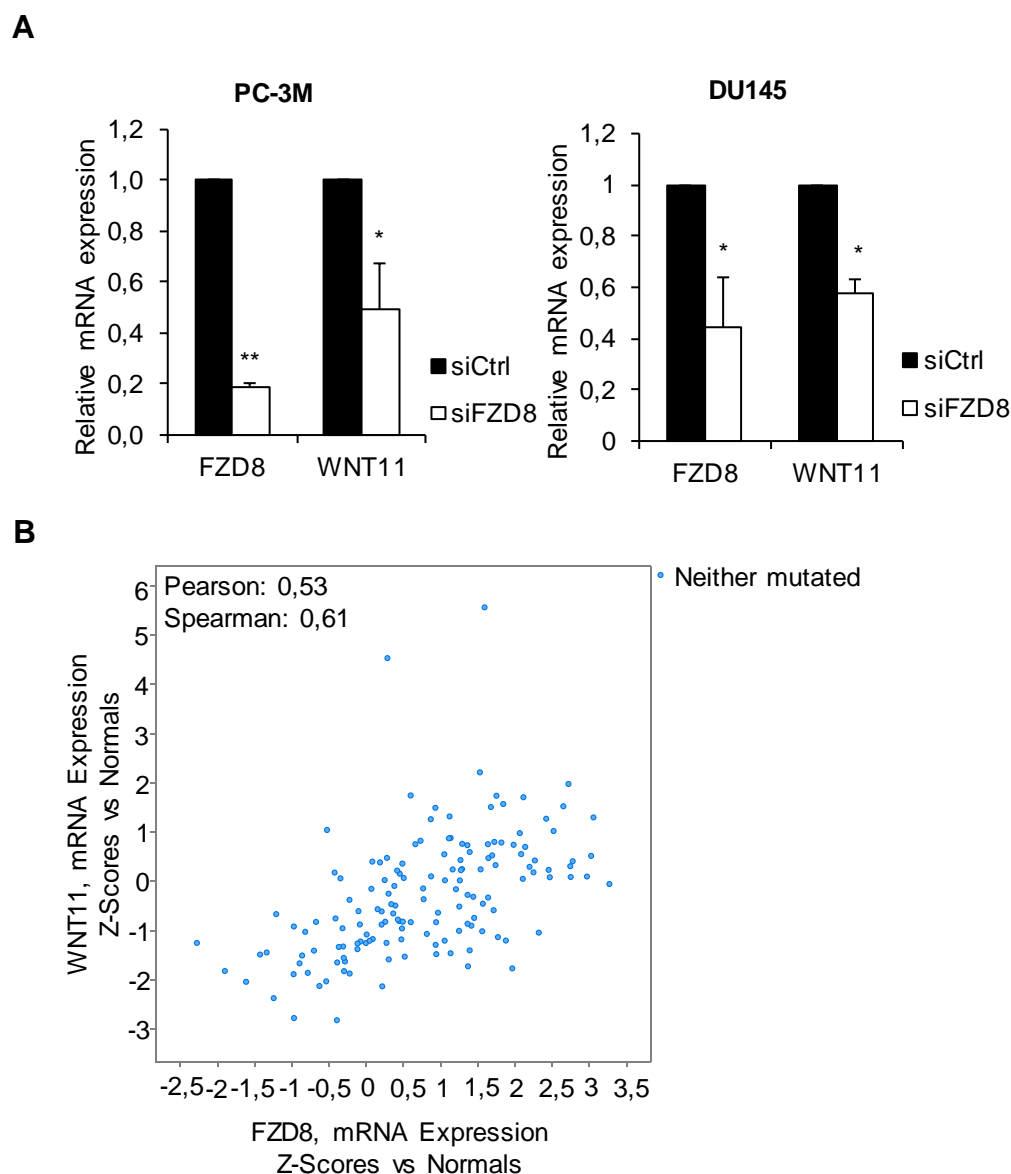


**Figure 52. FZD8 regulates *WNT11* expression.** (A) Q-RT-PCR analysis showing expression levels of the indicated genes, normalized to 36B4, in PC-3M and DU145 cells silenced with control (siCtrl) or FZD8 siRNAs, error bars show SD for four independent experiments. (B) Correlation plot for *FZD8* and *WNT11* mRNA expression in the MSKCC prostate cancer dataset, generated using cBioPortal; \*  $p < 0.05$ , \*\*  $p < 0.001$  by Student's t test.

### 2.1.2.3 EMT in organotypic 3D cultures

Since our observations demonstrate that FZD8 is involved in the regulation of EMT, we used 3D culture assays to examine organoid morphology, staining for laminin  $\alpha 1$  and vimentin, to distinguish epithelial, and well-differentiated structures from mesenchymal, and undifferentiated ones. Confocal analysis at the endpoint of the 3D culture from both PC-3M and PC-3 cells silenced for *FZD8* revealed that laminin  $\alpha 1$ , which was not detectable in control organoids, was clearly observed in *FZD8*-silenced organoids,



indicating the presence of a basal lamina characteristic of well-differentiated structures (**Fig. 53**). On the other hand, vimentin staining highlighted invasive cells migrating from control cell organoids but not from *FZD8*-silenced organoids, reflecting a reduction in invasive and mesenchymal properties of the latter (**Fig. 53**). Interestingly, a proportion of the *FZD8*-silenced organoids showed a total absence of vimentin staining, further supporting the importance of FZD8 for invasive behavior and EMT (**Fig. 53, upper panel**).

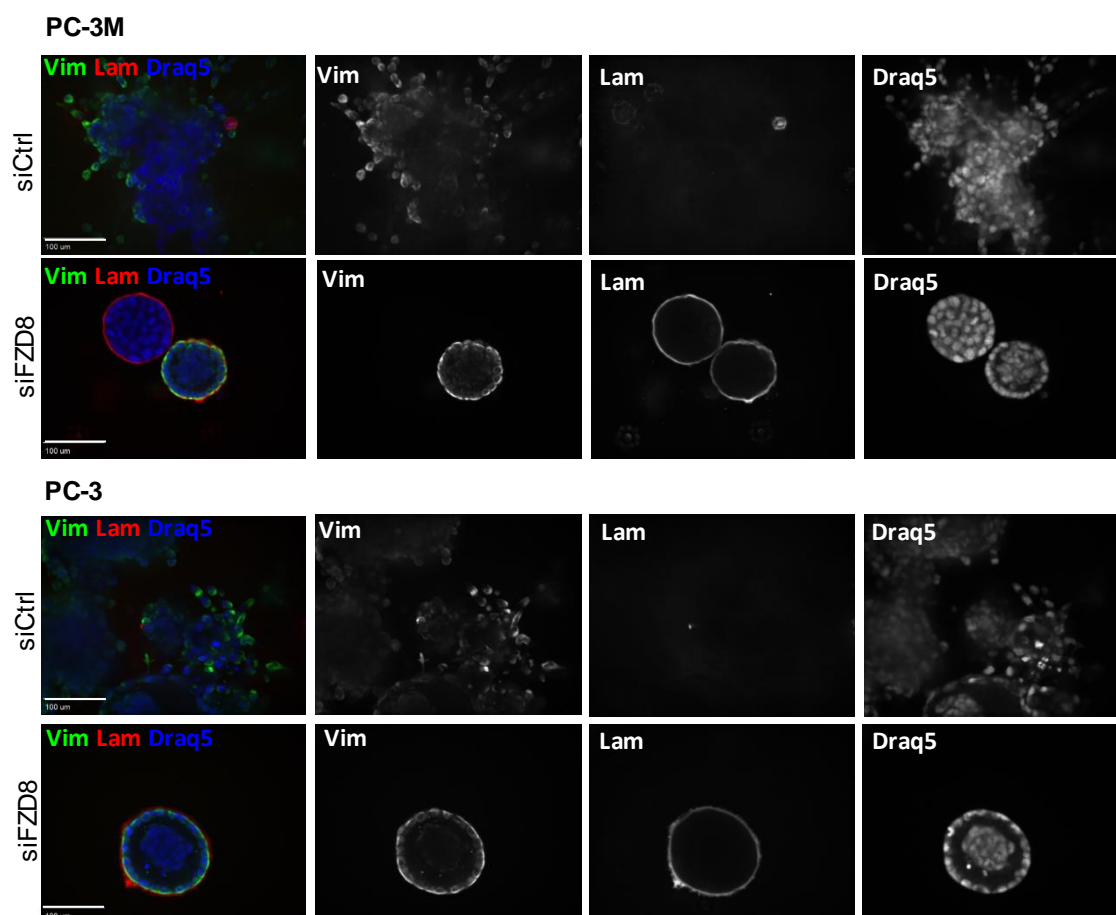


**Figure 53. Immunostaining of *FZD8* silenced cells in organotypic 3D cultures.** Confocal microscopy analysis of organoids derived from siCtrl and *FZD8* silenced PC-3M (upper panel) and PC-3 (lower panel) cells at day 9 of growth in 3D culture; immunostaining for vimentin (Vim) is shown in green and for laminin- $\alpha$ 1 (Lam) in red, blue staining shows cell nuclei (Draq5), scale bar 100  $\mu$ m.

## 2.2 Role of FZD8 in prostate pathogenesis: *in vivo* assays

### 2.2.1 *In vivo* chicken chorioallantoic membrane (CAM) model

Since our results highlight the malignant phenotype of FZD8 in prostate cancer, we decided to validate the functional role of FZD8 *in vivo* using the chorioallantoic membrane (CAM) model. This model is based on the properties of the CAM, which is a

highly vascular membrane found in chicken eggs that is easily accessible and that enables efficient tumor cell grafting and growth owing to the immunodeficient state of the chick embryo at this point in development. In this sense, the growth of tumor cells on the CAM mimics most of the characteristics of the carcinogenic process, including growth, invasion, angiogenesis and colonization of distant tissues (Deryugina & Quigley 2009) and also the cancer cell environment owing to its extracellular matrix protein content (Lokman et al. 2012). Control and *FZD8*-silenced PC-3 cells were grafted onto the exposed CAM of chicken embryos at developmental day 7 (EDD7) and allowed to grow for 3 days. At EDD10, tumors formed by *FZD8*-silenced PC-3 cells were significantly smaller than those formed by control cells (**Fig. 54A-C**), supporting the relevance of *FZD8* in prostate cancer growth *in vivo*. Evaluation of the extent of *FZD8* silencing at the moment of cell grafting onto the CAM and when tumors were excised indicated that silencing was maintained during the course of the assay (**Fig. 54D**).

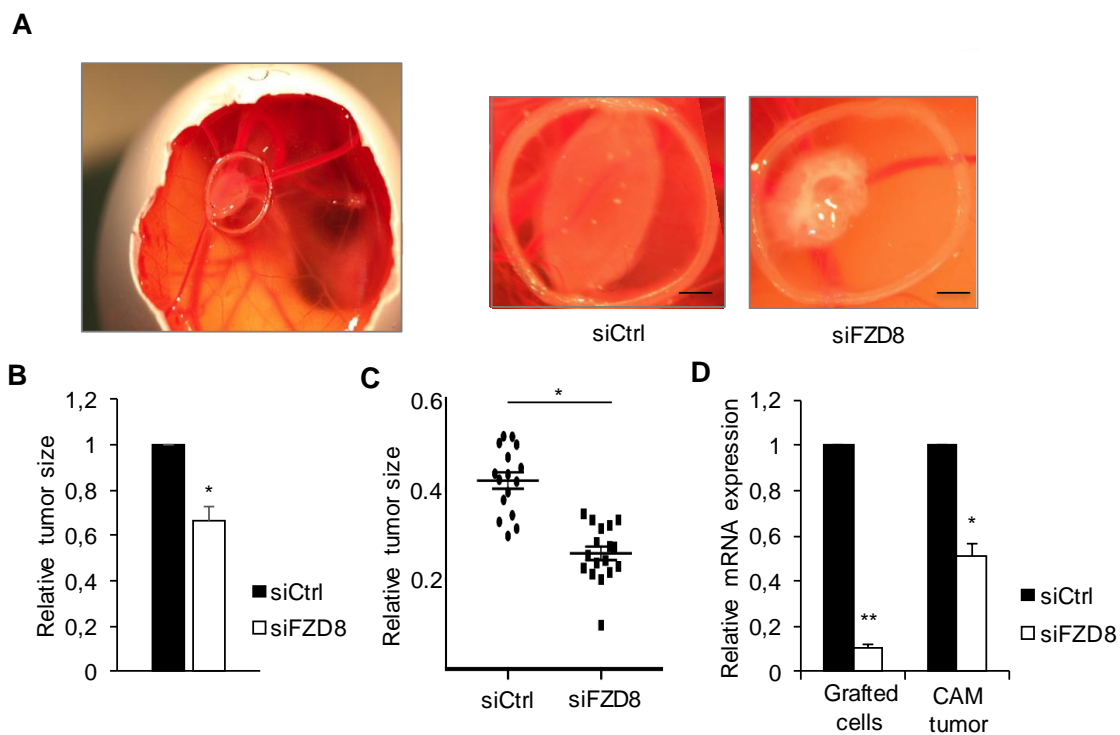


**Figure 54. *FZD8* is required for tumor growth *in vivo* in the CAM model. (A)** Representative pictures of PC-3 derived tumors implanted on the CAM for 3 days. Left, overview of the egg; right, representative tumors from PC-3 cells silenced for *FZD8*; scale bars ~5 mm. **(B)** Average tumor size, as determined by ImageJ, relative to control tumors, error bars indicate SD from three independent experiments, each with 12-15 eggs per condition. **(C)** Boxplot of tumor size in a representative experiment. **(D)** *FZD8* expression levels at day 0, when cells were implanted on the CAM and at the endpoint, when CAM tumors were excised from the egg; error bars indicate SD of three independent experiments \*  $p < 0.05$ , \*\*  $p < 0.001$  by Student's t test.

As a way to study prostate cancer metastasis in this *in vivo* model, we analyzed the expression of vimentin, which contributes to prostate cancer invasiveness (Wei et al. 2008; Y et al. 2008; Singh et al. 2003) in CAM tumors from control and siFZD8 PC-3 cells. Immunohistochemical analysis of the CAM tumor sections allowed us to determine that tumors in which *FZD8* was silenced exhibited lower levels of vimentin than control tumors, consistent with the role of FZD8 in prostate tumor cell invasion (**Fig. 55**). Of note, together with being a marker for invasiveness, immunostaining for vimentin distinguishes prostate cancer cells from CAM cells, which are negative for this marker (**Fig. 55, arrows**).

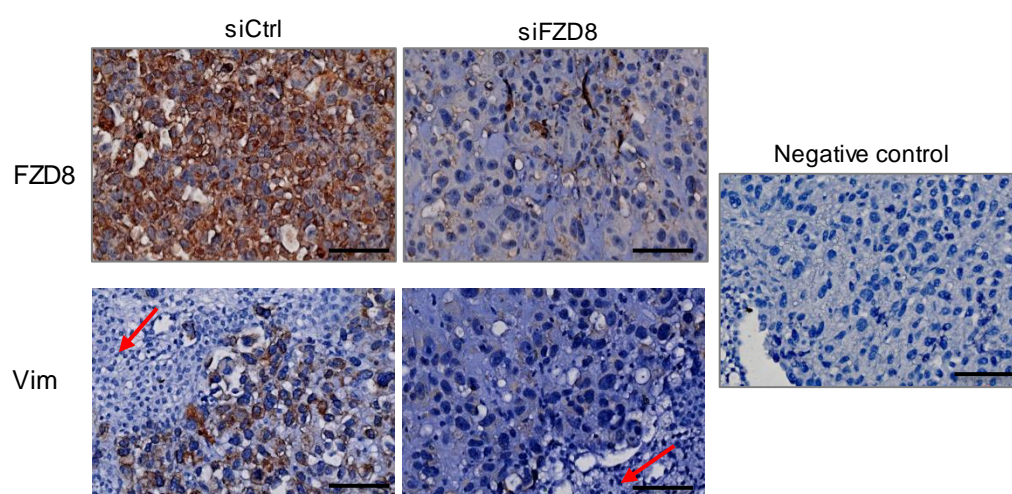


**Figure 55. Immunohistochemistry of FZD8 and vimentin in the CAM.** Representative images of sections from CAM tumors silenced for FZD8; arrows show chick embryo cells, distinguished from PC-3 cells by the absence of vimentin staining, scale bar 50  $\mu$ m.

### 2.2.2 *In vivo* mouse model

Orthotopic mouse models are based on directly implantation of the human cell line of interest into their organ of origin. In our case, human PCa PC3-M cell line is directly implanted into the prostate of athymic mice. After 4-6 weeks, tumor size, presence of circulating tumor cells (CTCs), and metastasis to the lungs and lymph nodes can all be quantified (Pavese et al. 2013). Taking advantage of some sections from mice in which PC-3M cells were orthotopically implanted to generate prostate tumors, immunohistochemistry was used to determine the levels of FZD8 and Wnt-11 in lymph node metastases (**Fig. 56**). Consistent with a role for Wnt-11/FZD8 signaling in prostate cancer metastasis, both proteins were detected in lymph nodes from the mice. Vimentin staining was also used to distinguish prostate cancer cells from host cells.

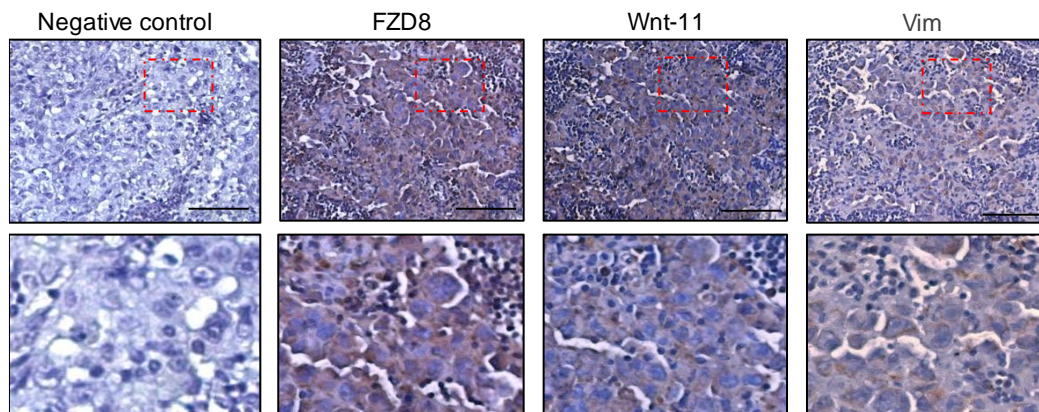


**Figure 56. Immunohistochemical staining of a lymph node metastasis from a PC-3 mouse xenograft.** Sections were stained for FZD8, Wnt-11 and vimentin; scale bars in upper pictures 50  $\mu$ m; lower pictures show zoom areas from upper ones.

### 2.3 Role of FZD8 in prostate tumorigenesis: analysis of patient samples

The use of human samples in biomedical research has expanded our concept of cell biology and contributed to the evolution and progress of basic biomedical research. Based on the wide use of human samples to identify biomarkers that can predict prostate cancer progression, relapse, therapy response and survival, we explored the potential of FZD8 as a biomarker in prostate cancer using tissues from PCa patients.

#### 2.3.1 Bioinformatics analysis of prostate cancer datasets

Aiming to corroborate our hypothesis of FZD8 being an indicator of prostate cancer progression, we performed a closer examination of FZD8 expression in prostate cancer datasets from the Oncomine database. The analysis showed that *FZD8* mRNA was significantly upregulated in the highest number of datasets when comparing prostate carcinoma and benign prostate (**Fig. 57A**). Analysis of *FZD8* mRNA expression in others datasets from the cBioPortal for Cancer Genomics (Cerami et al. 2012; Gao et al. 2013) also revealed elevated *FZD8* mRNA expression (z-score threshold  $\pm 1.5$ ) in 10% of tumors from the TCGA dataset (Abeshouse et al. 2015) as well as in 6% of tumors from the SU2C/PCF Metastatic Prostate Cancer dataset (Robinson et al. 2015). Interestingly, *FZD8* mRNA expression correlated with the presence of the *TMPRSS2-ERG* gene fusion and *ERG* mRNA expression (**Fig. 57B**), which has been found in 50% of prostate tumors. Moreover, this observation was confirmed in a second dataset (Grasso; Oncomine™ database, **Fig. 57C**).

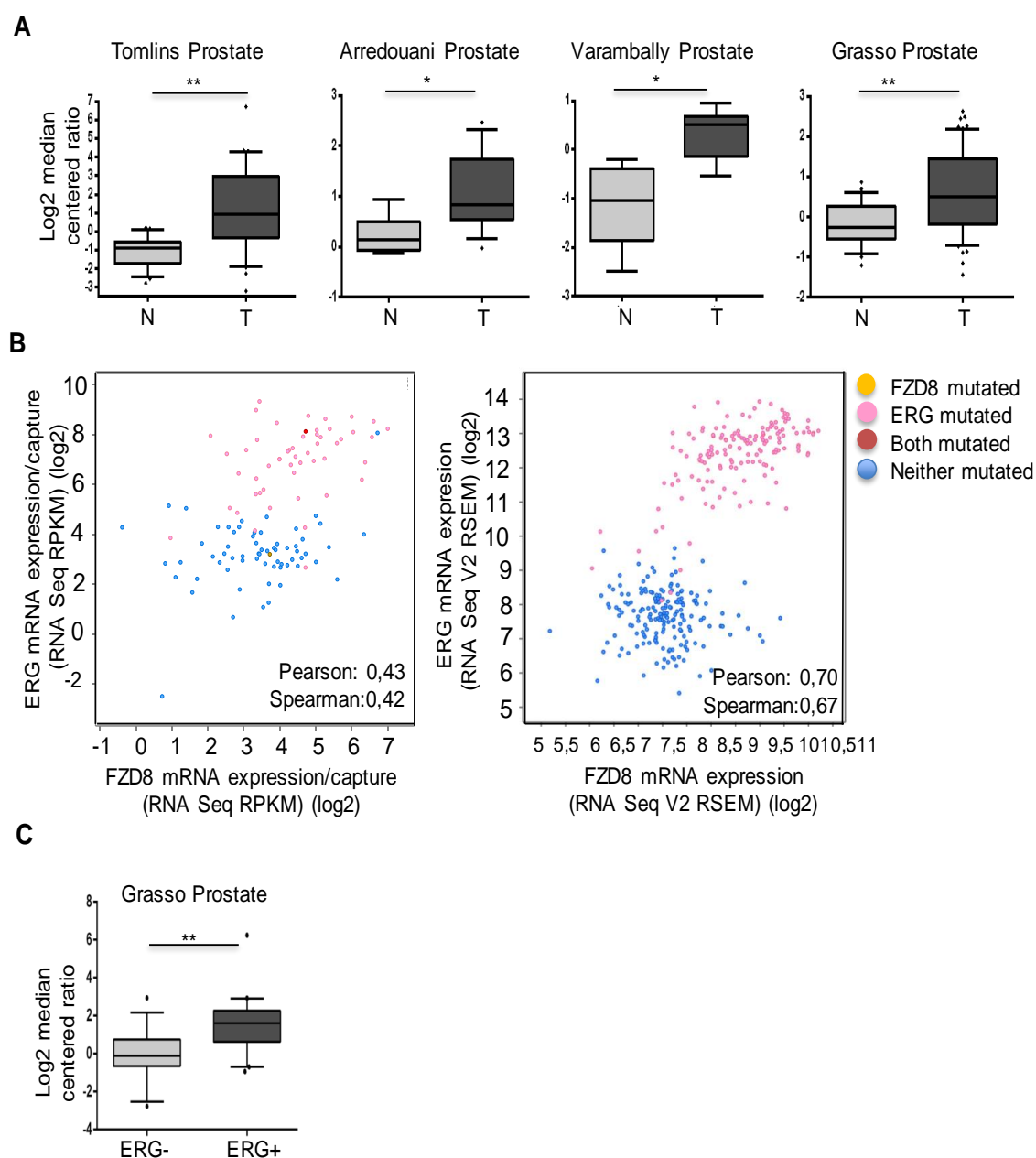


**Figure 57. *FZD8* is upregulated in patient prostate tumors. (A)** Analysis of *FZD8* expression in four different datasets taken from OncoPrint™: Tomlins (22 prostate glands and 30 prostate carcinomas), Arredouani (8 prostate glands and 13 prostate carcinomas), Varambally (6 prostate glands and 7 carcinomas) and Grasso (26 prostate glands and 59 carcinomas); prostate gland was defined as normal (N) and prostate carcinoma as tumor (T); only datasets with  $p < 0.05$  and fold-change  $> 1.5$  were considered. **(B)** Correlation of *FZD8* and *ERG* mRNA expression in prostate cancer datasets from cBioPortal, SU2C/PCF Dream Team Metastatic Prostate Cancer dataset (Robinson et al., 2015) (left) and TCGA prostate cancer dataset (Cancer Genome Atlas Research Network, Cell, 2015) (right). **(C)** *FZD8* expression in prostate tumors with (ERG+) and without (ERG-) *ERG* rearrangement from the Grasso dataset from OncoPrint™.



The results from our studies in prostate cancer cell lines suggest a model in which FZD8 transduces Wnt-11 signals that promote EMT and prostate cancer cell invasion. In order to evaluate *FZD8* and *WNT11* gene expression during prostate cancer progression, we performed bioinformatics studies using the MSKCC dataset (Taylor et al. 2010). Importantly, the analysis revealed a clear upregulation of FZD8 in prostate cancer compared to normal prostate and in prostate cancer metastases compared to primary tumors. Both *FZD8* and *WNT11* were upregulated in high Gleason score tumors and in tumors that had spread to the lymph nodes (**Fig. 58A**). Moreover, expression of *WNT11* correlated significantly ( $p = 0.014$ ) and *FZD8* showed a trend ( $p = 0.057$ ) with increased biochemical recurrence (**Fig. 58B**).

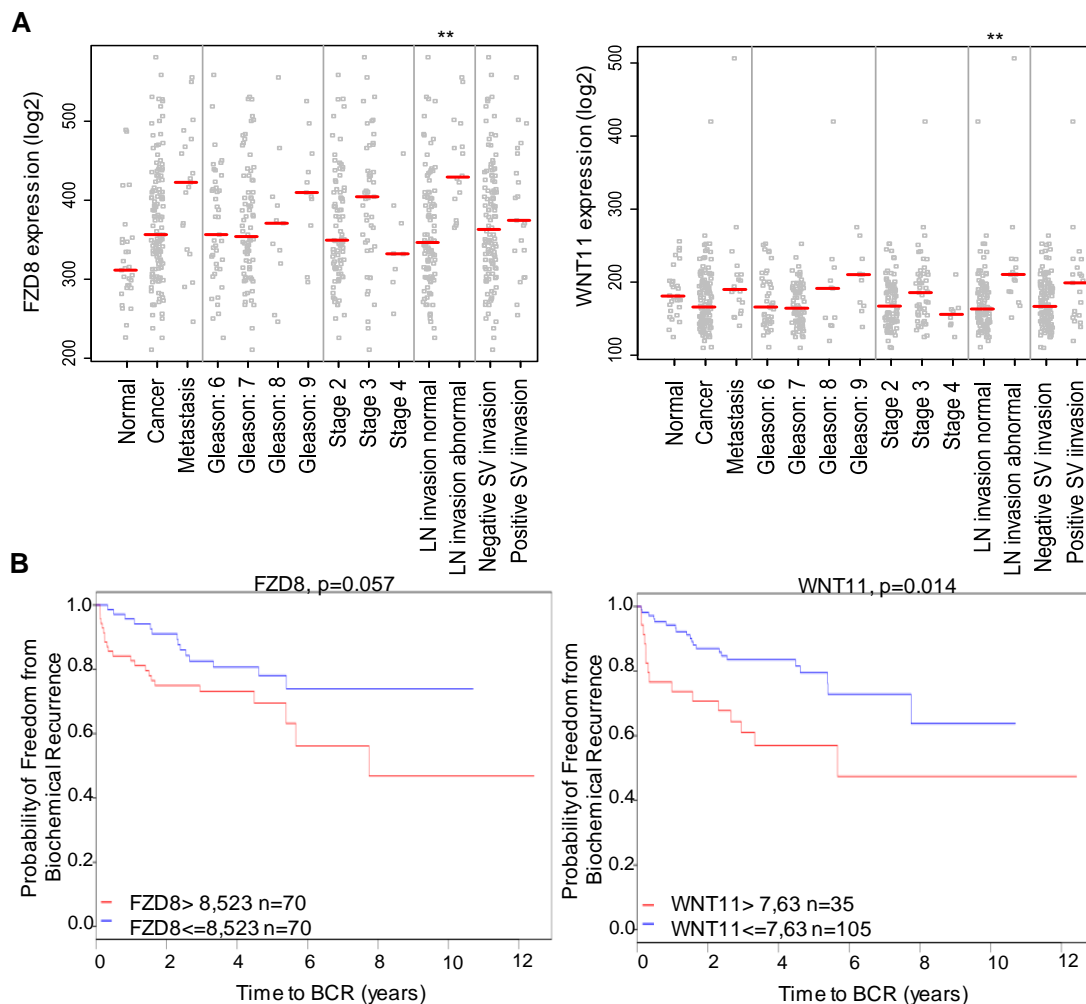


**Figure 58. Correlation of *FZD8* and *WNT11* with prostate cancer relapse. (A)** Bioinformatics analysis of *FZD8* (left) and *WNT11* (right) expression in prostate cancer using the MSKCC dataset. **(B)** Recurrence analysis based on *FZD8* (left) and *WNT11* (right) expression in the MSKCC dataset, determined using CamcAPP.

A deeper analysis of the MSKCC dataset also showed that elevated expression of both *FZD8* and *WNT11* was more prevalent in patients with recurrent disease, as compared to disease-free patients ( $p = 0.049$ , Fisher's exact test, two-sided) (**Fig. 59**), which lends support to the relevance of the Wnt-11-FZD8 signaling pathway in prostate cancer progression.

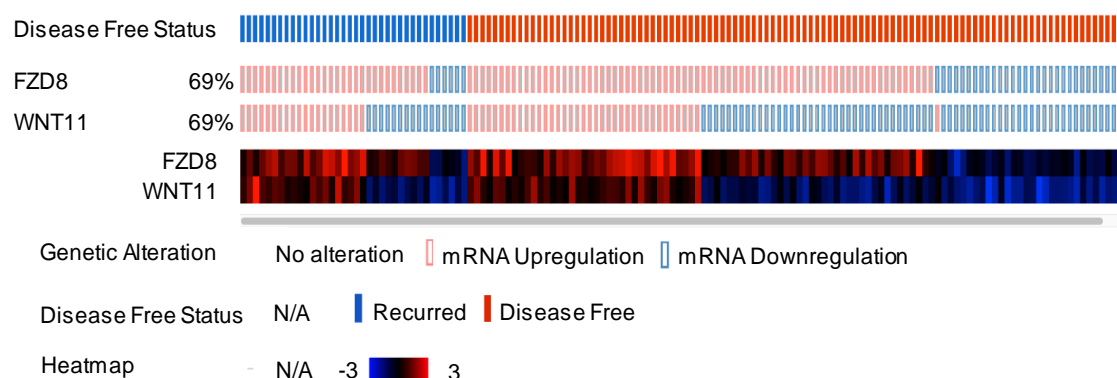


**Figure 59. *FZD8* and *WNT11* expression and disease free status.** Comparison of tumors with changes in *FZD8* and *WNT11* expression (up, red; down, blue) and disease-free status of patients, from cBioPortal.

### 2.3.2 Analysis of *FZD8* and Wnt-11 protein expression in prostate cancer patient TMAs

To confirm these *in silico* data, we used a TMA comprising sections of benign and malignant prostate from 90 prostate cancer patients and performed immunohistochemistry to detect *FZD8* and Wnt-11 protein expression. As expected, the evaluation of the staining revealed significantly higher levels of *FZD8* and Wnt-11 in tumor cells compared to benign epithelium from the same patients (**Fig. 60**).

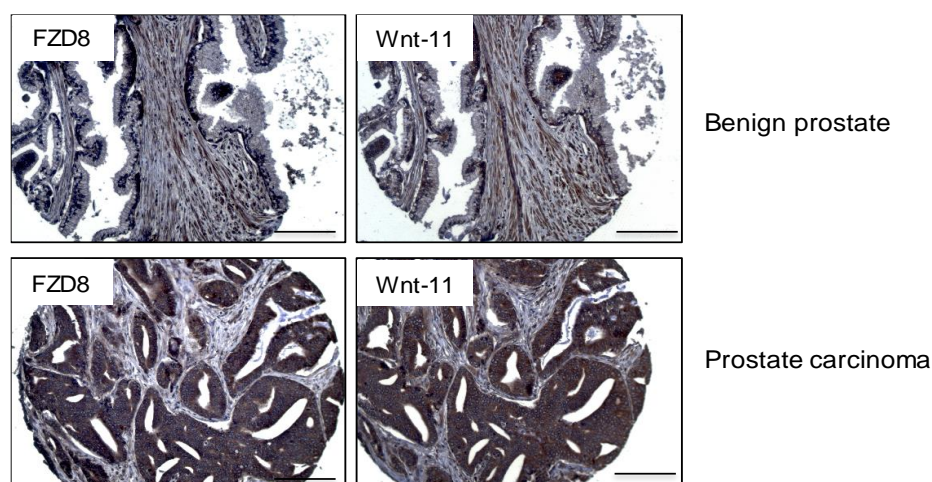


**Figure 60. *FZD8* and Wnt-11 expression are increased in prostate cancer.** Immunohistochemical staining of *FZD8* and Wnt-11 in adjacent sections of prostate cancer (Gleason 4+3) and benign prostate from the same patient; scale bar 25  $\mu$ m.

Moreover, the previous observation was supported by the finding of a significant correlation in the levels of FZD8 and Wnt-11 in benign and tumor epithelia and stroma (**Fig. 60, 61 and Table 18**).

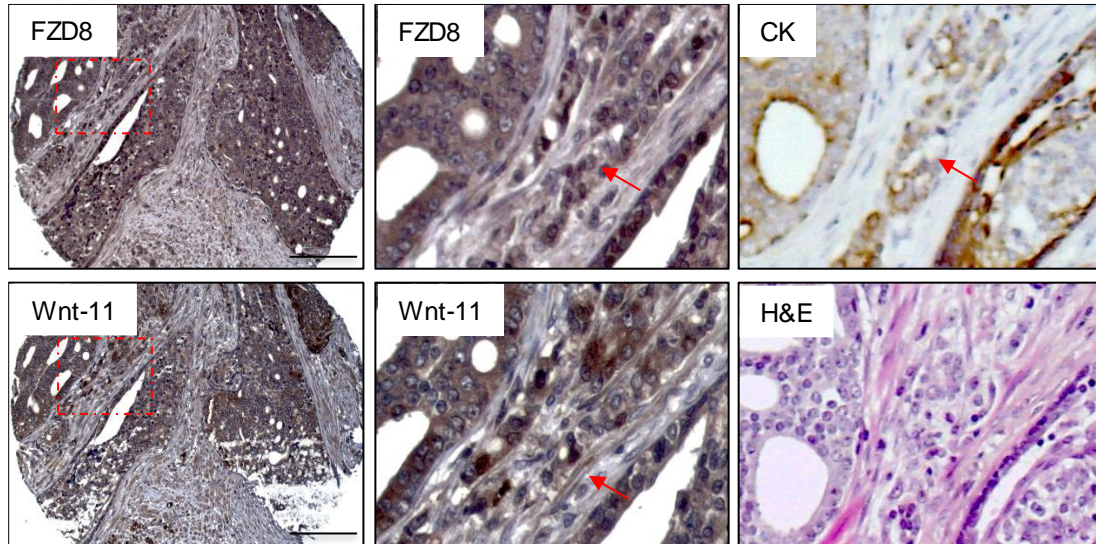


**Figure 61. FZD8 and Wnt-11 are expressed in disseminated tumor cells.** Immunohistochemical staining of FZD8 and Wnt-11 in a section of prostate cancer (Gleason 4+3) from another patient; scale bar 25  $\mu$ m. High magnification images for FZD8, Wnt-11, epithelial cyokeratins and H&E are also shown. Arrows show disseminated tumor cells positive for FZD8, Wnt-11 and epithelial cyokeratins.

Correlation	Cancer vs Normal		C.stroma vs N.stroma	
	FZD8	Wnt-11	FZD8	Wnt-11
Chi Pearson	<0.001	<0.001	<0.001	<0.001
Fisher Exact Two tails	1.13E-11	4.56E-09	7.27E-15	4.68E-12

**Table 18. Correlation analysis of FZD8 and Wnt-11 protein expression in normal and cancer.** Comparison of tumor and benign epithelium and cancer stroma and benign stroma.

Interestingly, it was observed that FZD8 and Wnt-11 were also both significantly lower in tumor stroma than in the benign stroma (**Fig. 62 and Table 19**), suggesting that elevated expression in cancer epithelial cells is accompanied by reduced expression in tumor-associated stroma, possibly reflecting a common mechanism of regulation of Wnt-11 and FZD8.



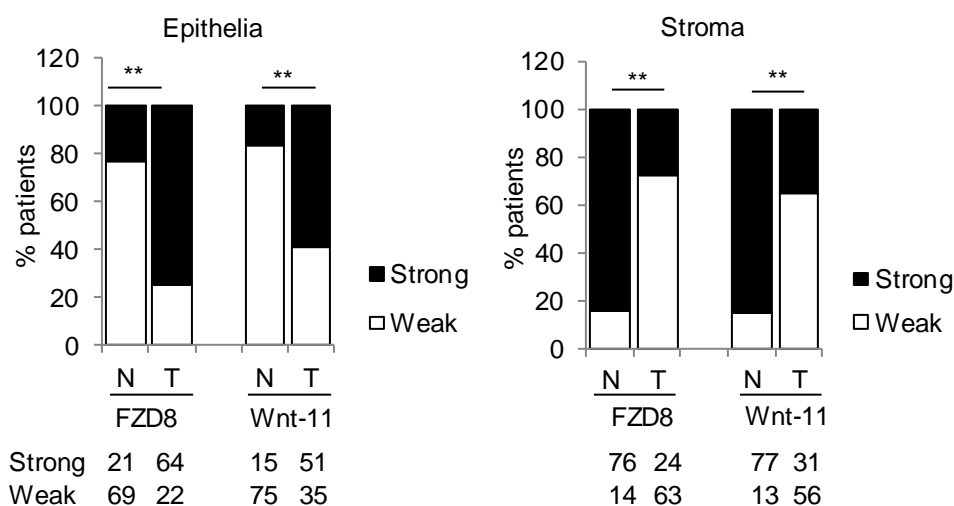


**Figure 62. Both FZD8 and Wnt-11 expression are increased in tumor epithelia and reduced in prostate cancer stroma.** Stratification of FZD8 and Wnt-11 expression in cancer (T) and benign (N) epithelia and stroma. \*\* $p < 0.001$  with Chi-Squared test and Fisher's exact test, two sided.

Correlation	FZD8	Wnt-11	Chi-square; Fisher Exact
<b>Cancer</b>			
		Low	High
	Low	17	5
	High	18	46
<b>Benign</b>			
		Low	High
	Low	61	8
	High	14	7
<b>Cancer stroma</b>			
		Low	High
	Low	46	17
	High	10	14
<b>Benign stroma</b>			
		Low	High
	Low	5	9
	High	8	68

**Table 19. Correlation analysis of FZD8 and Wnt-11.** Pearson Chi-square test with correction and Fisher's exact test, two-sided were used.

Despite our observations showing that FZD8 and Wnt-11 levels were higher in prostate cancer than in benign prostatic epithelium, there was no significant correlation between high expression and Gleason score in this patient cohort (**Table 20**). In this regard, larger studies will be needed to clarify the role of Wnt-11/FZD8 as markers of prostate cancer progression and patient mortality.

Antigen Staining score	Category n (%)	Category n (%)	Chi-Square; Fisher's Exact
<b>FZD8</b>			
	Benign	Cancer	<0.001; 1.13E-11
Low	69 (76,7)	22 (25,6)	
High	21(23,3)	64 (74,4)	
	Gleason ≤ 3,4	Gleason ≥4,3	NS
Low	47 (52,8)	19 (12,3)	
High	21 (23,6)	2 (2,24)	
	pT2	pT3	NS
Low	16 (17,9)	7 (7,8)	
High	33 (37,1)	33 (37,1)	
	PNI+	PNI-	NS
Low	7 (7,8)	16 (17,9)	
High	28 (31,4)	38 (42,7)	
<b>Wnt-11</b>			
	Benign	Cancer	<0.001; 4.56E-9
Low	75 (83,3)	35 (40,7)	
High	15 (16,6)	51 (58,6)	
	Gleason ≤ 3,4	Gleason ≥4,3	NS
Low	36 (41,3)	15 (17,2)	
High	31 (35,6)	5(5,7)	
	pT2	pT3	NS
Low	23 (26,4)	13 (14,9)	
High	25 (28,7)	26 (29,8)	
	PNI+	PNI-	NS
Low	12 (13,8)	24 (27,6)	
High	28 (32,2)	23 (26,4)	
<b>FZD8 stroma</b>			
	Benign	Cancer	<0.001; 7.27E-15
Low	14 (15,5)	63 (72,4)	
High	76 (84,4)	24 (27,6)	
	Gleason ≤ 3,4	Gleason ≥4,3	NS
Low	22 (24,7)	2 (2,2)	
High	46 (51,7)	19 (21,3)	
<b>Wnt-11 stroma</b>			
	Benign	Cancer	<0.001; 4.68E-12
Low	13 (14,4)	56 (64,4)	
High	77 (85,5)	31 (35,6)	
	Gleason ≤ 3,4	Gleason ≥4,3	NS
Low	24 (27,3)	7 (7,9)	
High	44 (50)	13 (14,7)	

**Table 20. Statistical analysis of FZD8 and Wnt-11 expression in TMAs.** Staining was classified as low (score 0 or 1) or high (score 2 or 3). Entries are absolute numbers with % in parentheses. Statistical significance was determined using Chi-squared test, Pearson correction and Fisher's exact test, two-sided; \* p < 0.05

## Chapter 3. Elucidation of the mechanism underlying the effects of FZD8 in prostate cancer pathogenesis

Our results have revealed the contribution of FZD8 to prostate cancer pathogenesis, promoting migration and invasion abilities of tumor cells as well as EMT, which together may drive prostate cancer progression and metastasis. However, the mechanisms mediating this tumor promoter role of FZD8 in prostate cancer remain undetermined. Multiple studies have outlined the capability of Wnt signaling to activate other pathways in various types of cancer. Crosstalk between the Wnt pathway and the PI3K/AKT, Ras or mTOR pathways has been widely reported. Moreover, Wnt pathway crosstalk with growth factor signaling pathways such as EGF, VEGF, HGF, IGF, FGF or TGF- $\beta$  are fairly prevalent in the development and progression of cancer. In this regard, all these pathways could represent the mechanism driving FZD8 effects on prostate cancer.

### 3.1 Involvement of FZD8 in TGF- $\beta$ signaling

Among all the various signaling pathways, crosstalk between TGF- $\beta$  and Wnt signaling is one of the best characterized and more extensively studied (Guo & Wang 2009; Attisano & Wrana 2013). Moreover, by analyzing the expression levels of the major components of the TGF- $\beta$  signaling pathway, we observed high expression of *TGF $\beta$ 1*, *TGFBRI*, *TGFBRII*, *SMAD2* and *SMAD3* in both metastatic prostate cancer cell lines PC-3M and DU145 (Fig. 63).

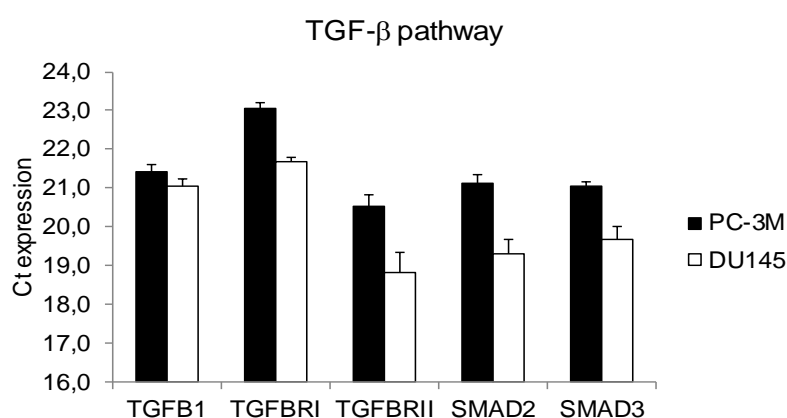


**Figure 63. Expression of the major components of the TGF- $\beta$  signaling pathway.** mRNA expression with Ct values of the indicated genes in PC-3M and DU145 cells. 36B4 Ct values were  $\approx$  16 in all experiments; error bars show SD of three independent experiments. Of note, lower Ct indicates higher mRNA expression.

In light of the fact that FZD8 is required for Wnt-11/ATF2 signaling, regulation of cell migration and invasion and expression of EMT-related genes, and based on the well reported implication of TGF- $\beta$  in these events and on the high expression of TGF- $\beta$

components in PCa cell lines, we hypothesized that FZD8 could be mediating its effects by playing a direct role in regulating TGF- $\beta$  signaling. To corroborate this hypothesis, the activation of TGF- $\beta$  signaling was evaluated using gene reporter assays, analysis of TGF- $\beta$  target gene expression and TGF- $\beta$  dependent Smad phosphorylation, as well as through analysis of TGF- $\beta$  dependent cell invasion and regulation of TGF- $\beta$  dependent EMT.

### 3.1.1 Analysis of TGF- $\beta$ -dependent transcriptional activity

In order to determine if FZD8 could regulate TGF- $\beta$  signaling at the transcriptional level, we first evaluated activation of the CAGA reporter, a Smad-dependent gene reporter that contains 12 copies of the PAI-1 promoter (a TGF- $\beta$  target gene). *FZD8* silencing in both PC-3M and DU145 cells significantly reduced TGF- $\beta$ -dependent activation of the CAGA reporter (**Fig. 64A and B**). Moreover, this effect was also observed when *FZD8* was silenced using an unrelated Dicer-substrate siRNA in PC-3M cells (**Fig. 64C**).

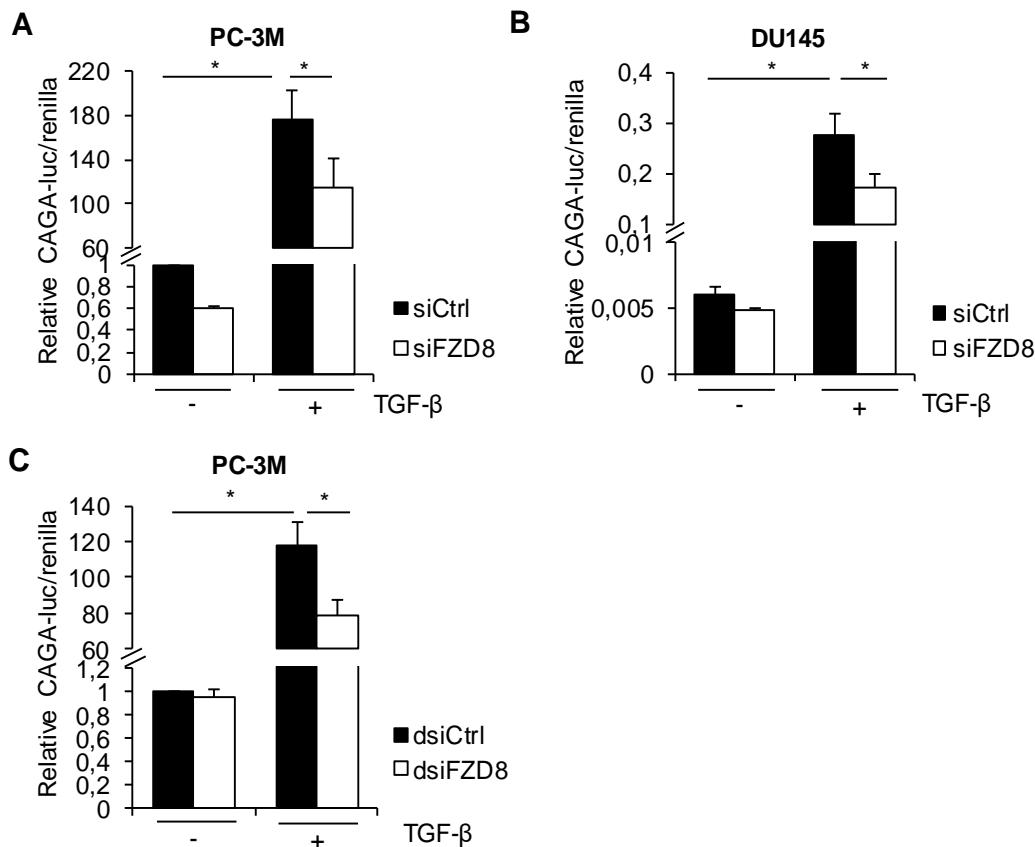


**Figure 64. FZD8 is required for TGF- $\beta$ -dependent gene reporter activity. (A-C)** CAGA12-luciferase/renilla activity in PC-3M (**A and C**) and DU145 (**B**) cells, respectively, silenced with siFZD8 or dsiFZD8 and treated with -/+ 1-0,1 ng/mL TGF- $\beta$  for 24 h; error bars show SD from three independent experiments. \* p < 0.05, \*\* p < 0.001 by Student's t test or ANOVA with Tukey post-hoc test where required.

### 3.1.2 Evaluation of target gene expression and Smad phosphorylation

To further characterize the regulation of TGF- $\beta$  signaling by FZD8, we analyzed the expression of some TGF- $\beta$  target genes as well as the levels of Smad phosphorylation, which is considered to be a good indication of activation of the pathway. Consistent with our previous observations, *FZD8* silencing was found to reduce the expression of the TGF- $\beta$  target genes *MMP9* and *PAI1*, both in PC-3M and DU145 cells (**Fig. 65A and B**). Furthermore, through a deeper analysis of the pathway by western blotting, we also found that silencing of *FZD8* reduced TGF- $\beta$ -dependent Smad2 phosphorylation and Smad2/3 protein levels in both cell lines (**Fig. 65C and D**), further supporting the involvement of FZD8 in TGF- $\beta$ /Smad-dependent signaling.

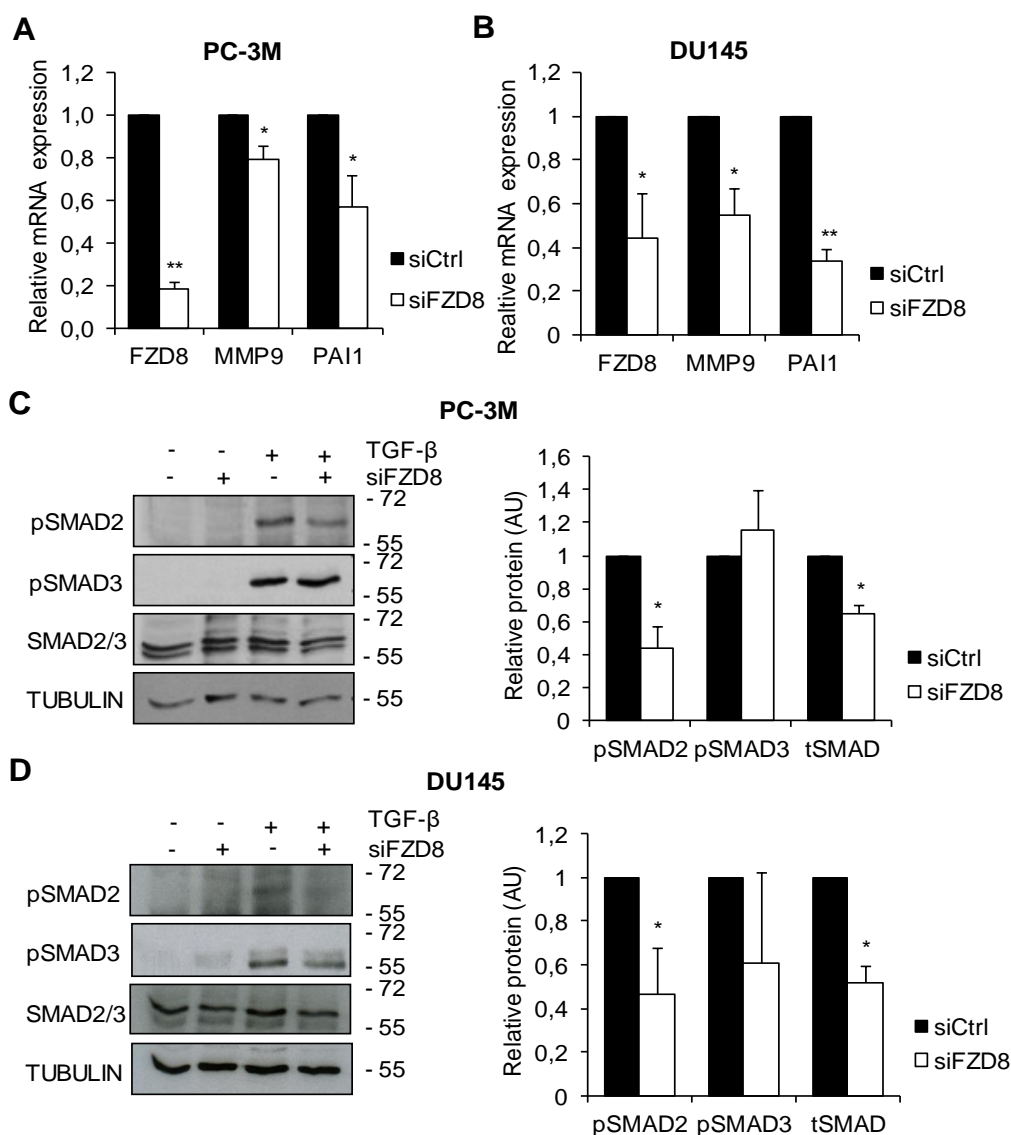


**Figure 65. FZD8 is required for expression of TGF- $\beta$  target genes and TGF- $\beta$ -dependent Smad phosphorylation.** Relative mRNA expression of the indicated genes in PC-3M (**A**) and

DU145 (B) cells silenced for *FZD8*; error bars show SD of four independent experiments. Western blots of PC-3M (C) and DU145 (D) cells silenced for *FZD8* and treated with 1 ng/mL of TGF- $\beta$  for 30 min. pSmad2, pSmad3, Smad2/3 and  $\beta$ -tubulin were used for blotting; graph shows relative protein levels, as determined by densitometry analysis of bands from TGF- $\beta$ -treated extracts, normalized to  $\beta$ -tubulin and relative to control siRNA, from three independent experiments \*  $p < 0.05$ , \*\*  $p < 0.001$  by Student's t test.

### 3.1.3 Analysis of TGF- $\beta$ -dependent cell invasion

Since TGF- $\beta$  signaling has been shown to promote cell invasion and our results are consistent with a requirement for FZD8 in TGF- $\beta$  signaling, we evaluated if *FZD8* silencing reduced invasion through its ability to inhibit TGF- $\beta$  signaling. In fact, *FZD8* silencing significantly reduced TGF- $\beta$ -induced cell invasion both in PC-3M (Fig. 66A, C and D) and DU145 cells (Fig. 66B, E and F) without affecting cell number (Fig. 67), supporting a role for FZD8 in regulating TGF- $\beta$  signaling and its consequent effects.

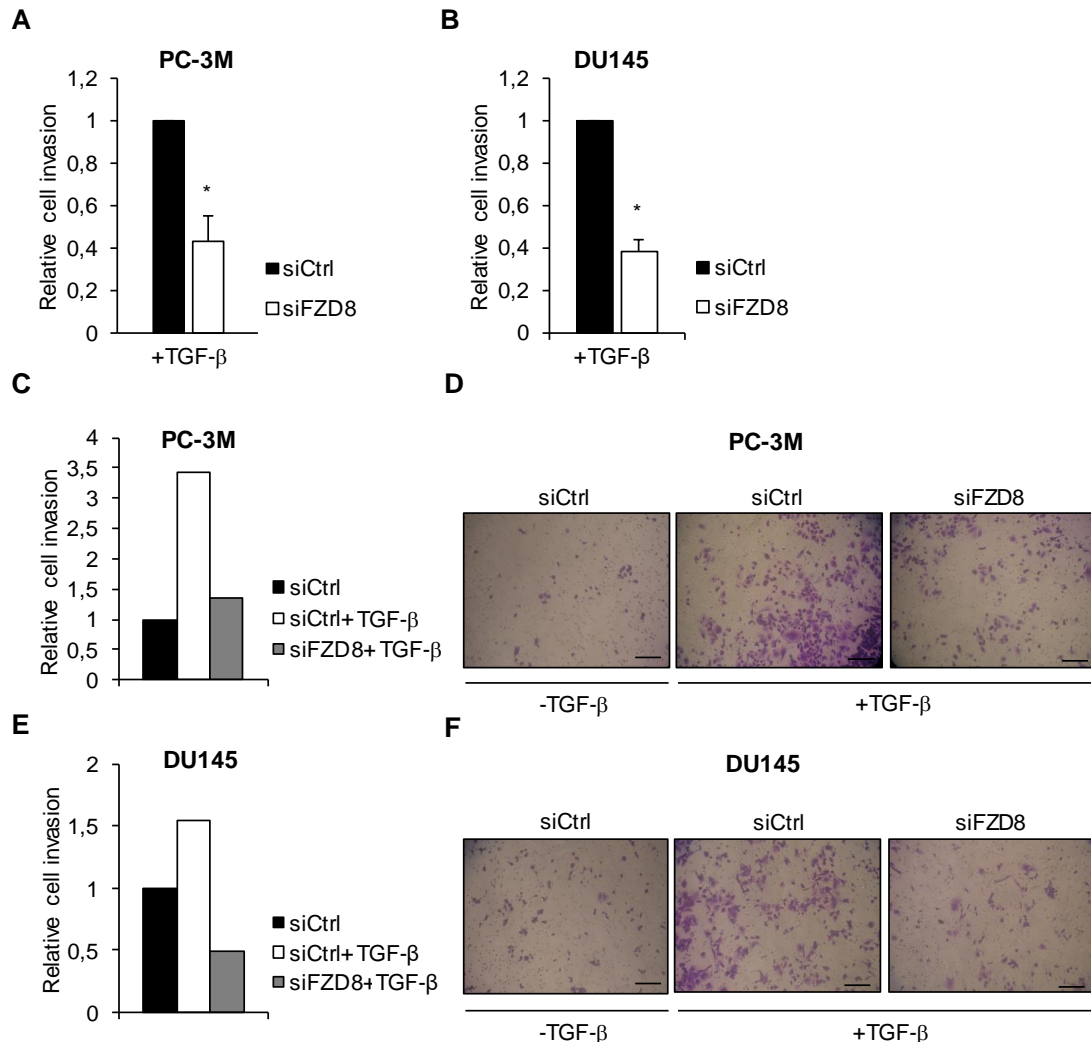


**Figure 66. FZD8 is required for TGF- $\beta$ -dependent cell invasion.** Relative cell invasion of PC-3M (A) and DU145 (B) cells silenced for *FZD8* and treated with 5 ng/mL of TGF- $\beta$  for 48 h; error bars represent SD of three independent experiments. (C-F) Relative cell invasion in a representative experiment and representative pictures of invading cells for PC-3M (C and D) and DU145 (E and F) cells. \*  $p < 0.05$  by Student's t test.

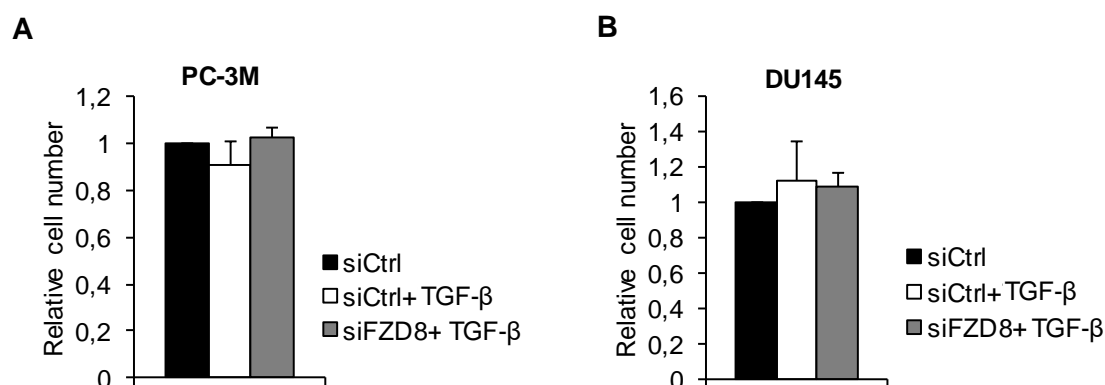


**Figure 67. Cell number analysis for invasion assays.** (A) and (B) show cell number for PC-3M and DU145 cells, respectively silenced for *FZD8* and treated with 5 ng/mL of TGF- $\beta$  for 48 h; error bars represent SD of three independent experiments. These data were used to normalize numbers of invading cells in Fig. 66. \*  $p < 0.05$ , \*\*  $p < 0.001$  by Student's t test.

### 3.1.4 Study of TGF- $\beta$ -dependent-EMT regulation

To extend our findings regarding *FZD8* regulation of TGF- $\beta$  signaling, we determined if *FZD8* silencing was also able to reduce EMT gene expression via inhibition of TGF- $\beta$  signaling. To do this, the effects of TGF- $\beta$  on the expression of EMT related genes were first examined. While TGF- $\beta$  treatment increased *MMP9* and *PAI1* expression (Fig. 68A and B) in both PC-3M and DU145 cells, it did not affect expression of EMT-related genes in PC-3M cells, apart from a small increase in *CDH2* and *CDH1* (Fig. 68C), being the latter expected to decrease with TGF- $\beta$  treatment (Cao & Kyprianou 2015; Papageorgis 2015). In contrast, TGF- $\beta$  treatment of DU145 cells increased *VIM*, *SNAI1/2* and *ZEB1* expression and reduced expression of *CDH1* (Fig. 68D). Not only that, TGF- $\beta$  treatment also increased *FZD8* and *WNT11* expression (Fig. 68E), supporting the idea of a positive feedback loop in the regulation of EMT. These results suggest that although both cell lines are highly metastatic, they display different features regarding EMT gene expression, which makes DU145 cells more sensitive to TGF- $\beta$  treatment than PC-3M cells.

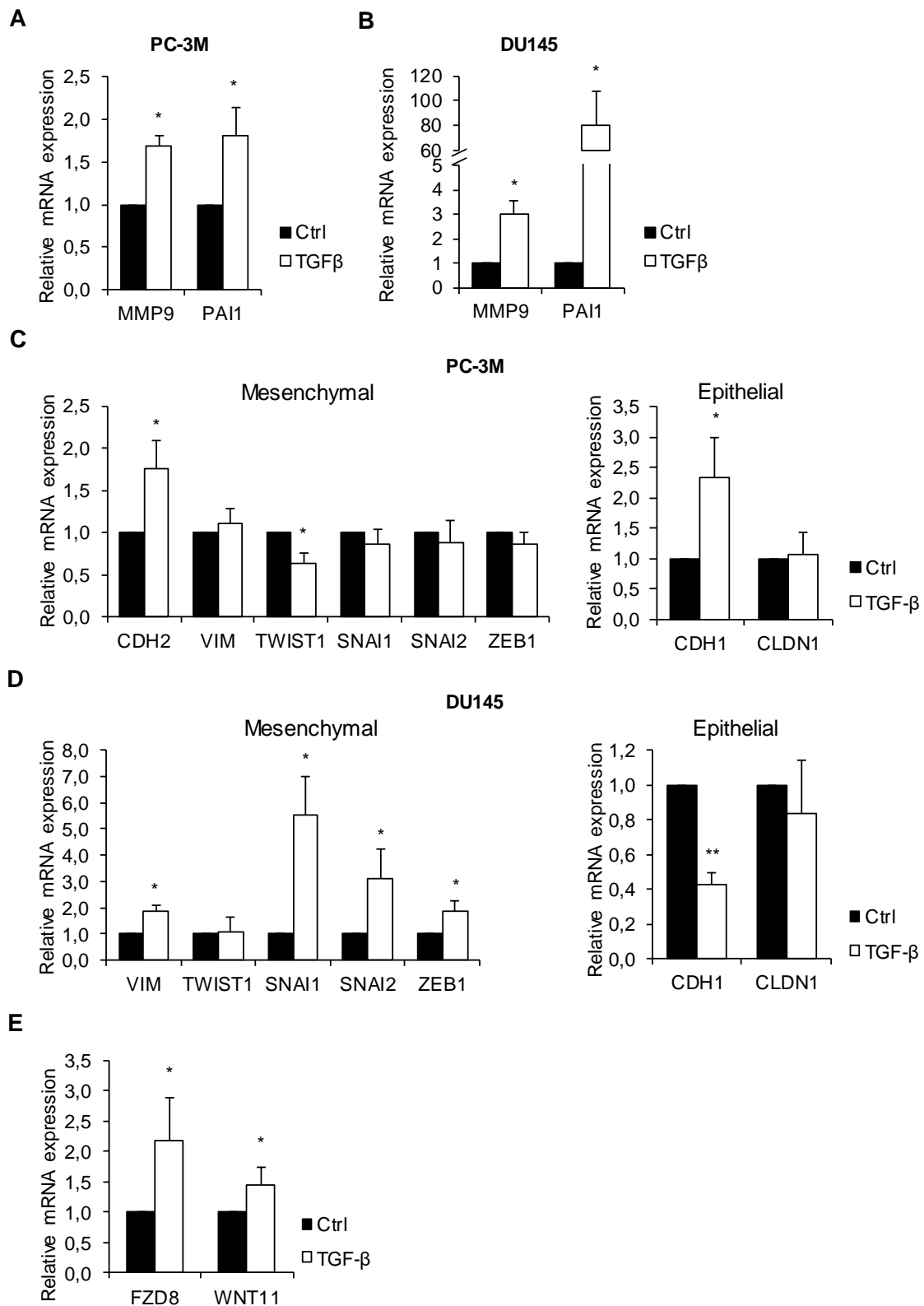


**Figure 68. Effects of TGF- $\beta$  on EMT gene expression.** (A-D) Q-RT-PCR analysis after treatment with 1 ng/mL TGF- $\beta$  for 24 h of TGF- $\beta$  target genes in PC-3M (A) and DU145 (B) cells as well as of EMT markers in PC-3M (C) and DU145 (D) cells. (E) Q-RT-PCR analysis of *FZD8* and *WNT11* in DU145 cells after treatment with 1 ng/mL TGF- $\beta$  for 24 h; in all cases error bars show SD for four independent experiments; \*  $p < 0.05$ , \*\*  $p < 0.001$  by Student's t test.



After evaluating the effects of TGF- $\beta$  in both cell lines, we decided to use DU145 cells, where TGF- $\beta$  effects were evident, aiming to determine if *FZD8* silencing could affect TGF- $\beta$ -dependent EMT gene expression. Examination of EMT-related genes upon TGF- $\beta$  treatment by q-RT-PCR revealed that *FZD8* silencing inhibited TGF- $\beta$ -induced expression of *VIM*, *SNAI1/2*, *ZEB1*, *MMP9* and *PAI-1* and increased expression of *CLDN1* (Fig. 69A and B). Together, these results provide evidence for a functional role for *FZD8* in regulating TGF- $\beta$ -mediated EMT gene expression.

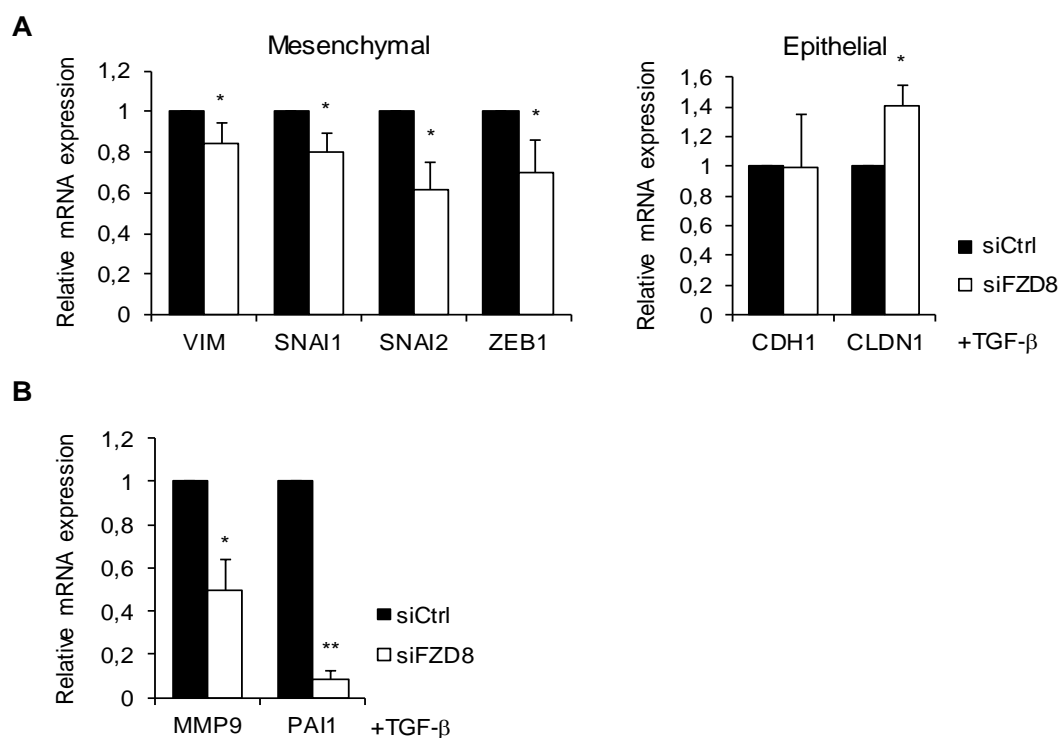


**Figure 69. FZD8 regulates TGF- $\beta$ -dependent expression of EMT-related genes.** Relative mRNA expression of the indicated EMT genes (A) as well as of the TGF- $\beta$  target genes (B), relative to 36B4, in DU145 cells silenced for *FZD8* and treated with 1 ng/mL TGF- $\beta$  for 24 h; error bars show SD for four independent experiments. \*  $p < 0.05$ , \*\*  $p < 0.001$  by Student's t test.

## 3.2 Mechanism of regulation of TGF- $\beta$ signaling by FZD8

### 3.2.1 Regulation at the intracellular level

The observations found in this work indicate that FZD8 is involved in both Wnt-11/ATF2 and TGF- $\beta$ /Smad signaling. Interestingly, in addition to the traditional crosstalk between Wnt and TGF- $\beta$  pathways observed at the level of Smad and  $\beta$ -catenin, ATF2 has also been reported to associate with Smad proteins (Sano et al. 1999). This suggests that Wnt-11/FZD8 signaling might regulate TGF- $\beta$ /Smad via ATF2. In order to assess the contribution of ATF2 to TGF- $\beta$  signaling, we evaluated the effects of a dominant-negative form of ATF2,  $\Delta$ -ATF2, which binds and inhibits the activities of ATF2 and its AP-1 family partners (Vinson et al. 2002). Gene reporter assays showed that  $\Delta$ -ATF2 significantly reduced TGF- $\beta$  activation of the Smad-dependent reporter CAGA-12 (**Fig. 70A**), indicating that ATF2 and/or other AP-1 family members play a role in TGF- $\beta$ /Smad signaling. An inhibitory effect of  $\Delta$ -ATF2 was also observed when using the 3TP-lux reporter, which contains both Smad and AP-1 binding sites (**Fig. 70B**). Moreover,  $\Delta$ -ATF2 significantly reduced TGF- $\beta$ -induced expression of *VIM*, *SNAI2* and *ZEB1* and increased the expression of *CDH1* in DU145 cells (**Fig. 71**) indicating a requirement for ATF2 for the expression of a subset of TGF- $\beta$ -regulated EMT genes.

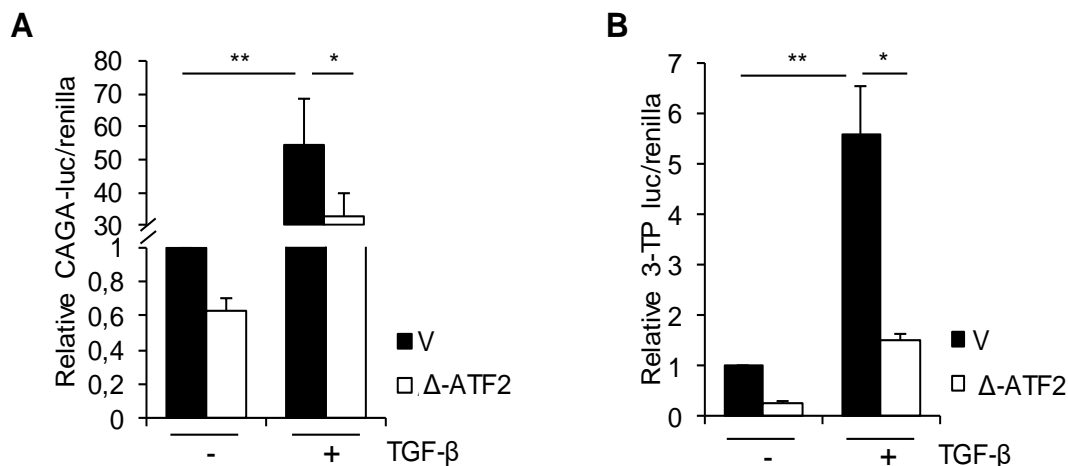


**Figure 70. ATF2 is required for TGF- $\beta$ -dependent gene reporter activity.** Gene reporter assays of CAGA12-luciferase (**A**) or 3-TP-luciferase (**B**) activities in PC-3M cells transfected with empty vector CMV500 (V) or dominant-negative ATF2 ( $\Delta$ -ATF2) and treated with 1 ng/mL TGF- $\beta$  for 24 h; error bars show SD for three independent experiments; \*  $p < 0.05$ , \*\*  $p < 0.001$  by ANOVA with Tukey post-hoc test.

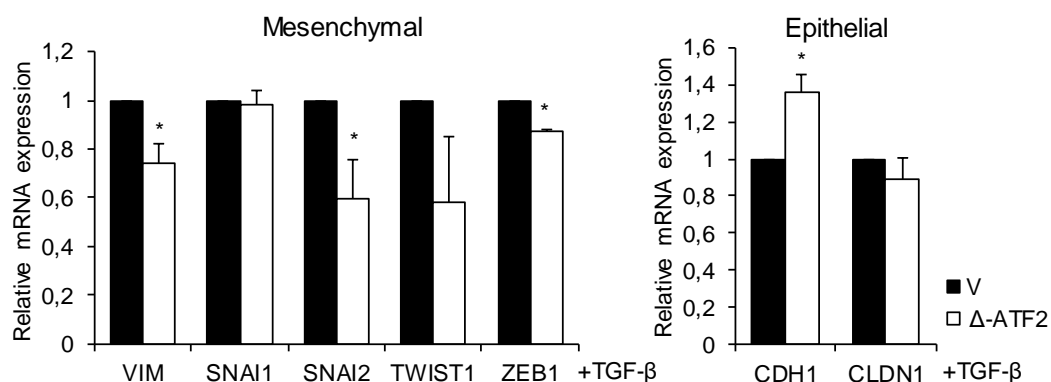


**Figure 71. ATF2 regulates TGF- $\beta$ -dependent expression of EMT-related genes.** Q-RT-PCR analysis showing mRNA expression of the indicated genes in DU145 cells transfected with empty vector CMV500 (V) or  $\Delta$ -ATF2 and treated with 1 ng/mL TGF- $\beta$  for 24 h; error bars show SD for four independent experiments; \*  $p < 0.05$  by Student's t test.

Since all these results together suggest that FZD8 may promote TGF- $\beta$ /Smad-dependent signaling via activation of ATF2, and given the reported association of ATF2 with Smad2 and Smad3 (Sano et al. 1999), we wished to determine if this interaction was affected by *FZD8* silencing. However, we were unable to detect a stable complex between ATF2 and Smad2 or Smad3 by immunoprecipitation in prostate cancer cells (**Fig. 72**), suggesting that signaling crosstalk takes place at some other point in the TGF- $\beta$  signaling pathway.

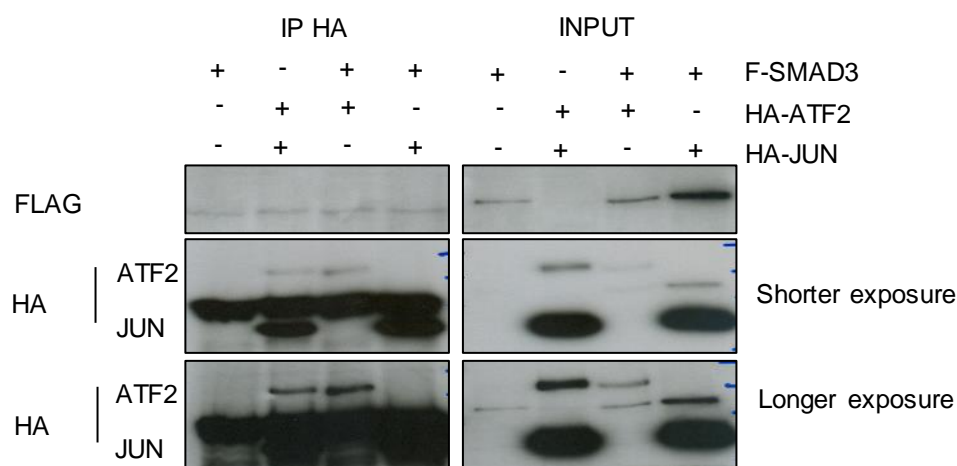


**Figure 72. ATF2 does not form a stable complex with Smad3.** Western blots of anti-HA immunoprecipitates (IP) and extracts (inputs) from PC-3M cells transfected for 24 h with HA-tagged ATF2 and c-JUN, and Smad3 plasmids were probed for ATF2 and c-JUN (HA) and Smad3 (Flag); blots are representative of two independent experiments.

### 3.2.2 Regulation at the cell membrane

#### 3.2.2.1 FZD8 binds to TGF- $\beta$ receptors

Based on our results excluding the regulation of TGF- $\beta$  signaling by FZD8 through Smad/ATF2 interaction, we next hypothesized that crosstalk between FZD8 and TGF- $\beta$  signaling might take place at the cell membrane. TGF- $\beta$  signaling is initiated by ligand binding to two transmembrane receptor kinases (TGF $\beta$ RI and TGF $\beta$ RII), with binding of TGF- $\beta$  to TGF $\beta$ RII being a prerequisite for efficient ligand binding to TGF $\beta$ RI (Shi & Massagué 2003). To test if FZD8 associated with TGF $\beta$  receptors, PC-3M cells were transfected with plasmids expressing epitope-tagged FZD8, TGF $\beta$ RI and TGF $\beta$ RII and subjected to immunoprecipitation analysis. Interestingly, a stable interaction was observed between FZD8 and both TGF $\beta$ RI and TGF $\beta$ RII (**Fig. 73A**). In addition, immunofluorescence analysis also showed that FZD8 partially co-localized with both TGF $\beta$ RI and TGF $\beta$ RII in transfected cells, lending further support to our hypothesis (**Fig. 73B**).

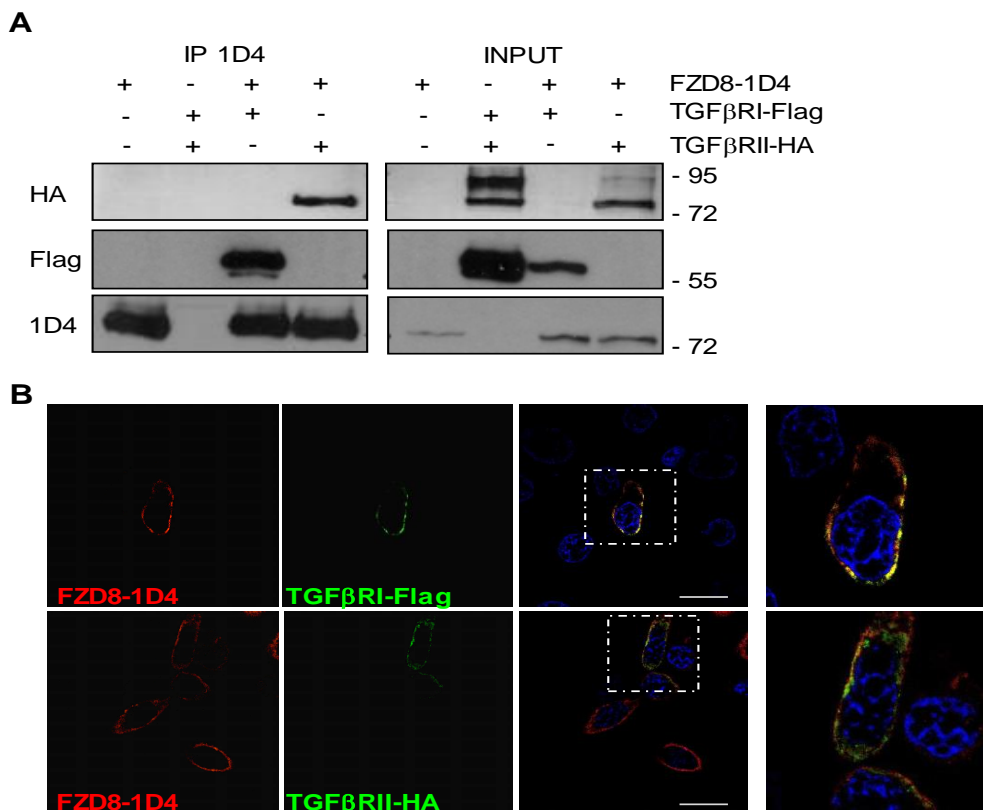


**Figure 73. FZD8 associates with TGF- $\beta$  receptors.** (A) Western blots of anti-1D4 immunoprecipitates (IP) and extracts (inputs) from PC-3M cells transfected with indicated plasmids; anti- HA, Flag and 1D4 were used for blotting. Blots are representative of three independent experiments and the positions of molecular mass markers are indicated. (B) Immunofluorescence analysis of PC-3M cells transfected with 1D4-tagged FZD8 (red) and Flag-tagged TGF $\beta$ RI or HA-tagged TGF $\beta$ RII (green) for 24 h; images are representative of three independent experiments, blue staining shows cell nuclei (DAPI); scale bar 25 $\mu$ m.

### 3.2.2.2 Analysis of interacting domains

FZD8, as all members of the FZD family, contains an extracellular N-terminal cysteine-rich domain (CRD), which is very well characterized owing to its involvement in Wnt binding. To determine whether the FZD8 CRD was involved in the association of FZD8 with TGF $\beta$  receptors, a plasmid encoding the FZD8 CRD fused to the Fc domain of human IgG was used. This fusion protein associated with TGF $\beta$ RI but not with TGF $\beta$ RII (**Fig. 74A**) suggesting that FZD8 associates with TGF $\beta$ RI and that the observed interaction with TGF $\beta$ RII (**Fig. 73A**) is mediated by endogenous TGF $\beta$ RI. In contrast to FZD8 CRD IgG, the extracellular domain of LRP6 fused to the Fc domain of human IgG did not bind either TGF $\beta$ RI or TGF $\beta$ RII (**Fig. 74A**). Furthermore, a tagged form of the TGF $\beta$ RI extracellular domain ( $\Delta$ TGF $\beta$ RI) readily associated with FZD8 CRD-IgG (**Fig. 74B**), which is consistent with the interaction between FZD8 and TGF $\beta$ RI involving the extracellular domains of both proteins.

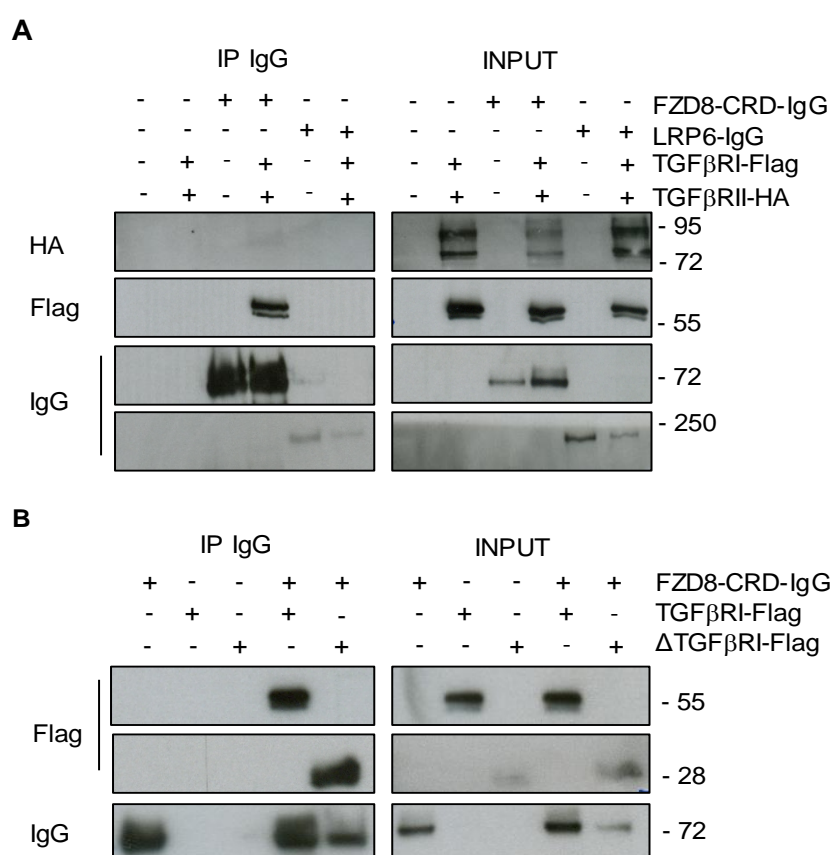


**Figure 74. FZD8 and TGF $\beta$ RI associate through their extracellular domains.** **(A)** Western blots of Protein A/G-agarose immunoprecipitates (IP IgG) and extracts (inputs) from PC-3M cells transfected for 24 h with indicated plasmids; anti-HA, -Flag and -IgG were used for blotting. Blots are representative of three independent experiments and the positions of molecular mass markers are indicated. **(B)** Western blots of Protein A/G-agarose pull-downs (IP IgG) and extracts (inputs) from PC-3M cells transfected for 24 h with indicated plasmids; Anti-Flag and -IgG were used for blotting. Blots are representative of three independent experiments and the positions of molecular mass markers are indicated.

### 3.2.2.3 Effects of TGF- $\beta$ on the interaction

To determine if the interaction of FZD8 with TGF $\beta$ RI/RII was ligand-regulated, experiments were carried out using cells treated with or without exogenous TGF- $\beta$ . Western blotting for phosphorylated Smad3 indicated that transfection of TGF $\beta$ RI/II was sufficient to activate TGF- $\beta$  signaling and that this was not affected by exogenous TGF- $\beta$  (**Fig. 75A**). However, treatment with TGF- $\beta$  reduced the interaction between FZD8 and TGF $\beta$ RII, whereas there was no significant effect on its association with TGF $\beta$ RI (**Fig. 75B**). These results are consistent with FZD8 interacting with TGF $\beta$ RII via TGF $\beta$ RI and TGF- $\beta$  treatment reducing binding of TGF $\beta$ RII to the FZD8-TGF $\beta$ RI complex.

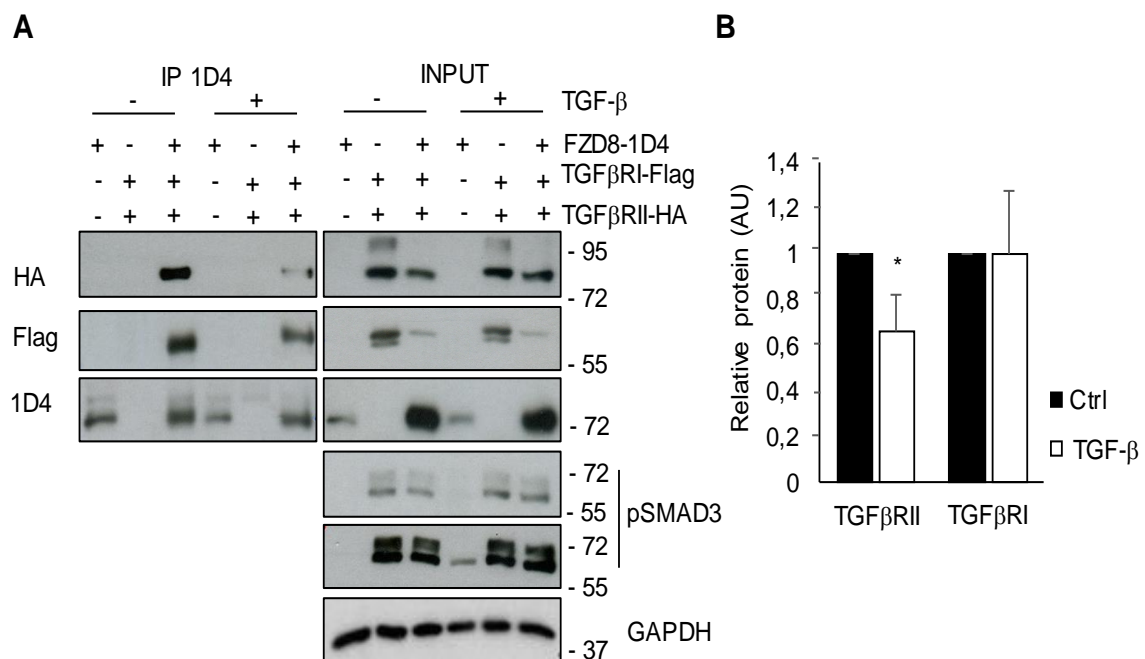


**Figure 75. The FZD8-TGF- $\beta$  receptor interaction is ligand-regulated.** (A) Western blots of anti-1D4 immunoprecipitates (IP) and extracts (inputs) from PC-3M cells transfected for 24 h with plasmids encoding 1D4-tagged FZD8, Flag-tagged TGF $\beta$ RI and HA-tagged TGF $\beta$ RII, serum-starved and treated +/- 1 ng/mL TGF- $\beta$  for 24 h. Anti-HA, Flag and 1D4 were used for blotting. Extracts were also probed for pSmad3 and GAPDH as a loading control. Blots are representative of three independent experiments and the positions of molecular mass markers are indicated. (B) Relative protein levels, as determined by densitometry analysis of bands from TGF- $\beta$ -treated extracts, relative to control (Ctrl), from three independent experiments.

### 3.2.2.4 Implication of Wnt-11 in FZD8-TGF $\beta$ RI binding

After demonstrating that the interaction between FZD8 and TGF $\beta$ RI/RII was TGF- $\beta$ -regulated, we wished to determine if Wnt-11 binding to FZD8 could prevent the FZD8-TGF $\beta$ RI/RII complex or if on the contrary, FZD8 could be binding both Wnt-11 ligand and TGF- $\beta$  receptors at the same time. Unexpectedly, co-immunoprecipitation analysis of tagged forms of Wnt-11, FZD8 and TGF $\beta$ Rs, indicated that Wnt-11 associated with FZD8 even when it was bound to TGF $\beta$ Rs (**Fig. 76**). Moreover, Wnt-11 also co-immunoprecipitated with TGF $\beta$ RI, which may indicate binding mediated by endogenous FZD8 receptors (**Fig. 76**).

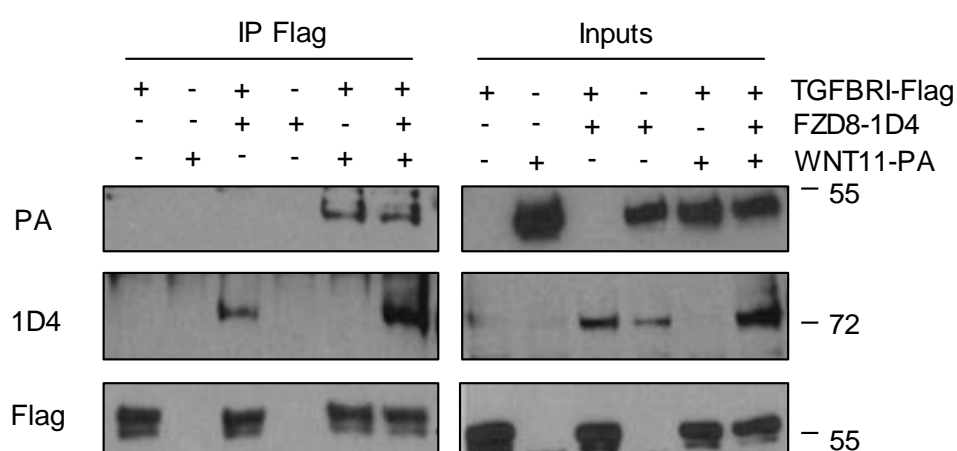


**Figure 76. Implication of Wnt-11 in FZD8-TGF $\beta$ RI binding.** Western blots of anti-Flag immunoprecipitates (IP) and extracts (inputs) from PC-3M cells transfected for 24 h with plasmids encoding 1D4-tagged FZD8, Flag-tagged TGF $\beta$ RI and PA-tagged Wnt-11. Anti-PA, 1D4 and Flag were used for blotting. Blots are representative of three independent experiments and the positions of molecular mass markers are indicated.

In conclusion, our data lead us to establish a model in which FZD8, by interacting both with Wnt-11 and TGF $\beta$ RI, is able to play a pivotal role in integrating Wnt and TGF- $\beta$  signals to drive EMT and invasion promoting prostate cancer progression and therefore, unveil FZD8 as an important target for the therapy of metastatic prostate cancer (**Fig. 77**).

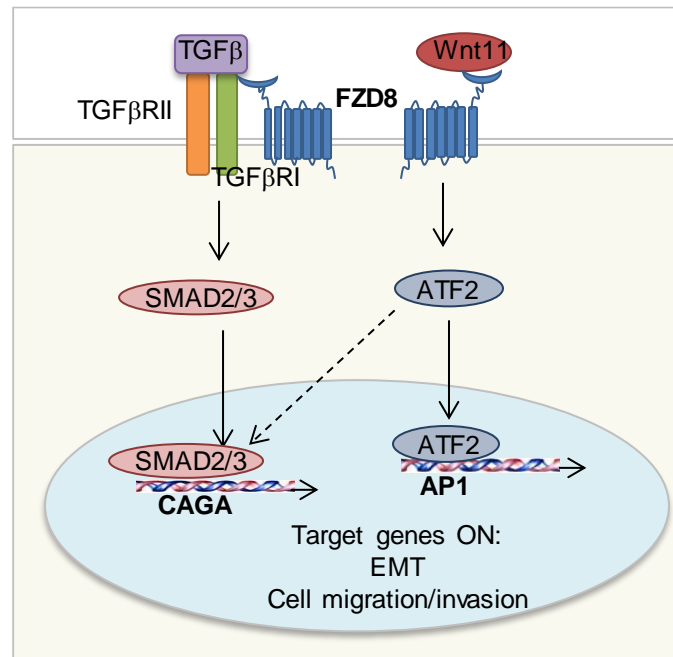


**Figure 77. Proposed model for FZD8 integration of Wnt-11 and TGF- $\beta$  signals.** Regulation at the level of the receptors and transcription factors is shown. Dashed arrow indicates potential regulation of Smad2/3 by ATF2, based on other published studies (see text).





---

# DISCUSSION

---



Prostate cancer is the second leading cause of death in men in industrialized countries. Owing to the crucial role of the androgen receptor in prostate carcinogenesis, androgen deprivation therapy is the main treatment option for prostate cancer patients. However, most patient tumors evolve to a castration resistant state in which tumor cells do not respond to hormonal therapy. Despite some recent therapies targeting AR and chemotherapy extend the life of prostate cancer patients, resistance to these treatments still appears, highlighting the urgent need for novel targets that do not rely on targeting the androgen receptor for the treatment of these patients. Interestingly, Wnt signaling has been shown to be altered at different stages of prostate cancer (Murillo-Garzón & Kypta 2017). Among these alterations, Wnt-11, a noncanonical Wnt ligand, has been shown to be upregulated in prostate tumors, particularly in metastasis (Zhu et al. 2004), as well as to promote prostate cancer cell migration and invasion and neuroendocrine-like differentiation features of aggressive disease (Uysal-Onganer et al. 2010). Several reports in the literature have shown the importance of targeting Wnt receptors as a strategy to inhibit aberrant Wnt signaling. Monoclonal antibodies such as Vantictumab, which targets FZD receptors (FZD1, 2, 5, 7 and 8)(Gurney et al. 2012); OTSA101, which targets FZD10 (Nagayama et al. 2005; Fukukawa et al. 2008) and Cirmtuzumab, which targets the ROR1 Wnt coreceptor (Choi et al. 2015) are in clinical trials for different cancer types (Murillo-Garzón & Kypta 2017).

Taking all this evidence into account and based on the requirement of Wnt ligands to activate their receptors and signal, we aimed to identify the receptors involved in Wnt-11 signaling in order to use them as therapeutic targets to inhibit Wnt-11 signaling in prostate cancer. During the work described in this thesis, we found that *FZD8* is highly expressed in metastatic prostate cancer cell lines as well as in prostate tumors, functioning as a major Wnt-11 receptor in metastatic prostate cancer. High *FZD8* expression was related to a tumor-promoting role in which it promotes prostate cancer cell migration, invasion and regulates EMT. Interestingly, we also found that this regulation is TGF- $\beta$ -dependent suggesting that FZD8 mediates crosstalk between Wnt-11 and TGF- $\beta$  signaling through binding to TGF $\beta$ RI. These findings support the fact that FZD8 could be a good therapeutic target for the treatment of metastatic prostate cancer.

## Chapter 1. Identification and characterization of Wnt-11 receptors in metastatic prostate cancer

The initial screen to identify Wnt receptors with increased expression in metastatic prostate cancer led us to select FZD2, FZD4 and FZD8 as the three main candidates for transducing Wnt-11 signals. Q-RT-PCR analysis of 23 Wnt receptors and coreceptors showed an increased expression of these receptors in PC-3M and VCaP cell lines, which are both highly metastatic and express the highest levels of *WNT11*.

The increasing expression of *FZD2* from less metastatic to more metastatic PCa cell lines is consistent with studies showing FZD2 involvement in prostate cancer aggressiveness through mediation of Wnt-5a signaling and binding to the ROR2 Wnt coreceptor (Yamamoto et al. 2010; Sato et al. 2010). Of note, a recent study has also reported association of high *FZD2* expression with metastasis and biochemical recurrence in prostate cancer (Sandsmark et al. 2017).

*FZD4* was also upregulated in metastatic prostate cancer cell lines, however its expression was higher in VCaP cells. These observations suggest a role for this receptor in *TMPRSS-ERG* positive tumors. Indeed, an association between *FZD4* and *ERG* has already been described (Gupta et al. 2010), where FZD4 was also found to be associated with EMT. Our analysis of Wnt receptor expression in prostate cancer datasets using the Oncomine database revealed that *FZD4* was also upregulated when comparing normal versus prostate cancer tissues, lending further support for a role of this receptor in a subset of prostate tumors.

Together with *FZD2* and *FZD4*, we found upregulation of *FZD8* in metastatic prostate cancer cell lines. Moreover, and distinct to *FZD2* and *FZD4*, this upregulation was supported by a strong colocalization between FZD8 and Wnt-11 found by immunofluorescence studies, suggesting a role for FZD8 as Wnt-11 receptor. Indeed, FZD8 has been reported to be a Wnt-11 receptor in the mouse, where Wnt-11 is required for the kidney development (Ye et al. 2011). Consistent with our finding of *FZD8* being upregulated in VCaP cells (*TMPRSS-ERG* fusion positive cell line), this receptor has also been reported to be induced by *ERG* (Brase et al. 2011), which was also confirmed by our bioinformatics analysis in different datasets. Furthermore, a recent study has also described that the expression of FZD8 is directly correlated with ERG expression in PCa, showing that ERG directly targets and activates FZD8 by binding to its promoter (Chakravarthi et al. 2018). *FZD8* expression was also found to be upregulated in a high number of prostate cancer datasets from the Oncomine and cBioPortal databases. In

addition, analysis of FZD8 protein expression in the ProteinAtlas also revealed its upregulation in PCa compared to normal prostate, consistent with studies showing increased expression of *FZD8* in prostate tumor epithelial cells, as compared to luminal epithelial cells from benign prostate (Pascal et al. 2009).

Interestingly, although our cell line data did not show a notable upregulation of any other Wnt receptor, our immunofluorescence assays also revealed a partial colocalization between Wnt-11 and FZD6 and Wnt-11 and FZD10. FZD6 has been reported to colocalize with Wnt-11 in breast cancer cell lines, where it activated noncanonical Wnt/PCP signaling and cell migration (Luga et al. 2012). Moreover, chip studies have shown an upregulation of *FZD6* in a panel of 54 prostate cancer patients (Wissman et al. 2003), suggesting that further investigation to clarify the role of this receptor in metastatic prostate cancer could be fruitful. Our analysis also showed a partial colocalization between FZD10 and Wnt-11 but the expression of this receptor was restricted to VCaP cells, where its expression was not very high. These results may suggest a possible role for FZD10 in ERG positive tumors, although additional studies will be needed to explore this hypothesis.

Despite its expression not being upregulated in highly metastatic prostate cancer cell lines, our q-RT-PCR analysis indicated that *FZD7* expression was increased in C4-2B cells cultured under hormone-deprived conditions (CSS) to induce NED, which also upregulates *WNT11* (Uysal-Onganer et al. 2010; Volante et al. 2016). Although FZD7 did not colocalize with Wnt-11 in our immunofluorescence studies, it has been reported to colocalize with Wnt-11 at the apical adherens junction in *Xenopus* embryos, where it regulates convergent extension movements (Djiane et al. 2000; Yamanaka & Nishida 2007; Kim et al. 2008). In addition, FZD7 mediates Wnt-11 signals during colon cancer cell invasion (Ueno et al., 2009). It would therefore be worthwhile investigating the possibility that FZD7 acts as a Wnt-11 receptor in neuroendocrine-like prostate cancer (for example, colocalization of Wnt-11 and FZD7 in CSS C4-2B cells).

Since the interaction between Wnt ligands and FZD receptors is context-dependent (Niehrs 2012), it is possible that different FZD receptors can bind to Wnt-11 in different cell types or conditions, as has been reported (Djiane et al. 2000; Penzo-Mendèz et al. 2003; Yamanaka & Nishida 2007; Cavodeassi et al. 2005; Witzel et al. 2006; Abdul-Ghani et al. 2011; Ye et al. 2011), which supports the potential involvement of more than one FZD family member functioning as Wnt-11 receptor in prostate cancer.

Regardless of the valuable information obtained through these approaches, the main limitation of this study is the lack of data based on Wnt receptor protein expression. Most

of the information deposited in available databases describes mRNA expression levels and it is more difficult to obtain information about protein expression. In addition, the fact that FZD receptors are cysteine-rich seven-pass-transmembrane domain proteins makes difficult to analyze them using western blotting because they readily form aggregates. However, when technically possible, specific antibodies for detecting Wnt receptors and coreceptors is essential to confirm that FZD protein expression levels reflect mRNA expression levels.

While the results described in this thesis are focused on FZD receptors, Wnt ligands also require binding to specific coreceptors in order to signal (Niehrs 2012). Our q-RT-PCR analysis showed an upregulation of *ROR1* in PC-3M prostate cancer cells, which is consistent with studies from Zhang et al. showing upregulation of this orphan tyrosine kinase receptor in 19 of 21 prostate tumors (S. Zhang et al. 2012). Even though there are few reports linking ROR1 to prostate cancer, several studies show that ROR1 is involved in other cancer types, such as leukemia, lung, breast and colon cancer (Kolb et al. 2016). Moreover, the closely related receptor ROR2 has been found to mediate Wnt-11 signaling in zebrafish, regulating convergent extension movements (Bai et al. 2014). ROR2 has also been extensively studied in different types of cancer, including prostate cancer, where it binds Wnt-5a through FZD2, to promote tumor aggressiveness (Yamamoto et al. 2010). Our *in silico* analysis of prostate cancer datasets also highlighted the upregulation of *PTK7* in several prostate cancer datasets, consistent with studies showing PTK7 as a predictor of lymph node metastasis and as a prognostic biomarker in prostate cancer (Zhang et al. 2014). Although not seen in our screen, other studies have shown the involvement of other Wnt coreceptors in Wnt-11 signaling, such as the tyrosine kinase receptor RYK in *Xenopus* models (Kim et al. 2008). These reports, together with our preliminary results for the study of coreceptors, highlight the requirement for further studies to identify those involved in Wnt-11 signaling in prostate cancer.

According to the widely characterized implication of Wnt-11 in noncanonical pathways (Uysal-Onganer & Kypta 2012), our data show that several FZD receptors can transduce Wnt-11-ATF2 noncanonical signaling. Interestingly, only FZD8 and FZD10 were able to enhance the activation that Wnt-11 produces in PC-3M cells. It is important to bear in mind that besides being a mediator of noncanonical Wnt signaling, ATF2 is also involved in the stress response, for example after chemotherapeutic agents such as cisplatin, doxorubicin or paclitaxel (Lo Iacono et al. 2015; Li et al. 2016). Since transfection of FZD receptors, may also activate ATF2 by inducing cell stress, we tried to strengthen the case

for FZD8 functioning as a Wnt-11 receptor using a more physiological approach. In this regard, we showed that silencing of *FZD8* significantly reduced Wnt-11 activation of the noncanonical ATF2 reporter, supporting the role of FZD8 as the major Wnt-11 receptor in metastatic prostate cancer. Importantly, immunoprecipitation assays confirmed that a stable interaction takes places between the ligand and the receptor, consistent with their strong colocalization in PC-3M cells. In light of the fact that FZD receptors can bind to different coreceptors (C. Li et al. 2008; Yamamoto et al. 2010; Carmon et al. 2012; Capurro et al. 2014) in order to signal, further studies will be needed to determine whether this binding is direct or requires a Wnt coreceptor. Of note, when analyzing ATF2 reporter activity, we observed *FZD2* silencing also significantly reduced Wnt-11 activation of ATF2. Although this effect was not as dramatic as that mediated by *FZD8* silencing, FZD2 has been described to promote tumorigenesis in prostate cancer through Wnt-5a signaling (Sato et al. 2010; Yamamoto et al. 2010; Sandsmark et al. 2017), encouraging additional studies to explore the role of FZD2 in Wnt-11 signaling.

Several reports have demonstrated the importance of FZD8 in different cancer types via binding to distinct Wnt ligands. In lung cancer, FZD8 has been described as a Wnt-2 receptor, activating the canonical pathway, with *FZD8* silencing reducing cell proliferation, suppressing A549 xenograft growth and sensitizing cells to chemotherapy (Wang et al. 2012; Bravo et al. 2013). FZD8 canonical signaling has also been described in triple negative breast cancer, where it is involved in resistance to chemotherapy (Yin et al. 2013). In head and neck squamous carcinomas, FZD8 is required for c-Met mediated canonical Wnt signaling and its overexpression rescues c-Met shRNA-induced impairment of sphere formation, tumor incidence and orthotropic tumor growth (Sun et al. 2014). While these studies implicate FZD8 in canonical Wnt signaling, other reports suggest that FZD8 can function as a canonical or a noncanonical Wnt receptor. Studies in renal cell carcinoma (RCC) have shown a dual role of FZD8, since its silencing reduces both canonical and noncanonical markers, including  $\beta$ -catenin and c-MYC but also Rho, Rac, JNK and ATF2 (Yang et al. 2017). FZD8 has been described as a noncanonical Wnt-5a receptor in airway smooth muscle cells, where it mediates JNK noncanonical signaling and is required for TGF- $\beta$  dependent ECM1 production (Kumawat et al. 2013), confirmed in later studies on the role of FZD8 in profibrotic signaling (A. I. R. Spanjer et al. 2016). In this project, we demonstrated that FZD8 functions as a Wnt-11 receptor in metastatic prostate cancer cells through the regulation of noncanonical Wnt signaling involving ATF2/AP-1 family of transcription factors. Moreover, FZD8 did not affect canonical Wnt signaling, as measured by a lack of effect on the TOP/FOP reporter and

expression of the  $\beta$ -catenin/Tcf target gene, *AXIN2*. A recent study by Li et al. also reported the upregulation of *FZD8* in prostate cancer, consistent with our results. However, they propose that *FZD8* activates Wnt/ $\beta$ -catenin signaling by increasing *WNT3A* expression. In contrast, our results indicate that Wnt/ $\beta$ -catenin signaling is not affected by *FZD8* silencing. Moreover, our data shows that Wnt/ $\beta$ -catenin signaling activity remains low in prostate cancer, which is consistent with reports from Sandsmark et al. 2017, showing that there was no alteration in the expression levels of  $\beta$ -catenin nor  $\beta$ -catenin translocation to the nucleus when comparing normal versus cancer samples. Their studies also described an upregulation of *AXIN2* or *GSK3* in cancer samples compared to normal, which suggests an increased activity of the destruction complex in prostate cancer, emphasizing the low  $\beta$ -catenin activity in prostate cancer cells (Sandsmark et al. 2017). How these contrasting mechanisms can be consolidated will require additional studies.

## Chapter 2. Implication of FZD8 in prostate cancer pathogenesis

The processes leading to the malignant transformation of cells are very complex but the ability of cells to invade surrounding tissues and metastasize are key events in tumor progression (Martin et al. 2000; Martin et al. 2013; W. G. Jiang et al. 2015). In this sense, understanding the mechanisms involved in tumor cell invasion may allow us to find ways to limit tumor progression and, as a result, lead to a reduction in cancer patient mortality (Martin et al. 2000; Martin et al. 2013).

In prostate cancer, previous studies by our group reported the involvement of Wnt-11 in PCa cell migration and invasion (Uysal-Onganer et al. 2010). In this thesis work, after identifying *FZD8* as major Wnt-11 receptor, we show that *FZD8* is also required for prostate cancer cell migration and invasion. Our analysis of the effects of both transient and stable *FZD8* silencing in different metastatic cell lines revealed it significantly reduced prostate cancer cell migration and invasion. Moreover, we were able to corroborate these 2D experiments using 3D organotypic cultures, showing that *FZD8*-silenced cells mature into well-differentiated organoids that do not form invasive structures, unlike control cells. In this regard, both 2D and 3D experiments support the role of *FZD8* in tumor progression through the regulation of migration and/or invasion activity in prostate cancer. It is important to highlight that the use of organotypic 3D cultures in our studies allowed us to overcome the limitations of 2D cultures, which despite being widely used in cancer research as a first approach to study different processes during tumor progression, usually represent more reductionist models that do



not into account the tumor microenvironment (TME) for tumor development and progression (Pampaloni et al. 2007; Härmä et al. 2010). In this regard, the use of 3D cultures allows one to address complex aspects of normal and malignant tissues, such as the extracellular matrix (ECM), basement membrane (BM), cell-cell and cell-matrix adhesion, tumor-stroma interactions, the formation of relevant tumor-like histology and more importantly in our case, to study tumor-cell invasion considering cell dynamics and tumor architecture (Härma et al. 2014).

Consistent with our findings, several studies have reported the implication of FZD receptors, including FZD8, in cell migration and invasion. In colorectal cancer, it has been described that FZD8 acts as a Wnt-2 receptor in cancer associated fibroblast (CAFs) being associated with a pro-migratory and pro-invasive phenotype, since both *WNT2* and *FZD8* knockdown reduced the migratory potential as well as the length of invasive sprouts of CAFs (Kramer et al. 2017). *FZD8* knockdown has also been shown to reduce the number of spheres formed by head and neck squamous carcinoma cells (HNSCC) (Sun et al. 2014), reflecting the important role of cancer stem cells in invasion and metastasis (Li et al. 2007; Sampieri & Fodde 2012). A recent study by Li et al. (2017) also reported the involvement of FZD8 in prostate cancer migration, invasion and stem like phenotypes, supporting a model in which FZD8 promote prostate cancer progression through regulation of invasive capacities.

The inhibition of Wnt signaling has traditionally relied on porcupine inhibitors which block Wnt secretion (Chen et al. 2009; Proffitt et al. 2013); tankyrase inhibitors, which inhibit  $\beta$ -catenin-dependent Wnt signaling by stabilizing Axin2 (Chen et al. 2009) or drugs that target  $\beta$ -catenin interactions with transcription factors (Anastas & Moon 2013). However, the elucidation of the structure of the XWnt-8-FZD8 CRD complex (Janda et al. 2012) has accelerated the development of drugs targeting the Wnt pathway at the receptor level (Gurney et al. 2012; Wei et al. 2011; Hojjat-Farsangi et al. 2013). Some years ago, a structure based study led to the identification of compounds that target the CRD domain of FZD receptors, preventing their binding to Wnt ligands (Lee et al. 2015). Our observation of the increased expression of FZD8 in metastatic prostate cancer cell lines and in a significant proportion of prostate tumors, together with the demonstrated inhibitory effect of *FZD8* silencing on prostate cancer cell migration and invasion, suggests that inhibition of Wnt-FZD8 interactions may be a useful approach for the treatment of patients with metastatic prostate cancer. Here, we found that two of the small molecule inhibitors that target the Wnt binding site on FZD (Lee et al. 2015) were able to reduce prostate cancer cell migration, lending support to our suggestion of FZD8

as a good therapeutic target. Nevertheless, it is important to bear in mind that these compounds are not specific for FZD8 and that the observed effects might be also due to inhibition of binding between different Wnt ligands and FZD receptors (Lee et al. 2015). A different approach that target Wnt-FZD binding is based on using peptides that block the interaction between ligand and receptor. In this regard, Foxy-5, a formylated hexapeptide which mimics Wnt-5a, has been reported to inhibits breast cancer metastasis (Säfhholm et al. 2006; Säfhholm et al. 2008) and is also in clinical trials for metastatic breast, colon and prostate cancer (Murillo-Garzón & Kypta 2017). Taking this into account, specific peptides blocking Wnt-11/FZD8 binding would benefit this study as tools to mimic the effects of *FZD8* silencing using a chemical approach.

The acquisition of invasive and metastatic phenotypes during tumor progression is often provoked by aberrant activation of the embryonic program EMT (Thiery 2002; Nieto et al. 2016). In the last few years, many studies have demonstrated the presence of EMT-like states in PCa, suggesting its involvement in prostate cancer development and metastasis (Grant & Kyprianou 2013; Montanari et al. 2017). E-cadherin loss correlates with prostate tumor progression and Gleason grade (Gravdal et al. 2007) and elevated N-Cadherin has been shown to be a significant predictor of clinical recurrence in prostate cancer patients following radical prostatectomy, as well as an effective therapeutic target in CRPC (Tanaka et al. 2010). Among the EMT inducers, Wnt signaling has been described as one of the crucial activators of this phenotypic change (Lamouille et al. 2014) and importantly, FZD receptors have been extensively related with the EMT program. In ERG positive prostate tumors, FZD4 has been shown to mediate loss of cell adhesion and EMT (Gupta et al. 2010). In addition, FZD2 was found to regulate EMT and metastasis in different cancer types, including breast, colon, hepatocellular carcinoma and lung cancer, where the expression of 75 EMT-associated genes were analyzed after FZD2 overexpression and depletion (Gujral et al. 2014). Moreover, a recent study has shown that activation of noncanonical Wnt signaling through Wnt-5a/FZD2 is associated with increased expression of EMT markers and higher Gleason score (Sandsmark et al. 2017). Furthermore, FZD7 has been shown to promote EMT in cervical cancer where *FZD7* knockdown inhibits invasion, metastasis, and EMT (Deng et al. 2015), and in oesophageal squamous cell carcinoma, where its high expression correlates with poor overall survival (Cao et al. 2017). In addition, FZD8 is involved in proliferation, migration and invasion of renal cell carcinoma, where it was able to induce the EMT program (Yang et al. 2017). Consistent with these studies, our work indicates that FZD8 regulates EMT in prostate cancer since its silencing reduces the expression of mesenchymal markers and increases the expression of epithelial markers, both at the

mRNA and protein levels. Moreover, the involvement of Wnt-11/FZD8 signaling in EMT is also supported by our bioinformatics analysis, which shows a positive correlation between *FZD8* and *WNT11* with mesenchymal markers and a negative correlation with epithelial ones. Notably, the fact that a proportion of 3D spheroids from *FZD8* silenced cells showed no vimentin staining also supports its role in EMT, although further staining experiments are needed to confirm that the organoids lacking vimentin are also negative for FZD8. Of particular interest, while FZD8 seems to regulate EMT favoring the mesenchymal phenotype in both PC-3M and DU145 cells, it is important to note that the EMT markers affected by *FZD8* silencing were not exactly the same; for example, in PC-3M cells, *FZD8* silencing downregulated *SNAI1* but not *SNAI2* expression, while both were downregulated in DU145 cells. These distinctions might be attributed to the different extents of *FZD8* silencing in the cell line, but it is also plausible that it reflects intrinsic differences between these cell lines. Although both are metastatic cell lines (the former to bone and the latter to brain) which do not express AR nor PSA and are androgen independent (Cunningham & You 2015), their different tumor origins make them display strong disparities. The more mesenchymal nature of PC-3M cells becomes evident when looking at the expression of EMT genes, such as *CDH2*, which is not expressed by DU145 cells but is highly expressed by PC-3M cells, and when treating the cells with TGF- $\beta$ , which induces changes in EMT genes in DU145 cells but not in PC-3M cells. In this way, it is possible that due to these distinctions, both cell lines may mediate the EMT process through regulation of different EMT-associated genes. The differences could also be explained by recent studies proposing that the EMT process is based on more dynamic changes characterized by cell fluidity and plasticity, in which different intermediate stages exist with induction of different EMT factors (Nieto et al. 2016). In this regard, it is still possible to consider that FZD8 does not drive a full EMT and that our observations of the different EMT markers affected in both cell lines is due to partial EMT phenotypes in each line.

Given all our observations suggesting that changes driven by FZD8 in the EMT program could be responsible for the observed effects in cell migration and invasion, we propose that FZD8 could therefore be involved in prostate cancer metastasis. Multiple studies during the last decade have shown that aberrant activation of one or more EMT-TFs may make a cell more prone to undergo EMT, and this is a necessary and sufficient condition to drive the invasion–metastasis cascade (Thiery 2002; Nieto et al. 2016). However, the idea of EMT promoting metastasis and invasion was recently challenged by two studies in mouse models of pancreatic (Zheng et al. 2015) and breast cancer (Fischer et al. 2015) in which *TWIST* or *SNAI1* knock-out or miR-200 overexpression

with the consequent suppression of *ZEB1*, respectively, did not affect the incidence of tumor metastasis. Although multiple interpretations were proposed, these new studies highlight the possibility of alternative mechanisms of cancer dissemination and metastasis that do not rely on aberrant overexpression of one or more EMT-TFs to alter cellular adhesion and invasion and drive metastasis (Nieto et al. 2016; Jolly et al. 2017). In this regard, our *in vivo* experiments using the CAM model highlight the importance of *FZD8* in tumor growth and although we haven't performed *in vivo* metastasis assays, recent studies by Lee et al. 2017 showed that downregulation of *FZD8* greatly suppressed the incidence of PCa bone metastasis *in vivo*, which is consistent with our data and support our idea of *FZD8* promoting EMT, subsequently regulating cell migration and invasion and therefore, driving prostate cancer metastasis.

There has been a lot of progress in recent years improving cancer diagnostics, prognostics and treatment, thanks to the combination of already established clinico-pathological features with the state-of-the-art -omics technologies, which together is defined as precision medicine (Shin et al. 2017). In the case of prostate cancer, precision medicine is distant from its application, since general parameters such as PSA, Gleason score or TNM grade are still mainly used to stratify patients. However, the extensive mutational landscape of metastatic CRPC lesions has pointed out the possibility of targeted therapies and precision medicine in CRPC (Mullane & Van Allen 2016). In this respect, the identification of the main players involved in cancer progression could contribute to a better stratification of the disease and consequently, to an improvement in the management of prostate cancer patients, through their use as biomarkers and therapeutic targets. In this project, we described that *FZD8* is involved in prostate cancer cell migration, invasion and EMT as well as it is required in tumor growth. Therefore, we hypothesize that *FZD8* may constitute a useful marker in prostate cancer progression. In fact, we demonstrate here that both *FZD8* and *Wnt-11* protein expression were upregulated in tissues from prostate cancer patients compared to benign tissues, which supports our hypothesis of *FZD8* as a biomarker in prostate cancer. Unfortunately, we could not find a correlation of *FZD8* with Gleason score. This could be explained by the low number of high Gleason samples in the TMA. Our bioinformatics analysis using the MSKCC dataset shows that *FZD8* expression is increased in metastatic patients and correlates with high Gleason score samples as well as with abnormal lymph node metastasis, and that *WNT11* expression positively correlates with patient survival and *FZD8* expression also shows a trend for this. Analysis of a larger cohort of patients is required to provide strong evidence for a role of *FZD8* as a prognostic factor in prostate cancer.

### Chapter 3. Elucidation of the mechanism underlying the effects of FZD8 in prostate cancer pathogenesis

In cancer, distinct pathways have predominant roles in the initiation and progression of EMT through the regulation of changes in morphology and gene expression that convert epithelial cells into motile mesenchymal cells which thereby stimulate tumor progression (Lamouille et al. 2014). The signals that cooperate to regulate EMT include TGF- $\beta$  signaling, integrin cascades, several growth factors that act through receptor tyrosine kinases (RTKs), such as EGF, FGF, HGF and VEGF and also PI3K-AKT and MAPK signaling cascades, together with Wnt, Notch, Hedgehog, interleukin-6 (IL6) and HIF signaling (Wendt et al. 2009; Lamouille et al. 2014). Importantly, TGF- $\beta$  signaling pathway is the best characterized inducer of the EMT process (Lamouille et al. 2014)

In normal prostate and early stages of prostate cancer, TGF- $\beta$  serves as a tumor suppressor by inducing cell cycle arrest and apoptosis. However, in advanced prostate cancer, TGF- $\beta$  acts as a tumor promoter driving tumor invasion and metastasis (Jones et al. 2009). Indeed, elevated TGF- $\beta$  levels in patient serum provide a significant prognostic value for highly aggressive metastatic disease and poor patient prognosis (Shariat et al. 2001). Moreover, dysfunctional TGF- $\beta$  receptor signaling accelerates prostate cancer progression in a mouse model via EMT and cytoskeleton changes in the tumor microenvironment (Pu et al. 2009). It has also been reported that elevated TGF- $\beta$  ligand levels correlate with increasing tumor grade in prostate cancer (Grant & Kyprianou 2013) and that TGF- $\beta$ 1 is able to induce EMT in prostate tumor epithelial cells and in mouse models, upregulating matrix metalloproteinase-9 (MMP-9) and promoting tumor invasion (Cao & Kyprianou 2015). Since TGF- $\beta$  is able to stimulate growth by its pleiotropic activities on both the cancer cell but also on the non-malignant stromal cell types of the tumor, it has also been shown that, particularly in prostate cancer, carcinoma-associated fibroblasts (CAF) derived from prostate tumors can stimulate tumor progression of non-transformed prostate epithelial cells (Jones et al. 2009).

According to the well reported role of TGF- $\beta$  in regulating EMT and its crosstalk with Wnt signaling pathway (Guo & Wang 2009; Attisano & Wrana 2013), in this thesis work, we demonstrate that Wnt-11/FZD8 axis also regulates TGF- $\beta$  signaling. Our analysis show that FZD8 is required for TGF- $\beta$ -dependent transcription and Smad phosphorylation as well as for the expression of TGF- $\beta$  target genes. In addition, we found that FZD8 also regulates TGF- $\beta$ -dependent EMT gene expression as well as TGF- $\beta$ -dependent cell invasion. The fact that *FZD8* silencing does not completely block the pathway may suggest that although FZD8 is involved in its regulation, it is not the only

factor and that TGF- $\beta$  signaling in prostate cancer cells is also regulated by other signals. Importantly, our results are consistent with the reported crosstalk between Wnt and TGF- $\beta$  signaling (Guo & Wang 2009; Attisano & Wrana 2013; Carstens et al. 2014), as well as with studies from Spanjer et al., who demonstrated a role for FZD8 in TGF- $\beta$ -induced profibrotic signaling through Wnt-5a, regulating collagen-a1, fibronectin, versican,  $\alpha$ -smooth muscle actin, and connective tissue growth factor (A. I. R. Spanjer et al. 2016). Our data also show that a dominant negative form of ATF2 is required for TGF- $\beta$  dependent transcription, as well as for the regulation of a subset of TGF- $\beta$ -dependent EMT genes. Although different reports have shown that Wnt-TGF- $\beta$  crosstalk can be mediated by the interaction between Smad and ATF2 or other members of the AP-1 family of transcription factors (Derynck et al. 1998; Sano et al. 1999; Hanafusa et al. 1999; Massagué 2000), we were unable to detect a stable complex between Smad3 and ATF2 by co-immunoprecipitation. This might be explained by the specific conditions used in the immunoprecipitation. However, it would be also plausible that the crosstalk between both pathways involves other Smads, rather than Smad3 or other AP-1 transcription factors, such as JUN, FOS, or MAF, highlighting the requirement of further studies to clarify this possible interaction.

However, since both Wnt and TGF- $\beta$  are secreted factors that acts through binding to specific cell surface receptors, it is still possible that FZD8 regulation of TGF- $\beta$  signaling may take place at the cell membrane. In this thesis work, we found that FZD receptors can interact with TGF $\beta$ Rs in the cell membrane and that this interaction is mediated through the FZD8-CRD and the extracellular domain of TGF $\beta$ RI. Moreover, we also found that this interaction was affected by exogenous TGF- $\beta$ , since its addition reduced the binding of TGF $\beta$ RII to FZD8 and not TGF $\beta$ RI binding, supporting our observations of TGF $\beta$ RI mediating the interaction. Although other proteins have been found to interact with FZD receptors, including the recent described interaction with *Clostridium difficile* toxin B (Chen et al. 2018), to our knowledge, this is the first work showing that FZD receptors can interact with TGF $\beta$ Rs. The molecular events that take place subsequent to TGF- $\beta$  binding are complex: in the absence of ligand, TGF $\beta$ RI and TGF $\beta$ RII may occur as monomers, homodimers and heterodimers. TGF $\beta$ RII homodimers and heterodimers are stabilized by contacts between the receptor cytoplasmic domains, whereas TGF $\beta$ RI homodimers do not require the TGF $\beta$ RI cytoplasmic domain. TGF- $\beta$  binding to TGF $\beta$ RII homodimers, leads to the recruitment of TGF $\beta$ RI homodimers and the formation of a heterohexamer complex of TGF- $\beta$ , TGF $\beta$ RI and TGF $\beta$ RII dimers. TGF $\beta$ RII then phosphorylates and activates TGF $\beta$ RI, which

propagates the signal (Shi & Massagué 2003; Massagué 2012). Our results suggest that being part of this complex, FZD8 plays a role in signal transduction subsequent to TGF $\beta$ RII phosphorylation and activation of TGF $\beta$ RI, which enables the regulation of TGF- $\beta$  signaling. However, since our experiments used transfected receptors, the exact events that take place in the FZD8-TGF $\beta$ R complex will require detailed study of the endogenous receptors. Our results also show that Wnt-11 can still bind FZD8 while the latter is bound to TGF $\beta$ RI, suggesting that although both Wnt and TGF $\beta$ RI bind to FZD8 through its CRD, different residues may be involved in the interaction. The novel model of Wnt-FZD signalosome, which shows that FZD receptors can dimerize through their CRD (DeBruine et al. 2017), increases the complexity of the interaction between FZD8 and TGF $\beta$ RI. In this regard, elucidating the regions involved in FZD8 binding to TGF $\beta$ RI, as well as the resolution of the crystal structure of the complex would contribute to a better understanding of Wnt-FZD-TGF $\beta$ RI crosstalk in prostate cancer and therefore, to design better approaches to target this pathway in disease. Importantly, extrapolation of these findings to different systems would allow us to determine whether this interaction is specific of prostate cancer or on the contrary, is a common event that would benefit the treatment of other types of cancer and other diseases, such as fibrosis.

In summary, we propose a model in which FZD8 can interact with Wnt-11 and TGF $\beta$ RI, integrating both Wnt and TGF- $\beta$  signaling pathways and thereby promoting EMT, cell migration and invasion, leading to prostate cancer metastasis. Hence, we believe that the role of FZD8 here described supports the potential of using this receptor as a therapeutic target in metastatic prostate cancer to block aberrant activation of both Wnt and TGF- $\beta$  signaling pathways.







---

# CONCLUSIONS

---



In summary, the results obtained throughout this thesis confirm our hypothesis and demonstrate that the identification and characterization of the receptors that mediate Wnt-11 migration and invasion in prostate cancer cells could represent a potential therapeutic target to improve the treatment of prostate cancer patients.

The results obtained lead to the following conclusions:

- 1) FZD8 is highly expressed in more aggressive prostate cancer cell lines as well as in prostate cancer compared to benign tissues.
- 2) FZD8 binds to Wnt-11 and acts as the main Wnt-11 receptor in metastatic prostate cancer, signaling through a noncanonical pathway.
- 3) FZD8 is required for the main hallmarks of prostate cancer progression such as cell migration, invasion, invasion in organotypic 3D cultures, regulation of EMT and tumor growth *in vivo*.
- 4) FZD8 and Wnt-11 expression correlate with prostate cancer progression.
- 5) FZD8 integrates Wnt and TGF- $\beta$  signaling pathways through its association with TGF $\beta$ RI, which enables the subsequent regulation of TGF- $\beta$  signaling.
- 6) FZD8 may constitute a therapeutic target in prostate cancer *per se* or in combination with TGF- $\beta$  inhibitors.





---

# **BIBLIOGRAPHY**

---



- Aaron, L. et al., 2016. Review of Prostate Anatomy and Embryology and the Etiology BPH. *Urol Clin North Am*, 43(3), pp.279–288.
- Abate-Shen, C. & Shen, M.M., 2000. Molecular genetics of prostate cancer. *Genes & Development*, (732), pp.2410–2434.
- Abdul-Ghani, M. et al., 2011. Wnt11 promotes cardiomyocyte development by caspase-mediated suppression of canonical Wnt signals. *Molecular and cellular biology*, 31(1), pp.163–178.
- Abeshouse, A. et al., 2015. The Molecular Taxonomy of Primary Prostate Cancer. *Cell*, 163(4), pp.1011–1025.
- Acebron, S.P. et al., 2014. Mitotic Wnt Signaling Promotes Protein Stabilization and Regulates Cell Size. *Molecular Cell*, 54(4), pp.663–674.
- Acebron, S.P. & Niehrs, C., 2016.  $\beta$ -Catenin-Independent Roles of Wnt/LRP6 Signaling. *Trends in Cell Biology*, pp.1–12.
- Albers, J. et al., 2013. Canonical Wnt signaling inhibits osteoclastogenesis independent of osteoprotegerin. *Journal of Cell Biology*, 200(4), pp.537–549.
- Ali, T.Z. & Epstein, J.I., 2007. Basal Cell Carcinoma of the Prostate: A Clinicopathologic Study of 29 Cases. *The American Journal of Surgical Pathology*, 31(5), pp.697–705.
- American Urological Association, 2017. Prostate. Normal histology and anatomic structures.
- van Amerongen, R., 2012. Alternative Wnt pathways and receptors. *Cold spring Harb Perspect Biol* 2012, 4(10).
- Anastas, J.N. & Moon, R.T., 2013. WNT signalling pathways as therapeutic targets in cancer. *Nature reviews. Cancer*, 13(1), pp.11–26.
- Angulo, J.C. et al., 2010. Primary transitional cell carcinoma of the prostate: a male disease with dismal prognosis despite cisplatin-based systemic chemotherapy. *Journal of Men's Health*, 7(1), pp.64–72.
- Attard, G. et al., 2016. Prostate cancer. *The Lancet*, 387(10013), pp.70–82.
- Attisano, L. & Wrana, J.L., 2013. Signal integration in TGF- $\beta$ , WNT, and Hippo pathways. *F1000prime reports*, 5(June 2013), p.17.
- Azimian-Zavareh, V. et al., 2018. Wnt11 alters integrin and cadherin expression by ovarian cancer spheroids and inhibits tumorigenesis and metastasis. *Experimental Cell Research*.
- Azzolin, L. et al., 2014. YAP/TAZ incorporation in the  $\beta$ -catenin destruction complex orchestrates the Wnt response. *Cell*, 158(1), pp.157–170.
- Bai, Y. et al., 2014. Ror2 receptor mediates wnt11 ligand signaling and affects convergence and extension movements in zebrafish. *Journal of Biological Chemistry*, 289(30), pp.20664–20676.
- Banyard, J. & Bielenberg, D.R., 2015. The Role of EMT and MET in Cancer Dissemination. *Connect Tissue Res*, 56(5), pp.403–413.

- Bartis, D. et al., 2013. Down-regulation of canonical and up-regulation of non-canonical Wnt signalling in the carcinogenic process of squamous cell lung carcinoma. *PLoS one*, 8(3), p.e57393.
- Benson, M.D. et al., 2017. A targeted approach to genome-wide studies reveals new genetic associations with central corneal thickness. *Molecular vision*, 23(December), pp.952–962.
- Bhanot, P. et al., 1996. A new member of the frizzled family from *Drosophila* functions as a Wingless receptor. *Nature*, 382(6588), pp.225–230.
- Bhavsar, A. & Verma, S., 2014. Anatomic Imaging of the Prostate. *BioMed Research International*, 2014.
- Bonkhoff, H. & Berges, R., 2009. The Evolving Role of Oestrogens and Their Receptors in the Development and Progression of Prostate Cancer. *European Urology*, 55(3), pp.533–542.
- Borcherding, N. et al., 2014. ROR1, an embryonic protein with an emerging role in cancer biology. *Protein and Cell*, 5(7), pp.496–502.
- Bovolenta, P. et al., 2008. Beyond Wnt inhibition: new functions of secreted Frizzled-related proteins in development and disease. *Journal of cell science*, 121(Pt 6), pp.737–46.
- Boyd, J.L. et al., 2015. Human-chimpanzee differences in a FZD8 enhancer alter cell-cycle dynamics in the developing neocortex. *Current Biology*, 25(6), pp.772–779.
- Brase, J.C. et al., 2011. TMPRSS2-ERG -specific transcriptional modulation is associated with prostate cancer biomarkers and TGF- $\beta$  signaling. *BMC cancer*, 11, p.507.
- Bravo, D.T. et al., 2013. Frizzled-8 receptor is activated by the Wnt-2 ligand in non-small cell lung cancer. *BMC Cancer*, 13(1), p.1.
- Cao, T.T. et al., 2017. FZD7 is a novel prognostic marker and promotes tumor metastasis via WNT and EMT signaling pathways in esophageal squamous cell carcinoma. , pp.65957–65968.
- Cao, Z. & Kyprianou, N., 2015. Mechanisms navigating the TGF- $\beta$  pathway in prostate cancer. *Asian Journal of Urology*, 2(1), pp.11–18.
- Capurro, M. et al., 2014. Glypican-3 binds to Frizzled and plays a direct role in the stimulation of canonical Wnt signaling. *Journal of cell science*, 127(Pt 7), pp.1565–75.
- Carmon, K.S. et al., 2012. LGR5 interacts and cointernalizes with Wnt receptors to modulate Wnt/ $\beta$ -catenin signaling. *Molecular and cellular biology*, 32(11), pp.2054–64.
- Carstens, J.L. et al., 2014. FGFR1-WNT-TGF- $\beta$  signaling in prostate cancer mouse models recapitulates human reactive stroma. *Cancer research*, 1(2), pp.609–620.
- Catalona, W.J., 2014. History of the discovery and clinical translation of prostate-specific antigen. *Asian Journal of Urology*, 1(1), pp.12–14.
- Cavodeassi, F. et al., 2005. Early stages of zebrafish eye formation require the



- coordinated activity of Wnt11, Fz5, and the Wnt/ $\beta$ -catenin pathway. *Neuron*, 47(1), pp.43–56.
- Center, M.M. et al., 2012. International Variation in Prostate Cancer Incidence and Mortality Rates. , 61, pp.1079–1092.
- Cerami, E. et al., 2012. The cBio Cancer Genomics Portal: An Open Platform for Exploring Multidimensional Cancer Genomics Data. *Cancer discovery*, 2(5), pp.401–404.
- Chakravarthi, B.V.S.K. et al., 2018. Wnt receptor Frizzled 8 is a target of ERG in prostate cancer. , (May).
- Chandrasekar, T. et al., 2015. Mechanisms of resistance in castration-resistant prostate cancer ( CRPC ). *Transl Androl Urol*, 4(3), pp.365–380.
- Chen, B. et al., 2009. Small molecule-mediated disruption of Wnt-dependent signaling in tissue regeneration and cancer. *Nat Chem Biol*, 5(2), pp.100–107.
- Chen, P. et al., 2018. Structural basis for recognition of frizzled proteins by Clostridium difficile toxin B. *Science (New York, N.Y.)*, 360(6389), pp.664–669.
- Choi, M.Y. et al., 2015. Pre-clinical specificity and safety of UC-961, a first-in-class monoclonal antibody targeting ROR1. *Clin Lymphoma Myeloma Leuk*, 15(0), pp.1–7.
- Clevers, H., 2006. Wnt/ $\beta$ -Catenin Signaling in Development and Disease. *Cell*, 127(3), pp.469–480.
- Coudreuse, D. & Korswagen, H.C., 2007. The making of Wnt: new insights into Wnt maturation, sorting and secretion. *Development (Cambridge, England)*, 134(1), pp.3–12.
- Cruciat, C.M. & Niehrs, C., 2013. Secreted and Transmembrane Wnt Inhibitors and Activators. *Cold Spring Harbor perspectives in biology*, 5(3), pp.1–26.
- Cunningham, D. & You, Z., 2015. In vitro and in vivo model systems used in prostate cancer research. *J Biol Methods*, 2(1), pp.1–28.
- Debruine, Z.J. et al., 2017. Wnt5a promotes Frizzled-4 signalosome assembly by stabilizing cysteine-rich domain dimerization. *Genes & Dev*, 31(9), pp.916–926.
- DeBruine, Z.J., Xu, H.E. & Melcher, K., 2017. Assembly and architecture of the Wnt/ $\beta$ -catenin signalosome at the membrane. *British Journal of Pharmacology*, 174(24), pp.4564–4574.
- Deng, B. et al., 2015. Down-regulation of Frizzled-7 expression inhibits migration, invasion, and epithelial-mesenchymal transition of cervical cancer cell lines. *Medical oncology (Northwood, London, England)*, 32(4), p.102.
- Dennler, S. et al., 1998. Direct binding of Smad3 and Smad4 to critical TGF  $\beta$  - inducible elements in the promoter of human plasminogen activator inhibitor-type 1 gene. , 17(11), pp.3091–3100.
- Derynck, R., Zhang, Y. & Feng, X.-H., 1998. Smad3 and Smad4 cooperate with c-Jun/c-Fos to mediate TGF- $\beta$ -induced transcription. *Nature*, 394(6696), pp.909–913.

- Deryugina, E.I. & Quigley, J.P., 2009. Chick embryo chorioallantoic membrane model systems to study and visualize human tumor cell metastasis. *Histochem Cell Biol*, 130(6), pp.1119–1130.
- Dijksterhuis, J.P., Petersen, J. & Schulte, G., 2014. WNT/Frizzled signalling: receptor-ligand selectivity with focus on FZD-G protein signalling and its physiological relevance: IUPHAR Review 3. *British journal of pharmacology*, 171(5), pp.1195–209.
- Djiane, A. et al., 2000. Role of frizzled 7 in the regulation of convergent extension movements during gastrulation in *Xenopus laevis*. *Development*, 127(14), pp.3091–100.
- Dwyer, M. a et al., 2010. WNT11 expression is induced by estrogen-related receptor alpha and beta-catenin and acts in an autocrine manner to increase cancer cell migration. *Cancer research*, 70(22), pp.9298–308.
- Eferl, R. & Wagner, E.F., 2003. AP-1: a double-edged sword in tumorigenesis. *Nature reviews. Cancer*, 3(11), pp.859–68.
- El-Khoueiry, A.B. et al., 2013. A phase I first-in-human study of PRI-724 in patients with advanced solid tumors. *J Clin Oncol*, 31.
- Emami, K.H. et al., 2004. A small molecule inhibitor of  $\beta$ -catenin/CREB-binding protein transcription. *Proceedings of the National Academy of Sciences*, 101(34), pp.12682–12687.
- Feldman, B.J. & Feldman, D., 2001. The development of androgen-independent prostate cancer. *Nat Rev Cancer*, 1(1), pp.34–45.
- Feng, X. & Derynck, R., 1996. Ligand-independent activation of transforming growth factor (TGF) beta signaling pathways by heteromeric cytoplasmic domains of TGF-beta receptors. *J Biol Chem*, 271(22), pp.13123–9.
- Fischer, K.R. et al., 2015. EMT is not required for lung metastasis but contributes to chemoresistance. *Nature*, 527(7579), pp.472–476.
- Flaherty, M.P. et al., 2008. Noncanonical Wnt11 signaling is sufficient to induce cardiomyogenic differentiation in unfractionated bone marrow mononuclear cells. *Circulation*, 117(17), pp.2241–2252.
- Fu, X. et al., 2016. Long noncoding RNA AK126698 inhibits proliferation and migration of non-small cell lung cancer cells by targeting Frizzled-8 and suppressing Wnt/ $\beta$ -catenin signaling pathway. *OncoTargets and therapy*, 9, pp.3815–27.
- Fukukawa, C. et al., 2008. Radioimmunotherapy of human synovial sarcoma using a monoclonal antibody against FZD10. *Cancer Science*, 99(2), pp.432–440.
- Gao, J. et al., 2013. Integrative analysis of complex cancer genomics and clinical profiles using the cBioPortal. *Sci Signal*, 6(269), pp.1689–1699.
- Geetha-Loganathan, P. et al., 2014. Avian facial morphogenesis is regulated by c-Jun N-terminal Kinase/Planar Cell Polarity (JNK/PCP) wingless-related (WNT) signaling. *Journal of Biological Chemistry*, 289(35), pp.24153–24167.
- Ghoshal, A. et al., 2015. Targeting Wnt Canonical Signaling by Recombinant sFRP1 Bound Luminescent Au-Nanocluster Embedded Nanoparticles in Cancer

- Theranostics. *ACS Biomaterial Science and Engineering*, 1(12), pp.1256–1266.
- Gleason, D., 1992. Histologic Grading of Prostate Cancer : A Perspective. *Human Pathology*, 23(3), pp.273–279.
- Globocan, 2012. <http://globocan.iarc.fr/old/FactSheets/cancers/prostate-new.asp>.
- Gnanasambandan, S.R.H. and K., 2013. Structure and Activation of MuSK, a Receptor Tyrosine Kinase Central to Neuromuscular Junction Formation. *Biochim Biophys Acta*, 1834(10), pp.2166–2169.
- Gonsalves, F.C. et al., 2011. An RNAi-based chemical genetic screen identifies three small-molecule inhibitors of the Wnt / wingless signaling pathway. *Proceedings of the National Academy of Sciences of the United States of America*, 108(15), pp.5954–5963.
- Gordetsky, J. & Epstein, J., 2016. Grading of prostatic adenocarcinoma : current state and prognostic implications. *Diagnostic Pathology*, 11(25), pp.2–9.
- Grandy, D. et al., 2009. Discovery and characterization of a small molecule inhibitor of the PDZ domain of dishevelled. *Journal of Biological Chemistry*, 284(24), pp.16256–16263.
- Grant, C.M. & Kyprianou, N., 2013. Epithelial mesenchymal transition (EMT) in prostate growth and tumor progression. *Translational andrology and urology*, 2(3), pp.202–211.
- Gravdal, K. et al., 2007. A switch from E-cadherin to N-cadherin expression indicates epithelial to mesenchymal transition and is of strong and independent importance for the progress of prostate cancer. *Clinical Cancer Research*, 13(23), pp.7003–7011.
- Green, J. & Nusse, R., 2014. The Role of Ryk and Ror Receptor Tyrosine Kinases in Wnt Signal Transduction. *Cold Spring Harbor Perspectives in Biology*, 6(2).
- Greenburg, G. & Hay, E.D., 1982. Epithelia suspended in collagen gels can lose polarity and express characteristics of migrating mesenchymal cells. *Journal of Cell Biology*, 95(1), pp.333–339.
- Gregory, M.A. et al., 2010. Wnt/Ca<sup>2+</sup>/NFAT signaling maintains survival of Ph<sup>+</sup> leukemia cells upon inhibition of Bcr-Abl. *Cancer Cell*, 18(1), pp.74–87.
- Grumolato, L. et al., 2010. Canonical and noncanonical Wnts use a common mechanism to activate completely unrelated coreceptors. *Genes & development*, 24(22), pp.2517–30.
- Gujral, T.S. et al., 2014. A Noncanonical Frizzled2 Pathway Regulates Epithelial-Mesenchymal Transition and Metastasis. *Cell*, 159(4), pp.844–856.
- Guo, X. & Wang, X.-F., 2009. Signaling cross-talk between TGF-beta/BMP and other pathways. *Cell research*, 19(1), pp.71–88.
- Gupta, S. et al., 2010. FZD4 as a mediator of ERG oncogene-induced WNT signaling and epithelial-to-mesenchymal transition in human prostate cancer cells. *Cancer Research*, 70(17), pp.6735–6745.
- Gurney, A. et al., 2012. Wnt pathway inhibition via the targeting of Frizzled receptors

- results in decreased growth and tumorigenicity of human tumors. *Proceedings of the National Academy of Sciences of the United States of America*, 109(29), pp.11717–22.
- Haikarainen, T., Krauss, S. & Lehtio, L., 2014. Tankyrases: structure, function and therapeutic implications in cancer. *Current pharmaceutical design*, 20(41), pp.6472–88.
- Hanafusa, H. et al., 1999. (smad-atf2) Involvement of the p38 Mitogen-activated Protein Kinase Pathway in Transforming Growth Factor- $\beta$ -induced Gene Expression \*. *The Journal of biological chemistry*, 274(38), pp.27161–27167.
- Hanahan, D. & Weinberg, R.A., 2011. Hallmarks of cancer: The next generation. *Cell*, 144(5), pp.646–674.
- Hanahan, D. & Weinberg, R.A., 2000. The hallmarks of cancer. *Cell*, 100(1), pp.57–70.
- Hanaki, H. et al., 2012. An Anti-Wnt5a Antibody Suppresses Metastasis of Gastric Cancer Cells In Vivo by Inhibiting Receptor-Mediated Endocytosis. *Molecular Cancer Therapeutics*, 11(2), pp.298–307.
- Hao, H.-X. et al., 2012. ZNRF3 promotes Wnt receptor turnover in an R-spondin-sensitive manner. *Nature*, 485(7397), pp.195–200.
- Hao, H.X., Jiang, X. & Cong, F., 2016. Control of Wnt receptor turnover by R-spondin-ZNRF3/RNF43 signaling module and its dysregulation in cancer. *Cancers*, 8(6), pp.1–12.
- Härma, V. et al., 2010. A Comprehensive Panel of Three-Dimensional Models for Studies of Prostate Cancer Growth , Invasion and Drug Responses. *PLoS ONE*, 5(5).
- Härma, V. et al., 2014. Quantification of Dynamic Morphological Drug Responses in 3D Organotypic Cell Cultures by Automated Image Analysis. *PLoS ONE*, 9(5).
- Härmä, V. et al., 2010. A Comprehensive Panel of Three-Dimensional Models for Studies of Prostate Cancer Growth , Invasion and Drug Responses. *PloS one*, 5(5).
- Harnden, P. et al., 2007. Should the Gleason grading system for prostate cancer be modified to account for high-grade tertiary components? A systematic review and meta-analysis. *Lancet Oncology*, 8(5), pp.411–419.
- Hatakeyama, J. et al., 2014. Vangl1 and Vangl2: planar cell polarity components with a developing role in cancer. *Society for Endocrinology*, 21(June), pp.1–30.
- Hayes, M. et al., 2013. Ptk7 promotes non-canonical Wnt/PCP-mediated morphogenesis and inhibits Wnt/ -catenin-dependent cell fate decisions during vertebrate development. *Development*, 140(10), pp.2245–2245.
- Hayward, S.W. & Cunha, G.R., 2000. The prostate: development and physiology. *Radiologic clinics of North America*, 38(1), pp.1–14.
- He, Z. et al., 2011. Transduction of Wnt11 promotes mesenchymal stem cell transdifferentiation into cardiac phenotypes. *wnt immuno. Stem cells and development*, 20(10), pp.1771–8.

- Heisenberg, C.P. et al., 2000. Silberblick/Wnt11 mediates convergent extension movements during zebrafish gastrulation. *Nature*, 405(6782), pp.76–81.
- Heldin, C.H. & Moustakas, A., 2016. Signaling Receptors for TGF-beta Family Members. *Cold Spring Harb Perspect Biol*, 8(8), pp.1–34.
- Hojjat-Farsangi, M. et al., 2013. Inhibition of the Receptor Tyrosine Kinase ROR1 by Anti-ROR1 Monoclonal Antibodies and siRNA Induced Apoptosis of Melanoma Cells. *PLoS ONE*, 8(4), pp.19–20.
- Huang, H. & Klein, P.S., 2004. Protein family review The Frizzled family : receptors for multiple signal transduction pathways. *Genome biology*, 5(7), pp.1–7.
- Humphrey, P.A., 2012. Histological variants of prostatic carcinoma and their significance. *Histopathology*, 60, pp.59–74.
- Humphrey, P.A. et al., 2016. The 2016 WHO Classification of Tumours of the Urinary System and Male Genital Organs—Part B: Prostate and Bladder Tumours. *European Urology*, 70(1), pp.106–119.
- Lo Iacono, M. et al., 2015. ATF2 contributes to cisplatin resistance in non-small cell lung cancer and celastrol induces cisplatin resensitization through inhibition of JNK/ATF2 pathway. *International Journal of Cancer*, 136(11), pp.2598–2609.
- Janda, C.Y. et al., 2012. Structural basis of Wnt recognition by Frizzled. *Science (New York, N. Y.)*, 337(6090), pp.59–64.
- Janssens, N. et al., 2004. Alteration of frizzled expression in renal cell carcinoma. *Tumor Biology*, 25(4), pp.161–171.
- Jiang, Q. et al., 2015. MicroRNA-100 suppresses the migration and invasion of breast cancer cells by targeting FZD-8 and inhibiting Wnt/??-catenin signaling pathway. *Tumor Biology*.
- Jiang, W.G. et al., 2015. Tissue invasion and metastasis: Molecular, biological and clinical perspectives. *Seminars in Cancer Biology*, 35, pp.S244–S275.
- Jolly, M.K. et al., 2017. EMT and MET: necessary or permissive for metastasis? *Molecular Oncology*, 11(7), pp.755–769.
- Jones, E., Pu, H. & Kyprianou, N., 2009. Targeting TGF- b in prostate cancer : therapeutic possibilities during tumor progression. *Expert Opin. Ther. Targets*, 13(2), pp.227–234.
- Karen E. Livermore, Munkley, J. & Elliott, D.J., 2016. Androgen receptor and prostate cancer. *AIMS Molecular Science*, 3(2), pp.280–299.
- Kawano, Y. & Kypta, R., 2003. Secreted antagonists of the Wnt signalling pathway. *Journal of cell science*, 116(Pt 13), pp.2627–34.
- Khan, N.I., Bradstock, K.F. & Bendall, L.J., 2007. Activation of Wnt/ $\beta$ -catenin pathway mediates growth and survival in B-cell progenitor acute lymphoblastic leukaemia. *British Journal of Haematology*, 138(3), pp.338–348.
- Kim, G., Her, J. & Han, J., 2008. Ryk cooperates with Frizzled 7 to promote Wnt11-mediated endocytosis and is essential for *Xenopus laevis* convergent extension movements. *The Journal of cell biology*, 182(6), pp.1073–82.

- Kirby, R.S. et al., 2004. Benign Prostatic Hyperplasia. *Book*.
- Klaus, A. & Birchmeier, W., 2008. Wnt signalling and its impact on development and cancer. *Nature reviews. Cancer*, 8(5), pp.387–398.
- Kohn AD, M.R., 2005. Wnt and calcium signaling: beta-catenin-independent pathways. *Cell Calcium*, 38(3–4), pp.439–446.
- Kolb, R. et al., 2016. ROR1 is an Intriguing Target for Cancer Therapy ROR1-Based Targeted Therapies ROR1-Mediated Oncogenic Signalling. *Molecular Enzymology and Drug Targets*, 2, pp.1–3.
- Komiya, Y. & Habas, R., 2008. Wnt signal transduction pathways. *Organogenesis*, 4(2), pp.68–75.
- Korinek, V. et al., 1997. Constitutive Transcriptional Activation by a  $\beta$ -Catenin–Tcf Complex in APC<sup>-/-</sup> Colon Carcinoma. *Science*, 275(5307), pp.1784–7.
- Kramer, N. et al., 2017. Autocrine WNT2 signaling in fibroblasts promotes colorectal cancer progression. *Oncogene*, 36(39), pp.5460–5472.
- Kubiczkova, L. et al., 2012. TGF- $\beta$  – an excellent servant but a bad master. *Journal of translational medicine*, 10(183), pp.1–24.
- Kumar, V.L. & Majumder, P.K., 1995. Prostate gland: Structure, functions and regulation. *International Urology and Nephrology*, 27(3), pp.231–243.
- Kumawat, K. et al., 2013. Noncanonical WNT-5A signaling regulates TGF- $\beta$ -induced extracellular matrix production by airway smooth muscle cells. *FASEB journal : official publication of the Federation of American Societies for Experimental Biology*, 27(4), pp.1631–43.
- Lako, M. et al., 1998. Isolation, characterisation and embryonic expression of WNT11, a gene which maps to 11q13.5 and has possible roles in the development of skeleton, kidney and lung. *Gene*, 219(1–2), pp.101–10.
- Lamouille, S., Xu, J. & Derynck, R., 2014. Molecular mechanisms of epithelial-mesenchymal transition. *Nature reviews. Molecular cell biology*, 15(3), pp.178–96.
- Le, P., McDermott, J.D. & Jimeno, A., 2015. Targeting the Wnt pathway in human cancers: therapeutic targeting with a focus on OMP-54F28. *Pharmacol Ther*, 0, pp.1–11.
- Lee, E.Y.H.P. & Muller, W.J., 2010. Oncogenes and tumor suppressor genes. *Cold Spring Harbor perspectives in biology*, 2(10), p.a003236.
- Lee, H.J. et al., 2015. Structure-based discovery of novel small molecule Wnt signaling inhibitors by targeting the cysteine rich domain of Frizzled. *Journal of Biological Chemistry*, p.jbc.M115.673202.
- Lee, J.M. et al., 2006. The epithelial-mesenchymal transition: New insights in signaling, development, and disease. *Journal of Cell Biology*, 172(7), pp.973–981.
- Li, C. et al., 2008. Ror2 modulates the canonical Wnt signaling in lung epithelial cells through cooperation with Fzd2. *BMC molecular biology*, 9, p.11.
- Li, F. et al., 2007. Beyond tumorigenesis: Cancer stem cells in metastasis. *Cell*

- Research*, 17(1), pp.3–14.
- Li, Q. et al., 2016. ATF2 translation is induced under chemotherapeutic drug-mediated cellular stress via an IRES-dependent mechanism in human hepatic cancer Bel7402 cells. *Oncology Letters*, 12(6), pp.4795–4802.
- Li, Q. et al., 2017. FZD8, a target of p53, promotes bone metastasis in prostate cancer by activating canonical Wnt/ $\beta$ -catenin signaling. *Cancer Letters*, 402, pp.166–176.
- Li, X. et al., 2008. Prostate tumor progression is mediated by a paracrine TGF- $\beta$ /Wnt3a signaling axis. *Oncogene*, 27(56), pp.7118–7130.
- Li, Y. et al., 2008. Sfrp5 coordinates foregut specification and morphogenesis by antagonizing both canonical and noncanonical Wnt11 signaling. *Genes and Development*, 22(21), pp.3050–3063.
- Liu, J. et al., 2013. Targeting Wnt-driven cancer through the inhibition of Porcupine by LGK974. *Proceedings of the National Academy of Sciences*, 110(50), pp.20224–20229.
- Logan, C.Y. & Nusse, R., 2004. The Wnt signaling pathway in development and disease. *Annu. Rev. Cell Dev. Biol*, 20, pp.781–810.
- Lokman, N.A. et al., 2012. Chick chorioallantoic membrane (CAM) assay as an in vivo model to study the effect of newly identified molecules on ovarian cancer invasion and metastasis. *International Journal of Molecular Sciences*, 13(8), pp.9959–9970.
- Lopez-bergami, P., 2011. Emerging roles of ATF2 and the dynamic AP1 network in cancer. , 10(1), pp.65–76.
- Lowsley, O., 1912. The development of the human prostate gland with reference to the development of other structures at the neck of the urinary bladder. *Am J Anat* 1912 ; 13 : 299-346. , p.13 : 299-346.
- Luga, V. et al., 2012. Exosomes mediate stromal mobilization of autocrine Wnt-PCP signaling in breast cancer cell migration. *Cell*, 151(7), pp.1542–1556.
- MacDonald, B.T & He, X., 2012. Frizzled and LRP5/6 Receptors for Wnt/ $\beta$ -Catenin Signaling. *Cold spring Harb Perspect Biol*, 4(12).
- MacDonald, B.T., Tamai, K. & He, X., 2009. Wnt/ $\beta$ -catenin signaling: components, mechanisms, and diseases. *Developmental cell*, 17(1), pp.9–26.
- Madan, B. et al., 2016. Wnt addiction of genetically defined cancers reversed by PORCN inhibition. *Oncogene*, 35(August 2015), pp.2197–2207.
- Majumdar, A. et al., 2003. Wnt11 and Ret/Gdnf pathways cooperate in regulating ureteric branching during metanephric kidney development. *Development (Cambridge, England)*, 130, pp.3175–3185.
- Malik, R.D. et al., 2011. Squamous Cell Carcinoma of the Prostate. *Reviews iç*, 13, pp.56–60.
- Malinauskas, T. & Jones, E.Y., 2014. Extracellular modulators of Wnt signalling. *Current Opinion in Structural Biology*, 29, pp.77–84.

- Mancini, M. & Toker, A., 2009. NFAT proteins: emerging roles in cancer progression. *Nature reviews. Cancer*, 9(11), pp.810–20.
- Martin, T.A. et al., 2000. Cancer Invasion and Metastasis: Molecular and Cellular perspective. *Madame Curie Bioscience Database [Internet]. Landes Bioscience, Austin.*
- Martin, T.A. et al., 2013. Cancer Invasion and Metastasis: Molecular and Cellular Perspective. *Landes Bioscience.*
- Martinez, S. et al., 2015. The PTK7 and ROR2 protein receptors interact in the vertebrate WNT/Planar cell polarity (PCP) pathway. *Journal of Biological Chemistry*, 290(51), pp.30562–30572.
- Masiakowski, P. & Carroll, R.D., 1992. A novel family of cell surface receptors with tyrosine kinase-like domain. *Journal of Biological Chemistry*, 267(36), pp.26181–26190.
- Massagué, J., 2000. How cells read TGF-beta signals. *Nature reviews. Molecular cell biology*, 1(3), pp.169–178.
- Massagué, J., 2012. TGFβ signalling in context. *Nat Rev Mol Cell Biol*, 13(10), pp.616–630.
- Massagué, J., Seoane, J. & Wotton, D., 2005. Smad transcription factors. , pp.2783–2810.
- Maye, P. et al., 2004. Multiple Mechanisms for Wnt11-mediated Repression of the Canonical Wnt Signaling Pathway. *J. Biol. Chem.*, 279(23), pp.24659–24665.
- McNeal, J.E., 1981. The zonal anatomy of the prostate. *The Prostate*, 2(1), pp.35–49.
- Meeks, J. & Schaeffer, E.M., 2011. Genetic Regulation of Prostate Development. *J Androl*, 32(3), pp.210–217.
- Miao, C. et al., 2015. miR-375 regulates the canonical Wnt pathway through FZD8 silencing in arthritis synovial fibroblasts. *Immunol Lett*, 164(1), pp.1–10.
- Mihara, E. et al., 2016. Active and water-soluble form of lipidated Wnt protein is maintained by a serum glycoprotein afamin/α-albumin. *eLife*, 5, pp.1–19.
- Mikels, A. & Nusse, R., 2006. Wnts as ligands: processing, secretion and reception. *Oncogene*, 25(57), pp.7461–8.
- Mochmann, L.H. et al., 2011. Genome-wide screen reveals WNT11, a non-canonical WNT gene, as a direct target of ETS transcription factor ERG. *Oncogene*, 30, pp.2044–2056.
- Montanari, M. et al., 2017. Epithelial-mesenchymal transition in prostate cancer: an overview. *Oncotarget*, 8(21), pp.35376–35389.
- Morin, P.J. et al., 1997. Activation of beta -Catenin-Tcf Signaling in Colon Cancer by Mutations in beta -Catenin or APC. *Science*, 275(5307), pp.1787–1790.
- Morris, M. et al., 2018. Optimizing Anticancer Therapy in Metastatic Non-Castrate Prostate Cancer: American Society of Clinical Oncology Clinical Practice Guideline. *J Clin Oncol*, 36(15), pp.1521–1539.



- Mottet, N. et al., 2016. Guidelines on Prostate Cancer. *European Association of Urology*.
- Mullane, S.A. & Van Allen, E.M., 2016. Precision medicine for advanced prostate cancer. *Curr Opin Urol*, 26(3), pp.231–239.
- Murillo-Garzón, V. et al., 2018. Frizzled-8 integrates Wnt-11 and transforming growth factor- $\beta$  signaling in prostate cancer. *Nature Communications*, (2018).
- Murillo-Garzón, V. & Kypta, R., 2017. WNT signalling in prostate cancer. *Nature Reviews Urology*, 14(11), pp.683–696.
- Nadal, R., Street, N.B. & Eisenberger, M.A., 2014. Small cell carcinoma of the prostate. *Nat Rev Urol*, 11(4), pp.213–219.
- Nagayama, S. et al., 2005. Therapeutic potential of antibodies against FZD 10, a cell-surface protein, for synovial sarcomas. *Oncogene*, 24(41), pp.6201–12.
- Nevedomskaya, E., Baumgart, S.J. & Haendler, B., 2018. Recent advances in prostate cancer treatment and drug discovery. *International Journal of Molecular Sciences*, 19(5).
- Nichols, A.S. et al., 2013. Frizzled receptors signal through G proteins. *Cell Signal.*, 25(6), pp.1468–1475.
- Niehhs, C., 2012. The complex world of WNT receptor signalling. *Molecular cell biology*, 13(12), pp.767–79.
- Nieto, M.A. et al., 2016. EMT: 2016. *Cell*, 166(1), pp.21–45.
- NIH, 2016. <https://www.cancer.gov/types/prostate/psa-fact-sheet#q3>.
- Nile, A.H. et al., 2017. Unsaturated fatty acyl recognition by Frizzled receptors mediates dimerization upon Wnt ligand binding. *PNAS*, 114(16), pp.4147–4152.
- Nishioka, M. et al., 2013. Possible involvement of Wnt11 in colorectal cancer progression. *Molecular Carcinogenesis*, 52(3), pp.207–217.
- Nusse, R., 2018. The Wnt homepage.
- Nusse, R. & Varmus, H., 1982. Many tumors induced by mouse mammary tumor virus contain a provirus integrated in the same region of the host chromosome. *Cell*, 31(1), pp.99–109.
- Nusse, R. & Varmus, H.E., 1992. Wnt Genes Review. , 69.
- Ohkawara, B. & Niehhs, C., 2011. An ATF2-based luciferase reporter to monitor non-canonical Wnt signaling in *Xenopus* embryos. *Developmental dynamics : an official publication of the American Association of Anatomists*, 240(1), pp.188–94.
- Ouko, L. et al., 2004. Wnt11 Signaling Promotes Proliferation, Transformation, and Migration of IEC6 Intestinal Epithelial Cells. *J Biol Chem*, 279(25), pp.26707–26715.
- Padua, D. & Massagué, J., 2009. Roles of TGF $\beta$  in metastasis. *Cell research*, 19(1), pp.89–102.
- Pampaloni, F., Reynaud, E.G. & Stelzer, E.H.K., 2007. The third dimension bridges the

- gap between cell culture and live tissue. *Nature Reviews Molecular Cell Biology*, 8(10), pp.839–845.
- Pandur, P. et al., 2002. Wnt-11 activation of a non-canonical Wnt signalling pathway is required for cardiogenesis. *Nature*, 418, pp.636–646.
- Pang, L. et al., 2016. Transcriptomic study of high-glucose effects on human skin fibroblast cells. *Molecular Medicine Reports*, 13(3), pp.2627–2634.
- Papageorgis, P., 2015. TGF $\beta$  Signaling in Tumor Initiation, Epithelial-to-Mesenchymal Transition, and Metastasis. *Journal of oncology*, 2015, p.587193.
- Park, H.W. et al., 2015. Alternative Wnt Signaling Activates YAP/TAZ. *Cell*, 162(4), pp.780–794.
- Pascal, L.E. et al., 2009. Gene expression relationship between prostate cancer cells of Gleason 3, 4 and normal epithelial cells as revealed by cell type-specific transcriptomes. *BMC cancer*, 9, p.452.
- Pavese, J., Ogden, I.M. & Bergan, R.C., 2013. An Orthotopic Murine Model of Human Prostate Cancer Metastasis. *Journal of Visualized Experiments*, (79), pp.1–9.
- Penzo-Mendèz, A. et al., 2003. Activation of G $\beta\gamma$  signaling downstream of Wnt-11/Xfz7 regulates Cdc42 activity during *Xenopus* gastrulation. *Developmental Biology*, 257(2), pp.302–314.
- Peradziryi, H., Tolwinski, N.S. & Borchers, A., 2012. The many roles of PTK7: A versatile regulator of cell-cell communication. *Archives of Biochemistry and Biophysics*, 524(1), pp.71–76.
- Perlmutter, M.A. & Lepor, H., 2007. Androgen deprivation therapy in the treatment of advanced prostate cancer. *Reviews in urology*, 9 Suppl 1(Suppl 1), pp.S3-8.
- Peter E Lonergan, D.J.T., 2011. Androgen receptor signaling in prostate cancer development and progression. *J Carcinog*, 10(20).
- Polakis, P., 2000. Wnt signaling and cancer. *Genes & Dev*, 14, pp.1837–1851.
- Polakis, P., 2012. Wnt signaling in cancer. *Cold Spring Harb.Perspect.Biol.*, 4(5). pii(May), p.a008052.
- Proffitt, K.D. et al., 2013. Pharmacological inhibition of the Wnt acyltransferase PORCN prevents growth of WNT-driven mammary cancer. *Cancer Research*, 73(2), pp.502–507.
- Pu, H. et al., 2009. Dysfunctional transforming growth factor- $\beta$  receptor II accelerates prostate tumorigenesis in the TRAMP mouse model. *Cancer Research*, 69(18), pp.7366–7374.
- PubMed Health, 2016. How does the prostate work?
- Puppo, F. et al., 2011. Protein tyrosine kinase 7 has a conserved role in Wnt/ $\beta$ -catenin canonical signalling. *EMBO Reports*, 12(1), pp.43–49.
- Railo, A. et al., 2008. Wnt-11 signaling leads to down-regulation of the Wnt/ $\beta$ -catenin, JNK/AP-1 and NF-kappaB pathways and promotes viability in the CHO-K1 cells. *Exp Cell Res*, 314(13), pp.2389–99.

- Rao, A.R., Motiwala, H.G. & Karim, O.M.A., 2008. The discovery of prostate-specific antigen. *BJU International*, 101(1), pp.5–10.
- Rebagay, G. et al., 2012. ROR1 and ROR2 in Human Malignancies: Potentials for Targeted Therapy. *Frontiers in oncology*, 2(April), p.34.
- Reeves, F. et al., 2016. *Chapter 29 - The Surgical Anatomy of the Prostate* Second Edi., Elsevier Ltd.
- Rhodes, D.R. et al., 2004. ONCOMINE: A Cancer Microarray Database and Integrated Data-Mining Platform. *Neoplasia*, 6(1), pp.1–6.
- Rijsewijk, F. et al., 1987. The Drosophila homology of the mouse mammary oncogene int-1 is identical to the segment polarity gene wingless. *Cell*, 50(4), pp.649–657.
- Rishi, V. et al., 2004. SREBP-1 dimerization specificity maps to both the helix-loop-helix and leucine zipper domains: Use of a dominant negative. *Journal of Biological Chemistry*, 279(12), pp.11863–11874.
- Robinson, D. et al., 2015. Integrative clinical genomics of advanced prostate cancer. *Cell*, 161(5), pp.1215–1228.
- Säfhholm, A. et al., 2006. A formylated hexapeptide ligand mimics the ability of Wnt-5a to impair migration of human breast epithelial cells. *Journal of Biological Chemistry*, 281(5), pp.2740–2749.
- Säfhholm, A. et al., 2008. The Wnt-5a-derived hexapeptide Foxy-5 inhibits breast cancer metastasis in vivo by targeting cell motility. *Clinical Cancer Research*, 14(20), pp.6556–6563.
- Saitoh, T., Hirai, M. & Katoh, M., 2001. Molecular cloning and characterization of human. *Int J Oncol*, 18(5), pp.991–6.
- Sampieri, K. & Fodde, R., 2012. Cancer stem cells and metastasis. *Seminars in Cancer Biology*, 22(3), pp.187–193.
- van der Sanden, M.H.M. et al., 2004. Induction of CCAAT/enhancer-binding protein (C/EBP)-homologous protein/growth arrest and DNA damage-inducible protein 153 expression during inhibition of phosphatidylcholine synthesis is mediated via activation of a C/EBP-activating transcription factor- $\alpha$ . *The Journal of biological chemistry*, 279(50), pp.52007–15.
- Sandsmark, E. et al., 2017. A novel non-canonical Wnt signature for prostate cancer aggressiveness. *Oncotarget*, 8(6), pp.9572–9586.
- Sano, Y. et al., 1999. ATF-2 is a common nuclear target of smad and TAK1 pathways in transforming growth factor- $\beta$  signaling. *Journal of Biological Chemistry*, 274(13), pp.8949–8957.
- Sato, A. et al., 2010. Wnt5a regulates distinct signalling pathways by binding to Frizzled2. for explaining wnt ineficiency binding. *The EMBO journal*, 29(1), pp.41–54.
- Schenkelaars, Q. et al., 2015. Insights into Frizzled evolution and new perspectives. *Evolution and Development*, 17(2), pp.160–169.
- Schrslder, F.H. et al., 1992. The TNM Classification of Prostate Cancer. , 138, pp.129–

138.

- Schulte, G., 2010. International Union of Basic and Clinical Pharmacology. LXXX. The Class Frizzled Receptors. *The American Society for Pharmacology and Experimental Therapeutics*, 62(4), pp.632–667.
- Schulte, G. & Bryja, V., 2007. The Frizzled family of unconventional G-protein-coupled receptors. *Trends in Pharmacological Sciences*.
- Selman, S.H., 2011. The McNeal prostate: A review. *Urology*, 78(6), pp.1224–1228.
- Semënov, M., Tamai, K. & He, X., 2005. SOST is a ligand for LRP5/LRP6 and a Wnt signaling inhibitor. *Journal of Biological Chemistry*, 280(29), pp.26770–26775.
- Semenov, M. V et al., 2001. Head inducer Dickkopf-1 is a ligand for Wnt coreceptor LRP6. *Current Biology*, 11, pp.951–961.
- Shariat, B.S.F. et al., 2001. Preoperative Plasma Levels of Transforming Growth Factor Beta1 (TGF- $\beta$ 1) Strongly Predict Progression in Patients Undergoing Radical Prostatectomy. *Journal of Clinical Oncology*, 19(11), pp.2856–2864.
- Shen, H. et al., 2017. MiR-99a inhibits keratinocyte proliferation by targeting Frizzled-5 (FZD5) / FZD8 through  $\beta$ -catenin signaling in psoriasis. *Pharmazie*, 72(8), pp.461–467.
- Shen, M. & Abate-Shen, C., 2010. Molecular genetics of prostate cancer: new prospects for old challenges. *Genes & development*, (212), pp.1967–2000.
- Shi, Y. & Massagué, J., 2003. Mechanisms of TGF-beta signaling from cell membrane to the nucleus. *Cell*, 113(6), pp.685–700.
- Shin, S.H., Bode, A.M. & Dong, Z., 2017. Precision medicine: the foundation of future cancer therapeutics. *Precision Oncology*, 1(12).
- Shultz, M.D. et al., 2013. Identification of NVP-TNKS656: The Use of Structure–Efficiency Relationships To Generate a Highly Potent, Selective, and Orally Active Tankyrase Inhibitor. *Journal of Medicinal Chemistry*, 56(16), pp.6495–511.
- Siegel, R.L., Miller, K.D. & Jemal, A., 2017. Cancer Statistics , 2017. , (February), pp.7–30.
- Silberstein, J.L. et al., 2013. Current clinical challenges in prostate cancer. *Translational andrology and urology*, 2(3), pp.122–36.
- Singh, S., Sadacharan, S. & Su, S., 2003. Overexpression of Vimentin : Role in the Invasive Phenotype in an Androgen-independent Model of Prostate Cancer. *Cancer research*, (63), pp.2306–2311.
- Smolich, B.D. et al., 1992. Wnt Family Proteins Are Secreted and Associated with the Cell Surface. , (December 1993), pp.1267–1275.
- Spanjer, A.I.R. et al., 2016. A pro-inflammatory role for the Frizzled-8 receptor in chronic bronchitis. *Thorax*, 71(4), pp.312–322.
- Spanjer, A.I.R. et al., 2016. TGF $\beta$ -induced profibrotic signaling is regulated in part by the WNT receptor Frizzled-8. *The FASEB Journal*, 30(5), pp.1823–35.

- Sreenath, T.L. et al., 2011. Oncogenic activation of ERG: A predominant mechanism in prostate cancer. *J Carcinog*, 10(37).
- Stamey, T.A. et al., 1987. Prostate-specific antigen as a serum marker for adenocarcinoma of the prostate. *The New England journal of medicine*, 317(15), pp.909–916.
- Storm, E.E. et al., 2015. Targeting PTPRK-RSPO3 colon tumours promotes differentiation and loss of stem-cell function. *Nature*, 529(7584), pp.97–100.
- Sun, S. et al., 2014. Targeting the c-Met/FZD8 signaling axis eliminates patient-derived cancer stem-like cells in head and neck squamous carcinomas. *Cancer Research*, 74(24), pp.7546–7559.
- Takada, S. et al., 2017. JB Special Review-Wnt Signaling: Biological Functions and Its Implications in Diseases Differences in the secretion and transport of Wnt proteins. *Journal of Biochemistry*, 161(1), pp.1–7.
- Tamai, K. et al., 2000. LDL receptor-related proteins in Wnt signal transduction. *Nature*, 407(407), pp.530–535.
- Tan, M.E. et al., 2015. Androgen receptor: structure, role in prostate cancer and drug discovery. *Acta Pharmacologica Sinica*, 36(1), pp.3–23.
- Tanaka, H. et al., 2010. Monoclonal antibody targeting of N-cadherin inhibits prostate cancer growth, metastasis and castration resistance. *Nat Med*, 16(12), pp.1414–1420.
- Tao, L. et al., 2016. Frizzled are colonic epithelial receptors for Clostridium difficile toxin B. *Nature*, 538(7625), pp.350–355.
- Tao, Q. et al., 2005. Maternal Wnt11 activates the canonical Wnt signaling pathway required for axis formation in Xenopus embryos. *Cell*, 120(6), pp.857–871.
- Taylor, B., Schultz, N. & Hieronymus, H., 2010. Integrative genomic profiling of human prostate cancer. *Cancer cell*, 18(1), pp.11–22.
- Thiele, S. et al., 2011. Expression profile of WNT molecules in prostate cancer and its regulation by aminobisphosphonates. *Journal of Cellular Biochemistry*, 112(6), pp.1593–1600.
- Thiery, J.P., 2002. Epithelial-mesenchymal transitions in tumour progression. *Nature reviews. Cancer*, 2(6), pp.442–54.
- Thompson, M., Nejak-Bowen, K. & Monga, S.P.S., 2011. *Crosstalk of the Wnt Signaling Pathway*,
- Thorpe, A. & Neal, D., 2003. Benign prostatic hyperplasia. *Lancet (London, England)*, 361(9366), pp.1359–67.
- Toyama, T. et al., 2010. Noncanonical Wnt11 Inhibits Hepatocellular Carcinoma Cell Proliferation and Migration. *Molecular Cancer Research*, 8(2), pp.254–265.
- Uysal-Onganer, P. et al., 2010. Wnt-11 promotes neuroendocrine-like differentiation, survival and migration of prostate cancer cells. *Molecular cancer*, 9, p.55.
- Uysal-Onganer, P. & Kypta, R., 2012. Wnt11 in 2011 - the regulation and function of a

- non-canonical Wnt. *Acta Physiologica*, 204(1), pp.52–64.
- Veeck, J. & Dahl, E., 2012. Targeting the Wnt pathway in cancer: The emerging role of Dickkopf-3. *Biochimica et Biophysica Acta - Reviews on Cancer*, 1825(1), pp.18–28.
- Veeman, M. et al., 2003. Zebrafish Prickle, a Modulator of Noncanonical Wnt/Fz Signaling, Regulates Gastrulation Movements. *Medical Engineering & Physics*, 25, pp.75–78.
- Veeman, M.T., Axelrod, J.D. & Moon, R.T., 2003. A Second Canon: Functions and Mechanisms of  $\beta$ -Catenin-Independent Wnt Signaling. *Developmental Cell*, 5(3), pp.367–377.
- Vinson, C. et al., 2002. Classification of Human B-ZIP Proteins Based on Dimerization Properties. *Asha*, 22(18), pp.6321–6335.
- Vinson, C. & Adler, P., 1987. Directional non-cell autonomy and the transmission of polarity information by the frizzled gene of Drosophila. *Nature*, 329(17), pp.219–222.
- Vinson, C., Conover, S. & Adler, P., 1989. A Drosophila tissue polarity locus encodes a protein containing seven potential transmembrane domains. *Nature*, 338(6212), pp.263–4.
- Vivanco, M.D. et al., 1995. A transition in transcriptional activation by the glucocorticoid and retinoic acid receptors at the tumor stage of dermal fibrosarcoma development. *The EMBO journal*, 14(10), pp.2217–28.
- Volante, M. et al., 2016. Androgen deprivation modulates gene expression profile along prostate cancer progression. *Human Pathology*, 56, pp.81–88.
- Wang, H. et al., 2012. Frizzled-8 as a putative therapeutic target in human lung cancer. *Biochemical and Biophysical Research Communications*, 417(1), pp.62–66.
- Wang, K. et al., 2018. Recent advances on the progressive mechanism and therapy in castration-resistant prostate cancer. *OncoTargets and Therapy*, 11, pp.3167–3178.
- Wang, M. et al., 2017. Role of tumor microenvironment in tumorigenesis. *Journal of Cancer*, 8(5), pp.761–773.
- Wang, M.T. et al., 2015. K-Ras Promotes Tumorigenicity through Suppression of Non-canonical Wnt Signaling. *Cell*, 163(5), pp.1237–1251.
- Watson, P.A., Arora, V.K. & Sawyers, C.L., 2015. Emerging mechanisms of resistance to androgen receptor inhibitors in prostate cancer. *Nature reviews. Cancer*, 15(12), pp.701–11.
- Wei, J. et al., 2008. Overexpression of vimentin contributes to prostate cancer invasion and metastasis via Src regulation. *Anticancer Research*, 28(1 A), pp.327–334.
- Wei, W. et al., 2011. Soluble Frizzled-7 receptor inhibits Wnt signaling and sensitizes hepatocellular carcinoma cells towards doxorubicin. *Molecular cancer*, 10(1), p.16.
- Wendt, M., Allington, T. & Schiemann, W., 2009. Mechanisms of Epithelial-Mesenchymal Transition by TGF- $\beta$ . *Future Oncol*, 5(8), pp.1145–1168.

- Willert, K. et al., 2003. Wnt proteins are lipid-modified and can act as stem cell growth factors. , 176(May).
- Willert, K. & Nusse, R., 2012. Wnt proteins. *Cold Spring Harb.Perspect.Biol.*, 4, p.a007864.
- Wissman, C. et al., 2003. WIFI, a component of the Wnt pathway, is down-regulated in prostate, breast, lung, and bladder cancer. *Journal of Pathology*, 201(2), pp.204–212.
- Witzel, S. et al., 2006. Wnt11 controls cell contact persistence by local accumulation of Frizzled 7 at the plasma membrane. *The Journal of cell biology*, 175(5), pp.791–802.
- Wrana, J. et al., 1992. TGF beta signals through a heteromeric protein kinase receptor complex. *Cell*, 71(6), pp.1003–1014.
- Wu, L. et al., 2013. ERG is a critical regulator of Wnt/LEF1 signaling in prostate cancer. *Cancer Research*, 73(19), pp.6068–6079.
- Y, Z. et al., 2008. Vimentin affects the mobility and invasiveness of prostate cancer cells. *Cell biochem Funct*, 26(5), pp.571–7.
- Yamamoto, A. et al., 2005. Shisa promotes head formation through the inhibition of receptor protein maturation for the caudalizing factors, Wnt and FGF. *Cell*, 120(2), pp.223–235.
- Yamamoto, H. et al., 2010. Wnt5a signaling is involved in the aggressiveness of prostate cancer and expression of metalloproteinase. *Oncogene*, 29(14), pp.2036–2046.
- Yamanaka, H. & Nishida, E., 2007. Wnt11 stimulation induces polarized accumulation of Dishevelled at apical adherens junctions through Frizzled7. *Genes to Cells*, 12(8), pp.961–967.
- Yang, P. et al., 2008. Wnt Signaling Requires Retromer-Dependent Recycling. *Developmental cell*, 14, pp.140–147.
- Yang, Q. et al., 2017. Frizzled 8 promotes the cell proliferation and metastasis of renal cell carcinoma. *Oncotarget*, 8, pp.78989–79002.
- Ye, X. et al., 2011. Genetic mosaic analysis reveals a major role for frizzled 4 and frizzled 8 in controlling ureteric growth in the developing kidney. *Development (Cambridge, England)*, 138(6), pp.1161–72.
- Ye, Z. et al., 2013. Wnt5a uses CD146 as a receptor to regulate cell motility and convergent extension. *Nature Communications*, 4.
- Yin, S. et al., 2013. Tumor Initiating Cells and FZD8 play a major role in drug resistance in Triple-Negative Breast Cancer. *Mol Cancer Ther*, 12(4), pp.491–498.
- Yu H, Ye X, Guo N, N.J., 2012. Frizzled 2 and frizzled 7 function redundantly in convergent extension and closure of the ventricular septum and palate: evidence for a network of interacting genes. *Development*, 139(23), pp.4383–4394.
- Yun, C. & DasGupta, R., 2015. Luciferase reporter assay in Drosophila and mammalian tissue culture cells. *Current Protocols in Molecular Biology*, 6(1),

pp.7–23.

- Zanconato, F. et al., 2016. YAP/TAZ as therapeutic targets in cancer. *Current Opinion in Pharmacology*, 29, pp.26–33.
- Zhan, T., Rindtorff, N. & Boutros, M., 2017. Wnt signaling in cancer. *Oncogene*, 36(11), pp.1461–1473.
- Zhang, H. et al., 2014. Protein tyrosine kinase 7 (PTK7) as a predictor of lymph node metastases and a novel prognostic biomarker in patients with prostate cancer. *International journal of molecular sciences*, 15(7), pp.11665–77.
- Zhang, P. et al., 2012. Activation of Wnt11 by transforming growth factor- $\beta$  drives mesenchymal gene expression through non-canonical Wnt protein signaling in renal epithelial cells. *The Journal of biological chemistry*, 287(25), pp.21290–302.
- Zhang, S. et al., 2012. The onco-embryonic antigen ROR1 is expressed by a variety of human cancers. *American Journal of Pathology*, 181(6), pp.1903–1910.
- Zhang, Y.E., 2009. Non-Smad pathways in TGF-beta signaling. *Cell research*, 19(1), pp.128–39.
- Zheng, X. et al., 2015. EMT Program is Dispensable for Metastasis but Induces Chemoresistance in Pancreatic Cancer. *Nature*, 527(7579), pp.525–530.
- Zhou, W. et al., 2007. Modulation of morphogenesis by noncanonical Wnt signaling requires ATF/CREB family-mediated transcriptional activation of TGF $\beta$ 2. *Nature Genetics*, 39, pp.1225–1234.
- Zhu, H. et al., 2004. Analysis of Wnt Gene Expression in Prostate Cancer : Mutual Inhibition by WNT11 and the Androgen Receptor. *Cancer Research*, 64, pp.7918–7926.





---

**SCIENTIFIC  
CONTRIBUTIONS**

---



✚ Al Shareef Z, Karooni H, **Murillo-Garzón V**, Domenici G, Stylianakis E, Steel JH, Rabano M, Gorroño-Etxebarria I, Zabalza I, Vivanco MDM, Waxman J, Kypta RM. Protective effect of stromal Dickkopf-3 in prostate cancer: opposing roles for TGFBI and ECM-1. *Oncogene*. 2018 Jun 1. doi: 10.1038/s41388-018-0294-0. [Epub ahead of print] PubMed PMID: 29858602.

### **Abstract**

Aberrant transforming growth factor- $\beta$  (TGF- $\beta$ ) signaling is a hallmark of the stromal microenvironment in cancer. Dickkopf-3 (Dkk-3), shown to inhibit TGF- $\beta$  signaling, is downregulated in prostate cancer and upregulated in the stroma in benign prostatic hyperplasia, but the function of stromal Dkk-3 is unclear. Here we show that DKK3 silencing in WPMY-1 prostate stromal cells increases TGF- $\beta$  signaling activity and that stromal cell-conditioned media inhibit prostate cancer cell invasion in a Dkk-3-dependent manner. DKK3 silencing increased the level of the cell-adhesion regulator TGF- $\beta$ -induced protein (TGFBI) in stromal and epithelial cell-conditioned media, and recombinant TGFBI increased prostate cancer cell invasion. Reduced expression of Dkk-3 in patient tumors was associated with increased expression of TGFBI. DKK3 silencing reduced the level of extracellular matrix protein-1 (ECM-1) in prostate stromal cell-conditioned media but increased it in epithelial cell-conditioned media, and recombinant ECM-1 inhibited TGFBI-induced prostate cancer cell invasion. Increased ECM1 and DKK3 mRNA expression in prostate tumors was associated with increased relapse-free survival. These observations are consistent with a model in which the loss of Dkk-3 in prostate cancer leads to increased secretion of TGFBI and ECM-1, which have tumor-promoting and tumor-protective roles, respectively. Determining how the balance between the opposing roles of extracellular factors influences prostate carcinogenesis will be key to developing therapies that target the tumor microenvironment.

✚ **Murillo-Garzón V**, Gorroño-Etxebarria I, Åkerfelt M, Puustinen MC, Sistonen L, Nees M, Carton J, Waxman J, Kypka RM. Frizzled-8 integrates Wnt-11 and transforming growth factor- $\beta$  signaling in prostate cancer. *Nat Commun.* 2018 May 1;9(1):1747. doi: 10.1038/s41467-018-04042-w. PubMed PMID: 29717114; PubMed Central PMCID: PMC5931552.

### **Abstract**

Wnt-11 promotes cancer cell migration and invasion independently of  $\beta$ -catenin but the receptors involved remain unknown. Here, we provide evidence that FZD<sub>8</sub> is a major Wnt-11 receptor in prostate cancer that integrates Wnt-11 and TGF- $\beta$  signals to promote EMT. FZD8 mRNA is upregulated in multiple prostate cancer datasets and in metastatic cancer cell lines in vitro and in vivo. Analysis of patient samples reveals increased levels of FZD<sub>8</sub> in cancer, correlating with Wnt-11. FZD<sub>8</sub> co-localizes and co-immunoprecipitates with Wnt-11 and potentiates Wnt-11 activation of ATF2-dependent transcription. FZD8 silencing reduces prostate cancer cell migration, invasion, three-dimensional (3D) organotypic cell growth, expression of EMT-related genes, and TGF- $\beta$ /Smad-dependent signaling. Mechanistically, FZD<sub>8</sub> forms a TGF- $\beta$ -regulated complex with TGF- $\beta$  receptors that is mediated by the extracellular domains of FZD<sub>8</sub> and TGFBR1. Targeting FZD<sub>8</sub> may therefore inhibit aberrant activation of both Wnt and TGF- $\beta$  signals in prostate cancer.

✚ **Murillo-Garzón V**, Kypta R. WNT signalling in prostate cancer. *Nat Rev Urol.* 2017 Nov;14(11):683-696. doi: 10.1038/nrurol.2017.144. Epub 2017 Sep 12. Review. PubMed PMID: 28895566.

**Abstract**

Genome sequencing and gene expression analyses of prostate tumours have highlighted the potential importance of genetic and epigenetic changes observed in WNT signalling pathway components in prostate tumours - particularly in the development of castration-resistant prostate cancer. WNT signalling is also important in the prostate tumour microenvironment, in which WNT proteins secreted by the tumour stroma promote resistance to therapy, and in prostate cancer stem or progenitor cells, in which WNT- $\beta$ -catenin signals promote self-renewal or expansion. Preclinical studies have demonstrated the potential of inhibitors that target WNT receptor complexes at the cell membrane or that block the interaction of  $\beta$ -catenin with lymphoid enhancer-binding factor 1 and the androgen receptor, in preventing prostate cancer progression. Some WNT signalling inhibitors are in phase I trials, but they have yet to be tested in patients with prostate cancer.

✚ Cautain B, de Pedro N, **Murillo-Garzón V**, Muñoz de Escalona M, González Menéndez V, Tormo JR, Martín J, El Aouad N, Reyes F, Asensio F, Genilloud O, Vicente F, Link W. High-content screening of natural products reveals novel nuclear export inhibitors. *J Biomol Screen*. 2014 Jan;19(1):57-65. doi: 10.1177/1087057113501389. Epub 2013 Sep 17. PubMed PMID: 24045581.

### **Abstract**

Natural products are considered an extremely valuable source for the discovery of new drugs against diverse pathologies. As yet, we have only explored a fraction of the diversity of bioactive compounds, and opportunities for discovering new natural products leading to new drugs are huge. In the present study, U2nesRELOC, a previously established cell-based imaging assay, was employed to screen a collection of extracts of microbial origin for nuclear export inhibition activity. The fluorescent signal of untreated U2nesRELOC cells localizes predominantly to the cytoplasm. Upon treatment with the nuclear export inhibitor leptomycin B, the fluorescent-tagged reporter proteins appear as speckles in the nucleus. A proprietary collection of extracts from fungi, actinomycetes, and unicellular bacteria that covers an uncommonly broad chemical space was used to interrogate this nuclear export assay system. A two-step image-based analysis allowed us to identify 12 extracts with biological activities that are not associated with previously known active metabolites. The fractionation and structural elucidation of active compounds revealed several chemical structures with nuclear export inhibition activity. Here we show that substrates of the nuclear export receptor CRM1, such as Rev, FOXO3a and NF- $\kappa$ B, accumulate in the nucleus in the presence of the fungal metabolite MDN-0105 with an IC<sub>50</sub> value of 3.4  $\mu$ M. Many important processes in tumor formation and progression, as well as in many viral infections, critically depend on the nucleocytoplasmic trafficking of proteins and RNA molecules. Therefore, the disruption of nuclear export is emerging as a novel therapeutic approach with enormous clinical potential. Our work highlights the potential of applying high-throughput phenotypic imaging on natural product extracts to identify novel nuclear export inhibitors.

## **RESUMEN: VERSIÓN EXTENDIDA**

### **INTRODUCCIÓN**

En la actualidad, el cáncer de próstata representa en varones el tipo de cáncer más frecuentemente diagnosticado y la tercera causa más común de muerte en los países industrializados. Los principales factores de riesgo asociados a este tipo de cáncer son la edad y la raza, aunque otros factores como la herencia genética, la dieta o el consumo de alcohol se han visto asociados como un mayor riesgo.

El cáncer de próstata tiene su origen en las neoplasias prostáticas intraepiteliales que normalmente progresan a neoplasias de alto grado dando lugar frecuentemente a carcinomas de próstata. Durante este proceso de transformación las células adquieren alteraciones a nivel molecular que determinan la progresión del cáncer hasta estadios invasivos y metastáticos.

Marcadores como el antígeno específico de próstata (PSA) se han empleado en el diagnóstico del cáncer de próstata lo que ha contribuido a una mejora en el diagnóstico de este tipo de tumores. Inicialmente, el tratamiento del cáncer de próstata se basa en el seguimiento y la vigilancia debido a la lenta progresión de dichos tumores. Posteriormente, cuando el tumor está localizado la principal terapia es la prostatectomía radical y/o la radioterapia. Cuando los tumores comienzan a metastatizar, la terapia de deprivación de andrógenos (ADT) es la opción más empleada debido al requerimiento de andrógenos de las células del cáncer de próstata para proliferar. Sin embargo, muchos pacientes desarrollan resistencia a esta terapia y aunque nuevos tratamientos están siendo desarrollados, no se han observado mejoras en la supervivencia, lo que estimula la investigación en los mecanismos que dan lugar a esta resistencia con el fin de identificar nuevas dianas que mejoren el tratamiento de esta enfermedad.

La familia de proteínas de Wnt juega un papel fundamental en procesos como el desarrollo, la proliferación, la polaridad, la migración y la supervivencia de las células y por todo ello, alteraciones en los niveles de dichas proteínas se han visto implicados en enfermedades como el cáncer. Entre los miembros de esta familia, Wnt-11 (miembro no canónico por señalar independientemente de  $\beta$ -catenina) se encuentra altamente expresado en líneas celulares de cáncer de próstata, así como en tumores de próstata. Además, Wnt-11 promueve la migración y la invasión celular lo que sugiere su implicación en la progresión y la metástasis del cáncer de próstata.

En base a la implicación de Wnt-11 en el cáncer de próstata y a la necesidad que estas proteínas tienen de unirse a receptores de membrana para activar la señalización y mediar sus efectos, en esta tesis se plantea que la identificación y caracterización de los receptores de Wnt-11 puede representar una nueva diana terapéutica para inhibir los efectos de este ligando en la progresión del cáncer de próstata. Así, los objetivos principales de este trabajo consisten en identificar los receptores de Wnt-11 y caracterizar los efectos funcionales que ejercen en el cáncer de próstata, así como analizar los mecanismos moleculares que subyacen a esta ruta de señalización y evaluar el potencial de dichos receptores como biomarcadores y dianas terapéuticas en la progresión del cáncer de próstata.

## **MATERIALES Y MÉTODOS**

En esta tesis se han llevado a cabo cultivos celulares tanto en 2D como en 3D y se han empleado diversas técnicas de biología molecular tales como extracción de RNA, PCR, western blotting e inmunoprecipitaciones. También se han llevado a cabo análisis de actividad reportera, microscopía de inmunofluorescencia, inmunohistoquímicas con muestras de pacientes y ensayos en modelos *in vivo* como la membrana corioalantoidea (CAM) del pollo.

## **RESULTADOS**

### Capítulo 1. Identificación y caracterización de los receptores de Wnt-11 en cáncer de próstata metastático

Previos estudios demostraron una elevada expresión de Wnt-11 en líneas celulares de cáncer de próstata, así como en tumores de próstata, sobre todo, en metástasis. En base a esta implicación de Wnt-11 en el cáncer de próstata y al requerimiento de la unión entre las proteínas Wnt y sus receptores para señalizar y realizar su función, el objetivo inicial de esta tesis es la identificación de los receptores de Wnt que muestran una expresión elevada en cáncer de próstata y que, por ello, pueden jugar un papel fundamental en la progresión y la metástasis de este tipo de cáncer.

Para ello, inicialmente, se llevó a cabo un análisis de la expresión de un amplio panel de receptores de Wnt incluyendo la familia de receptores Frizzled (FZD1-10), los receptores tirosina quinasa ROR1, ROR2, RYK, PTK7 and MuSK y otros coreceptores como LRP4-6, LGR4 and 5 and GPC4. En primer lugar, se analizó la expresión de estos receptores en diferentes líneas celulares representando diferentes estadios del cáncer de próstata mediante qRT-PCR. En este análisis, se observó que algunos receptores incluyendo FZD2, FZD4 y FZD8 se encuentran altamente expresados en las líneas celulares más agresivas. Además, el patrón de expresión de



estos receptores correlaciona con el patrón de Wnt-11, lo que sugiere que estos receptores pueden tener una implicación en la progresión del cáncer de próstata mediando la señalización de Wnt-11. La expresión de estos receptores también se evaluó mediante un análisis *in silico* usando bases de datos de pacientes con cáncer de próstata. De este modo, se observó que FZD4 y FZD8 y el correceptor PTK7 se encuentran altamente expresados en muestras de pacientes tumorales comparadas con tejido sano en diferentes bases de datos. Finalmente, el análisis conjunto de ambas estrategias de *screening* permitió la identificación de candidatos potenciales que se encuentran altamente expresados en cáncer de próstata y que, por tanto, pueden estar implicados en la patogénesis de esta enfermedad.

Con el fin de evaluar cuál de los potenciales candidatos podía actuar como receptor de Wnt-11 en las células metastáticas de cáncer de próstata, se llevaron a cabo ensayos de colocalización por inmunofluorescencia entre los diez miembros de la familia de receptores FZD y Wnt-11. Este análisis permitió concluir que FZD8 es el receptor que mejor colocaliza con Wnt-11 aunque FZD6 y FZD10 también lo hacen parcialmente.

Por último, para determinar qué receptor podía mediar la señalización de Wnt-11 se emplearon ensayos de silenciamiento génico y actividad reportera. Estos experimentos permitieron concluir que FZD8 actúa como el receptor principal de Wnt-11 en las células metastáticas del cáncer de próstata, ya que su silenciamiento génico reduce la activación que Wnt-11 ejerce sobre el reportero de ATF2 y de AP1 (ambos reporteros de la ruta no canónica de Wnt). Además, ensayos de inmunoprecipitación mostraron que FZD8 se une de forma estable a Wnt-11, lo que sostiene su papel como receptor principal de Wnt-11 en cáncer de próstata.

## Capítulo 2: Implicación de FZD8 en la patogénesis del cáncer de próstata

Numerosos eventos se han visto implicados en la progresión tumoral incluyendo las capacidades de migración e invasión que las células adquieren durante el proceso metastático. Debido al papel de Wnt-11 en la migración e invasión celular, el siguiente objetivo de esta tesis se basa en estudiar el papel de su receptor, FZD8, en estas habilidades de las células metastáticas.

En primer lugar, se llevaron a cabo ensayos de migración e invasión celular en cultivos en 2D usando canales Boyden. Estos experimentos permitieron concluir que el silenciamiento de FZD8 reduce la migración e invasión de las células de cáncer de próstata metastático. Estos efectos se corroboraron también con líneas celulares establemente silenciadas para FZD8 y con inhibidores químicos de la unión entre Wnt

y los receptores FZD. Además, los efectos de FZD8 sobre la invasión celular se estudiaron también mediante ensayos en 3D empleando cultivos organotípicos que simulan de una forma más fisiológica el comportamiento de las células en el organismo. Con estos estudios se comprobó que el silenciamiento de FZD8 reduce la invasión celular en 3D, reduciendo parámetros como el número y la longitud de los apéndices y aumentando la esfericidad de los organoides.

Ya que uno de los eventos implicados en la adquisición de las capacidades de invasión y migración celular en los tumores es el proceso de transición epitelio-mesénquima (EMT), se evaluó si FZD8 estaba implicado en este proceso. El análisis por PCR de diversos genes implicados en este proceso, así como a nivel proteico por western blot permitió determinar que el silenciamiento de FZD8 reduce la expresión de los factores mesenquimales y aumenta la expresión de los epiteliales apoyando el papel de FZD8 en el proceso de EMT.

En segundo lugar, se trató de evaluar el papel de FZD8 en ensayos *in vivo* utilizando el modelo de la membrana corioalantoidea (CAM) del pollo que permite implantar células tumorales y evaluar el crecimiento tumoral. Así, tras implantar células de cáncer de próstata metastático silenciadas para FZD8 se pudo observar que éstas producían tumores de un menor tamaño que las controles, implicando a FZD8 en el crecimiento tumoral.

Por último, se emplearon muestras de pacientes sanos y con cáncer de próstata contenidas en un array de tejido (TMA) para analizar la expresión de FZD8 y Wnt-11. El análisis por inmunohistoquímica de la expresión de ambos permitió observar que tanto FZD8 como Wnt-11 se encontraban altamente expresados en cáncer de próstata con respecto a los tejidos sanos. Aunque no se observó una correlación con el grado de Gleason de los pacientes, el análisis de la expresión en bases de datos mediante bioinformática sugiere que los pacientes con alta expresión de FZD8 y Wnt-11 tienen una menor tasa de supervivencia.

Así, todos estos resultados sostienen la implicación de FZD8 en el proceso metastático del cáncer de próstata y su posible uso como biomarcadores y como dianas terapéuticas en esta enfermedad.

### Capítulo 3. Estudio del mecanismo que subyace a los efectos de FZD8 en la patogénesis del cáncer de próstata

Los resultados obtenidos hasta este punto revelan la contribución de FZD8 en la patogénesis del cáncer de próstata promoviendo la migración e invasión celular y el proceso de EMT. Sin embargo, los mecanismos moleculares que median este proceso

se desconocen. La ruta de señalización de Wnt interacciona con otras muchas rutas durante la progresión del cáncer. Entre ellas, la ruta de señalización de TGF- $\beta$ , además de interactuar con Wnt, se ha visto implicada en los eventos mediadores del proceso metastático como la migración e invasión celular y el proceso de EMT. Así, el último objetivo de esta tesis consistió en determinar si FZD8 media sus efectos regulando la señalización de TGF- $\beta$ .

En primer lugar, se llevó a cabo un análisis de la actividad transcripcional de TGF- $\beta$  que permitió concluir que el silenciamiento de FZD8 reduce la ruta de TGF- $\beta$ . Además, el silenciamiento de FZD8 reduce la expresión de los genes diana de TGF- $\beta$  y los niveles de fosforilación de SMAD2 analizados mediante PCR y western blot, respectivamente lo que sostiene la implicación de FZD8 en la señalización de TGF- $\beta$ .

Debido a la implicación de FZD8 en los procesos de migración e invasión celular y de EMT, se pretendió evaluar si FZD8 mediaba estos efectos a través de TGF- $\beta$ . Así, el silenciamiento de TGF- $\beta$  redujo tanto la invasión como el proceso de EMT dependiente de TGF- $\beta$ .

FZD8 está implicado en la ruta no canónica de Wnt activando ATF2 y, además, en la señalización de TGF- $\beta$ . En base a estos resultados, se analizó la posibilidad de que el requerimiento de FZD8 sobre TGF- $\beta$  estuviese mediado por ATF2. De este modo, el análisis de actividad reportera mostró que un dominante negativo de ATF2 es capaz de reducir el reportero de TGF- $\beta$  así como el proceso de EMT dependiente de TGF- $\beta$ , indicando un posible requerimiento de ATF2 en esta ruta de señalización.

Dado que diferentes estudios han mostrado que los factores de transcripción SMAD y ATF2 pueden interactuar en el núcleo, en este trabajo se planteó que FZD8 podría estar regulando esta interacción. Sin embargo, mediante análisis de inmunoprecipitación no se pudo detectar una unión estable entre los factores SMAD y ATF2 lo que llevó a descartar esta hipótesis. Posteriormente, se planteó que dado que ambas rutas, Wnt y TGF- $\beta$ , se activan por unión de los ligandos a receptores de membrana, podría ser posible que FZD8 estuviese interactuando con los receptores de TGF- $\beta$  en la membrana celular. Inesperadamente, mediante ensayos de inmunoprecipitación e inmunofluorescencia, se observó que FZD8 interacciona con los receptores de TGF- $\beta$  (TGF $\beta$ RI y TGF $\beta$ RII). Además, se pudo comprobar que esta interacción está mediada por los dominios extracelulares de FZD8 y de TGF $\beta$ RI y que la unión entre FZD8 y los receptores de TGF- $\beta$  se ve afectada por la presencia de ligando (TGF- $\beta$ ), el cuál disminuye la interacción entre FZD8 y TGF $\beta$ RII. Así mismo,

se pudo observar que en presencia de Wnt-11, FZD8 todavía puede unirse a los receptores de TGF- $\beta$

Todos estos resultados son consistentes con un modelo en el que FZD8 integra ambas rutas de señalización, Wnt y TGF- $\beta$ , y así promueve la migración e invasión celular además del proceso de EMT dando lugar a la metástasis del cáncer de próstata. Consecuentemente, FZD8 puede representar una óptima diana terapéutica en el cáncer de próstata metastático con el fin de bloquear los efectos de ambas rutas, Wnt y TGF- $\beta$ .

## CONCLUSIONES

Los resultados de esta tesis permiten concluir que:

- FZD8 se encuentra altamente expresado en las líneas celulares más agresivas de cáncer de próstata, además de en tejidos de cáncer de próstata y en metástasis con respecto a tejidos sanos.
- FZD8 se une a Wnt-11 y actúa como receptor principal en cáncer de próstata metastático mediando una ruta no canónica de Wnt.
- FZD8 está implicado en las principales características de la progresión tumoral tales como la migración, la invasión, la invasión en cultivos organotípicos en 3D y el proceso de EMT.
- FZD8 promueve el crecimiento tumoral *in vivo*.
- La expresión de FZD8 y WNT11 correlaciona con la progresión del cáncer de próstata.
- FZD8 integra las rutas de señalización de Wnt y TGF- $\beta$  a través de su asociación con TGF $\beta$ RI.
- FZD8 puede constituir una diana terapéutica para el cáncer de próstata metastático *per se* o en combinación con inhibidores de la ruta de TGF- $\beta$ .



